Master's thesis

NTNU
Norwegian University of Science and Technology
Faculty of Natural Sciences
Department of Materials Science and Engineering

Fride Müller

Heavy Metal Emissions from Primary Aluminium Production

Master's thesis in Materials Science and Engineering
Supervisor: Gabriella Tranell
Co-supervisor: Thor Anders Aarhaug
June 2022

NTNU
Norwegian University of
Science and Technology

Fride Müller

Heavy Metal Emissions from Primary Aluminium Production

Master's thesis in Materials Science and Engineering
Supervisor: Gabriella Tranell
Co-supervisor: Thor Anders Aarhaug
June 2022

Norwegian University of Science and Technology
Faculty of Natural Sciences
Department of Materials Science and Engineering

NTNU
Norwegian University of
Science and Technology

NTNU – Trondheim
Norwegian University of
Science and Technology

TMT4920 Master in Materials Science and Engineering

Heavy Metal Emissions from Primary Aluminium Production

Author: Fride Müller

Supervisor: Gabriella Tranell, NTNU
Co-Supervisor: Thor Anders Aarhaug, SINTEF

June 10, 2022

Preface

This thesis is written as a part of the fifth year course TMT4920 *Master in Materials Science and Engineering* and marks the ending of a five year educational program in material science and engineering at the Norwegian University of Science and Technology, NTNU.

I would like to thank my supervisor, Professor Gabriella Tranell for excellent guidance through this year with both project assignment and master thesis. I greatly appreciate the discussions from the weekly meetings, field trips to Høyanger and Mosjøen, being able to experience the annual TMS conference in Los Angeles and the social events throughout the year.

I would also like to thank my co-supervisor Thor Anders Aarhaug for helping me with the sensor system set up, as well as patiently guiding me through the associated data analyses in MATLAB.

Thank you to Ellen Bromstad Myrvold, Asbjørn Magnus Kjønnås and Kim Ronny Elstad at Alcoa for always welcoming me with open arms upon my visits and providing me with help and knowledge during my emission measurements. I would also like to thank Morten Isaksen, Nancy Jorunn Holt and Eirik Manger at Hydro for sharing their knowledge, as well as providing samples and organising a visit to Hydro Høyanger.

Finally, I would like to extend my gratitude to my family and friends for always believing in me. Without your unconditional support i would not be where I am today.

Abstract

Heavy metals in airborne particulate matter (PM), or dust, are considered a health and environmental concern. A better understanding of the formation and composition of the dust emissions are necessary to improve monitoring and control measures regarding heavy metal emissions.

Fugitive dust emissions from two Norwegian aluminium smelters were investigated by different characterisation methods and in-situ particulate matter emission measurements. Both settled and airborne dust mainly from Hydro Høyanger, were characterised by means of Bruaner, Emmet and Teller method (BET), Scanning electron microscope (SEM), X-ray diffraction (XRD), Inductively Coupled Plasma Mass Spectrometry (ICP-MS) and particle size distribution analyser. PM emissions were measured for three weeks at Alcoa's plant in Mosjøen by optical PM sensors based on laser scattering technology. The sensors measured temperature and humidity, number concentration and mass concentration for $PM_{1.0}$, $PM_{2.5}$, $PM_{4.0}$ and PM_{10}. The purpose of this work was to map the composition and variation in fugitive potroom emissions that occur in different areas and in connection with different operational processes within the electrolysis hall, with a focus on heavy metals and particle size distribution.

Heavy metal particles were often found as inclusions or on the surface of larger carbon particles. Nickel and iron were found to be phosphorous or sulfuric compounds and nickel appeared to be present as nickel sulfide in some cases. Particle size distribution for settled and airborne dust were mainly found to be in PM_{10+} range, while the average particle size fraction for particles measured by the sensor system were found to be around 0.6 µm at roof and floor level. Correlation between specific operational activities and increased emissions were observed, where anode change caused higher emissions than metal tapping and temperature measurements. Emissions produced during anode change mainly consisted of $PM_{2.5}$, while tapping caused more PM_{10} emissions.

Sammendrag

Tungmetallutslipp i form av luftbårne partikler, eller støv, anses som en miljøbelastning og kan være helseskadelig for både mennesker og dyr. En bedre forståelse av forekomst og sammensetningen er derfor nødvendig for å kontrollere og overvåke slike utslipp på en best mulig måte, samt innføre utslippsreduserende tiltak.

Diffuse støvutslipp fra to norske aluminiumssmelteverk ble undersøkt ved hjelp av ulike karakteriseringsmetoder og utslippsmålinger. Luftbårne partikler og avsatt støv, hovedsakelig fra Hydro Høyanger, ble undersøkt ved hjelp av Bruaner, Emmet og Teller-metoden (BET), elektronmikroskop (SEM), røntgendiffraksjon (XRD), massespektrometri (ICP-MS) og partikkelstørrelse analysator. Partikkelutslipp ble målt ved hjelp av optiske sensorer i en periode på tre uker, ved Alcoas anlegg i Mosjøen. Sensorene målte temperatur, fuktighet, tallkonsentrasjon og massekonsentrasjon for $PM_{1.0}$, $PM_{2.5}$, $PM_{4.0}$ og PM_{10}. Hensikten med dette var å kartlegge sammensetning og variasjon i diffuse støvutslipp som oppstår i ulike områder, og i forbindelse med forskjellige driftsprosesser i en elektrolysehall med fokus på tungmetaller og partikkelstørrelsesfordeling.

Tungmetallpartikler ble ofte observert som inneslutninger eller på overflaten av større karbonpartikler. Nikkel og jern ble funnet som fosfor- eller svovelholdige forbindelser og nikkel ble i noen tilfeller antatt å være tilstede som nikkelsulfid. For luftbårne partikler og avsatt støv ble partikkelstørrelsesfordelingen hovedsakelig funnet å være over PM_{10}, mens gjennomsnittlig partikkelstørrelsesfraksjon målt av sensorsystemet ble funnet å være rundt 0.6 µm ved tak- og gulvnivå. Korrelasjon mellom spesifikke driftsaktiviteter og periodevis økt utslipp ble observert, hvor anodeskift forårsaket høyere målte utslipp enn metalltapping og temperaturmålinger. Utslipp som oppstod under anodeskift bestod hovedsakelig av $PM_{2.5}$, mens tapping forårsaket høyere nivå av PM_{10} utslipp.

Contents

List of Abbrevations

Table 1: List of abbrevations

Abbrevation	**Meaning**
UN	United Nations
EEA	European Economic Area
Alumina	Aluminium Oxide
CPC	Calcined Petroleum Coke
ACM	Anode Cover Mass
SPL	Spent Pot Lining
GTC	Gas Treatment Center
SGA	Smelter Grade Alumina
SEM	Scanning Electron Microscope
TEM	Transmission Electron Microscope
ICP-MS	Inductively Coupled Plasma Mass Spectrometry
PM	Particulate Matter
NEA	Norwegian Environmental Agency
SSB	Statistics Norway
FEG	Field Emission Gun
EDS	Energy Dispersive Spectroscopy
XRD	X-ray Diffraction
PSD	Particle Size Distribution
WD	Working Distance
BSE	Back Scatter Electron

List of Figures

List of Tables

Chapter 1

Introduction

To achieve the UN's climate goals by 2030, Norwegian companies have been part of the European quota system through the EEA agreement since 2008. This involves reducing greenhouse gases, as well as managing and monitoring hazardous waste and emissions of heavy metals in relation to industrial processes. Over time, the number of quotas will be reduced, which will lead to stricter requirements for Norwegian industry.

Metal production is one of Norway's largest export industries, whereas aluminium production is the largest. Norway is one of the biggest producer of primary aluminium in Europe, and every year about 1.2 million tons is produced [11]. Although Norway is one of the leading countries regarding clean industry and energy-efficiency, high demands are placed on occupational health, environmental impact and sustainable production.

During aluminium production, dust or particulate matter, is produced. This is microscopic particles of solid or liquid matter suspended in the air. Through this type of pollution heavy metals can be introduced to the human body and the environment. Heavy metals are non-biodegradable and can cause serious health problems, affecting the nervous system, liver, kidney and respiratory functions. Including this, heavy metals can damage living organisms both on land and in water by causing diseases, reduced growth and reproduction problems [12].

Today, the heavy metal emissions are measured in Norwegian aluminium plants and reported to the government on a regular basis. However, these measurements are often problematic in terms of collecting enough sample material and only represents a short period of time in a continuous production process. The knowledge about heavy metals, its behaviour in the electrolysis cell and how it ends up as fugitive emissions must increase to monitor these emissions in the best possible way.

1.1 Aim of Work

This thesis is a continuation of work performed by the author in relation to course TMT4500 specialisation project at NTNU during fall 2021. The overall goal of the specialisation project was to describe the extent of emissions and dispersion of heavy metals which originate from impurities in the raw materials to the outside environment. This was done through characterisation of dust from the aluminium electrolysis cell raw gases. Main observations obtained during this work were:

- Heavy metals were mostly found on the surface or as inclusions in carbon particles.
- Nickel and iron were often found as both sulphuric and phosphorous compounds.

For this thesis, the composition of fugitive dust emissions were investigated by means of several characterisation methods. Both airborne and settled potroom dust, mainly from Hydro Høyanger, were investigated. Mapping the particle size distribution of the dust with the purpose to investigate how heavy metals are distributed between size fractions were also performed. Sensors measuring PM emissions were placed at different elevations inside the electrolysis hall at Alcoa Mosjøen. These sensors provided continuous data for three weeks which were analysed and compared to operational data provided by the industry. The purpose of this was to identify what operational activities that accounts for the majority of the particulate emissions. To be able to monitor and control heavy metal emissions, a better understanding of the composition and activities related to enhanced PM emissions, is necessary. As a result, measures for a safer work environment can be adapted, reducing the health risks associated with heavy metals, as well as implementing measures to reduce the environmental impacts.

The project is a part of related activities in SFI Metal Production, which is a collaboration between industry, research institutes and academia with a purpose to make resource efficient metal production from a clean industry possible.

Chapter 2

Theory

This chapter will cover the relevant theoretical content necessary for a comprehensive overview and understanding of this thesis' issues and discussion. This includes the theoretical background for production of primary aluminium, followed by impurities found in the electrolysis originating mainly from anodes and alumina. Composition and particle size distribution of fugitive emissions and potroom dust are included as a literature study. Finally some theoretical background for sensor systems and sampling methods used today, as well as emission regulations are presented.

2.1 Primary Aluminium Production

Primary aluminium is produced from electrolysis of aluminium oxide (Al_2O_3), also called alumina, which is extracted from bauxite through the Bayer process. Most modern aluminium plants today is based on the pre-bake anode technology. This involves production of anodes in a separate facility where they are pre-baked and inserted to the electrolysis cell. This allows for good control regarding anode quality and emission capturing compared to the previously dominating Sødeberg technology. The composition of the raw materials used in production of anodes is analysed and must meet the standards and quality requirements to be used in anode production. During baking of anodes off-gases will occur, these gases are transported to a gas treatment center connected to the baking plant. This baking process is a continuous process that takes place in the electrolysis halls for the Sødeberg technology. As a result, the emissions of the harming off-gases are not as controlled and monitored as for the pre-bake technology. The anodes are almost completely consumed and replaced within a specific interval (2-4 weeks). The remaining parts of the anodes are called *butts* and are reused in production of new anodes.

The alumina is usually point-fed to the cell by automatic feeders at a set time interval. These feeders are built in to the superstructure of the cell. Small and rapid additions of alumina allows for good dissolution and mixing in the cryolite. Thus, minimising the risk of sludge formation and reducing alumina losses due to dusting during feeding [13].

The molten aluminium is extracted from the cell on a daily basis. This operation is called tapping and involves the liquid metal being siphoned off into a crucible using vacuum. The aluminium is then weighed and transported to an open-heart furnace in the cast house. Here, impurities are removed from the molten aluminium through skimming, fluxing gas and/or salt fluxing. Finally, the aluminium is cast into different types of forms from smaller ingots of 25 kg to large 15-25 ton aluminium slabs [13].

2.1.1 Electrolysis

Aluminium is produced through the Hall-Héroult process based on electrochemical reduction of alumina. The electrolysis cell consists of a steel box lined with carbon, which works as the cathode[1], consumable carbon anodes and a fume hood to collect and transport off-gases, see figure 2.1.

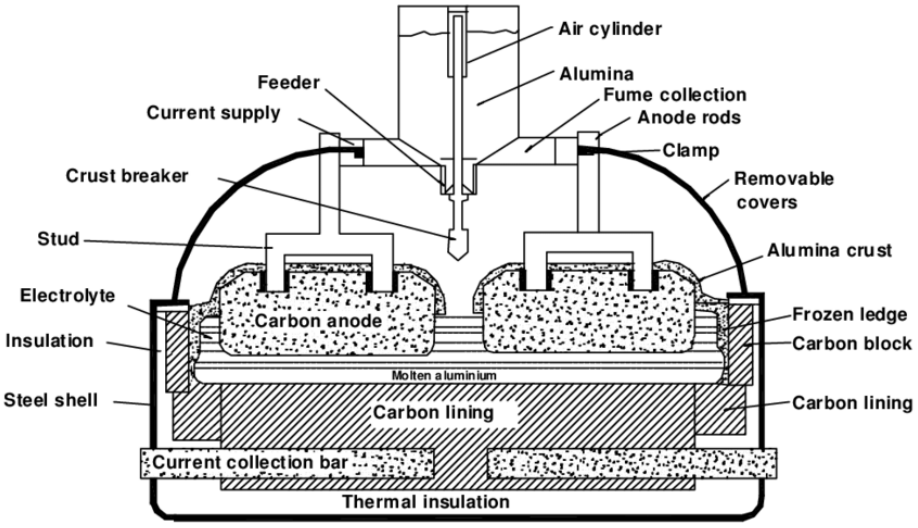

Figure 2.1: Cross section of a pre-baked Hall-Héroult electrolysis cell [1].

Aluminium can not be produced through electrolysis of alumina dissolved in water due to the high reactivity between aluminium and the protons of water. The protons (H^+) will be reduced before the Al^{3+} ions causing formation of hydrogen gas. As

[1]Electrochemically correct, the working cathode is the surface of the molten aluminum[14].

a result, the alumina is dissolved in an electrolyte consisting of cryolite (Na_3AlF_6) and different mixtures of additives, under a high intensity electrical current. The typical composition of the additives is 9-11% aluminium fluoride (AlF_3), 4-6% calcium fluoride (CaF_2) and 1.5-4% alumina. The purpose of adding AlF_3 is to reduce the melting point of the bath from 1012 °C to around 960 °C, which improves the current efficiency. The molten mixture of cryolite and additives is usually referred to as *bath* [13]. The oxygen from the dissolved alumina reacts with the carbon in the anodes as shown in Reaction 2.1.

$$C_{(s)} + 2\,O^{2-}_{(bath)} \longrightarrow CO_{2(g)} + 4\,e^- \tag{2.1}$$

The aluminium cations at the cathode are reduced to molten aluminium, as seen in the simplified Reaction 2.2.

$$Al^{3+}_{(bath)} + 3\,e^- \longrightarrow Al_{(l)} \tag{2.2}$$

In reality the aluminium is found in anion complexes, such as AlF_4^{4-} and AlF_6^{3-} before being reduced to molten aluminium [13].

The overall reaction in the Hall-Héroult process can be written as a combination of the two reactions mentioned above.

$$\frac{1}{2}\,Al_2O_{3(bath)} + \frac{3}{4}\,C_{(s)} \longrightarrow Al_{(l)} + \frac{3}{4}\,CO_{2(g)} \tag{2.3}$$

2.1.2 Carbon Anodes

Carbon anodes are made of a mixture of 60-70% calcined petroleum coke (CPC), 15-20% recycled anode butts and 12-17% coal tar pitch binder. The anodes are usually produced in a separate plant where the mixture is formed to a solid block called green anodes by vibroforming or pressing and heating from 600-800 °C. Further, the green anodes are exposed to a heat treatment with a duration of two/three weeks at 1200-1250 °C, with a purpose to carbonise the liquid pitch into solid pitch coke [15].

Carbon anodes used in aluminium production mainly consists of petroleum coke. Coke is produced as a by-product from the oil refining industry in a step called cracking. High value products like diesel fuels and gasoline are usually prioritised regarding quality, causing variations within the coke production with different impurity levels and structures [15]. Coal tar pitch consists of liquid hydrocarbon with more than 90% carbon and is distilled from the coal tar from the steel industry coke [14].

Anode grade coke

CPCs are often classified as needle coke, sponge coke and shot coke based on their structural form. Needle coke is often referred to as premium grade coke and have a low impurity and S content. Needle coke and sponge coke is similar regarding porosity, but the former has a layered or anisotropic structure. Shot coke has a granular highly isotropic texture and is usually higher in impurities [16].

Sponge coke, also referred to as anode grade coke, is the most common type of coke used in aluminium production. The porous structure allows for the coal tar pitch to penetrate CPC during mixing, resulting in a good and mechanically strong interlocked structure [17]. Sponge coke is usually classified as anisotropic like needle coke, but due to large variations some grains may have dominating isotropic structure making it more similar to shot coke [15]. Anode grade coke usually have a sulfur level between 0.5-4%, vanadium level between 50-400 ppm and nickel level between 50-250 ppm. However, the increase in aluminium production through the years have led to higher demands of CPC. This, combined with reduced availability in quality coke, results in a trend toward higher impurity levels. Thus, these impurity levels are not definite and a wider range of isotropic structured coke with higher amounts of impurities are used [16][17].

2.1.3 Gas Treatment

The off-gas produced during aluminium electrolysis mainly consists of hydrogen fluoride (HF), sulphur dioxide (SO_2) and dust, including CO_2 and CO. In the early 1970's a gas treatment system was included in the process to clean the HF gas from the emissions. In Table 2.1, a generalisation of the composition of the off-gas relative to the CO gas is attempted by Aarhaug and Ratvik [8].

Table 2.1: Generalisation of the off-gas composition relative to CO [8].

Gas	**Raw Gas**	**After Gas Treatment**
CO	1	1
CO_2	10	10
HF	0.07	0.001
SO_2	0.1	<0.1
COS	0.01	<0.01

.

The HF creation is showed in Reaction 2.4, where the hydrogen originates from moisture in the alumina.

$$\frac{1}{3}\,\mathrm{AlF}_{3(s)} + \frac{1}{2}\,\mathrm{H_2O} \longrightarrow \frac{1}{6}\,\mathrm{Al_2O_3} + \mathrm{HF}_{(g)} \tag{2.4}$$

The creation of SO_2 is expressed in Reactions 2.5 and 2.6, where carbonyl sulfide (COS) is firstly formed in the anode and then burned under the fume hood.

$$\frac{1}{3}\,\mathrm{Al_2O_{3(s)}} + \mathrm{C}_{(s)} + \mathrm{S}_{(s)} \longrightarrow \frac{2}{3}\,\mathrm{Al}_{(l)} + \mathrm{COS}_{(g)} \tag{2.5}$$

$$\mathrm{COS}_{(g)} + \frac{3}{2}\,\mathrm{O}_{2(g)} \longrightarrow \mathrm{CO}_{2(g)} + \mathrm{SO}_{2(g)} \tag{2.6}$$

The off-gas is extracted with suction and lead to the dry scrubber, or the gas treatment center (GTC). Here the gas is exposed to primary alumina, where AlF_3 is produced when reacting with HF. This process have an efficiency rate of 99% where most of the HF is cleaned from the off-gas. The secondary alumina and AlF_3 is reintroduced to the furnace, while the remaining off-gas is cleaned in the wet scrub where sea water capture SO_2 as sulphate [8]. Figure 2.2 shows an illustration of the gas treatment process and the fluoride cycle.

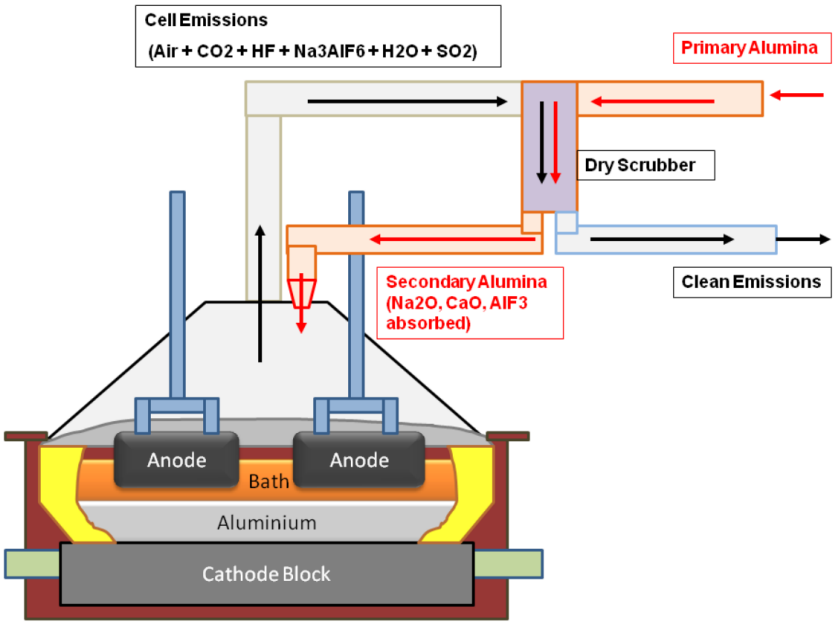

Figure 2.2: Gas treatment system and alumina route in an aluminium electrolysis cell [2].

2.1.4 Material Consumption

Producing 1 ton aluminium usually requires 420 kg carbon, 1920 kg alumina and 16 kg AlF_3. Due to other chemical reactions, losses and impurities in the system, the actual consumption will be higher than the theoretical consumption.

Carbon Consumption

From stochiometric calculations the theoretical consumption of carbon is found to be only 333 kg C/t Al, producing 1.22 kg CO_2 (see Reaction 2.3). The excess carbon consumption is mainly due to chemical reactions between anodes, oxygen and CO_2, resulting in the actual CO_2 produced being closer to 1.5 kg. The air reactivity, given in Reaction 2.7, happens when exposed carbon reacts with air. This often occurs in the pitch binder matrix and leads to physical loss of coke particles, which can cause dust generation that floats on the surface of the bath. The anodes are covered in anode cover mass (ACM), consisting of a mixture of alumina and crushed bath, to reduce and control the air reactivity [15][13].

$$O_{2(g)} + C_{(s)} \longrightarrow CO_{2(g)} \tag{2.7}$$

The CO_2 produced from the Hall-Héroult reaction further reacts with the carbon from the anodes. Reaction 2.8, also referred to as the Boudouard reaction, may occur on any surface of the anode and block the anode-electrolyte interface [15].

$$CO_{2(g)} + C_{(s)} \longrightarrow 2\,CO_{(g)} \tag{2.8}$$

Alumina Consumption

The theoretical alumina consumption is estimated to be 1889 kg/ton Al based on stochiometric calculations. The alumina provided to the cell consists of impurities and moisture in addition to Al_2O_3. The phase content of the alumina is also an important aspect regarding actual consumption. Various alumina phases will have different effects on the energy balance of the cell due to different enthalpy. Modern plants mainly uses alumina with a high content of gamma phase (γ-Al_2O_3) and low content alpha phase (α-Al_2O_3). The excess alumina usage may also be a result of dusting during transport and leaks [2].

Alumina feeding and content in the bath is also important regarding effective dissolving and reduction of losses. Too high alumina content in the bath can cause excessive amounts of undissolved alumina sludge assembling underneath the metal pad. However,

lower alumina content risks a change in the anode process, which can cause a phenomenon called the anode effect[2] [14].

Energy Consumption

The theoretical minimum energy consumption for cells operating at 95% current efficiency producing 1 kg aluminium is 6.42 kWh. However, modern aluminium smelters require an average of 13 kWh/kg Al, resulting in the actual energy efficiency to be only approximately 50%. The excess energy input is lost to surroundings as heat [13]. Some impurities are found to lower the energy efficiency such as phosphorous and vanadium [14].

In addition to Reaction 2.3, some of the metal produced at the cathode will dissolve into the electrolyte in the boundary layer at the metal-bath interface. The metal is transported to the reaction zone where it oxidizes, forming CO and Al_2O_3 when reacting with CO_2. This is called the back reaction and is given in Reaction 2.9.

$$2\,Al_{(dissolved)} + 3\,CO_{2(g)} \longrightarrow Al_2O_{3(dissolved)} + 3\,CO_{(g)} \tag{2.9}$$

The back reaction will cause a loss in current efficiency. Additions of AlF_3 as well as controlled amounts of Al_2O_3 dissolved in the melt, low electrolyte temperature, a balanced current distribution to the anodes and sufficient inter electrode distance, will all contribute to minimise the back reaction frequency [13].

Spent Pot Lining

The steel box or the pot containing the molten aluminium and bath is, as mentioned, lined with carbon materials and thermal insulation. Over time, this material becomes saturated with cryolytic bath, causing expansion, cracking and chemical degradation. Thus, the spent pot lining (SPL) needs to be replaced every 5-10 years. SPL is considered hazardous waste in most countries due to the amounts of absorbed fluorides and traces of cyanide. Aluminium plants usually produce 40-60 kg mixed waste per ton Al produced where SPL being the major contribute [13].

2.2 Impurities in the Electrolysis Cell

Impurities are always present in the commercial Hall-Héroult electrolysis cell. These are often introduced to the process through alumina feeding, anode consumption, use

[2]When an electrically insulating gas forms under the anodes causing the anode gas composition to mainly consist of CO, CF_4 and C_2F_6 where the two latter have a particularly high global warming potential and is harmful for the work environment [14].

of tools etc. Impurities can have several negative effects on the production process such as reduced current efficiency and metal quality, increased carbon consumption and harmful emissions to surrounding environment.

2.2.1 Anode Impurities

The anode grade coke used in modern plants today is, as mentioned, of varying quality. The CPCs may contain higher amounts of impurities such as heavy metals, due to mixing of different quality cokes [16]. The metals are introduced to the process through continuous anode exchange and will theoretically eventually end up in the Al melt, compromising the quality of the product [18]. In Table 2.2 some of the trace elements found in anode coke and associated concentrations are given.

Table 2.2: Representative concentration of trace elements in anode coke [ppm] [8].

Element	**Low**	**High**	**Element**	**Low**	**High**
Fe	50	350	**Cu**	20	50
Ni	50	500	**Cr**	1	50
V	30	500	**P**	5	30
Pb	3	10	**S %wt**	0.5	5
Mo	10	20	**Na**	20	140
Al	20	250	**K**	10	20
Zn	2	150	**Mg**	50	200

Various concentrations of sulfur is always present in anodes used in primary aluminium production. The sulfur can be found as a part of the carbon lattice, attached to chains on the surface of clustered molecules or on surfaces and pores bound by capillary condensation, adsorption, or chemisorption [15]. Sulfur is considered to reduce the CO_2 reactivity which is beneficial for the anode performance. As a result, 1.5-2 wt% S is usually present in anodes [8]. However, V, Ni and Fe are found to have a negative impact on the CO_2 reactivity and may act as catalysts. Traces of Fe and Ni in the anode show enhanced air reactivity and increased Boudouard reaction. Higher vanadium content in the coke will also lead to an increase in the Boudouard reaction [19].

A study done by Jahrsengene et al. [20] showed that V, Ni and Fe are most likely present in high-sulfur coke as hexagonal sulfides rather than as metal porphyrins. An Extended X-ray Absorption Fine Structure analysis (EXAFS) was performed to determine the identity of V, Ni and Fe impurities by comparing the metal structures with known crystal structures. V was found mainly as V_3S_4, Ni as hexagonal NiS and

Fe as hexagonal FeS. From the experiments the author found that the metal was well spread in the carbon matrix, and not present as large crystalline inclusions.

As mentioned, the increase in aluminium production in the world will lead to reduced anode quality and increased impurity concentration [16]. Including less dense coke materials, the quality change will have an impact on the anode performance in the electrolysis cell. Anodes with more porous structure will be more exposed to air and CO_2 reactivity which will also be affected by increased metal impurities [13].

2.2.2 Secondary Alumina

The primary alumina used in aluminium production, also referred to as smelter grade alumina (SGA), requires low impurity levels to retain the bath chemistry [13]. Typical trace elements found in SGA is given in Table 2.3. However, during dry scrubbing other impurities and particles from the off-gas will be mixed with the secondary alumina and AlF_3. Thus, the secondary alumina will have a generally higher impurity level than the SGA.

Table 2.3: Typical impurity content in smelter grade alumina [%wt] [8].

Impurity	**%wt**	**Impurity**	**%wt**
$\mathbf{SiO_2}$	0.007-0.02	$\mathbf{P_2O_5}$	0.0004-0.0011
$\mathbf{Fe_2O_3}$	0.008-0.022	$\mathbf{Cr_2O_3}$	0.002
$\mathbf{TiO_2}$	0.002-0.008	$\mathbf{Ga_2O_3}$	0.007-0.008
CaO	0.003-0.035	$\mathbf{Na_2O}$	0.3-0.45
ZnO	0.001-0.011	$\mathbf{Li_2O}$	0-0.001
$\mathbf{V_2O_5}$	0.0012-0.004	$\mathbf{K_2O}$	0.01-0.08

Impurities in the secondary alumina is found to accumulate in the finer alumina fractions. Since the system between the cells and scrubber can be considered a closed loop, the possibility to purify the secondary alumina have been studied by Kalyavina et al. [21], amongst others.

2.2.3 Impurity Cycling

All though recycling of anodes and using secondary alumina from dry scrubbing is both economical and environmental beneficial, it can lead to some challenges. Impurity cycling is an unwanted and negative effect caused by reusing the raw materials. During gas treatment, all particulate matter will theoretically be transported back to the cell with the secondary alumina. Impurities that do not escape as fugitive emissions will therefore eventually accumulate in the bath or oxidise in the aluminium melt [8].

Sulfur

Sulfur is mainly introduced to the process as coke impurity. It is believed to reduce the Boudouard reaction and is therefore wanted in controlled amounts [20]. However, the sulfur emissions need to be closely monitored due to environmental impacts, as a result governmental restrictions are often imposed. Through recycling of anodes and secondary alumina, sulfur is continuously introduced to the process. This, in combination with gradually higher impurity in the raw materials, can eventually lead to accumulation above wanted concentrations in the process [8].

Phosphorous

Phosphorous in the cell mostly originates from the alumina. With the recycling of increased amounts of impurities with the secondary alumina, more phosphorous ends up in the electrolyte and molten aluminium than in the past. This element will in low amounts in aluminium reduce the corrosion resistance and increase the brittleness. Phosphorous can appear in different valence states from -3 to +5. Even for low amounts of phosphorous, this can cause a reduced current efficiency [22]. Sterten et al. [3] reported a linear decrease in current efficiency in the range 0.1-0.7% per 0.01 wt% impurity cations present in the electrolyte for some elements plotted in Figure 2.3.

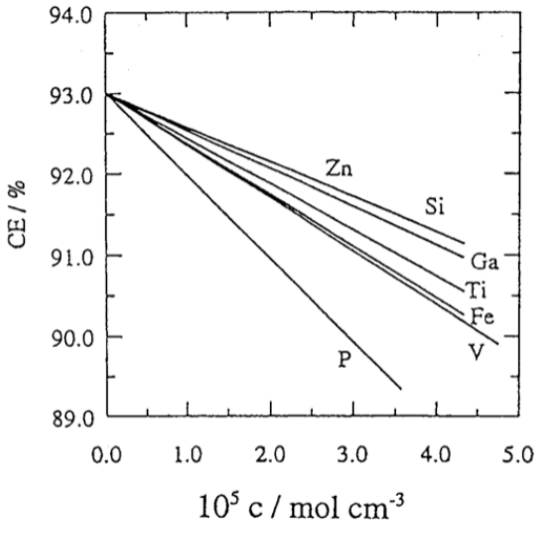

Figure 2.3: Current efficiency as a function of the concentration of impurities [mol/cm^3] [3].

Previous study performed by the author also found traces of phosphor in combination with metal impurities when analysing small carbon particles from the off-gas. This corresponds well with a study performed by Haugland et al. [22] where the behaviour of phosphorus impurities in aluminium electrolysis cells were studied. The authors found that dissolved P species can also be reduced by impurities in the bath, where small carbon particles may act as nucleation sites. They also found that loss of phosphorous from the cell was due to evaporation of gaseous elemental phosphorous and phosphorus attached to carbon dust.

Fluorides

Fluorides are the main element recycled in the system with the secondary alumina, considering the dry scrubbing system was invented to clean the off-gas for damaging HF gas and transport the fluorides back to the cell. Most of the fluoride losses is due to fugitive emissions in the form of particulates or gases. $NaAlF_4$ is the main fluoride containing compound lost to potroom emissions. This compound is evaporated bath and escapes the cell during operational processes where open bath is exposed [8].

Metals

Work performed related to PhD thesis by H. Gaertner [23] found that by the use of an EPA standard cyclone operated with a cut-size of about 11µm and below, approximately 2.4 wt% of metallic impurities was be obtained. This corresponds to roughly 4-5 kg dust per ton Al produced. The author found that by reducing the cut size, the metal quality and current efficiency would improve as a result of certain elements (Ni, Fe, P, V and Ti) and carbon dust no longer would be recycled in the cell.

2.3 Fugitive Emissions and Potroom Dust

During production of aluminium a large amount of dust will occur. The dust usually originates from daily operational processes such as anode change, anode covering processes and metal tapping, but also from leaks of alumina or ACM and condensed bath. Several studies have been conducted with a purpose to characterize and determine composition, sources and nature of potroom dust and fugitive emissions.

Fugitive dust emissions are here defined as the potline emissions of particulate material that are not captured by the fumehood and transported to GTC. These emissions are either airborne or settled in the electrolysis hall, where the former will eventually end up as settled dust or emitted to the environment.

2.3.1 Composition and Classification

Höflich et al. [9] collected and characterised potroom particles from two aluminium smelters (one with Sødeberg and one with prebake technology) with aerodynamic diameters between 0.18 µm and 10 µm with a purpose to asses health effects from inhaling. Sampling was executed by means of five-stage cascade impactors in breathing zones of workers close to the cell. From this study relative abundances and 95% interval of different particle groups were found and listed in table 2.4. The carbon rich particles detected were mostly found as soot agglomerates. However, larger pieces of carbon were also observed which were most likely splinters from anodes.

Table 2.4: Relative abundances [%] and 95% confidence intervals (in parenthesis) of particle groups [9].

Particle group	**Prebake (1006 particles)**
Aluminium oxides	8.0 (5.0-12.4)
Cryolite	11.4 (7.8-16.4)
Aluminium oxides- cryolite mixtures	64.6 (58.0-70.8)
Soot	6.6 (3.9-10.7)
Silicates	1.3 (0.4-3.9)
Sea Salt	4.5 (2.4-8.2)
Brass (sample holder)	1.8 (0.7-4.6)
Fe/Ti oxides	0.8 (0.2-3.2)
Calcium carbonate	0.1 (0.005-2.0)
Silicon	0.1 (0.005-2.0)
Other particles	0.9 (0.2-3.3)

Wong et al. [24] performed a study on the composition of the dust as a function of its material source. The authors analysed and compared the composition of airborne and settled dust from four different smelters. By means of X-ray diffraction, the major component phases of dust unregarding where the sample was collected showed a composition of:

- Bath related compounds: cryolite, chiolite ($Na_5Al_3F_{14}$) and calcium chiolite ($Na_2Ca_3Al_2F_{14}$)
- Transitional aluminas (γ-, γ' and θ-Al_2O_3)
- α-Al_2O_3 and graphitic carbon

As a part of TMT4500 Specialisation Project [7] the current author characterised dust from the GTC, i.e not fugitive emissions. The samples were taken from the gas duct

from an aluminium smelter in Norway, and studied with SEM and TEM, amongst others. In addition to finding phosphorous and sulfur in combination with metal impurities as inclusions in small carbon particles, heavy metals were also often found in combination with bath fumes.

From an ICP-MS analysis performed during this project the chemical composition of the dust were analysed. The average of some of the most relevant elements and associated error are given in Table 2.5.

Table 2.5: Average measurements of some elements included associated standard error [mg/kg] [7].

Element	**Average**	**Error**
Al	318333	±159167
Ca	4950	±2475
Fe	2033	±1017
Pb	177	±88
Ni	4633	±2317
P	500	±250
K	1097	±548
Na	64500	±32250
S	11783	±5892
Ti	73	±37
V	263	±132

A study performed by Clos et al. [25] found that off gas particles from aluminium production consists of four distinguishable particle compositions. These were large unstructured alumina particles, small spherical bath condensates consisting of Al-Na-F phases, smaller particles consisting of S and Ni and scarce C particles.

2.3.2 Particle Size Distribution

Wong et al. [4] also conducted a study where particle size distribution and composition were examined. Sampling of dust at different heights within the potroom showed that coarser dust such as anode cover material and feed alumina tend to settle at surfaces (floor, cell exterior, different structures). Particles were found to decrease in size at increasing height and bath fumes were the dominating contributor to the fines/ultrafines found at roof level. Figure 2.4 show how particle terminal velocity ($v_{particle}$) varies as a function of particle size. Due to gravitational settings, a particle

settles when the upward air flow velocity (v_{air}) < $v_{particle}$ and remain airborne when $v_{air} > v_{particle}$.

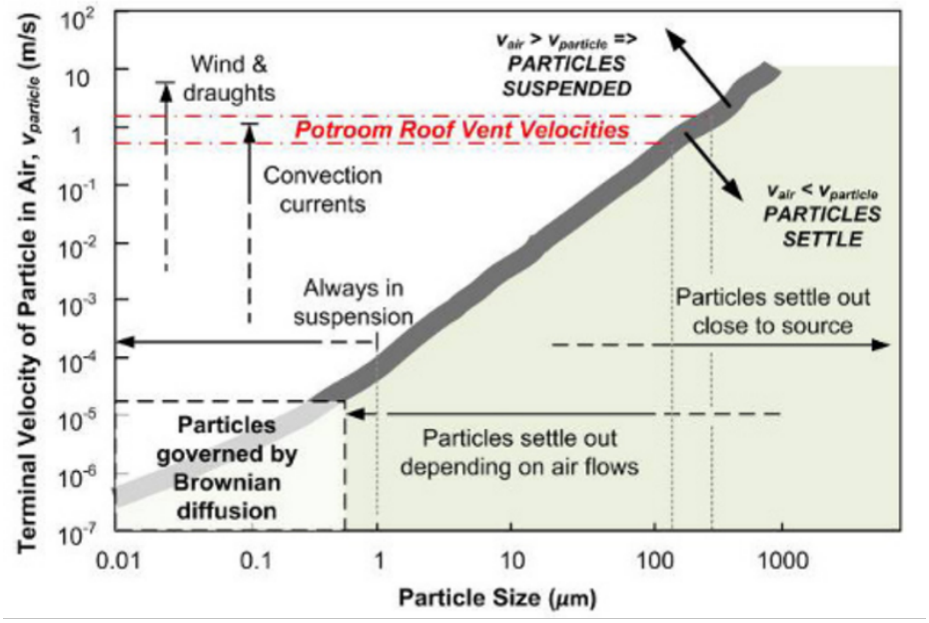

Figure 2.4: Terminal velocity of particle in air [m/s] as a function of particle size [µm] [4].

A 24 hour case study examining sources of fugitive dust emissions of roof and operating floor level was also performed by Wong et al. [26] The observations from this study implied that anode change was the main contributor to fugitive roof emissions followed by metal tapping, loading of cover material and dust sweeping. The floor level dust emissions were mainly related to the same operations as roof level, but included housekeeping by operators, movement by anode tending vehicles and PTM cranes.

Weather conditions may also effect periodic high fugitive roof emissions. During strong gusts of wind, the settled dust will swirl up and be transported around the hall and out through the roof. This is one of the main reasons sampling of fugitive emissions and dust is so challenging in an aluminium plant.

2.3.3 Sources and Formation of Potroom Dust

From the mentioned various studies above, it is fair to say that the likely major sources of potroom dust are different forms of alumina, pot fumes and bath-related compounds.

Pot fumes can be defined as particulate material generated inside the pot. This is usually extracted together with the off-gases and transported to the GTC. In addition to being a critical source for potroom dust, pot fumes can form a hard gray scale on the inside of the gas extraction system which has caused the industry a lot of challenges. Pot fumes can carry alumina, ACM and carbon, in addition to condensed bath and are highly enriched with fluorides and sulfur, as well as other impurities such as iron and phosphorous. Pot fumes are recognised to be of very fine particles and at least 50% of the particles are <20 µm [27]. Thus, the pot fume have a tendency to escape through the roof due to high mobility. However, this is only relevant when the pot fume escapes the cell and gas extraction system. This usually occurs in relation with operational processes where it is necessary to remove fume hoods or doors covering the pot. Figure 2.5 illustrates how pot fumes escape during anode change [5].

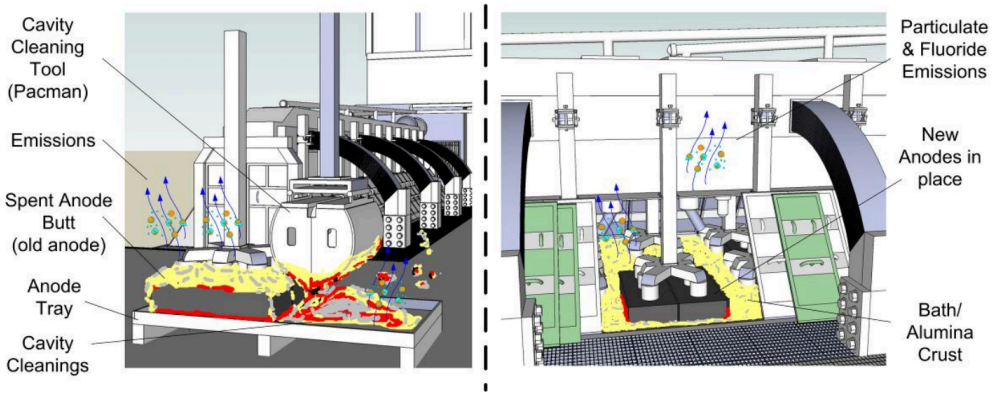

Figure 2.5: Illustrations of pot fume emission during different operational processes such as removal of butt and cavity cleaning (left) and inserting of new anodes (right) [5].

Alumina is as mentioned a large contributor to potroom dust. Alumina is primarily present in the potroom as feed alumina and as a part of ACM. Hyland et al. [27] summarise formation of alumina based dust from listed sources:

- Leaks and spillages related to delivery, transportation and storage
- Alumina carried out with rising hot pot fume during feeding to the cell
- Leaks and spillages during delivery, transportation and cell tending operations of ACM

Spilling of bath related compounds such as ACM also contribute a great deal to the total potroom dust generation, in addition to the vaporised bath carried out with the pot fume. This dust mainly consists of alumina and crushed bath and usually consists of coarse particles compared to the volatile pot fume. As a result, it is more likely that this type of dust settles on surfaces and potroom floor rather than escaping through the roof [5].

2.4 Sensor Systems and Sampling Devices

Dust, or airborne particulate matter (PM), is considered a health- and environmental concern regarding metal production. Close qualitative and quantitative monitoring and measuring of PM is therefore an important subject. There are several methods for sampling of this kind, such as filter sampling, optical sensors or light absorption or extinction methods [10].

Exposure to particles of different proportions is often linked to health problems such as asthma, decreased lung function and respiratory problems, amongst other. PM is often distinguished based on particle size or more precisely, particle diameter. PM_{10} generally includes particles with a diameter of 10 µm or smaller. These are inhalable particles that can get deep into the lungs and may in some cases even get into the bloodstream, causing damaging health effects. $PM_{2.5}$ includes particles with a diameter of 2.5 µm and smaller, also known as fine particles. These pose the greatest risk to health when inhaled [28].

2.4.1 Current Sampling and Monitoring Procedures

The most common procedure for monitoring fugitive emissions is by the use of filter systems. There are different setups for this type of monitoring, but nevertheless this usually includes tubes and pumps. These allow the air from the potroom to be lead through a filter which collects the dust. This procedure usually needs some time to gather enough dust for different analyses, but will provide accurate monitoring of its content. However, this method will only give an average over the measured period and does not consider variations within production processes, weather conditions and different size fractions of the dust. Other dust measuring techniques are given in Table 2.6, adapted from [10].

Table 2.6: Different dust measuring methods, adapted from [10].

Type	Description
Nephelometer	Measure scattered light at an angle for all particles in a chamber
Optical particle counters	Measures scattered light by each individual particle in a flow
Optical transmission device	Measures forward light scattering or opacity from a light source passing over a longer distance
Cascade impactors	Separates particles based on their inertia

Myklebust et al. [6] investigated the reliability and functionality of a system based on affordable (<200$) microsensors for monitoring fugitive emissions from primary aluminium production. The system was setup to measure PM_{10} and $PM_{2.5}$, temperature and relative humidity. From this study the authors found that the microsensors gave reliable data that correlated with operational processes such as different particle size fractions related to different operational activities. In Figure 2.6 a scatter plot of concentration $PM_{2.5}$ as a function of PM_{10} - $PM_{2.5}$ for specific time periods related to a specific operational process. For the time period 10:25-11:00 during anode change, higher concentrations of $PM_{2.5}$ were detected than during the two other processes. Both the processes performed during the time period 14:45-15:15 and 20:15-21:00 involved covering with ACM. The emissions detected during these operations were found to have a higher concentration of larger particles.

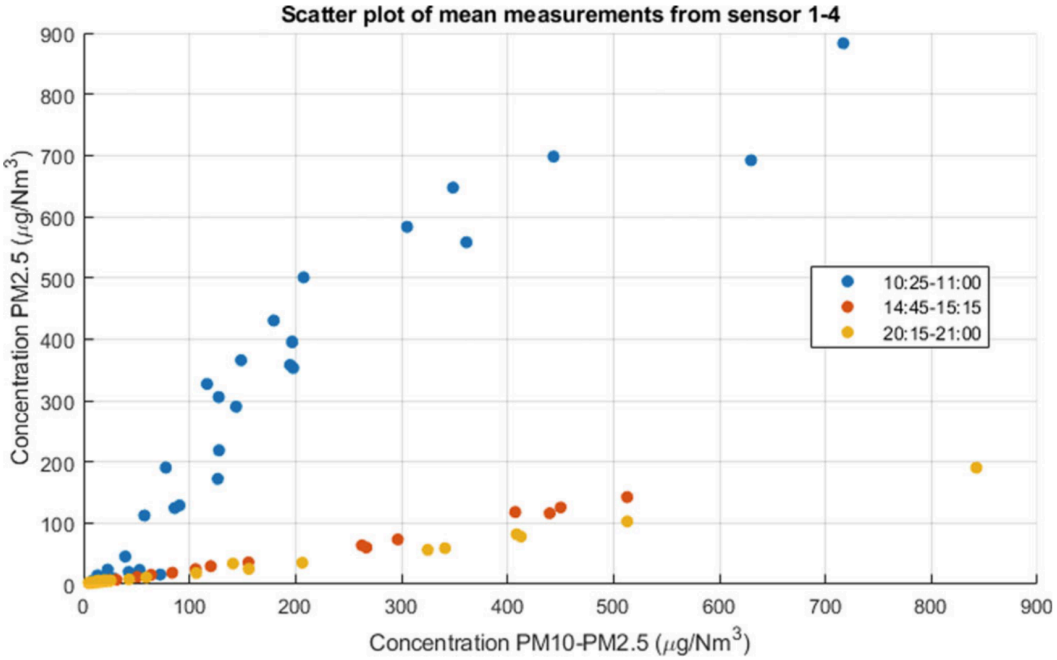

Figure 2.6: Mean values of PM10 and PM 2.5, each color corresponds to a specific process performed in a time period, adapted from [6].

Alcoa Mosjøen

To ensure that measurements are performed according to recognized measurement principles, Alcoa uses a procedure based on Norwegian standards NS 4861, NS 4863 and SINTEF report STF21 F898012. This procedure includes measurements of dust and gas from the electrolysis halls and is adapted to the use of YH pumps for collecting gas samples. The pumps are rechargeable and contain cellulose sheets impregnated with 10% KOH solution containing 50% ethanol. A flow meter is used to measure the pump capacity. The sampling lasts for about 24 hours or 1440 minutes, before the samples are brought to the lab for analyses.

For the heavy metal sampling, Gast vacuum pump with 589/3 whatman filters (150 mm diameter) and neoprene hose and probe, is used. Here, the heavy metal concentration in dust is measured through measuring campaigns. The heavy metal emission is calculated by combining the annual dust emission with the heavy metal

profile for the emission source. Calculations are based on the assumption that the heavy metals are only bound to the dust particles. For the analyses, at least 250 mg dust needs to be collected which usually takes several days.

Hydro Høyanger

Hydro's plant in Høyanger have an unique rooftop design compared to other Norwegian aluminium smelters. Distributed over the roof, are 18 chimneys through which the fugitive emissions from the electrolysis hall passes. In every other chimney there are fixed mounted probes, making it nine probes in total. During sampling a so called 'environmental fan' is turned on, which extracts dust and gas from all the nine probes at once. At the sampling point a multi-probe consisting of eight probes is mounted and connected to their respective filters. The sampling takes place for seven days, gathering dust at one filter each day. Solenoid valves ensure that the sample changes to the next day after 24 hours.

Heavy metal sampling is required to be performed 4 times a year from the electrolysis. Filter holders are prepared as usual with a support filter and a dust filter. Also here a minimum of 250 mg dust is required, resulting in sampling for about two-three weeks. During heavy metal sampling, the valves are fully opened causing the gas velocity to be whatever the vacuum pump can handle. This will give as much dust as possible. Also here the heavy metal emission is calculated by combining the annual dust emission with the heavy metal profile for the emission source.

2.4.2 Emission Regulations

The Norwegian Environment Agency (NEA) is a state executive agency with the main purpose of reducing greenhouse gas emissions, protect Norwegian nature and prevent pollution. Through control acts and regulations NEA can set frameworks for companies in terms of emissions and pollution, but also production volume as this is often related [29].

Together with Statistics Norway (SSB), NEA collect and calculate emission data of some important components on annual basis. From this database the total emissions of some heavy metals from all land based industry during the year 2020 is listed in Table 2.7 and compared to the total emissions from the industry of Primary Aluminium Production. Companies qualifying for this industry according to this database are listed below:

- Hydro Aluminium
  - Høyanger
  - Karmøy
  - Sunndal
  - Årdal metallverk
- Hydro Vigelands brug AS
- Alcoa
  - Lista
  - Mosjøen
- Metallco Aluminium AS
- Sør-Norge Aluminium
- Herøya Industripark

Table 2.7: Heavy metal emissions from land based industries and emissions from the industry of primary aluminium production in 2020 [kg] [7]

Metal	Land based industry	Primary Al production industry	Ratio from Al industry [%]
Ni	10143,34	2880,33	28,40
Pb	2410,5	260,39	10,80
V	732,53	95,65	13,06
Cd	140,57	26,13	18,59
Zn	22158,24	897,64	4,05

The sector *Land Based Industry* includes most of the industrial activities on land of a certain size [30].

Chapter 3

Experimental Method

This chapter includes the experimental observations and methods used to achieve the desired results. A description of the materials investigated, how and when it was collected and what type of analyses that were performed are included. The experimental work is divided into two main methodologies. This includes collection and analysing of data as well as different characterisational methods such as SEM, BET, XRD, particle size distribution by laser scattering and ICP-MS. Finally a short description and theoretical background of the equipment used for these examinations are also included in this chapter.

3.1 Materials

The materials examined in this thesis consists of dust from fugitive emissions in the potroom of two aluminium smelter, Hydro Høyanger and Alcoa Mosjøen. In addition to this, results from the authors previous work are included and compared to results obtained through this thesis. The main origin of this type of dust is explained in the previous chapter (Chapter 2). Collection of the dust is based on different methodologies and a full overview of sample, origin and performed analyses is given in Table 3.1. Some of the samples are collected by contacts in the industry and sent to the author, while other samples are collected by the author. Samples categorised as settled dust are collected by filling a sample holder with dust from different surfaces in the electrolysis hall. The samples categorised as airborne are either collected by filter or by scraping of dust from inside the chimney. The latter only applies to Hydro Høyanger as Alcoa Mosjøen have a different design of rooftop outlet.

In addition to this, old samples collected with a SINTEF sampler system in 2008 at Høyanger were analysed. These samplers are based on filter systems and collected

airborne dust in the fan room above the electrolysis hall. In addition to dust collection and analyses, data of PM emissions at different size fractions were collected by the use of small sensors. This data were analysed by means of digital platforms such as MATLAB and Excel. Data regarding industrial methods and operational events were provided by the industry.

Table 3.1: Overview of samples and analysis performed

Sample	ICP-MS	BET/BJH	SEM	XRD	PSD	About sample
1	x	x	x			Airborne Høyanger, sent from industry
2	x		x			Airborne Høyanger, sent from industry
3	x	x	x	x	x	Settled Høyanger, sent from industry
4	x					SINTEF samplers Høyanger 2008
5	x					SINTEF samplers Høyanger 2008
6	x					SINTEF samplers Høyanger 2008
7	x					SINTEF samplers Høyanger 2008
8	x	x		x	x	Airborne Høyanger, sampled by author 23.03.22
9	x		x	x	x	Airborne Høyanger, sampled by author 23.03.22
10	x				x	Airborne Høyanger, sampled by author 23.03.22
11	x	x		x	x	Settled Høyanger, sampled by author 23.03.22
13			x			Filters Høyanger, sent from industry
14					x	Settled Mosjøen, sampled by author 25.04.22

3.2 Characterisation

In this thesis, dust samples were characterised by means of a Micromeritics 3Flex 3500 Surface Area and Porosity Analyzer with N_2 as adsorptive. A Zeiss ULTRA 55 scanning electron microscope (SEM) with a field emission gun (FEG) was also used with chemical composition analyses by means of energy dispersive spectroscopy (EDS). Including this, inductively coupled plasma mass spectrometry (ICP-MS) analysis was executed by external lab ALS Scandinavia in Luleå, Sweden. Bruker D8 A25 DaVinci X-ray diffractometer was used for x-ray diffraction (XRD) analyses. Lastly, Laser Scattering Particle Size Distribution (PSD) Analyzer Horiba LA-960 was used to attempt a mapping of particle size distribution.

3.2.1 BET and BJH

The method of Brunauer, Emmet and Teller (BET) is used for determination of specific surface area. Surface area helps determine such things as how solids burn, dissolve, and react with other materials. This is done by degassing the sample, which involves preheating the sample by applying some combination of heat, vacuum and/or flowing gas to remove adsorbed contaminants such as water and CO_2. The sample is then cooled to cryogenic temperature (77K) and an adsorptive, usually nitrogen, is dosed

to the sample in controlled increments. Between each dose the pressure equilibrate and the quantity adsorbed is calculated. This amount defines an adsorption isotherm, from which the quantity of gas required to form a monolayer over the external surface of the solid, is determined. With the area covered by each adsorbed gas molecule known, the surface area can be calculated.

The samples were placed in a sample holder and weighed before placed in a degasser over night. Here, the samples were heated up to 250°C before cooling down the samples to room temperature in an atmosphere of nitrogen. The heating steps are given in Table 3.2. Further, the samples were weighed again before being placed in the 3Flex 3500. Nitrogen were used as adsorptive and the analysis bath temperature were around 78K (-195°C).

Table 3.2: Degassing steps in sample preparation.

Sample prep: Stage	**Temperature (°C)**	**Ramp Rate (°C/min)**	**Time (min)**
1	30	10	10
2	90	10	60
3	250	10	820
4	25	10	60

The Barret-Joyner-Haleda (BJH) method is used for determination of porosity, pore sizes and pore distributions. Surface area determinations involve creating the conditions required to adsorb an average monolayer of molecules onto a sample. By extending this process so the gas is allowed to condense in the pores, the samples fine pore structure can be evaluated. The gas will condense in the pores with the smallest dimensions first, as the pressure increases. The pressure is increased until saturation is reached, when all pores are filled with liquid. Further, the adsorptive gas pressure is reduced incrementally, evaporating the condensed gas from the system. Evaluation of the adsorption and desorption branches of these isotherms and the hysteresis between them reveals information about the size, volume, and area of pores.

3.2.2 SEM

The dust were placed on carbon tape for good conducting effects. In addition to this, the samples were coated with carbon with the purpose of giving the best possible results regarding imaging and analyses. The primary electron energy was set to 15 KeV with a working distance (WD) of 10 mm, however, some of the SEM images will show a WD at 15 mm. This was due to a malfunction in the stage control and the displayed WD was not correlated with the actual WD. The purpose of examining

the samples in SEM was to get an adequate picture of the morphology and chemical composition as well as variation in particle size and shape. By the use of imaging with backscatter electrons (BSE), elements with different atomic numbers were possible to distinguish. The heavier elements have bigger nuclei and can therefore deflect incident electrons more strongly than lighter elements. As a result, heavier elements appear brighter than lighter elements. This made it possible to locate potential heavy metals and perform mapping analyses by the use of EDS, in these areas.

The SEM was also used to get an indication of the average particle size, especially for the carbon particles. This was done by manually measuring particles with a measuring device in the smartSEM software and calculating an average based on approximately 100 measurements. An example of how this procedure would look like is given in Figure 3.1. For these analyses the dust was placed on conducting Cu-tape to easily distinguish the carbon particles from the tape.

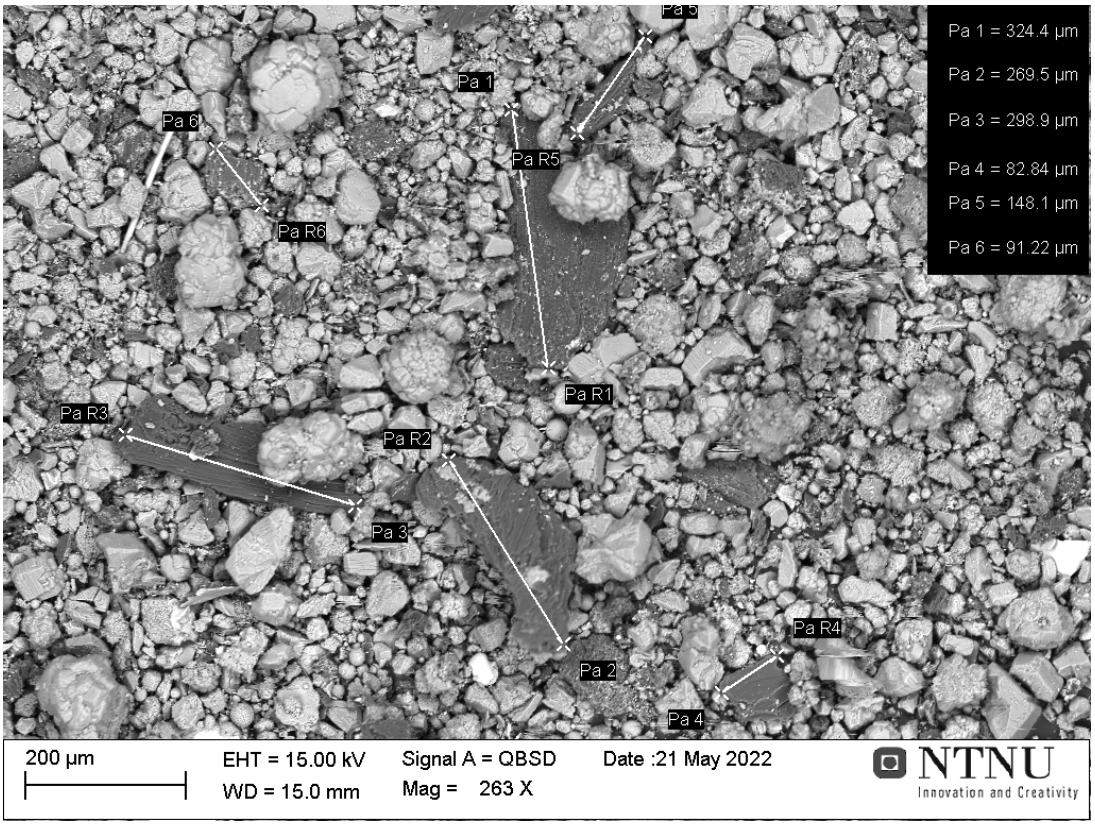

Figure 3.1: Example of how manually carbon particle size measurements were performed in SEM.

3.2.3 XRD

The DaVinci1 was operated with CuKα and LynxEye SuperSpeed detector with 40 kV and 40 mA. Scans were measured over a 2θ range from 10-90°for 60 min. EVA analysis software was used to identify different crystalline phases in four samples, two settled dust and two airborne dust samples. XRD is used to identify the different crystalline phases in the sample based on the diffraction pattern.

3.2.4 Particle Size Distribution

6 samples were analysed in a PSD analyser. For each sample, at least three analyses were performed. The Horiba LA-960 can measure particle sizes between 0.1-5000 µm and is based on laser diffraction technology. The analyser is able to measure both dry and dispersed powder where in this case, the dry measurement technology was used. The reason for this was to be able to measure water-soluble particles. The sample is placed on a vibratory feeder before falling into the dispersion chamber. There, the sample flows through a venturi nozzle where any agglomerates are dispersed using 360° compressed air. The geometry of the dispersion nozzle is designed so that the air is accelerated to supersonic velocity. The now-dispersed powder flows into the measurement zone where powder is measured and then evacuated though the bottom of the system automatically by vacuum.

3.2.5 ICP-MS

The samples were sent to the lab ALS Scandinavia AB in Sweden for Inductively coupled plasma mass spectrometry (ICP-MS). ICP-MS is an elemental analysis technology which is able to detect very small traces of heavy metals in small amounts of dust samples. 12 samples were prepared and sent for a semiquantitative screening of elements in industrial material.

3.3 Sensors and Data Collection

Sensirion SPS30 is an optical PM sensor of the type nephelometer, based on laser scattering technology. The sensors provide information about:

- Mass concentration: $PM_{1.0}$, $PM_{2.5}$, PM_4 and PM_{10}
- Number concentration: $PM_{0.5}$, $PM_{1.0}$, $PM_{2.5}$, PM_4 and PM_{10}
- Temperature

- Relative humidity

The system consist of three sensors connected to a low-cost, small sized computer called Raspberry pi, visualised in Figure 3.2. This system collects data which can be accessed by an external computer, giving continuous measurements of particulate emissions.

Figure 3.2: Sensor system and raspberry pi, where one sensor is connected marked 1BF5039.

Three systems were placed at different places and elevations in the electrolysis hall (hall 3) at Alcoa, Mosjøen. Figure 3.3 illustrates the location of the three different systems. One of the sensor systems was placed at floor level, while the other two were placed at roof level near a rooftop outlet. For each system there are three sensors.

DH1 and DH2 were placed at roof-level on each side of the drip catcher. One sensor was placed above the drip catcher while two sensors are lowered down in the hall, for each system. DH3 was placed at floor-level where all three sensors are at similar heights. The sensors provide information about variation in PM emissions at a specific period of time. By comparing this to documented operational events in the hall on furnaces close to the sensors, it is possible to get an indication of which processes lead to increased emissions.

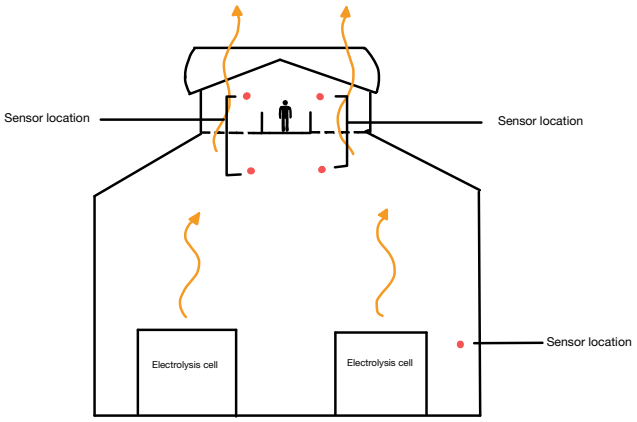

Figure 3.3: Location of the sensors marked as red dots DH1 and DH2 is located at roof-level, DH3 is located at floor-level.

In Figure 3.4 an overview of sensor location and furnace number closest to the sensors is given. DH1 and DH2 are as mentioned placed at roof level, while DH3 is placed at floor level.

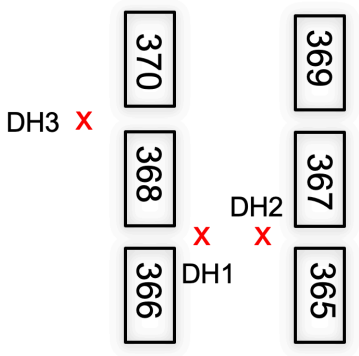

Figure 3.4: Location of the sensors in connection with cell row and furnace number.

Chapter 4

Results

This chapter concerns the results achieved through different experiments and practical research. The practical research includes data collection and analysis from small sensors handled by the author as well as documentation and data collected by the industry. The study includes various characterisation methods such as BET, SEM, XRD and ICP-MS.

4.1 Characterisation

Different characterisation methods were used with the intention of mapping the composition and variations in dust from primary aluminum production that occur in different areas of the smelter and in relation to different processes.

4.1.1 BET

4 samples were analysed by means of the BET method with the purpose to determine specific surface area. Full analyses are found in Appendix A.

Nitrogen adsorption and desorption isotherms are given in Figure 4.1. The isotherms are similar to the type II isotherms, common for non-porous adsorbents or adsorbents having relatively large pores. A small hysteresis is observed for all the samples with a step down of the desorption branch at p/p° 0.45-0.50. The isotherms for sample 3 and 11 show a steady increase in the intermediate zone before a rapid increase in the final zone. This behaviour is common for mesoporous and macroporous materials which usually have pores in the size range 2-50 nm. The same trend can be observed in isotherms for sample 1 and 8, only with approximately half the adsorbed quantity.

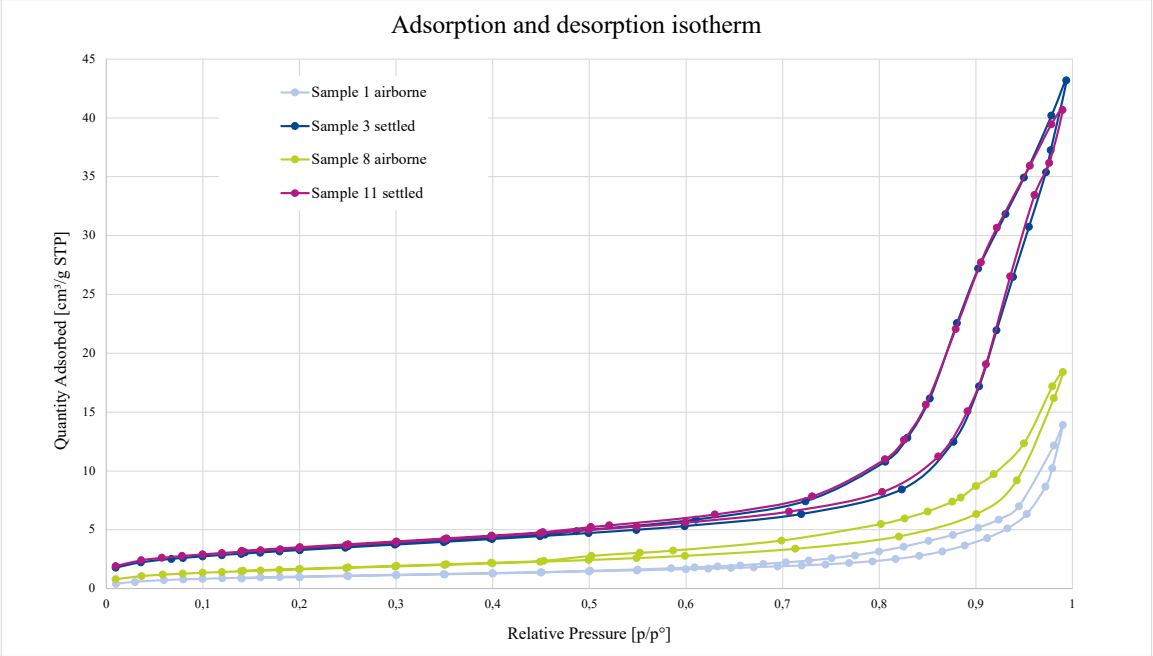

Figure 4.1: Isotherms for sample 1, 3, 8 and 11 showing quantity of nitrogen adsorbed [cm^3/g STP] at varying relative pressures [$p/p°$].

Table 4.1 show the measured surface area for airborne and settled dust. These results show a lower surface area for airborne dust at approximately 3.7 and 6.0 m^2/g compared to settled dust at approximately 11.8 and 12.4 m^2/g. Similar measurements are performed on the primary alumina by Hydro Høyanger on every alumina delivery. An average based on measurements from January 2021-April 2022 of this alumina give a surface area of approximately 76 m^2/g. Including surface area, Table 4.1 present pore volume by single point desorption, where total pore volume of pores with a diameter less than 200 nm are measured at $p/p° = 0{,}989971592$. This indicate smaller pore volume in airborne dust, which correlates well with the surface area. Pore size is given as adsorption average pore diameter and is found between 19 and 23 nm for the samples. This agrees with the range of mesoporous and macroporous materials.

Table 4.1: Surface area, pore size and volume for airborne and settled dust

	Airborne		Settled	
Sample number	**1**	**8**	**3**	**11**
Surface area [m^2/g]	3,733	6,014	11,746	12,369
Pore volume [cm^3/g]	0,022	0,029	0,066	0,063
Pore size [nm]	23,095	19,013	22,112	20,417

4.1.2 SEM

The following section presents results and observations obtained from SEM analyses. This includes variation in morphology, chemical composition and particle size for airborne and settled dust, as well as dust collected by filter.

Morphology

In Figure 4.2, filter, airborne and settled dust from Hydro Høyanger are imaged with a magnification of 100x. A clear difference in structure is observed, where the settled dust is found to be coarser than the filter and airborne dust. The airborne dust have areas with fine particles as the filtered dust, but with occasional larger particles. Larger versions of all images included in this subsection are included in Appendix B.

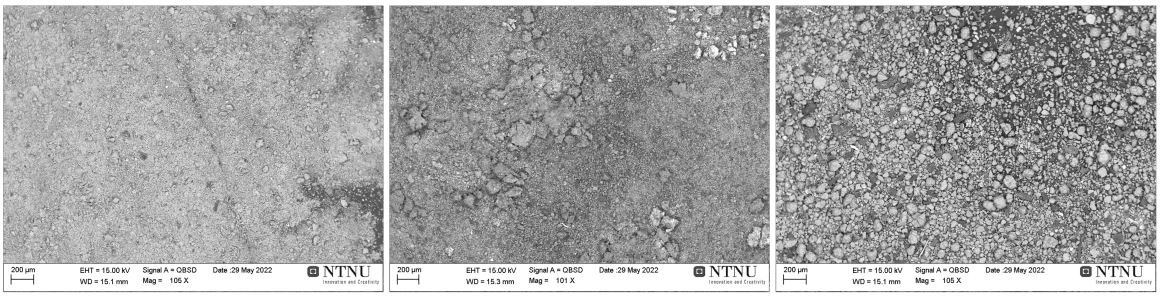

Figure 4.2: From left: Filter, airborne and settled dust with a magnification of 100x.

In Figure 4.3, morphology of filter, airborne and settled dust are given with a magnification of 500x. A gradually increase in grain size from filter to airborne and again to settled dust is observed. The dust collected by filter seem to have a fume like structure, compared to the settled dust with large separate particles.

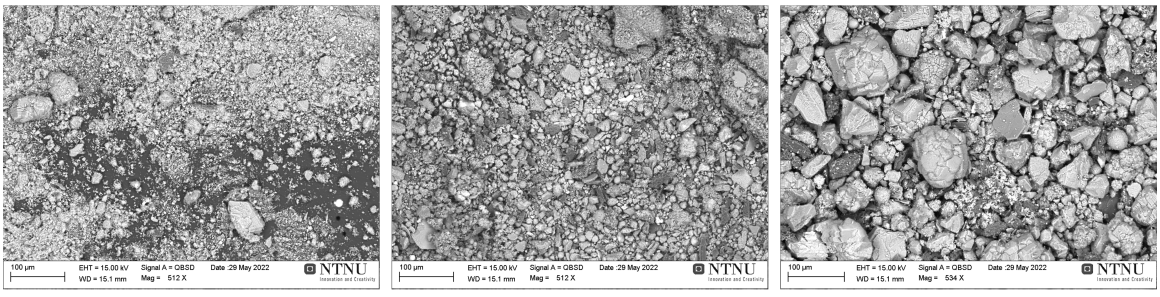

Figure 4.3: From left: Filter, airborne and settled dust with a magnification of 500x.

In Figure 4.4, filter, airborne and settled dust are imaged with a magnification of 1000x. The fume structure for filter dust is more prominent with this magnification.

This may indicate more bath related compounds and vaporised particles in the filtered dust. The airborne and settled dust is observed to have a more similar structure at this magnification than with 100x and 500x.

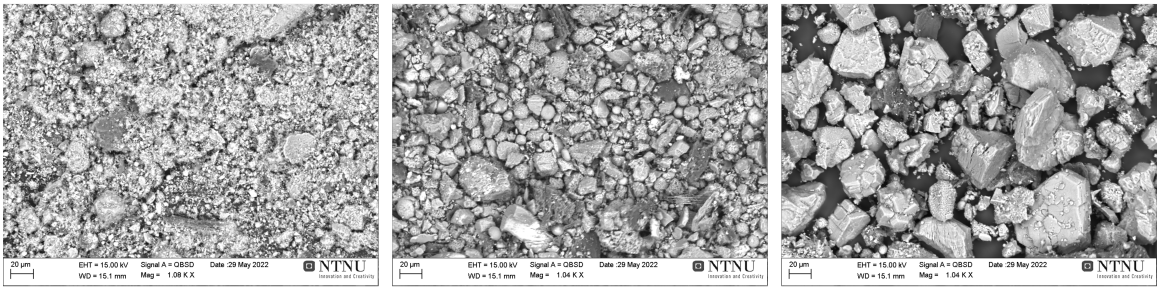

Figure 4.4: From left: Filter, airborne and settled dust with a magnification of 1000x.

Chemical Composition

Figure 4.5 show four examples of what a typical carbon particle found in both settled and airborne dust looks like. All images are taken with BSE, hence, heavier elements are observed on the surface of each particle marked with red arrow. During the authors previous work [7], it was observed that heavy elements tended to accumulate on the surface of carbon particles. Even though the dust analysed in this thesis originates from fugitive emissions and not from the gas duct, similarities regarding heavy metal accumulation are observed.

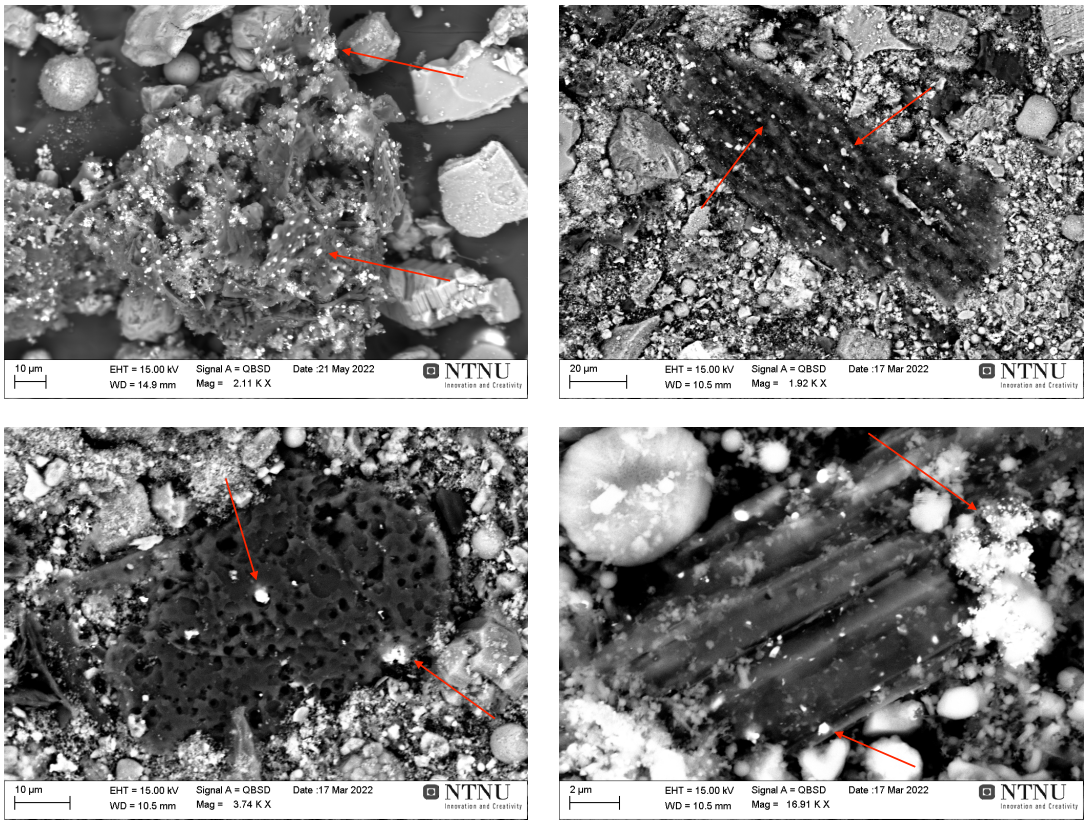

Figure 4.5: Typical carbon particles found in fugitive dust.

Figure 4.6 show a carbon particle imaged with BSE. The areas marked with 1, 2 and 3 show where point analyses were executed by means of EDS. The quantitative analysis is given in Table 4.2. From this table the composition of the main particle is observed as carbon with a concentration of 92.7 %. The bright spots consists of mainly iron and nickel with a concentration of 32.2 and 18.7 % for point 1, respectively, and 41.2 and 14 % for point 2. From the quantitative analyses, the concentration of sulfur and nickle could indicate that nickel is present as nickel sulfide (NiS). This type of analysis was performed on several particles where similar results were observed. the bright areas often had high concentrations of either iron or nickel or both, while the main particle consists of mostly carbon. Traces of aluminium, sodium and fluoride are almost consistently detected. Sulfur is usually present in higher concentrations in the bright areas.

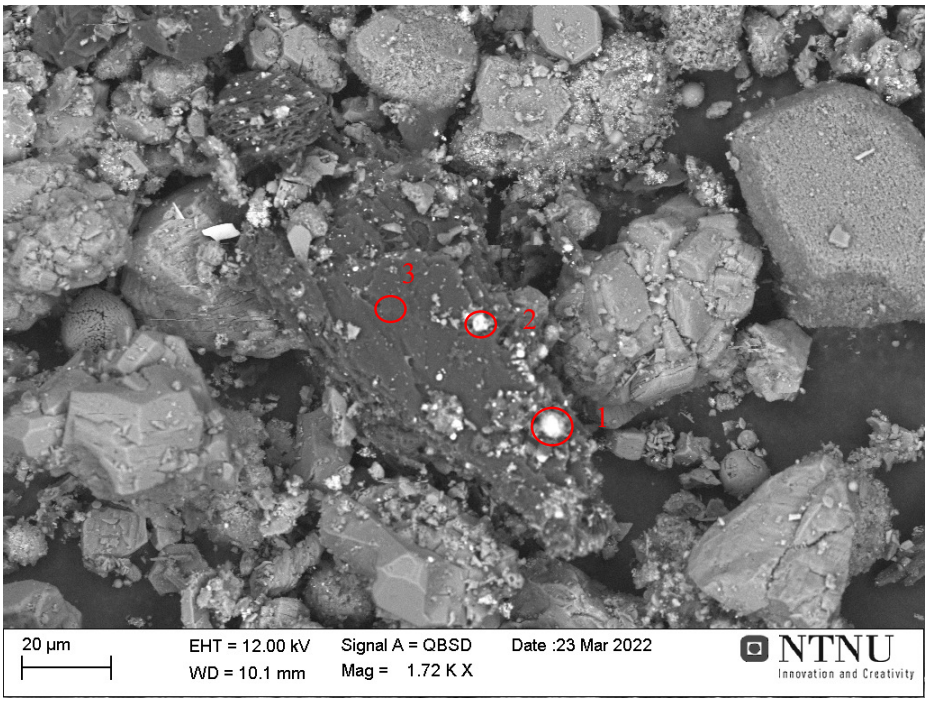

Figure 4.6: Point analysis of a carbon particle.

Table 4.2: Normalised concentration [%wt]

Element	**1**	**2**	**3**
Fe	32,31	41,22	-
Ni	18,67	13,97	-
O	9,78	14,16	-
S	8,99	7,00	1,97
Na	8,53	6,19	1,60
F	8,16	5,37	2,15
Al	7,70	4,97	1,57
C	5,86	6,68	92,72
Ca	-	0,43	-

Besides point analyses, mapping of entire particles was performed. In Figure 4.7 and Figure 4.8 an example of such analyse is given. Within the marked area in Figure 4.7, the mapping analysis was performed. This particle is observed with several heavy elements on the surface by the use of BSE imaging.

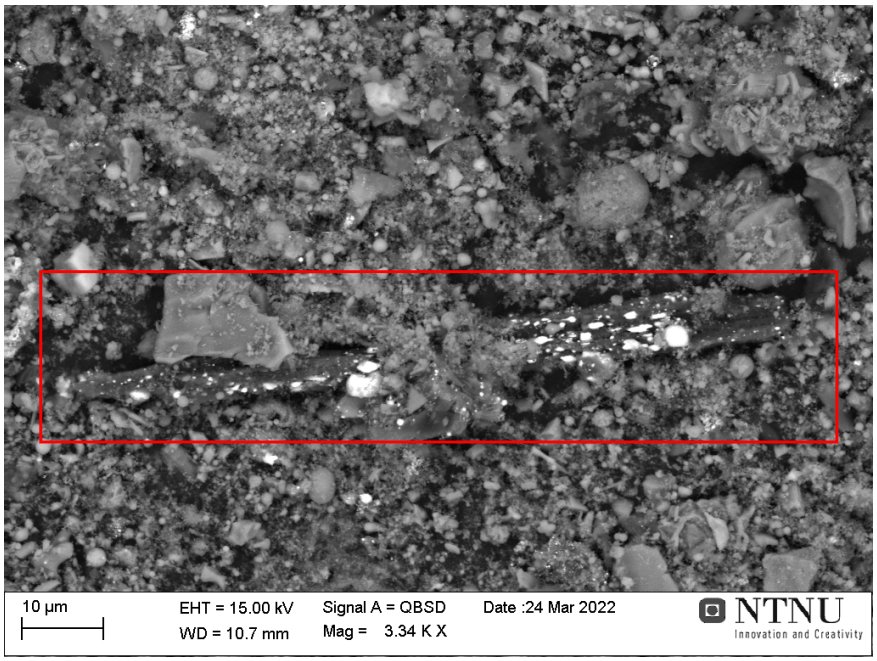

Figure 4.7: SEM image of a particle with heavy elements on the surface

The mapping analyses also show a composition of the main particle to contain large amounts of carbon (green). Both nickel (turquoise) and iron (pink) are detected on the surface of the particle, where both correlate well with the sulfur map (blue). This observation was common for several of the mapped particles where heavy elements were detected with BSE. More mapping analyses are given in Appendix B.

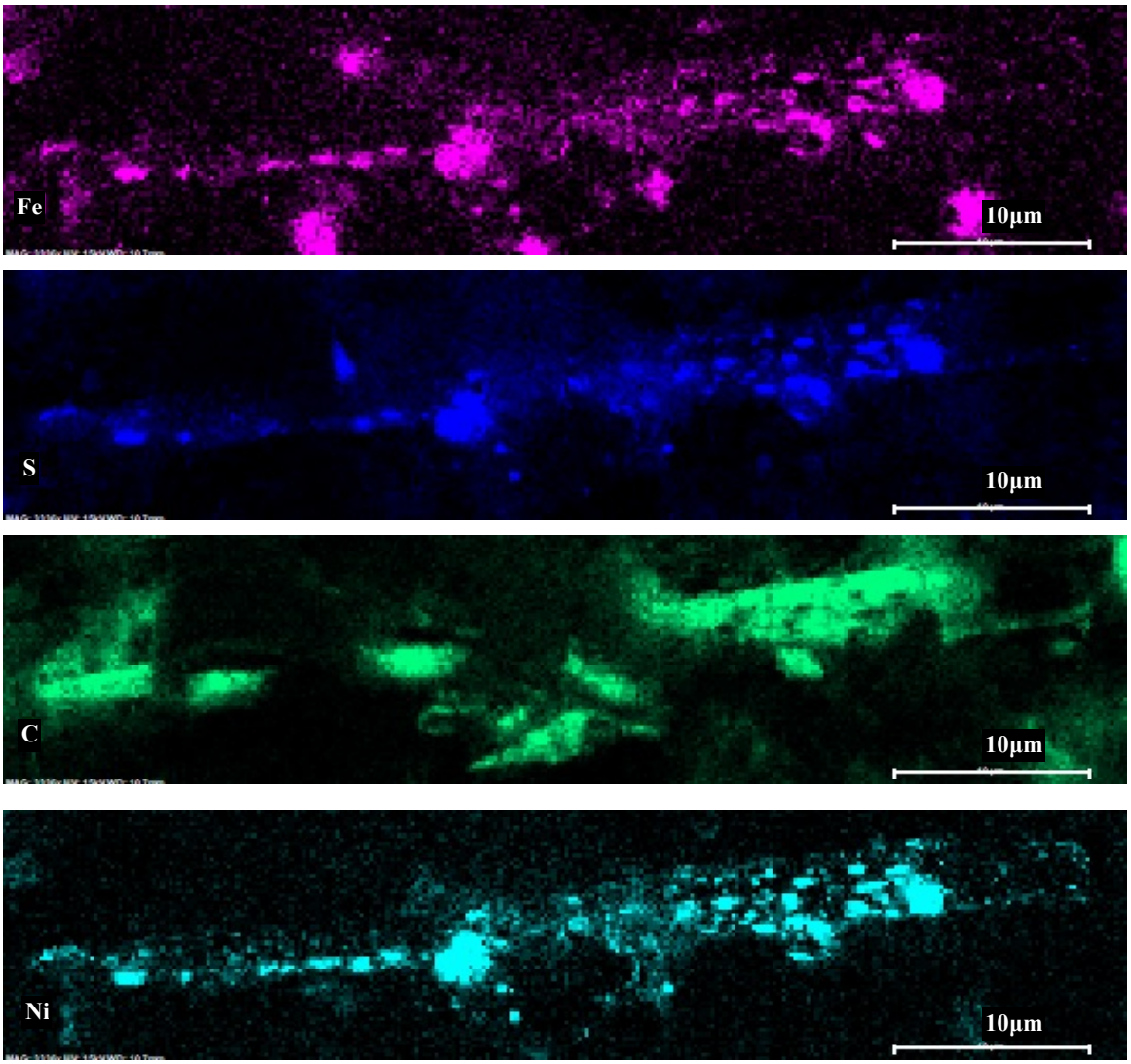

Figure 4.8: Mapping analysis of particle showing from the top: Fe, S, C and Ni maps.

Particle Size Measurements

Figure 4.9 show the carbon particle size distribution found by manually measuring 100 carbon particles in SEM for settled, airborne and filter dust from Hydro Høyanger. A correlation between airborne and filter dust is observed at the lower part of the graph. The settled dust is found to have larger variations than airborne and filter dust.

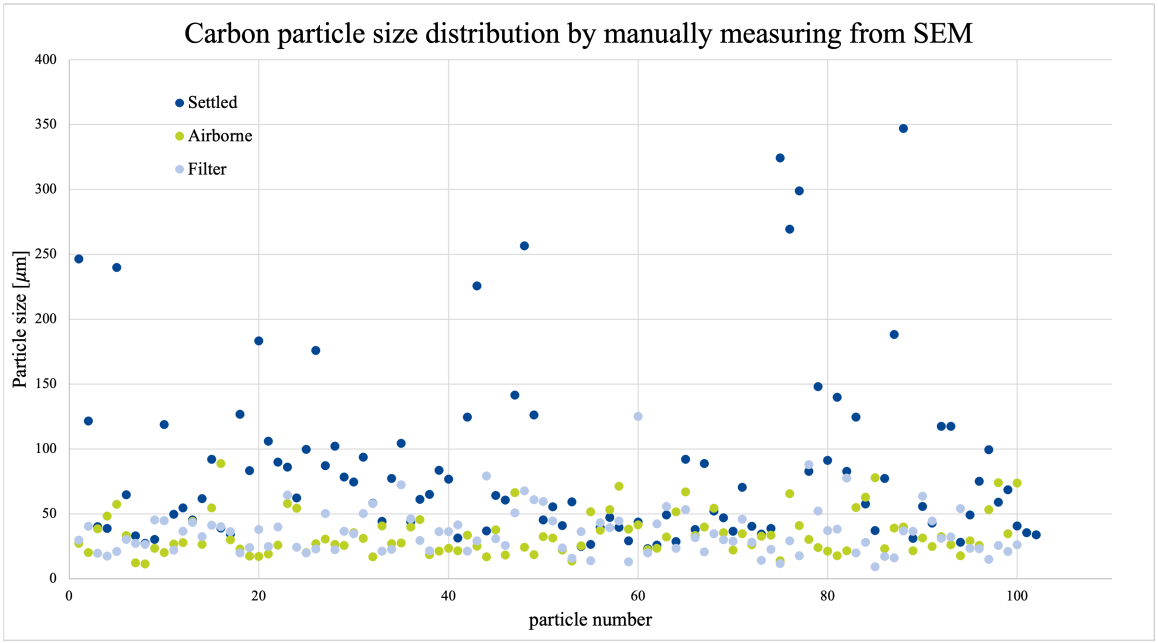

Figure 4.9: Carbon particle size distribution for settled, airborne and filter dust manually measured in SEM.

In Table 4.3 mean, median, min and max carbon particle size for settled, airborne and filter dust are given. Average carbon particle size for airborne and filter dust are observed to be quite similar at 34 and 36 µm, respectively. The average carbon particle size for settled dust at 85 µm is more than twice the size of airborne and settled at 34 µm and 35 µm, respectively. The median carbon particle size is also found to be twice the size of carbon particles in airborne and filter dust. The minimum value for settled dust is 23 µm, almost double the size of minimum value for airborne dust. An interesting observation is the maximum value for filter dust at 125 µm compared to maximum value for airborne at 89 µm. The maximum carbon particle size for settled dust is found at 347 µm which is relatively large and almost three times the maximum carbon particle size for filter dust.

Table 4.3: Particle size for carbon particles in settled, airborne and filter dust.

Carbon particle size [µm]	**Settled**	**Airborne**	**Filter**
Mean	85,34	34,24	35,58
Median	62,04	30,12	31,34
Min.	23,26	11,50	9,22
Max.	346,9	88,85	125,1

4.1.3 XRD

Four samples were analysed by means of XRD. The software EVA was used to identify crystalline phases in the dust samples. In Figure 4.10, the crystalline patterns for sample 8 and 11 are given, showing a main composition of corundum (α-Al_2O_3), cryolite and chiolite. The patterns of airborne and settled dust are observed to be quite similar also for the other samples investigated, see Appendix C for complete XRD-analysis.

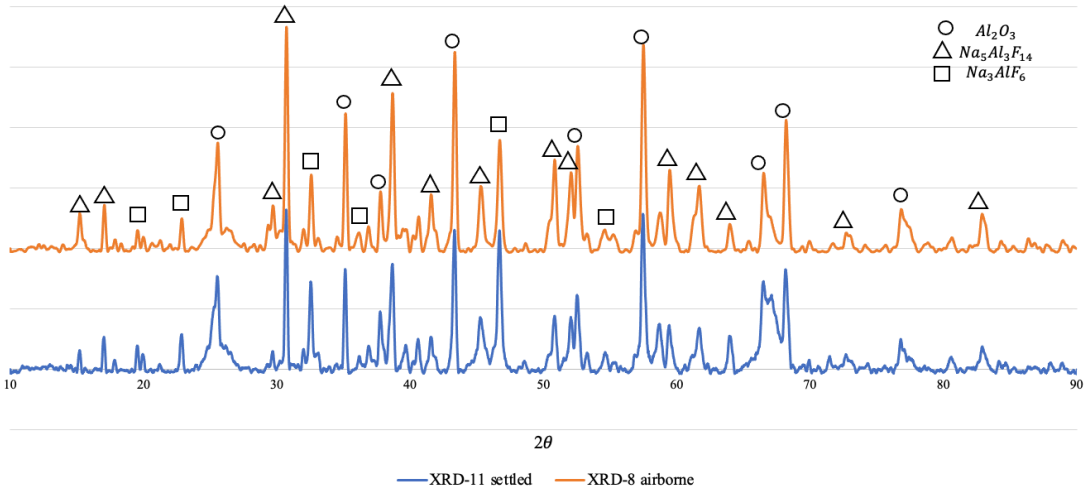

Figure 4.10: XRD analysis of settled and airborne dust.

In Table 4.4, semi-quantification of the different elements based on the XRD-analyses are given. No significant difference between settled and airborne dust was observed.

Table 4.4: Semi-quantification of elements found in airborne and settled dust.

	Settled		Airborne	
Element	**3**	**11**	**8**	**9**
O	14,3	12,8	14,4	16,4
F	38,7	40,5	38,7	36,3
Na	20,8	21,8	20,1	19,2
Al	26,2	25,0	26,7	28,1

4.1.4 Particle Size Distribution

Figure 4.11 show the particle size distribution for settled dust, where the particle diameter (µm) is given as a function of particle size distribution vector (%). The particle size is observed to be quite similar for all samples. However, sample 14 is positioned slightly to the right of the other two samples, indicating coarser particles. This is also substantiated in the overview of mean and median particle sizes in Table 4.5, where sample 14 have the largest particle size for both mean and median values.

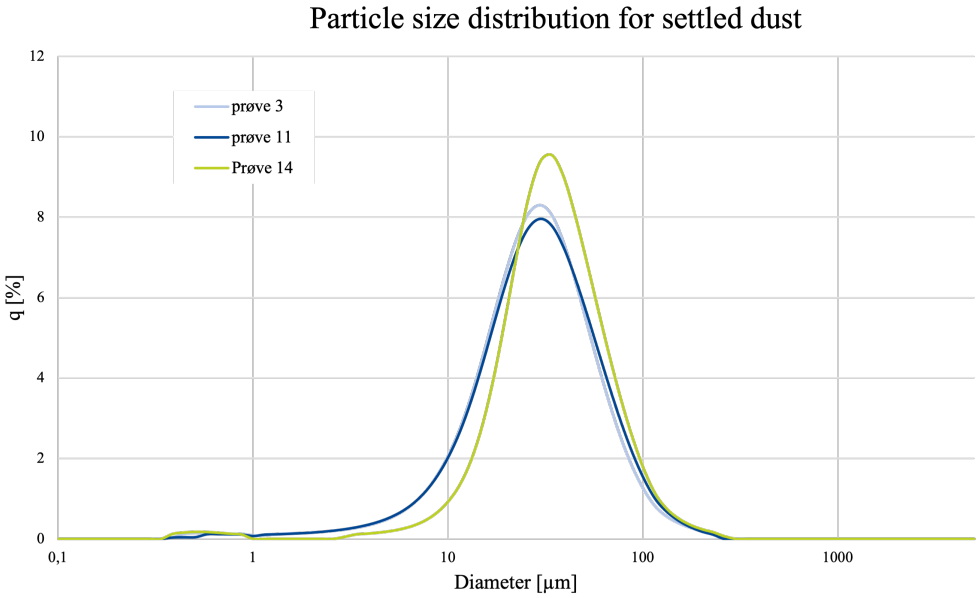

Figure 4.11: Particle size distribution for settled dust.

Figure 4.12 show the particle size distribution for airborne dust. Also here the particle sizes are observed to be similar. However, an indication of a small peak is observed around diameter 100-200 µm.

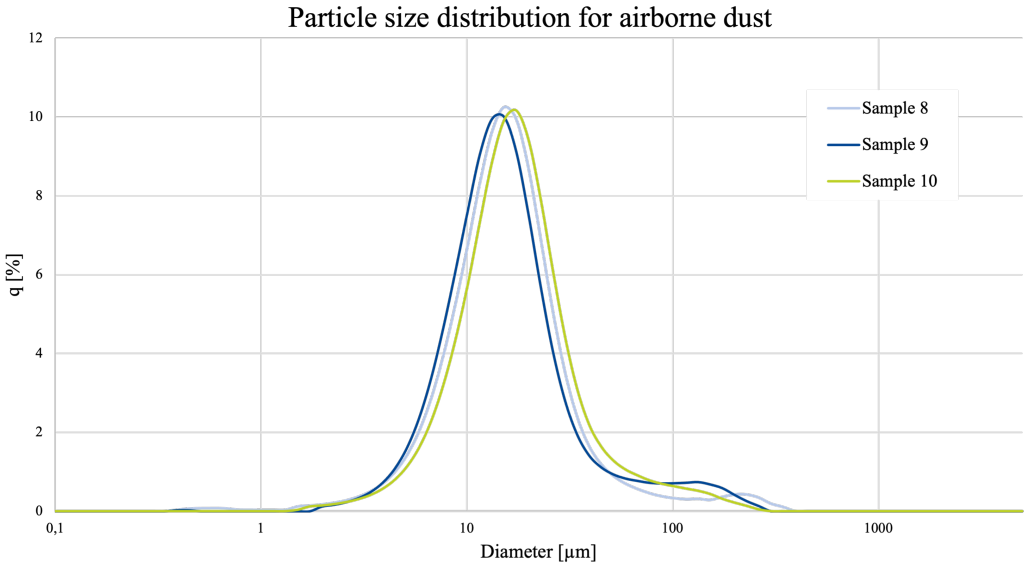

Figure 4.12: Particle size distribution for airborne dust [µm].

Table 4.5 present the median and mean size for airborne and settled dust. Airborne dust is observed to have smaller median and mean particle size than settled dust. The analyses indicate that the mean size for airborne dust is between 13 µm and 15 µm, while between 26 µm and 31 µm for settled dust. Mean size is found to be around 21 µm for airborne and 32-38 µm for settled dust. In addition, D10 and D90 which indicate what diameter 10% and 90% of the distribution lies below, are included. For airborne 10% of the distribution is found below 6-7 µm, while for settled dust it is found to be below 10-11 µm. 90 % of the particle size distribution for airborne dust is found below the diameters between 38 µm and 47 µm, while for settled dust this lies between 49 µm and 65 µm.

Table 4.5: Particle size distribution for airborne and settled dust [µm].

	Airborne			Settled		
Particle size [µm]	**8**	**9**	**10**	**3**	**11**	**14**
Median size	14,33	13,63	15,74	26,58	27,37	31,94
Mean size	21,43	21,67	21,86	32,82	34,07	38,65
D10	6,63	6,57	7,37	10,03	10,10	11,00
D90	47,31	45,99	38,40	61,92	65,65	49,40

In Figure 4.13 a clear difference between airborne and settled dust is observed regarding particle size distribution. Sample 8, 9 and 10 represents airborne dust and are found as the narrower peaks to the left. Sample 3, 11 and 14 represents settled dust and is found as the broader peaks to the right.

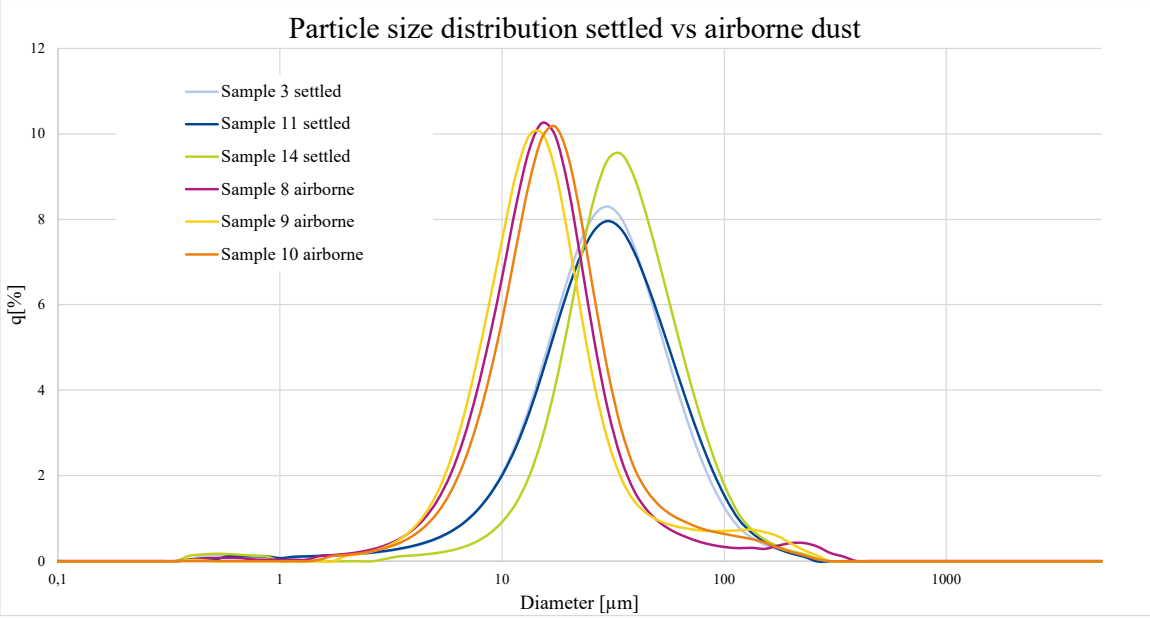

Figure 4.13: Particle size distribution for airborne and settled dust [µm].

4.1.5 ICP-MS

12 samples from different areas in a smelter were analysed by means of ICP-MS. For complete analyses see Appendix D. In Figure 4.14-4.17 the distribution of the 10 main elements in different categories are given. The samples were divided into airborne and settled dust as explained in Chapter 3. In addition, filter samples of airborne potroom dust from Høyanger from a SINTEF sampling system were analysed separately from the airborne dust, for the reason being that the dust was collected in 2008 by a different method than the other airborne samples. As a reference, airborne dust in gas duct from sunndalsøra was analysed. These ICP-MS analyses were performed by the author during the fall semester 2021 in relation to a project assignment [7]. The purpose of this categorisation is to see if there are major differences in composition based on where and how the dust is collected. Table 4.6 contains the average value of the 10 main elements and their distribution, which is used to produce the diagrams in Figure 4.14-4.17.

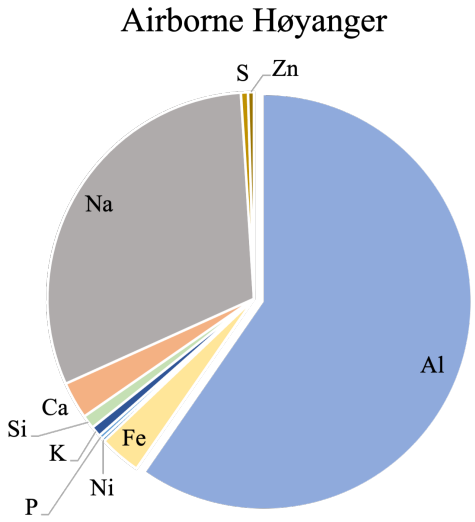

Figure 4.14: Average composition of main elements in airborne dust from Høyanger.

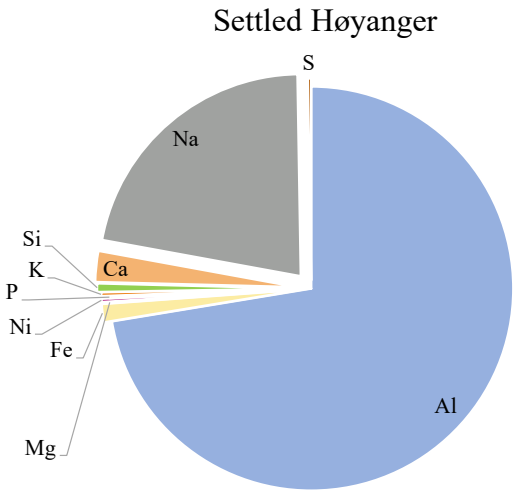

Figure 4.15: Average composition of main elements in settled dust from Høyanger.

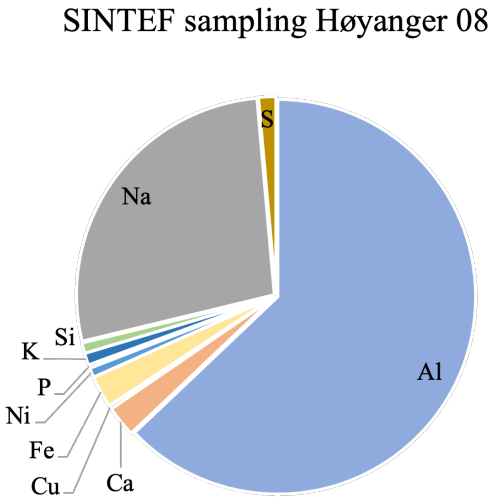

Figure 4.16: Average composition of main elements in dust collected with SINTEF samplers.

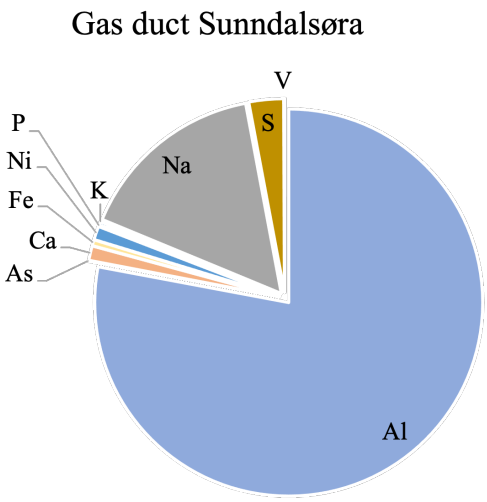

Figure 4.17: Average composition of main elements in dust from gas duct analysed in relation to project assignment [7].

From Table 4.6 a clear difference between the aluminium content in airborne dust and dust from gas duct is observed. Based on the main elements found in airborne dust approximately 60% of this is aluminium, compared to the almost 80% found in dust from gas duct. However, airborne dust have a composition of almost double the amount sodium found in the gas duct at 30% and 16%, respectively. The distribution of aluminium in settled dust is closer to the gas duct composition at 72% and a sodium content at 22%. The opposite trend is seen with the SINTEF sampler, lower content aluminum at 63% and higher content sodium at 27%. The nickel concentration is quite similar for all the categories, but a bit higher in the gas duct at 1,13%. Iron is more significant in airborne dust and dust collected with SINTEF samplers at around 3%, compared to settled and raw gas.

Table 4.6: Average distribution of the 10 main components in the dust from different areas [mg/kg].

Airborne			**Settled**			**SINTEF**			**Raw gas [7]**		
	mg/kg	%		mg/kg	%		mg/kg	%		mg/kg	%
Al	196000	59,64	**Al**	255000	72,40	**Al**	220000	62,90	**Al**	318333	77,96
Na	101000	30,73	**Na**	77000	21,86	**Na**	95750	27,37	**Na**	64500	15,80
Ca	9540	2,90	**Ca**	8700	2,47	**Ca**	8825	2,52	**Ca**	4950	1,21
Fe	10740	3,27	**Fe**	5100	1,45	**Fe**	9150	2,62	**Fe**	2033	0,50
Ni	846	0,26	**Ni**	910	0,26	**Ni**	2727,5	0,78	**Ni**	4633	1,13
P	1022	0,31	**P**	690	0,20	**P**	960	0,27	**P**	500	0,12
K	2700	0,82	**K**	1050	0,30	**K**	3425	0,98	**K**	1097	0,27
S	1820	0,55	**S**	925	0,26	**S**	4925	1,41	**S**	11783	2,89
Si	3480	1,06	**Si**	2400	0,68	**Si**	3025	0,86	**As**	238	0,06
Zn	1514	0,46	**Mg**	427	0,12	**Cu**	990	0,28	**V**	263	0,06

In Figure 4.18 the average composition of aluminium and sodium in dust from potroom, airborne and settled at Hydro Høyanger (HH), and raw gas Hydro Sunndalsøra (HS) are given. This chart show Al and Na as inversely proportional with higher Al amounts in dust from raw gas and lower in airborne dust in the potroom, while Na is higher in airborne dust than in raw gas.

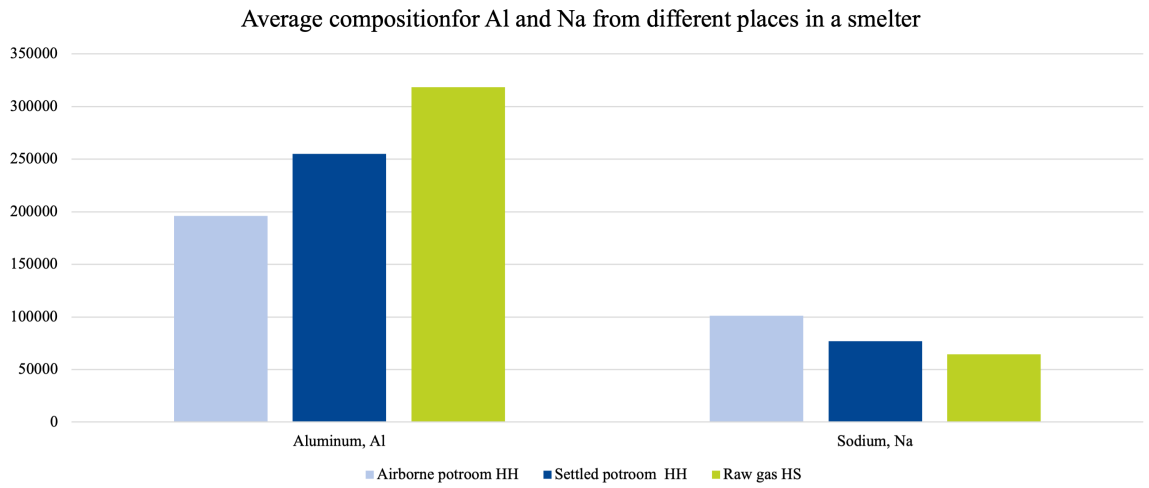

Figure 4.18: Average composition of aluminium and sodium in dust from airborne, settled and raw gas.

The average composition of some minor elements from both airborne and settled dust in potroom (HH), as well as dust from raw gas (SH) are given in Figure 4.19. Only small amounts of zinc are detected in the raw gas and settled dust compared to the airborne dust. Iron in airborne dust is found to be more than double the amount in settled dust, while iron in raw gas is found to be about 1/5 of the amount in airborne dust. Nickel in potroom dust is similar for both airborne and settled, while in raw gas the amount of Ni is found to be almost 80% more. More phosphorous is found in airborne dust than dust from raw gas. From Table 4.7 the average phosphorous in airborne dust is found to be around 1000 mg/kg while half of this is found in dust from raw gas at 500 mg/kg. The sulfur measured in dust from raw gas is 85% more than the sulfur in airborne dust and more than 90% than the settled dust.

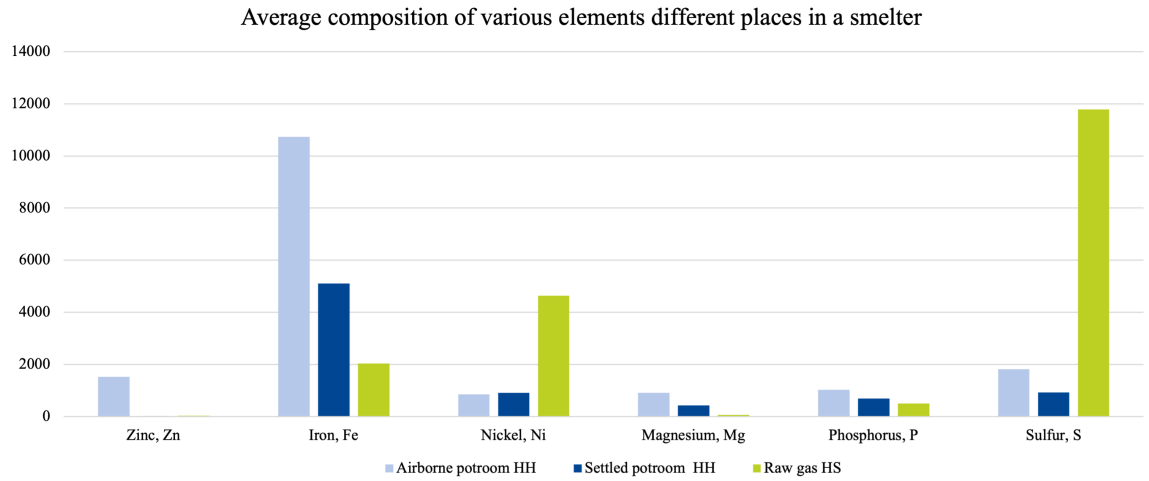

Figure 4.19: Average composition of various minor elements in dust from airborne, settled and gas duct.

Table 4.7: Average composition of various minor elements in dust from airborne, settled and gas duct [mg/kg].

Element	Airborne potroom	Settled potroom	Raw gas
Zinc, Zn	1514	20	33
Iron, Fe	10740	5100	2033
Nickel, Ni	846	910	4633
Magnesium, Mg	902	427	52
Phosphorus, P	1022	690	500
Sulfur, S	1820	925	11783

In Figure 4.20 the average of some trace elements found in dust from potroom, airborne and settled (HH), and in gas duct (SH), are given. Titanium in airborne dust differs from both settled and gas duct by almost 6 times. There is also detected more vanadium in airborne dust than in settled and gas duct, from Table 4.8 vanadium in airborne dust is found to be 438 mg/kg. There is almost 75% more lead in dust from gas duct than in airborne and 90% more than in settled dust. More arsenic is detected in dust from gas duct, while twice as much gallium is detected in airborne dust compared to settled and gas duct. Barium is generally found in low concentrations.

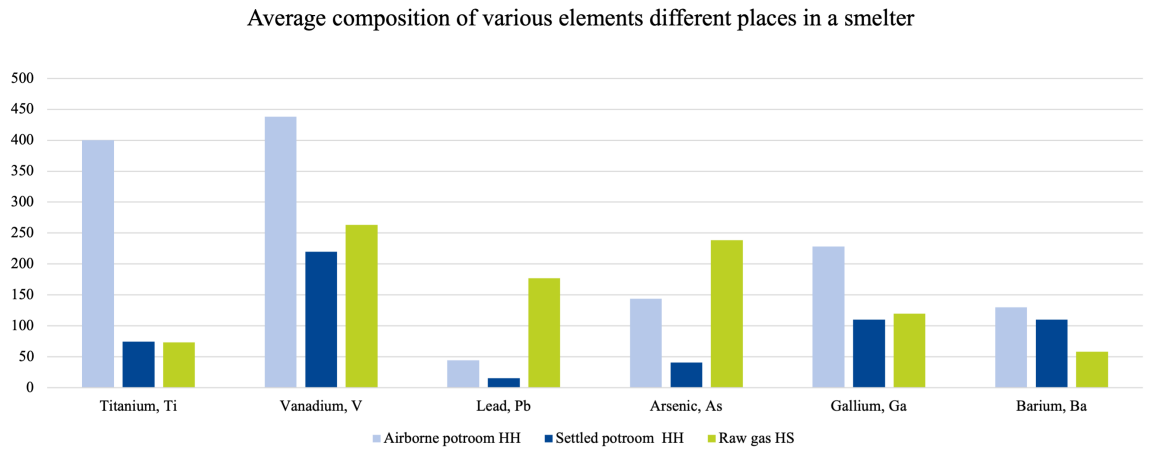

Figure 4.20: Average composition of various trace elements in dust from airborne, settled and gas duct.

Table 4.8: Average composition of various trace elements in dust from airborne and settled at HH, and gas duct at SH [mg/kg].

Element	Airborne potroom	Settled potroom	Raw gas
Titanium, Ti	400	74,5	73
Vanadium, V	438	220	263
Lead, Pb	44	15,5	177
Arsenic, As	144	40,5	238
Gallium, Ga	228	110	120
Barium, Ba	130	110	58

4.2 Emission Data

PM emissions, temperature and humidity data was collected for a period of almost three weeks at Alcoa Mosjøen. DH1 and DH2 represents the sensors at roof level, while DH3 represent the sensor at floor-level. Only data from the last week of data collection will be presented in this chapter for clarity. This period covers temperature and humidity variations corresponding to the entire measuring period, as well as variations in PM emissions and particle size distribution.

4.2.1 Temperature and Humidity

Figure 4.21 visualise the temperature variations during the period from 9th of May to 17th of May. DH1 and DH2 have, not surprisingly, detected generally higher temperatures than DH3. They have also detected similar temperatures, which is expected when placed in the same area. Temperature variations at floor level also appear to be more frequent than at roof level. During this period of time the average outside temperature was around 5°C which will contribute to lower temperatures in the hall [31].

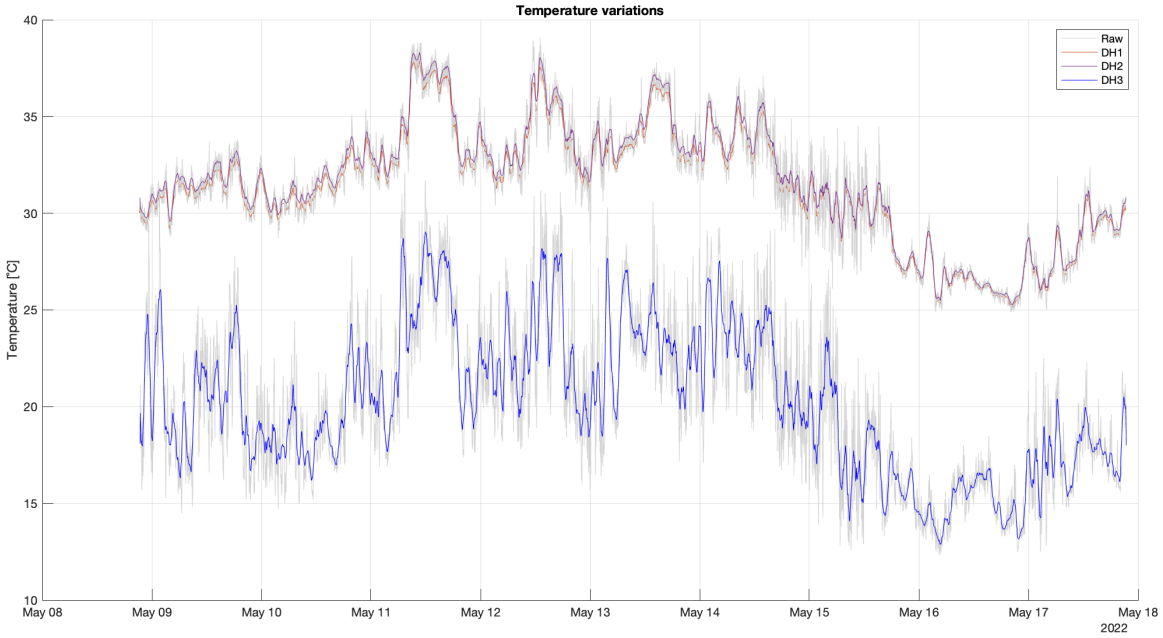

Figure 4.21: Variations in temperature detected at roof level (DH1 and DH2) and at floor level (DH3) [°C].

In Table 4.9 mean, min and max temperature for the different sensor systems are given for the period of 9-17th of May. The similar values for DH1 and DH2 confirms what can be seen from the graph in Figure 4.21 regarding similar temperature measurements.

Table 4.9: Temperature measurements for the three sensor systems [°C].

Temperature [°C]	**DH1**	**DH2**	**DH3**
Mean	31,3	31,7	20,2
Min.	24,9	25,0	12,3
Max.	38,6	39,1	32,1

In Figure 4.22 relative humidity is given for all three sensor systems. The humidity is measured significantly higher at floor level than roof level. This is expected due to cold air containing more water vapor than warm air.

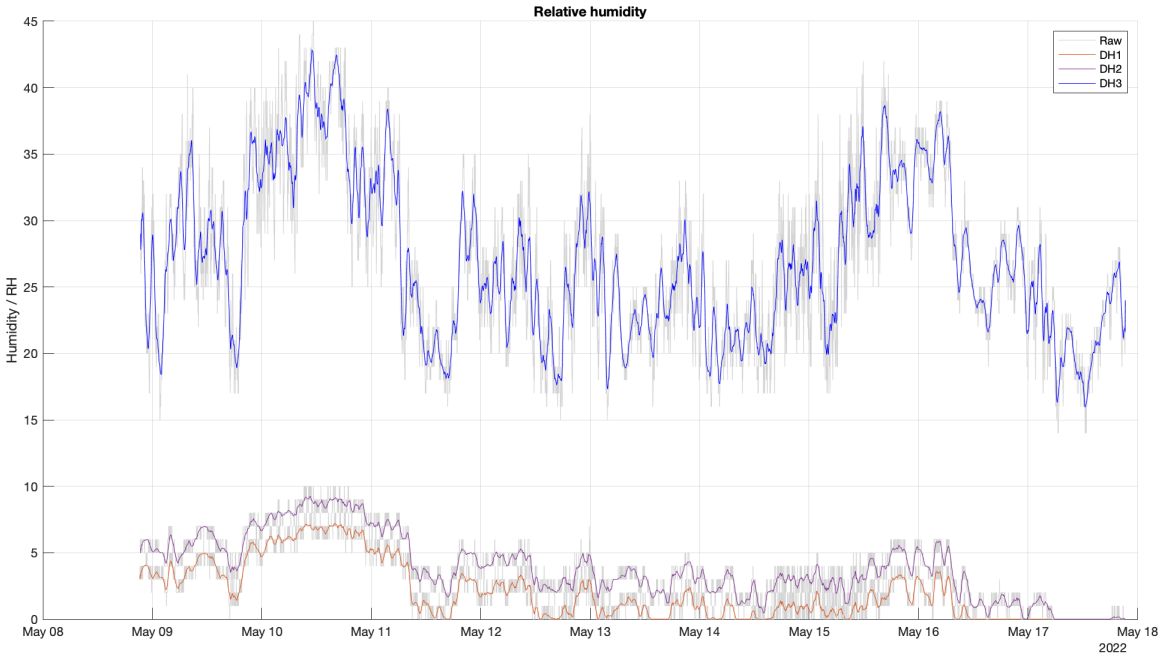

Figure 4.22: Variations in relative humidity detected at roof level (DH1 and DH2) and at floor level (DH3) [RH%].

In Table 4.10 mean, min and max measurements for relative humidity is given for the time period 9-17th of May. Mean humidity for DH1 and DH2 are significantly lower than for DH3 measured at 27%. Max humidity for roof level does not exceed 10%, while for floor level this is measured up to 45%. The average outdoor humidity for this period was around 86% based on data from a local weather station [31].

Table 4.10: Humidity measurements for the three sensor systems [%].

Relative Humidity [%]	**DH1**	**DH2**	**DH3**
Mean	2,03	3,84	27,0
Min.	0	0	14
Max.	8	10	45

4.2.2 Typical Particle Size and Fraction Distribution

In Figure 4.23 typical particle size for DH1, DH2 and DH3 are given. The majority of the measurements are found around 0.6 µm for all sensors. Greater variation in particle size is observed in the upper limit versus the lower limit. No significant difference between particle size on floor level and roof level is observed in this figure.

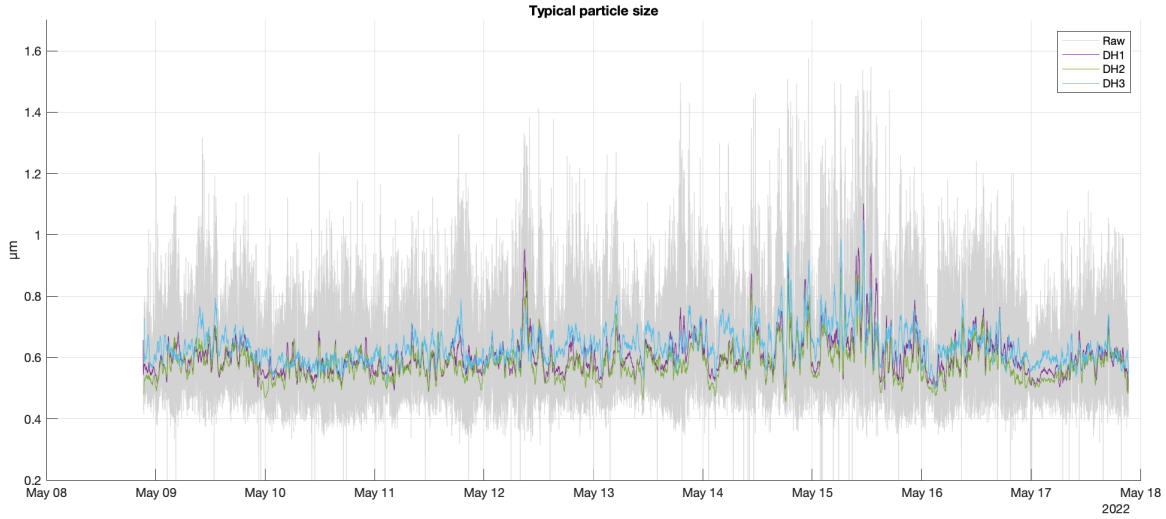

Figure 4.23: Typical particle sizes for all sensors [µm].

In Table 4.11 mean, min and max are given for typical particle size for DH1, DH2 and DH3. Mean particle size is approximately 0,61 µm and 0.58 µm for the roof level sensors. Floor level mean particle size is slightly larger at almost 0.64 µm. For min measurements, only values > 0 µm were included. This results in a minimum particle size at 0.32 µm for roof level and 0.33 µm for floor level. For maximum particle size, floor level measurements is found to be vaguely larger at 1.58 µm, compared to roof level at 1.55 µm and 1.46 µm.

Table 4.11: Typical particle size for DH1, DH2 and DH3 [µm].

Typical particle size [µm]	**DH1**	**DH2**	**DH3**
Mean	0,6045	0,5819	0,6375
Median	0,5774	0,5558	0,6134
Min.	0,3154	0,3213	0,3252
Max.	1,5471	1,4545	1,5764

Plotted in Figure 4.24 are $PM_{1.0}$ and $PM_{4.0}$ subtracted from PM_{10} at top and middle, respectively. The lower plot show PM_{10}, all for sensor DH1 at roof-level. Subtracting $PM_{4.0}$ from PM_{10} give concentrations up to approximately 100 µg/m^3, indicating that the majority of the PM_{10} fraction consists of smaller fractions such as $PM_{4.0}$.

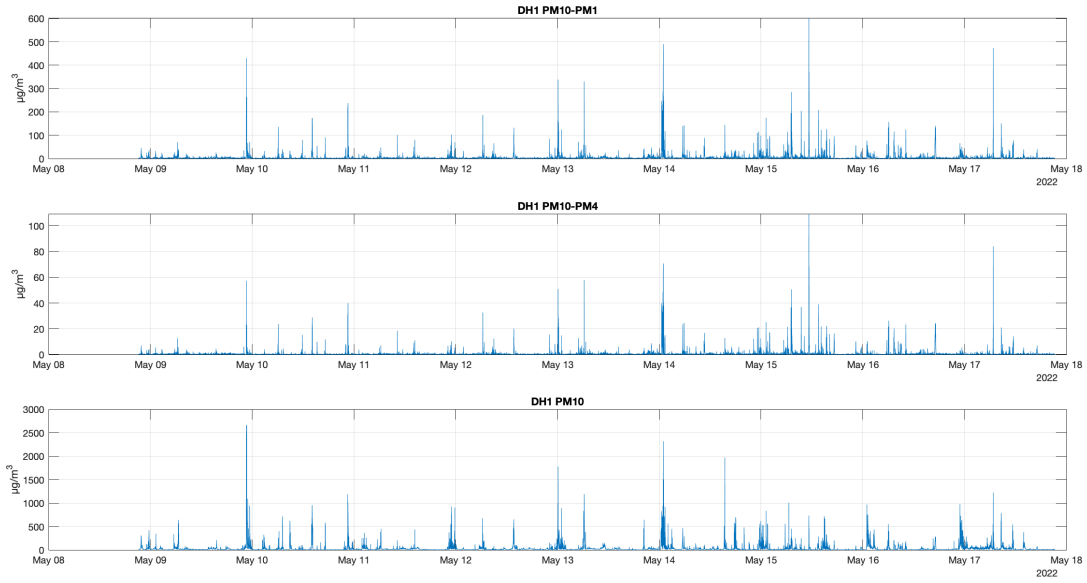

Figure 4.24: From the top: PM10-PM1, PM10-PM4, PM10 for sensor system DH1 at roof level.

In Table 4.12 the average mass concentration for each particle size fraction are given. Observations based on these numbers show that $PM_{1.0}$ amounts to 86% of PM_{10} at roof level, while at floor level the same fraction amounts to 77% of PM_{10}. $PM_{2.5}$ amounts to 95% of PM_{10} at roof level and 89% of PM_{10} at floor level. Lastly, $PM_{4.0}$ amounts to 98% and 96% of PM_{10} at roof and floor level, respectively.

Table 4.12: Average mass concentration for sensor DH1, DH2 and DH3 [µg/m^3].

Average mass concentration [µg/m^3]	**DH1**	**DH2**	**DH3**
PM_1	26,4097	29,5910	6,7483
$PM_{2.5}$	29,1085	32,5739	7,8697
PM_4	30,1212	33,6884	8,4796
PM_{10}	30,6383	34,2583	8,7912

4.2.3 Dust Load Variations and Operational Activities

In Figure 4.25 measured PM_{10} emissions for DH1, DH2 and DH3 are given for the time period 9-17th of May. A significant difference between floor level and roof level emissions is observed, where floor level dust is usually found at 1/10 of roof levels. One exception of this is May 15th, where dust levels on the floor reaches almost 2500 $\mu g/m^3$ for a short period of time. Generally, events on floor seems to be reflected under roof, but not necessarily vice versa. This can be expected as the roof leveled sensors are more exposed to activities in the hall, such as gusts of wind, vehicles and crane movements.

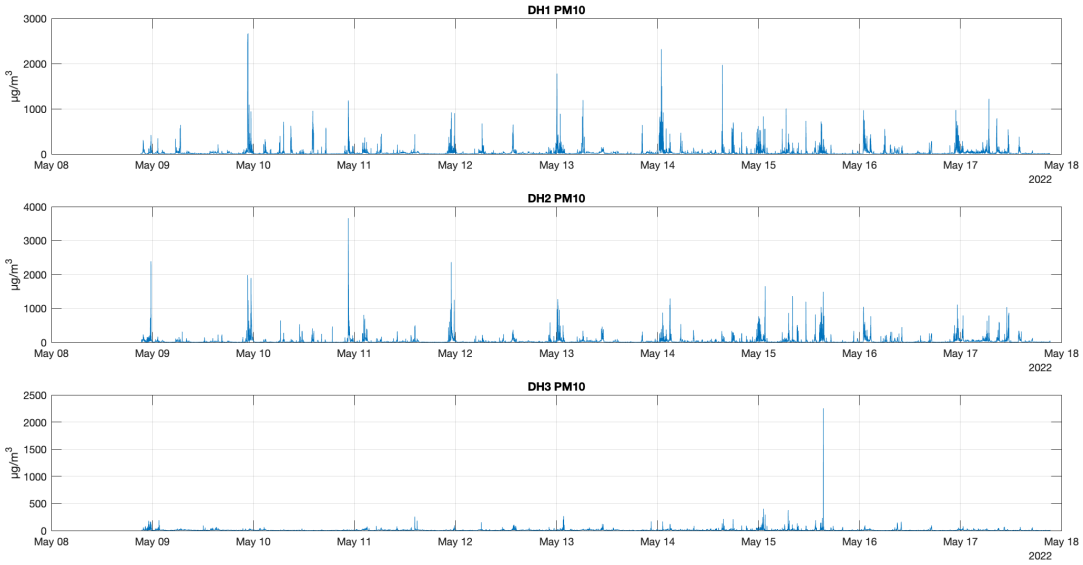

Figure 4.25: PM10 emissions for all sensor systems. From top DH1 and DH2 at roof level and DH3 at floor-level.

Operational data for the time period 9-17th of May were provided by Alcoa Mosjøen to compare with emission measurements. This included documented activities such as anode change, tapping and temperature measurements for relevant furnaces nearby the sensors. In Figure 4.26 the operational data are given as:

- 1 - Star probe, Temperature measurements
- 2 - Metal tapping
- 3 - Anode Change

During temperature measurements, one furnace cover is removed for the duration of measurements. For tapping, two furnace covers are removed while four covers are usually removed during anode change.

Observations from Figure 4.26 indicate that the highest emissions from 10, 13 and 14th of May correlates well with the timing of anode changes.

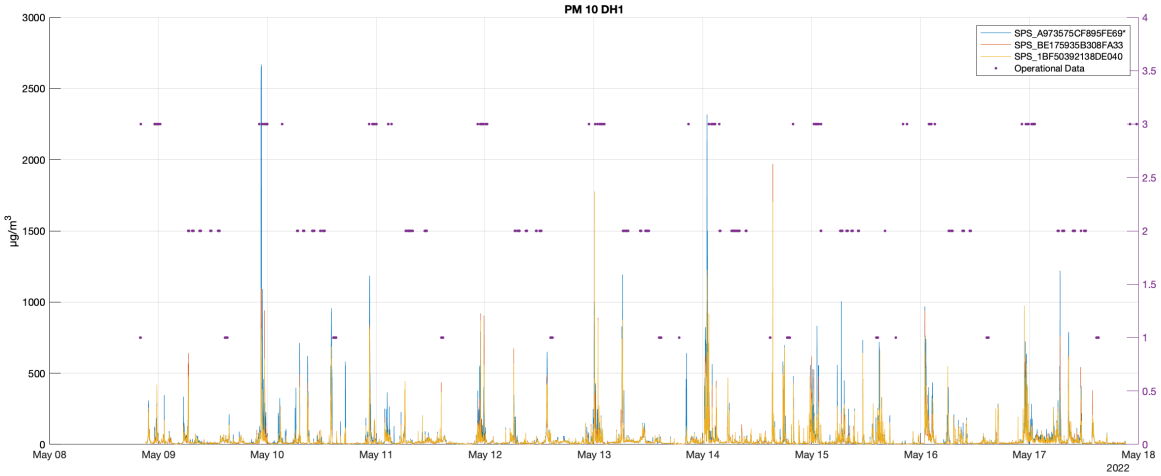

Figure 4.26: PM10 emissions for roof level compared to production activities where 1= temperature measurements, 2= tapping and 3= anode change.

Figure 4.27 show PM_{10} emissions at roof level for 12-13th of May. From this figure, the documented anode changes is observed to result in quite different emission concentrations. For the metal tapping there seem to be a period of increased emissions right before the procedure is completed for both days.

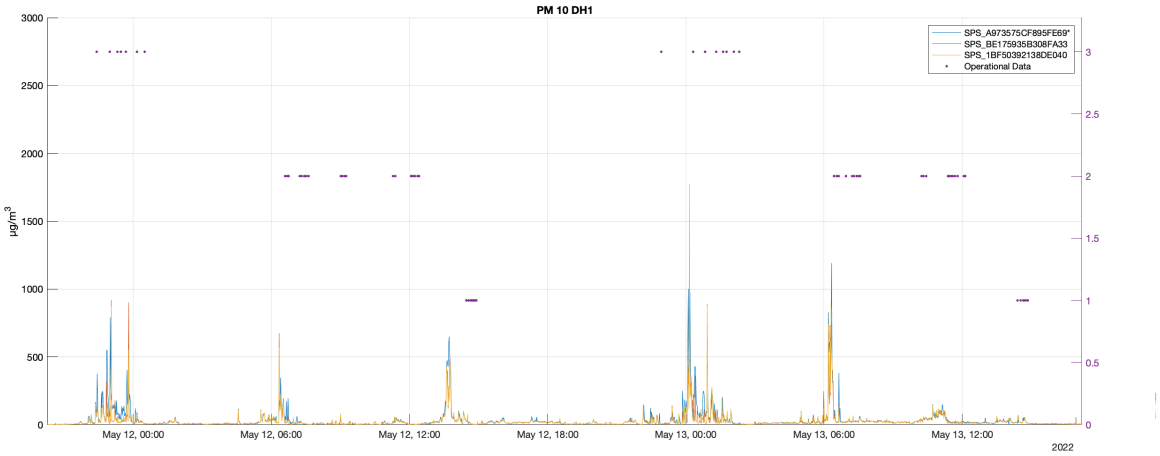

Figure 4.27: PM emissions 12-13th of May with operational activities.

Usually the emission concentrations at floor level is found at <500 µg/m^3. In Figure 4.28 an increase in emissions is detected at 2200 µg/m^3. This deviates from measurements from the entire period of three weeks. Looking at the operational data in this period, no clear source of the high emissions is observed based on the three process activities documented. The large peak is placed between temperature measurements and tapping, indicating that some other, undocumented event caused these measurements.

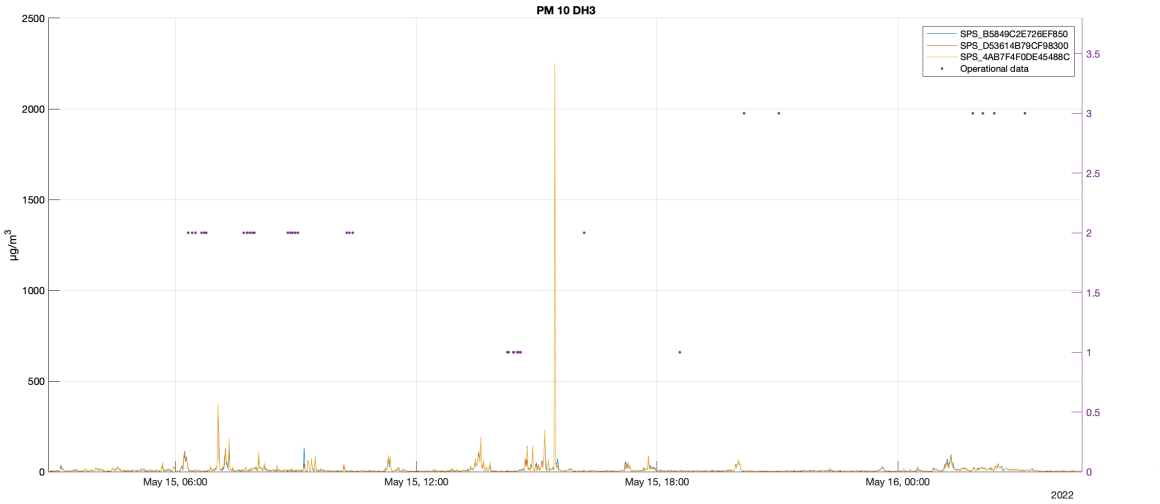

Figure 4.28: PM emissions 15th of May with operational activities at floor level.

In Figure 4.29, PM_{10} and $PM_{2.5}$ is given for the different operational activities at roof level. The top plot show emissions related to anode change at furnace 367, which is found directly below sensor DH2. These emissions are observed to consist mainly of $PM_{2.5}$. The middle plot represents emissions detected during metal tapping. The delay between registered tapping and top might be explained by the main emissions occurring after tapping, when the crucible is full of liquid metal and the siphoning lid is removed. The emissions seems to consist of more PM_{10} in this case, compared to anode change. During temperature measurements two small tops are detected. The first top seem to contain more fine particles compared to the second top.

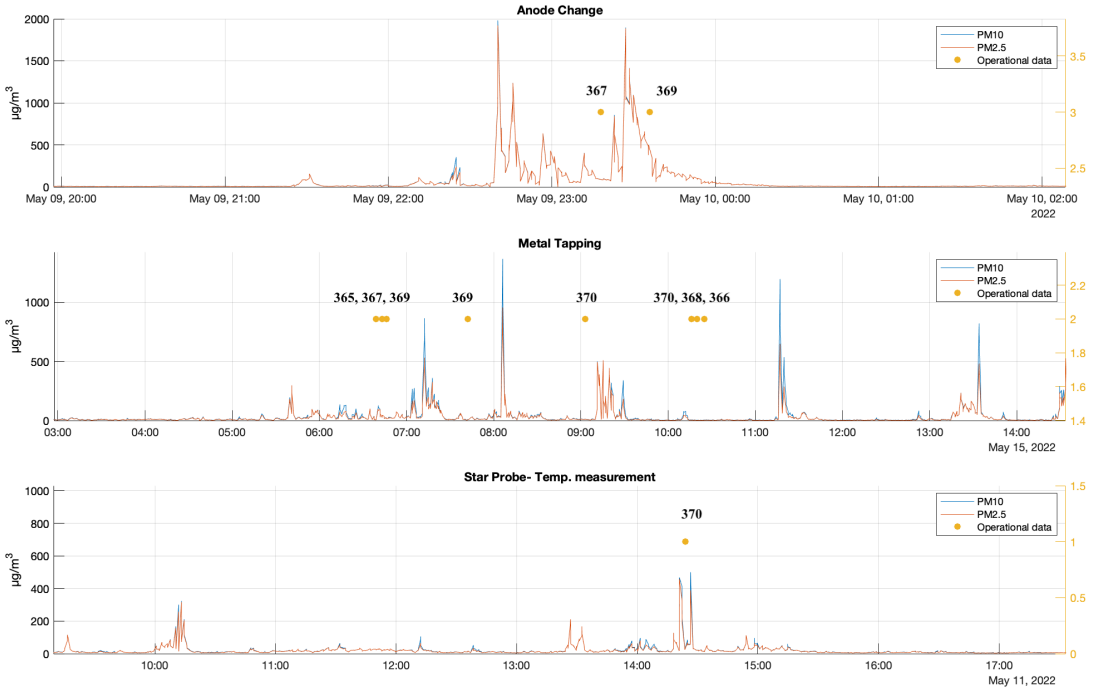

Figure 4.29: PM10 and PM2.5 emission data for DH2 during different operational activities.

Chapter 5

Discussion

This chapter will discuss the results achieved through experimental examinations. Observations of variations in morphology and chemical composition achieved through EDS, spectrometry and XRD, are included. In addition to this, discussion regarding particle size distribution as well as variations in emissions related to operational activities in the electrolysis hall, will be covered in this chapter.

5.1 Characterisation and Composition

This section will mainly discuss results obtained with SEM, XRD and ICP regarding chemical composition. The differences in morphology of settled and airborne dust observed during SEM analyses will also be highlighted and discussed.

5.1.1 Chemical Composition

As seen in previous studies by the author, the dust largely consists of Al and Na, regardless of where and how it was collected. However, when looking at the average composition of some main impurity elements given in Figure 5.1, the dust source seem to have an impact on variations regarding concentration. Ni concentration found in dust from the raw gas appears to be twice as high as found in airborne dust from SINTEF samplers in 2008 and almost 75% more than found in airborne dust collected from inside the chimney in Høyanger.

According to previous studies by Jahrsengene et al. [20] V, Ni and Fe were found to be present in coke as sulfides. From Figure 5.1, it can be observed that higher concentration of S correlates with higher concentration of Ni in dust from raw gas and from SINTEF samplers. However, this does not seem to be the case for Fe and V,

indicating that these metals might be present in airborne dust as other compounds as well.

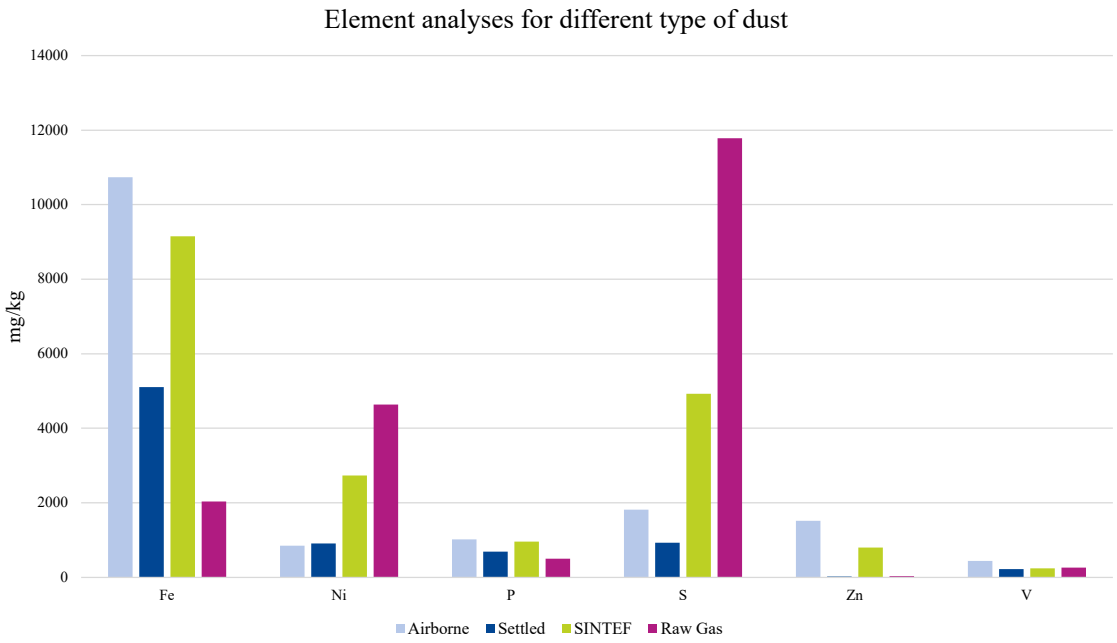

Figure 5.1: Average concentration of some elements found in airborne, settled, filtered and raw gas dust.

Fe was found to be 10 740 mg/kg dust in airborne dust collected from the chimney. This is almost double the amount dust found in settled dust, but quite similar to what was found in airborne filter samples by SINTEF from 2008. By disregarding the samples that were collected almost 15 years ago, it is reasonable to consider other factors influencing the high iron concentrations detected in airborne dust. The large deviation give reason to believe that contamination from the the anode rode is present. It can also be a result from the sampling method where the dust was scraped of a metallic plate inside the chimney, or due to erosion or corrosion from the interior of the chimney. Comparing this with fugitive dust collected at plants without the same type of outlet could be useful.

The ratio between the measured Fe concentrations is observed to correlate well with the P concentration ratio between the different type of dust, given in Figure 5.1. This is consistent with observations made during mapping of chemical composition in SEM where Fe and P particles were found to match well, indicating traces of iron and phosphorous compounds. Ni and S are also usually found with good correlation

in these types of maps. Figure 5.2 and 5.3 show the Ni/S map and Fe/P map of the same area, respectively. These maps show traces of Ni and Fe detected in the same areas indicating particles of nickel and iron compounds. However, previous study performed by this author [7] found Ni and Fe as separate and individual particles when examined in TEM. The intensity of the overlapping colours could therefore indicate what compound is most likely present. The white circles in Figure 5.2 show where nickel is most likely found as a sulfuric compound, while the red areas in Figure 5.3 indicate where iron is most likely present as phosphorous compounds.

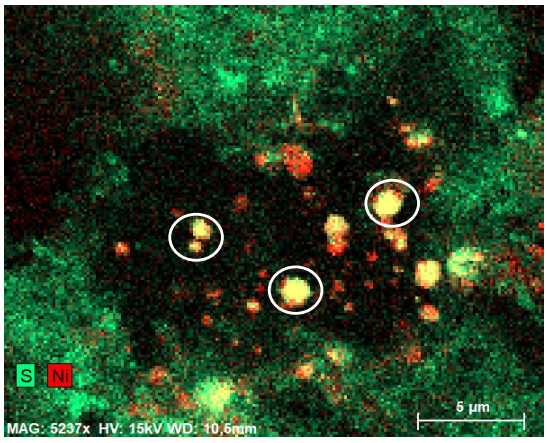

Figure 5.2: S (green) and Ni (red) map.

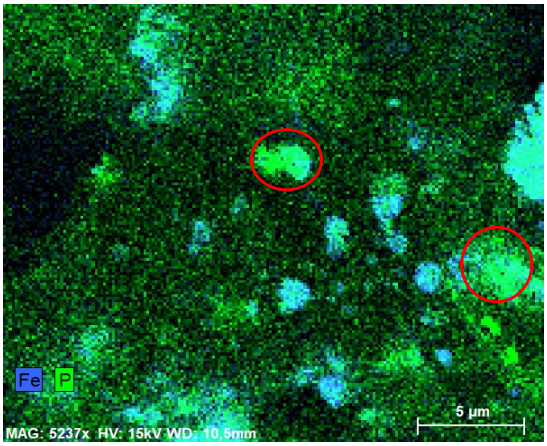

Figure 5.3: Fe (blue) and P (green) map.

Previous study performed by the author [7] found that heavy metals, especially Ni and Fe, were usually located on the surface of carbon particles when analysed in SEM. The same observations are made in this study during point and mapping analyses by means of EDS. this give reason to believe that the particles are a result of high sulfur coke material used in anodes, as reported by Jahrsengene et al. [20]. Including this, Höflich et al. [9] observed larger pieces of carbon particles, which were most likely splinters from anodes, in a potroom particle analysis. This can indicate that high sulfur anode material will not only effect the reactions within the cell, but potentially be a direct cause of higher concentrations of heavy metals in the fugitive emissions and potroom dust. This being said, the significant contrast that occurs between carbon particles and heavy metals when using BSE, might affect what particles are prioritised for such analyses. However, a connection between carbon particles and heavy metals is not to be overlooked, as anode raw material accounts for the majority of pollutants that are introduced to the process.

The major component phases for the dust were found to be corundum, cryolite and chiolite for both settled and airborne dust during XRD analyses. This agrees well

with findings made in a previous study conducted by Wong et al. [26], where the major component phases of dust were found to be a composition of cryolite, chiolite and alumina, amongst others. Considering that XRD only analyses crystalline phases, it is difficult to say anything about the degree of contamination of heavy metals as these fall below the detection limit for this type of characterisation. The most important observation here, is the fact that no significant difference between settled and airborne dust was observed.

5.1.2 Morphology

Looking at the dust in SEM provided information about different levels of coarsity for filter, airborne and settled dust. The dust from filter appears to consist of more sub-micron particles with fume like structure, while the settled dust have more large individual particles. Fume is found in the settled dust as well, but usually as deposition on the surface of large particles. The fume structure is usually found to be high in Al, Na and F concentration during mapping analyses, indicating bath condensates. This correlates well with findings made by Clos et al. [25] where small, spherical bath condensates of Al-Na-F phases, were found in off gas from aluminium production. The authors also reported large unstructured alumina particles and carbon particles, which can clearly be observed in Figure 4.4 for settled dust.

An interesting observation is how the airborne dust appears to be more similar to filter dust at 100x magnification in Figure 4.2. It has a fine structure with occasional larger particle. However, looking at the airborne dust with 1000x magnification, the structure appear to be more similar to settled dust. The airborne was as mentioned collected from inside the chimney at Høyanger. This is also the location of Høyanger's sampling system, and the airborne dust would be expected to be more similar to the filter dust. The differences regarding particle size and structure between filter and airborne dust could give rise to speculations weather the sampling system is able to collect all particle size fractions in the fugitive emissions, or if only the fine particles are captured.

5.2 Particle Size Distribution

This section mainly discuss and compare the results obtained through particle size distribution analyses by laser scattering, surface area by BET, size fraction distribution measured by the sensor system and finally the manually measured particle sizes for carbon particles in airborne and settled dust.

5.2.1 Surface Area

Surface area for settled dust was found to be more than twice the size of airborne dust during BET analyses. Observations made during SEM morphology-analyses proved that settled dust have a coarser structure and often contain more large alumina particles. The porosity and size of alumina particles will contribute to a larger surface area measurement. However, comparing the settled dust to the BET results of primary alumina provided by Hydro, the settled dust is only 1/6 of the alumina surface area.

From the ICP-MS analyses in Table 4.6 the aluminium concentration in settled dust were found to be 72% compared to airborne at 60%. Considering this, it is possible that lower concentrations of alumina also results in lower surface area. If so, this would mean even larger surface area for dust from the gas duct, where aluminium concentration was measured at almost 80%. Surface area analyses for dust from gas duct was unfortunately not conducted during the project assignment, but would be interesting to do for further work.

Porous carbon particles may also be a source for larger surface area. Unfortunately, quantitative analyses of carbon concentration was not included in the ICP-MS analyses. Thus, the differences between airborne, settled and filter regarding carbon concentration are still unclear. However, from the SEM analyses it was observed that larger carbon particles were found in settled dust, which could contribute to larger surface area.

5.2.2 Particle Size Measurements

From the PSD analyses by laser scattering, a difference in size distribution between airborne and settled dust were observed. This was expected due to the results obtained from the SEM morphology-analyses, where the airborne dust appeared to consist of finer particles. However, the average particle size of airborne dust were measured to be around 21 µm which is relatively large. Work performed related to PhD by H. Gaertner [23] found that 2.4 wt% of metallic impurities could be obtained by removing particles above 11 µm. According to the particle size distribution for settled dust, this would mean being left with only 10% of the dust.

By manually measuring carbon particles it was found that settled dust generally contain larger carbon particles than filter and airborne dust. During measurements of settled dust the carbon particles were easy to locate due to contrast and size. However, this might influence the result by omitting small particles from the measurements in favor of the large particles. Carbon particles in filter dust were harder to locate due

to fume structure covering the particles. To be able to detect carbon particles they had to be of a certain size to stand out from the fume. The carbon particles were also often only partly visible which could cause wrongful measurements.

Gaertner [23] reported that impurity content increased with increasing particle size, especially for nickel and iron. Based on this, it would be fair to assume more impurities in settled dust due to the larger particles. From the ICP-MS analyses, Ni and Fe were reported at 910 and 5100 mg/kg, respectively. However, the concentration of Ni and Fe in filter dust collected with the SINTEF samplers were reported to be 2728 and 9150 mg/kg, respectively. In combination with the observation made during manual measurements of carbon particles, this could indicate that the majority of heavy metals is found in the sub-micron range with bath compounds. This can be investigated further with the help of an impactor collecting different size fractions.

5.2.3 Size Fraction Distribution

Whats interesting to see from the PSD analyses, is the large fraction of particle sizes above 10 µm. Typical particle size measured by the sensor systems was found to be around 0.6 µm, compared to 21 µm for airborne dust measured by PSD analyses. PM_{10+} is a fraction which were not possible to measure with the sensor systems which may explain the conflicting results. However, a deviation this large could only be explained by several influential factors. The dust referred to as airborne in this thesis is by definition not airborne in the period of sampling collection, which may influence the results. Dust collected by filters would probably give more accurate results, however gathering enough dust for all these different characterisation methods would take more time than available for this thesis.

No significant difference between typical particle size at roof and floor level were detected by the sensor system in the electrolysis hall. However, when looking at fraction distribution in relation to PM_{10} in Figure 5.4, some differences were observed. PM_4 were found to amount for 98% of PM_{10} at roof level. At floor-level this number were found to be 96%. Although this is not a huge difference, it indicates that a small portion of the dust at floor level belongs to the larger fraction group. A reasonable assumption would be that the larger particles eventually ends up as settled dust. This correlates well with observations found by Wong et al. [4], where coarser dust tended to settle at surfaces. The authors found that particles decreased in size at increasing heights and bath fumes were the domination contributor to fines at roof level. The opportunity to measure floor level emissions with a PM_{10+} detector would be highly interesting in this case, and comparing the size distribution observations obtained from SEM and PSD analyses.

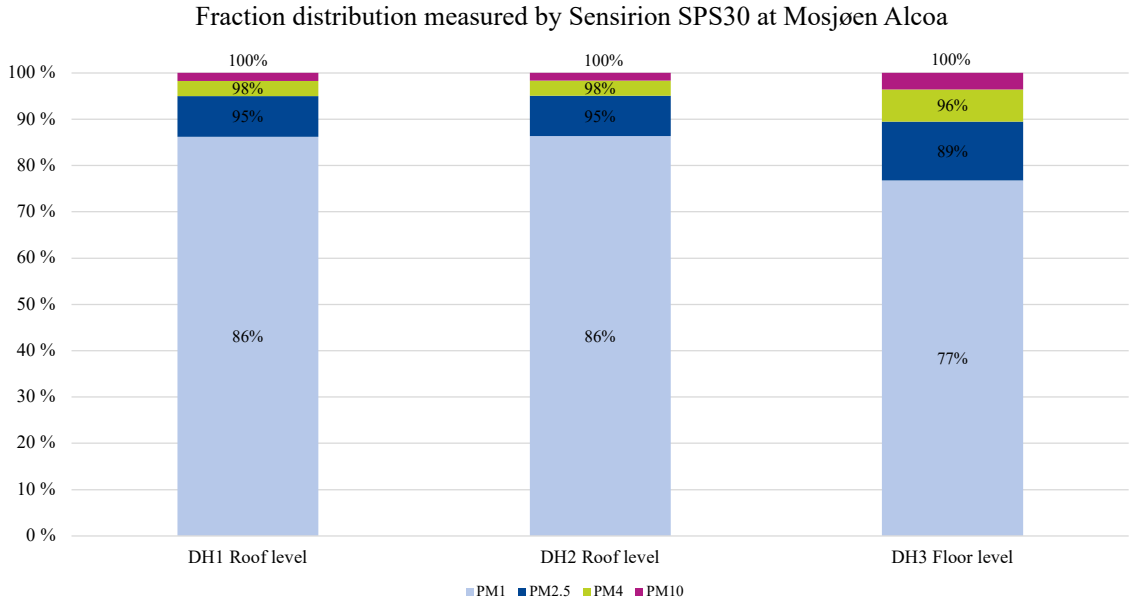

Figure 5.4: Fraction distribution between PM1, PM2.5, PM4 and PM10 measured by the three sensor systems in an aluminium electrolysis hall.

5.3 Emission Data and Operational activities

This section will discuss the observations achieved from the sensor systems. This includes temperature and humidity measurements, PM emissions related to specific operational activities as well as differences in PM emissions at roof and floor level.

5.3.1 Temperature and Humidity measurements

The temperature measurements at roof and floor level show the same trends in variation with an average of 10 °C colder at floor level. An attempt to see a connection between temperature variations and PM emissions was made. However, for such a short period of time, no correlating observations were possible to find. This would be an interesting study for a period covering several seasons and different weather conditions.

The humidity measurements correlates well between the sensors as well as with the temperature measurements. An attempt to compare emission data and humidity was also performed. However, the same observations made when comparing with temperature, were seen with humidity. No specific correlation between emissions and humidity were found.

5.3.2 Production Activities

By plotting the different processes, anode change, tapping and temperature measurements and the time they were performed in the emission concentration plot, it was possible to connect specific activities with emission trends in the hall. The documented anode change is observed to occur at a time when some of the highest concentrations of dust and particulate matter are measured, seen in Figure 4.26. This agrees with observations made by Wong et al. [26] during a 24 hour case study. By examining sources of fugitive dust emissions anode change were found to be the main contributor to fugitive roof emissions, followed by metal tapping and covering of anodes.

During tapping, the emissions are observed to be generally lower than for anode change. Tapping require two lids to be removed and only a small portion of the bath is exposed, compared to anode change where four lids are removed. The latter process also cause more exposed bath which tends to evaporate. However, a big contributor to emissions, is the process of covering anodes which usually causes significant amount of dusting. Covering is not performed to the same degree for anode change and tapping and might explain the difference regarding emissions for the two processes. The temperature measurements usually causes low emissions, however this may also vary depending on location of sensor versus location of measurements.

The emissions at floor level is generally low. It does not appear to be any clear indication that events measured by the roof level sensors are also detected at floor level. In Figure 4.28, PM emissions at about 2300 $\mu g/m^3$ were detected at floor level. This differs from the other measurements and is equal to more than four times higher than the second highest emission concentration measured during the time period 9-17th of may at floor level. None of the standard operational data provided by Alcoa correlates with this high peak, and might be a result of other more infrequent activities. This event does not seem to be reflected at roof level, which might indicate a local swirl of dust caused by housekeeping or transportation close to the sensor.

During anode change, the main fraction of the emissions appeared to consist of $PM_{2.5}$ compared to tapping, where emissions mainly consisted of PM_{10}. Myklebust et al. [6] reported large amounts of fine dust during anode change and a clear difference with coarser dust during covering of anodes. This was not observed in Figure 4.29 when investigating size fractions during anode change. However, the authors reported data and measurements over two days which might give a better overview of when different events during the operational processes occur. For this thesis, the measurements lasted for three weeks. When comparing with operational data, the only information available was i.e when the anode changes were performed. This means that no specific

information of when the crust breaking before, or anode covering after anode change, was provided. Nor was any information on any incidents that may have caused delays or increased emissions provided.

According to Wong et al. [4] coarse dust is usually associated with ACM or feed alumina. Emissions of coarse dust tend to occur during processes such as anode covering by crane. Therefore, PM_{10} being the large fraction of emissions related to metal tapping, was not expected. However, in Figure 5.5, the two first emission peaks are located approximately 30-20 min after the tapping started. This could be explained by the fact that when the tapping process is done, the tapping lid is removed from the crucible. Before the crucible is covered and transported out of the hall, it will be open and often vaporise and cause PM emissions in the hall. ACM and bath are often siphoned off with the metal, which often leads to a greater degree of vaporization from the crucible. This might also be the source of PM_{10} emissions.

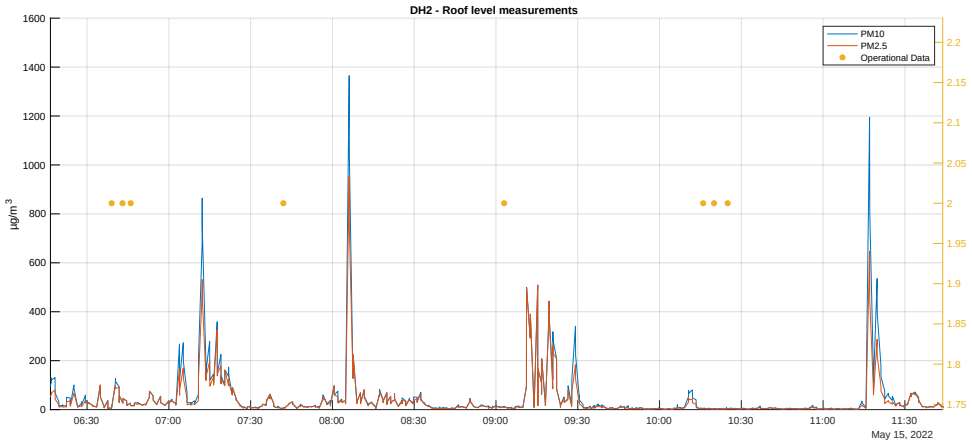

Figure 5.5: PM10 and PM2.5 emissions during metal tapping measured at roof level.

Chapter 6

Conclusion

Fugitive dust emissions from two Norwegian aluminium smelters were investigated by different characterisation methods and in-situ particulate matter emission measurements. Both settled and airborne dust mainly from Hydro Høyanger, were characterised by means of BET, SEM, XRD and particle size distribution analyser. In addition to this, ICP-MS analyses were performed by external lab ALS Scandinavia. PM emissions were measured for three weeks at Alcoa's plant in Mosjøen by optical PM sensors based on laser scattering technology. The sensors measured temperature and humidity, number concentration and mass concentration for $PM_{1.0}$, $PM_{2.5}$, $PM_{4.0}$ and PM_{10}.

By comparing the chemical composition analyses performed by means of ICP-MS and SEM with the authors previous work, it appears that most Ni ends up in the GTC. The high concentration of Fe in airborne dust gives reason to believe that it most likely originates from several sources as well as anode material. Further, important observations found during these analyses were:

- Heavy metals such as Ni and Fe were found to be mainly located as inclusions or at the surface of carbon particles.
- Ni and Fe appears to be present as phosphorous or sulfuric compounds and the former is believed to occasionally be present as nickel sulfide.

When examining the morphology of filter, airborne and settled dust in SEM, it was found that dust collected on filter consists mainly of sub-micron particles with fume structure, rich in Al, Na and F. The settled dust were found to consists of large individual particles which often are identified as alumina or carbon.

From the particle size analyses and measurements, it was found that large parts of the airborne and settled dust collected manually, had a particle size above PM_{10}.

Carbon particles in filter, airborne and settled dust were also found with a particle size mainly above PM_{10}.

- Average particle size of airborne and settled dust by means of PSD analyser were found to be approximately 21 µm and 35 µm, respectively.
- The average size fraction of particles measured with sensor systems were found to be around 0,6 µm at roof and floor level.
- Average particle size for carbon particles measured in filter, airborne and settled dust were found to be 36 µm, 34 µm, 85 µm, respectively.

By measuring particulate emissions with Sensirion SPS30 measurement system at Alcoa Mosjøen, a correlation between specific operational activities and increased emissions were observed. It was found that:

- Anode change cause short periods of increased emissions in the hall and usually contribute to higher emissions than tapping and temperature measurements.
- Emissions at floor level is usually very low and does not seem to be affected by operational activities to the same extent as at roof level.
- Emissions produced during anode change mainly consists of $PM_{2.5}$, while emissions produced during metal tapping mainly consists of PM_{10}.

6.1 Further Work

Based on results and observations obtained from this work, following research activities would be relevant for further work:

- Analyse distribution of heavy metals between different size fractions of fugitive dust by means of an impactor.

By collecting fugitive potroom dust with i.e a three stage impactor, it would be possible to characterise different size fractions of the dust. This could give more information of heavy metals behaviour in fugitive emissions and dispersion to the environment.

- Measure PM_{10+} emissions in the electrolysis hall.

As observed in this study, a large part of the potroom dust contain particles above PM_{10}. With a sensor system that can measure this fraction, it would be possible to learn more about how PM_{10+} particles behave in the potroom, as well as what operational activities that can be contected to these emissions.

- Collect enough filter dust to characterise by means of several characterisation methods.

Several of the characterisation methods used in this study require a certain amount of dust. Collecting enough airborne dust will take time, but will however contribute to a better understanding of the behaviour of the fine dust fraction in fugitive emissions.

- Analyse carbon concentration in fugitive emissions by means of LECO.

It would be interesting to study the amount of carbon in fugitive dust emissions, as heavy metals are often associated with carbon particles.

- Characterise and compare fugitive dust from Alcoa Mosjøen with Hydro Høyanger.

By comparing the composition of dust from different production plants, it would be possible to detect any differences that may occur. This will contribute to adapting and introducing measures to reduce heavy metal emissions, and will only be possible by continuing the collaboration and transparency between companies within the industry.

Bibliography

[1] S. Prasad. Studies on the hall-heroult aluminum electrowinning process. 2000. Journal of the Brazilian Chemical Society.

[2] V. Gusberti, D. Severo, B. Welch, and M. Skyllas-Kazacos. Modelling the aluminium smelting cell mass and energy balance- a tool based on the 1 st. law of thermodynamics. In *Light Metals 2012*, pages 929–934. Springer International Publishing.

[3] Å. Sterten, P. A. Solli, and E. Skybakmoen. Influence of electrolyte impurities on current efficiency in aluminium electrolysis cells. In *Journal of Applied Electrochemistry*, volume 28, pages 781–789. 1998.

[4] D. S. Wong, N. I. Tjahyono, and M. M. Hyland. The nature of particles and fines in potroom dust. In *Light Metals 2014*, pages 553–558. Springer International Publishing.

[5] D. S. Wong. Sources of potroom dust emissions from aluminium smelters. Technical report, 2013. The University of Auckland.

[6] H. A. H. O. Myklebust, T. A. Aarhaug, and G. Tranell. Measurement system for fugitive emissions in primary aluminium electrolysis. In *Light Metals 2020*, pages 735–743. Springer International Publishing.

[7] F. Müller. Heavy metal emissions from primary aluminium production. Technical report, 2021. NTNU.

[8] T. A. Aarhaug and A. P. Ratvik. Aluminium primary production off-gas composition and emissions: An overview. In *JOM*, volume 71, pages 2966–2977. 2019, Springer US.

[9] B. L. W. Höflich, S. Weinbruch, R. Theissmann, H. Gorzawski, M. Ebert, H. M. Ortner, A. Skogstad, D. G. Ellingsen, P. A. Drabløs, and Y. Thomassen. Characterization of individual aerosol particles in workroom air of aluminium

smelter potrooms. In *Journal of Environmental Monitoring*, volume 7, pages 419–424. 2005, Royal Society of Chemistry.

[10] H. A. H. O Myklebust. Fume formation and measurements in the metal-production industry. Technical report, 2021. NTNU, ISSN: 2703-8084.

[11] Norsk Industri. Om aluminiumsbransjen, 2022. Accessed: 28.04.2022. [Online]. Available: `https://www.norskindustri.no/bransjer/aluminium/om-aluminiumsbransjen/`.

[12] M. L. Sall, A. K. D. Diaw, D. Gningue-Sall, S. E. Aaron, and J. Aaron. Toxic heavy metals: impact on the environment and human health, and treatment with conducting organic polymers, a review. In *Environmental Science and Pollution Research*, volume 27, pages 29927–29942. 2020.

[13] A. T. Tabereaux and R. D. Peterson. Chapter 2.5 - aluminum production. In *Treatise on Process Metallurgy*, pages 839–917. Elsevier, 2014. https://doi.org/10.1016/B978-0-08-096988-6.00023-7.

[14] R. Lumley. *Fundamentals of Aluminium Metallurgy: Production, Processing and Applications*. Elsevier Science & Technology. 2010, ISBN:978-1-84569-654-2.

[15] G. Jahrsengene. Coke impurity characterisation and electrochemical performance of carbon anodes for aluminium production. Technical report, 2019. NTNU, ISBN : 9788232643004.

[16] L. Edwards, N. Backhouse, H. Darmstadt, and M. Dion. Evolution of anode grade coke quality. In *Light Metals 2012*, pages 1207–1212. Springer International Publishing.

[17] L. Edwards. The history and future challenges of calcined petroleum coke production and use in aluminum smelting. In *JOM*, volume 67, pages 308–321. 2015. https://doi.org/10.1007/s11837-014-1248-9.

[18] G. Jahrsengene, H. C. Wells, A. P. Rørvik, S.and Ratvik, R. G. Haverkamp, and A. M. Svensson. A XANES study of sulfur speciation and reactivity in cokes for anodes used in aluminum production. In *Metallurgical and Materials Transactions B*, volume 49, pages 1434–1443. 2018. https://doi.org/10.1007/s11663-018-1215-x.

[19] G. Jahrsengene, S. Rørvik, A. P. Ratvik, L. P. Lossius, R. G. Haverkamp, and A. M. Svensson. Reactivity of coke in relation to sulfur level and microstructure. In *Light Metals 2019*, pages 1247–1253. Springer International Publishing.

[20] G. Jahrsengene, H. C. Wells, C. Sommerseth, A. P. Ratvik, L. P. Lossius, K. H. Sizeland, P. Kappen, A. M. Svensson, and R. G. Haverkamp. An EXAFS and XANES study of v, ni, and fe speciation in cokes for anodes used in aluminum production. In *Metallurgical and Materials Transactions B*, volume 50, pages 2969–2981. 2019. https://doi.org/10.1007/s11663-019-01676-z.

[21] S. Kalyavina, A. P. Ratvik, and T. A. Aarhaug. Impurities in raw gas and secondary alumina. In *Light Metals 2013*, pages 195–200. Springer International Publishing.

[22] E. Haugland, G. M. Haarberg, E. Thisted, and J. Thonstad. The behaviour of phosphorus impurities in aluminium electrolysis cells. In *Essential Readings in Light Metals: Volume 2 Aluminum Reduction Technology*, pages 229–233. Springer International Publishing, 2016.

[23] H. Gaertner. Characteristics of particulate emissions from aluminium electrolysis cells. Technical report, 2013. NTNU, ISBN:978-82-471-4764-1.

[24] D. S. Wong, N. I. Tjahyono, and M. M. Hyland. Visualising the sources of potroom dust in aluminium smelters. In *Light Metals 2012*, pages 833–838. Springer International Publishing.

[25] D. P. Clos, P. Nekså, S. G. Johnsen, and R. E Aune. Investigation of scale formation in aluminium industry by means of a cold-finger. In *Light Metals 2019*, pages 707–719. Springer International Publishing.

[26] D. S. Wong, M. M. Hyland, N. I. Tjahyono, and D. Cotton. Potroom operations contributing to fugitive roof dust emissions from aluminium smelters. In *Light Metals 2019*, pages 905–912. Springer International Publishing.

[27] M.M. Hyland and M.P. Taylor. Origins and effects of potroom dust. In *Light Metals 2005*, pages 141–145. Springer International Publishing.

[28] United States Environmental Protection Agency. Health and environmental effects of particulate matter (PM), 2016. Accessed: 19.04.2022. [Online]. Available: `https://www.epa.gov/pm-pollution/health-and-environmental-effects-particulate-matter-pm`.

[29] Miljødirektoratet. Om miljødirektoratet, 2022. Accessed: 28.04.2022. [Online]. Available: `https://www.miljodirektoratet.no/om-oss/`.

[30] Miljødirektoratet og Statistisk Sentralbyråd. Landbasert industri, 2022. Accessed: 28.04.2022. [Online]. Available: `https://www.norskeutslipp.no/no/Landbasert-industri/?SectorID=600`.

[31] Værstasjon. Mosjøen, kulstaddalen, 2022. Accessed: 31.04.2022. [Online]. Available: `https://kulstaddalen.no/wxabout.php`.

Chapter 7

Appendices

A BET

Sample: prøve1
Operator:
Submitter:
File: C:\data\Fride M\1.SMP

Started:	4/5/2022 9:51:00 AM	Analysis adsorptive:	N2
Completed:	4/5/2022 5:37:32 PM	Analysis bath temp.:	-195,898 °C
Report time:	4/5/2022 5:56:32 PM	Thermal correction:	Yes
Sample mass:	0,2560 g	Ambient free space:	16,3455 cm³ Measured
Analysis free space:	57,7940 cm³	Equilibration interval:	10 s
Low pressure dose:	None	Sample density:	1,000 g/cm³
Automatic degas:	Yes		

Comments: Fra takvent tilsendt fra industri, prøve 1. gul avsetting på glass

Sample prep: Stage	Temperature (°C)	Ramp Rate (°C/min)	Time (min)
1	30	10	10
2	90	10	60
3	250	10	820
4	25	10	60

Summary Report

Surface Area

Single point surface area at p/p° = 0,300067047: 3,5578 m²/g

BET Surface Area: 3,7329 m²/g

Pore Volume

Single point desorption total pore volume of pores less than 1 929,241 Å diameter at p/p° = 0,989971592: 0,021553 cm³/g

Pore Size

Adsorption average pore diameter (4V/A by BET): 230,945 Å

Desorption average pore diameter (4V/A by BET): 230,945 Å

Sample: prøve1
Operator:
Submitter:
File: C:\data\Fride M\1.SMP

Started: 4/5/2022 9:51:00 AM
Completed: 4/5/2022 5:37:32 PM
Report time: 4/5/2022 5:56:32 PM
Sample mass: 0,2560 g
Analysis free space: 57,7940 cm³
Low pressure dose: None
Automatic degas: Yes

Analysis adsorptive: N2
Analysis bath temp.: -195,898 °C
Thermal correction: Yes
Ambient free space: 16,3455 cm³ Measured
Equilibration interval: 10 s
Sample density: 1,000 g/cm³

Comments: Fra takvent tilsendt fra industri, prøve 1. gul avsetting på glass

Sample prep: Stage	Temperature (°C)	Ramp Rate (°C/min)	Time (min)
1	30	10	10
2	90	10	60
3	250	10	820
4	25	10	60

Isotherm Tabular Report

Relative Pressure (p/p°)	Absolute Pressure (mmHg)	Quantity Adsorbed (cm³/g STP)	Elapsed Time (h:min)	Saturation Pressure (mmHg)
			01:52	748.194153
0.009969441	7.482910	0.3977	02:14	750.584717
0.029565259	22.210293	0.5738	02:34	751.229431
0.059566127	44.748497	0.7132	02:42	751.240662
0.079630670	59.807484	0.7814	02:47	751.060913
0.099784699	74.921432	0.8290	02:51	750.830872
0.119870382	90.013687	0.8749	02:56	750.925171
0.139692313	104.894066	0.9161	03:01	750.893616
0.159563871	119.823799	0.9543	03:04	750.945679
0.179585998	134.896729	0.9899	03:09	751.153931
0.199542997	149.868896	1.0209	03:12	751.060669
0.249386228	187.293137	1.0948	03:14	751.016357
0.300067047	225.385406	1.1678	03:17	751.116821
0.349325136	262.359253	1.2385	03:20	751.046021
0.399580963	300.132080	1.3118	03:23	751.117065
0.449581465	337.592133	1.3871	03:26	750.903137
0.499391476	375.167603	1.4643	03:29	751.249512
0.549299134	412.735504	1.5472	03:32	751.385681
0.599622238	450.274323	1.6446	03:34	750.929993
0.622969837	467.805328	1.6934	03:37	750.927734
0.646551543	485.639923	1.7486	03:40	751.123291
0.670171203	503.463989	1.8128	03:43	751.246826
0.694988354	521.948853	1.8843	03:47	751.018127
0.719739556	540.779724	1.9615	03:50	751.354736
0.744386555	559.204407	2.0546	03:52	751.228516
0.768849247	577.414185	2.1739	03:55	751.010925
0.793038760	595.611267	2.3255	03:58	751.049377
0.816791834	613.635803	2.5156	04:01	751.275635
0.841237418	631.950806	2.7817	04:04	751.215759
0.865227411	649.792175	3.1568	04:07	751.007385
0.888234571	667.158386	3.6558	04:10	751.106079
0.911568576	684.563965	4.3048	04:13	750.973633
0.932541177	700.300232	5.1136	04:16	750.959045
0.952693846	715.647522	6.3351	04:19	751.183105
0.972037809	729.916504	8.6685	04:22	750.913696
0.978977333	735.155212	10.2217	04:26	750.942017
0.989971592	743.412109	13.9087	04:29	750.942871
0.980541203	736.409485	12.1535	04:33	751.023499

Sample: prøve1
Operator:
Submitter:
File: C:\data\Fride M\1.SMP

Started: 4/5/2022 9:51:00 AM
Completed: 4/5/2022 5:37:32 PM
Report time: 4/5/2022 5:56:32 PM
Sample mass: 0,2560 g
Analysis free space: 57,7940 cm³
Low pressure dose: None
Automatic degas: Yes

Analysis adsorptive: N2
Analysis bath temp.: -195,898 °C
Thermal correction: Yes
Ambient free space: 16,3455 cm³ Measured
Equilibration interval: 10 s
Sample density: 1,000 g/cm³

Comments: Fra takvent tilsendt fra industri, prøve 1. gul avsetting på glass

Sample prep: Stage	Temperature (°C)	Ramp Rate (°C/min)	Time (min)
1	30	10	10
2	90	10	60
3	250	10	820
4	25	10	60

Isotherm Tabular Report

Relative Pressure (p/p°)	Absolute Pressure (mmHg)	Quantity Adsorbed (cm³/g STP)	Elapsed Time (h:min)	Saturation Pressure (mmHg)
0.825233898	619.472473	3.5676	04:54	750.662903
0.799659504	600.087158	3.1525	04:57	750.428345
0.774979955	581.793213	2.8272	05:00	750.720337
0.750838843	563.487000	2.5760	05:02	750.476624
0.727178325	545.673035	2.3808	05:06	750.397827
0.703161600	527.863464	2.2226	05:11	750.700073
0.680113504	510.341125	2.0944	05:14	750.376404
0.656095968	492.537659	1.9813	05:17	750.709778
0.632670630	474.741730	1.8934	05:20	750.377380
0.608735091	456.902649	1.8039	05:23	750.577148
0.584482755	438.622986	1.7237	05:26	750.446411
0.549881709	412.821075	1.6235	05:29	750.745239
0.500761753	375.674713	1.5073	05:32	750.206482
0.450518401	337.975555	1.3753	05:36	750.192566
0.400215861	300.331055	1.2885	05:39	750.422668
0.350281786	262.757904	1.2101	05:42	750.132935
0.300272272	225.310043	1.1354	05:45	750.352478
0.250251874	187.763123	1.0585	05:48	750.296570
0.200362198	150.346222	0.9735	05:51	750.372192
0.140393115	105.337784	0.8694	05:55	750.305908

Sample: prøve1
Operator:
Submitter:
File: C:\data\Fride M\1.SMP

Started:	4/5/2022 9:51:00 AM	Analysis adsorptive:	N2
Completed:	4/5/2022 5:37:32 PM	Analysis bath temp.:	-195,898 °C
Report time:	4/5/2022 5:56:32 PM	Thermal correction:	Yes
Sample mass:	0,2560 g	Ambient free space:	16,3455 cm³ Measured
Analysis free space:	57,7940 cm³	Equilibration interval:	10 s
Low pressure dose:	None	Sample density:	1,000 g/cm³
Automatic degas:	Yes		

Comments: Fra takvent tilsendt fra industri, prøve 1. gul avsetting på glass

Sample prep: Stage	Temperature (°C)	Ramp Rate (°C/min)	Time (min)
1	30	10	10
2	90	10	60
3	250	10	820
4	25	10	60

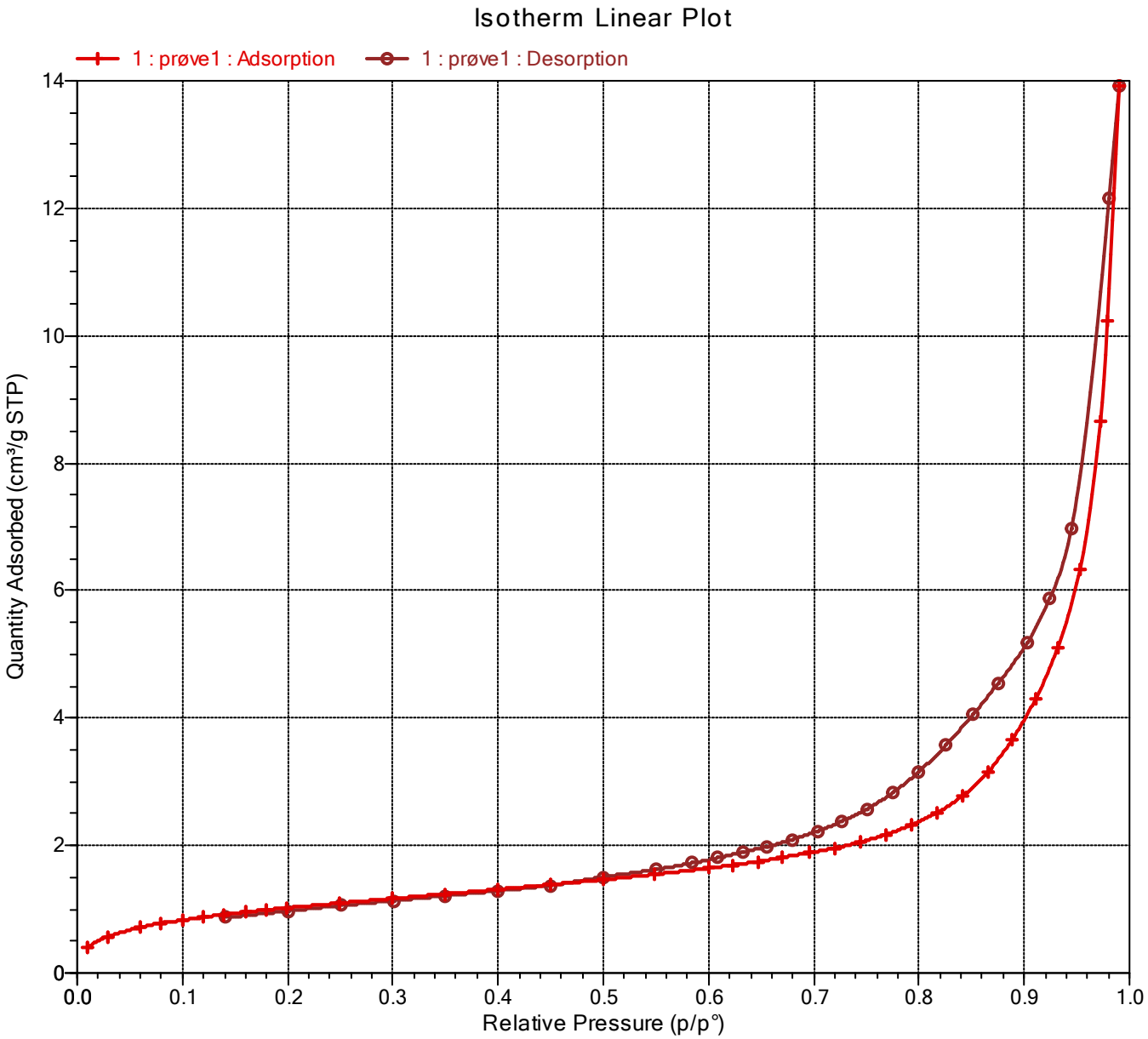

Sample: prøve1
Operator:
Submitter:
File: C:\data\Fride M\1.SMP

Started: 4/5/2022 9:51:00 AM
Completed: 4/5/2022 5:37:32 PM
Report time: 4/5/2022 5:56:32 PM
Sample mass: 0,2560 g
Analysis free space: 57,7940 cm³
Low pressure dose: None
Automatic degas: Yes

Analysis adsorptive: N2
Analysis bath temp.: -195,898 °C
Thermal correction: Yes
Ambient free space: 16,3455 cm³ Measured
Equilibration interval: 10 s
Sample density: 1,000 g/cm³

Comments: Fra takvent tilsendt fra industri, prøve 1. gul avsetting på glass

Sample prep: Stage	Temperature (°C)	Ramp Rate (°C/min)	Time (min)
1	30	10	10
2	90	10	60
3	250	10	820
4	25	10	60

BET Report

BET surface area: 3,7329 ± 0,0374 m²/g
Slope: 1,148053 ± 0,011507 g/cm³ STP
Y-intercept: 0,017937 ± 0,002005 g/cm³ STP
C: 65,005053
Qm: 0,8576 cm³/g STP
Correlation coefficient: 0,9995984
Molecular cross-sectional area: 0,1620 nm²

Relative Pressure (p/p°)	Quantity Adsorbed (cm³/g STP)	1/[Q(p°/p - 1)]
0.059566127	0.7132	0.088807
0.079630670	0.7814	0.110725
0.099784699	0.8290	0.133702
0.119870382	0.8749	0.155673
0.139692313	0.9161	0.177241
0.159563871	0.9543	0.198945
0.179585998	0.9899	0.221127
0.199542997	1.0209	0.244182
0.249386228	1.0948	0.303471
0.300067047	1.1678	0.367100

Sample: prøve1
Operator:
Submitter:
File: C:\data\Fride M\1.SMP

Started:	4/5/2022 9:51:00 AM	Analysis adsorptive:	N2
Completed:	4/5/2022 5:37:32 PM	Analysis bath temp.:	-195,898 °C
Report time:	4/5/2022 5:56:32 PM	Thermal correction:	Yes
Sample mass:	0,2560 g	Ambient free space:	16,3455 cm³ Measured
Analysis free space:	57,7940 cm³	Equilibration interval:	10 s
Low pressure dose:	None	Sample density:	1,000 g/cm³
Automatic degas:	Yes		

Comments: Fra takvent tilsendt fra industri, prøve 1. gul avsetting på glass

Sample prep: Stage	Temperature (°C)	Ramp Rate (°C/min)	Time (min)
1	30	10	10
2	90	10	60
3	250	10	820
4	25	10	60

BET Surface Area Plot

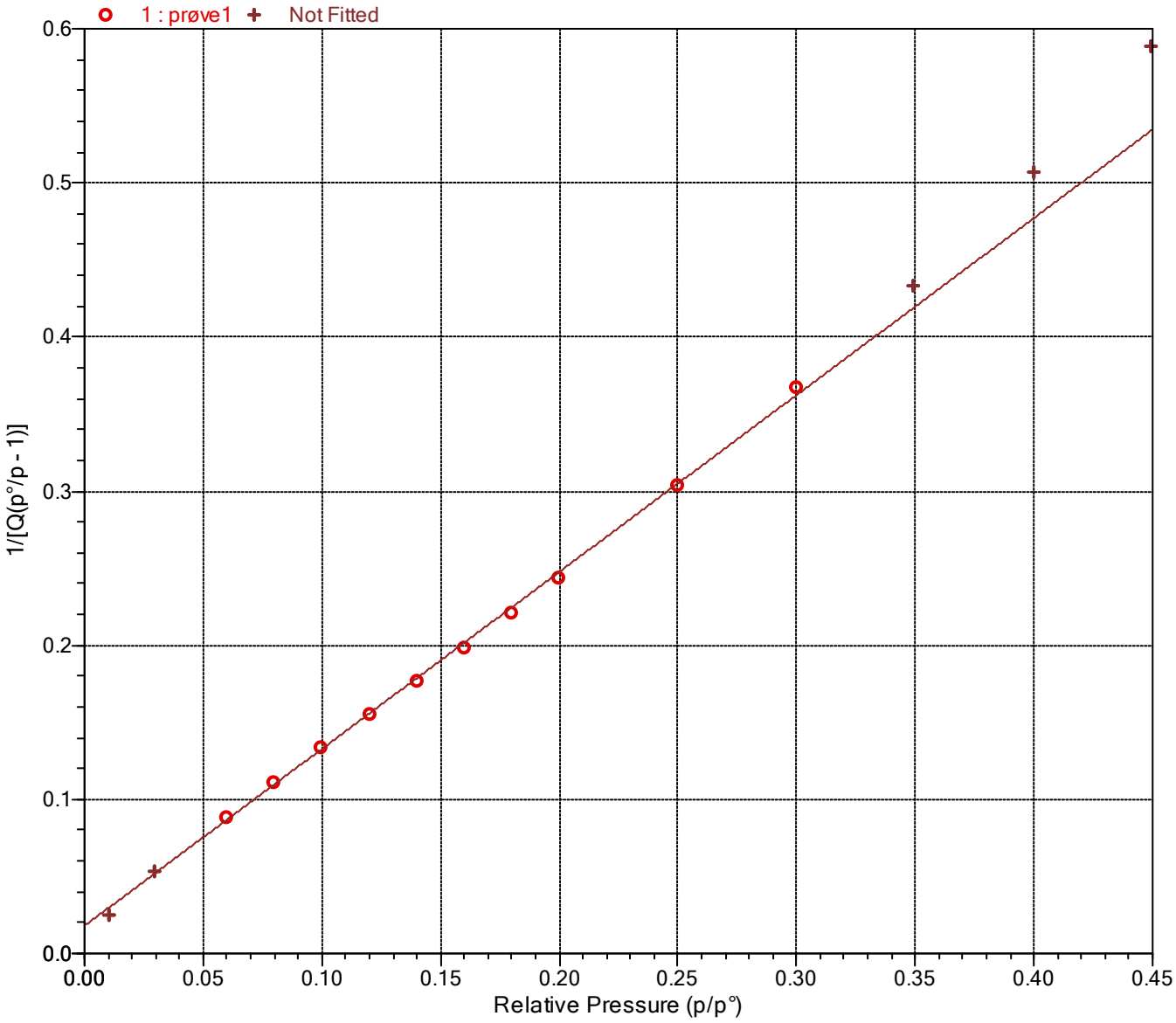

Sample: prøve1
Operator:
Submitter:
File: C:\data\Fride M\1.SMP

Started:	4/5/2022 9:51:00 AM	Analysis adsorptive:	N2
Completed:	4/5/2022 5:37:32 PM	Analysis bath temp.:	-195,898 °C
Report time:	4/5/2022 5:56:32 PM	Thermal correction:	Yes
Sample mass:	0,2560 g	Ambient free space:	16,3455 cm³ Measured
Analysis free space:	57,7940 cm³	Equilibration interval:	10 s
Low pressure dose:	None	Sample density:	1,000 g/cm³
Automatic degas:	Yes		

Comments: Fra takvent tilsendt fra industri, prøve 1. gul avsetting på glass

Sample prep: Stage	Temperature (°C)	Ramp Rate (°C/min)	Time (min)
1	30	10	10
2	90	10	60
3	250	10	820
4	25	10	60

BET Isotherm Plot

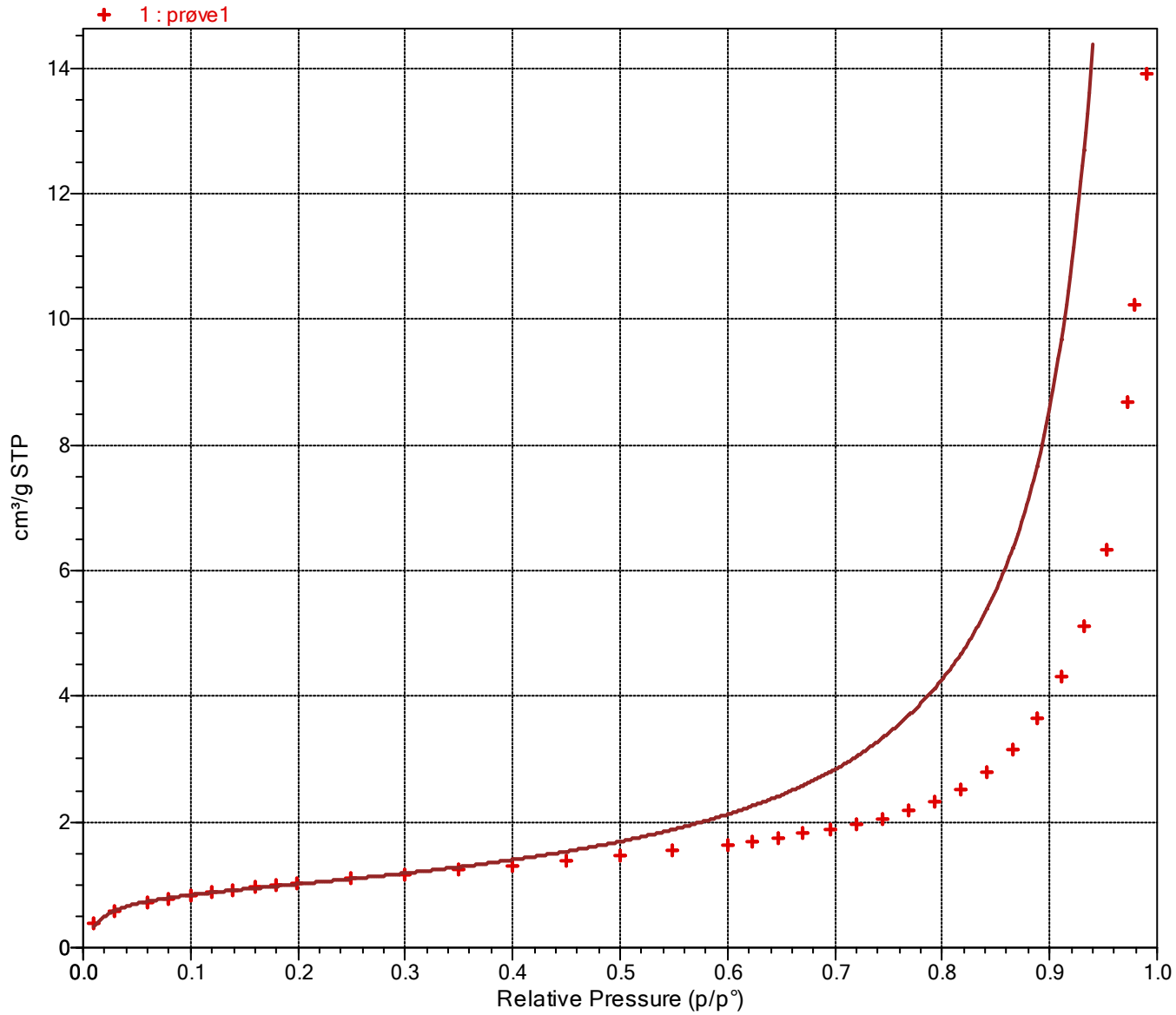

Sample: prøve1
Operator:
Submitter:
File: C:\data\Fride M\1.SMP

Started:	4/5/2022 9:51:00 AM	Analysis adsorptive:	N2
Completed:	4/5/2022 5:37:32 PM	Analysis bath temp.:	-195,898 °C
Report time:	4/5/2022 5:56:32 PM	Thermal correction:	Yes
Sample mass:	0,2560 g	Ambient free space:	16,3455 cm³ Measured
Analysis free space:	57,7940 cm³	Equilibration interval:	10 s
Low pressure dose:	None	Sample density:	1,000 g/cm³
Automatic degas:	Yes		

Comments: Fra takvent tilsendt fra industri, prøve 1. gul avsetting på glass

Sample prep: Stage	Temperature (°C)	Ramp Rate (°C/min)	Time (min)
1	30	10	10
2	90	10	60
3	250	10	820
4	25	10	60

t-Plot Report

Micropore volume:	-0,000249 cm³/g
Micropore area:	*
External surface area:	4,1857 m²/g
Slope:	0,270115 ± 0,006859 cm³/g·Å STP
Y-intercept:	-0,160462 ± 0,027868 cm³/g STP
Correlation coefficient:	0,998071
Surface area correction factor:	1,000
Density conversion factor:	0,0015496
Total surface area (BET):	3,7329 m²/g
Thickness range:	3,5000 to 5,0000 Å
Thickness equation:	Harkins and Jura

Thickness Curve

$$t = [\ 13.99 / (\ 0.034 - \log(p/p^\circ)\ )\ ]^{\wedge} 0.5$$

t-Plot Report - Data

Relative Pressure (p/p°)	Statistical Thickness (Å)	Quantity Adsorbed (cm³/g STP)	Fitted
0.059566127	3.3335	0.7132	
0.079630670	3.5141	0.7814	*
0.099784699	3.6766	0.8290	*
0.119870382	3.8269	0.8749	*
0.139692313	3.9673	0.9161	*
0.159563871	4.1029	0.9543	*
0.179585998	4.2358	0.9899	*
0.199542997	4.3659	1.0209	*
0.249386228	4.6859	1.0948	*
0.300067047	5.0126	1.1678	
0.349325136	5.3391	1.2385	
0.399580963	5.6881	1.3118	
0.449581465	6.0581	1.3871	
0.499391476	6.4569	1.4643	
0.549299134	6.8959	1.5472	
0.599622238	7.3907	1.6446	
0.622969837	7.6423	1.6934	
0.646551543	7.9135	1.7486	
0.670171203	8.2049	1.8128	
0.694988354	8.5356	1.8843	

* The micropore area is not reported because either the micropore volume is negative or the calculated external surface area is larger than the total surface area.

Sample: prøve1
Operator:
Submitter:
File: C:\data\Fride M\1.SMP

Started:	4/5/2022 9:51:00 AM	Analysis adsorptive:	N2
Completed:	4/5/2022 5:37:32 PM	Analysis bath temp.:	-195,898 °C
Report time:	4/5/2022 5:56:32 PM	Thermal correction:	Yes
Sample mass:	0,2560 g	Ambient free space:	16,3455 cm³ Measured
Analysis free space:	57,7940 cm³	Equilibration interval:	10 s
Low pressure dose:	None	Sample density:	1,000 g/cm³
Automatic degas:	Yes		

Comments: Fra takvent tilsendt fra industri, prøve 1. gul avsetting på glass

Sample prep: Stage	Temperature (°C)	Ramp Rate (°C/min)	Time (min)
1	30	10	10
2	90	10	60
3	250	10	820
4	25	10	60

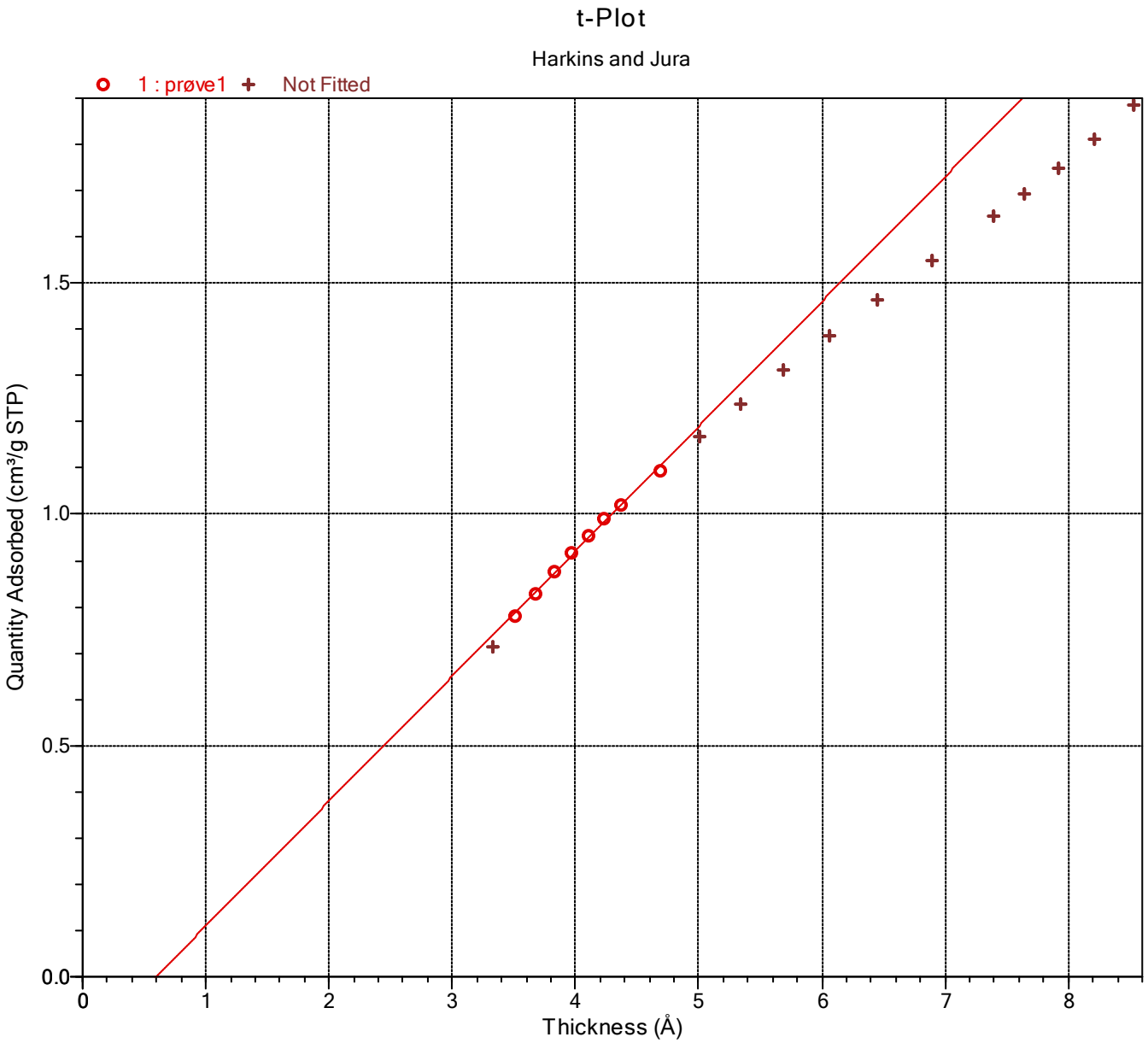

Sample: prøve1
Operator:
Submitter:
File: C:\data\Fride M\1.SMP

Started: 4/5/2022 9:51:00 AM
Completed: 4/5/2022 5:37:32 PM
Report time: 4/5/2022 5:56:32 PM
Sample mass: 0,2560 g
Analysis free space: 57,7940 cm³
Low pressure dose: None
Automatic degas: Yes

Analysis adsorptive: N2
Analysis bath temp.: -195,898 °C
Thermal correction: Yes
Ambient free space: 16,3455 cm³ Measured
Equilibration interval: 10 s
Sample density: 1,000 g/cm³

Comments: Fra takvent tilsendt fra industri, prøve 1. gul avsetting på glass

Sample prep: Stage	Temperature (°C)	Ramp Rate (°C/min)	Time (min)
1	30	10	10
2	90	10	60
3	250	10	820
4	25	10	60

BJH Adsorption Pore Distribution Report

Faas Correction
Harkins and Jura
$t = [13.99 / (0.034 - \log(p/p°))]^{0.5}$

Diameter range: 17,000 to 3 000,000 Å
Adsorbate property factor: 9,53000 Å
Density conversion factor: 0,0015496
Fraction of pores open at both ends: 0,00

Pore Diameter Range (Å)	Average Diameter (Å)	Incremental Pore Volume (cm³/g)	Cumulative Pore Volume (cm³/g)	Incremental Pore Area (m²/g)	Cumulative Pore Area (m²/g)
1926.3 - 930.1	1113.4	0.006068	0.006068	0.218	0.218
930.1 - 703.9	785.3	0.002600	0.008668	0.132	0.350
703.9 - 422.2	494.3	0.004024	0.012692	0.326	0.676
422.2 - 299.4	339.5	0.002136	0.014829	0.252	0.928
299.4 - 230.4	255.5	0.001424	0.016252	0.223	1.151
230.4 - 183.5	201.3	0.001147	0.017400	0.228	1.379
183.5 - 152.7	165.1	0.000884	0.018284	0.214	1.593
152.7 - 129.9	139.4	0.000648	0.018932	0.186	1.779
129.9 - 112.7	120.0	0.000434	0.019366	0.145	1.924
112.7 - 99.6	105.3	0.000289	0.019655	0.110	2.034
99.6 - 89.0	93.7	0.000214	0.019870	0.091	2.125
89.0 - 80.2	84.1	0.000151	0.020021	0.072	2.197
80.2 - 72.8	76.1	0.000099	0.020120	0.052	2.249
72.8 - 66.5	69.3	0.000070	0.020191	0.041	2.290
66.5 - 61.1	63.5	0.000065	0.020255	0.041	2.331
61.1 - 56.6	58.6	0.000060	0.020315	0.041	2.371
56.6 - 52.6	54.4	0.000043	0.020358	0.031	2.403
52.6 - 49.1	50.7	0.000033	0.020391	0.026	2.429
49.1 - 42.7	45.4	0.000067	0.020458	0.059	2.488
42.7 - 37.4	39.7	0.000047	0.020505	0.047	2.535
37.4 - 33.0	34.9	0.000046	0.020550	0.052	2.588
33.0 - 29.2	30.8	0.000051	0.020601	0.066	2.654
29.2 - 25.8	27.3	0.000052	0.020653	0.076	2.729
25.8 - 22.9	24.2	0.000052	0.020705	0.086	2.815
22.9 - 20.1	21.3	0.000055	0.020760	0.104	2.919
20.1 - 17.6	18.7	0.000057	0.020817	0.122	3.041
17.6 - 16.6	17.1	0.000025	0.020842	0.058	3.099

Sample: prøve1
Operator:
Submitter:
File: C:\data\Fride M\1.SMP

Started: 4/5/2022 9:51:00 AM
Completed: 4/5/2022 5:37:32 PM
Report time: 4/5/2022 5:56:32 PM
Sample mass: 0,2560 g
Analysis free space: 57,7940 cm³
Low pressure dose: None
Automatic degas: Yes

Analysis adsorptive: N2
Analysis bath temp.: -195,898 °C
Thermal correction: Yes
Ambient free space: 16,3455 cm³ Measured
Equilibration interval: 10 s
Sample density: 1,000 g/cm³

Comments: Fra takvent tilsendt fra industri, prøve 1. gul avsetting på glass

Sample prep: Stage	Temperature (°C)	Ramp Rate (°C/min)	Time (min)
1	30	10	10
2	90	10	60
3	250	10	820
4	25	10	60

BJH Desorption Pore Distribution Report

Faas Correction
Harkins and Jura
t = [13.99 / (0.034 - log(p/p°))] ^ 0.5

Diameter range: 17,000 to 3 000,000 Å
Adsorbate property factor: 9,53000 Å
Density conversion factor: 0,0015496
Fraction of pores open at both ends: 0,00

Pore Diameter Range (Å)	Average Diameter (Å)	Incremental Pore Volume (cm³/g)	Cumulative Pore Volume (cm³/g)	Incremental Pore Area (m²/g)	Cumulative Pore Area (m²/g)
1928.4 - 1005.4	1197.9	0.002888	0.002888	0.096	0.096
1005.4 - 363.0	431.3	0.009220	0.012108	0.855	0.952
363.0 - 267.3	300.0	0.001975	0.014083	0.263	1.215
267.3 - 210.9	232.0	0.001229	0.015312	0.212	1.427
210.9 - 167.9	184.2	0.001104	0.016416	0.240	1.667
167.9 - 140.5	151.6	0.000908	0.017324	0.240	1.906
140.5 - 120.2	128.7	0.000897	0.018221	0.279	2.185
120.2 - 105.1	111.5	0.000778	0.018999	0.279	2.464
105.1 - 93.6	98.6	0.000600	0.019598	0.243	2.707
93.6 - 84.5	88.5	0.000445	0.020043	0.201	2.908
84.5 - 77.0	80.4	0.000325	0.020368	0.162	3.070
77.0 - 70.6	73.5	0.000243	0.020610	0.132	3.202
70.6 - 65.3	67.7	0.000183	0.020794	0.108	3.310
65.3 - 60.5	62.7	0.000147	0.020941	0.094	3.404
60.5 - 56.3	58.2	0.000092	0.021033	0.063	3.467
56.3 - 52.5	54.3	0.000103	0.021136	0.076	3.543
52.5 - 49.1	50.7	0.000082	0.021218	0.065	3.608
49.1 - 44.8	46.8	0.000089	0.021307	0.076	3.684
44.8 - 39.7	41.9	0.000071	0.021378	0.068	3.752
39.7 - 35.2	37.1	0.000139	0.021518	0.150	3.903
35.2 - 31.4	33.0	0.000007	0.021524	0.008	3.910
31.4 - 22.3	23.5	0.000008	0.021532	0.013	3.923
22.3 - 19.8	20.9	0.000040	0.021572	0.076	3.999
19.8 - 16.8	18.0	0.000037	0.021608	0.081	4.080

Sample: prøve1
Operator:
Submitter:
File: C:\data\Fride M\1.SMP

Started:	4/5/2022 9:51:00 AM	Analysis adsorptive:	N2
Completed:	4/5/2022 5:37:32 PM	Analysis bath temp.:	-195,898 °C
Report time:	4/5/2022 5:56:32 PM	Thermal correction:	Yes
Sample mass:	0,2560 g	Ambient free space:	16,3455 cm³ Measured
Analysis free space:	57,7940 cm³	Equilibration interval:	10 s
Low pressure dose:	None	Sample density:	1,000 g/cm³
Automatic degas:	Yes		

Comments: Fra takvent tilsendt fra industri, prøve 1. gul avsetting på glass

Sample prep: Stage	Temperature (°C)	Ramp Rate (°C/min)	Time (min)
1	30	10	10
2	90	10	60
3	250	10	820
4	25	10	60

Sample Log

Date	Time	Log Message
4/4/2022	10:35:58 AM	Start degas stage 1 of 4: ramp to 30 °C at 10 °C/min/min and hold for 10 minutes.
4/4/2022	10:54:58 AM	Start degas stage 2 of 4: ramp to 90 °C at 10 °C/min/min and hold for 60 minutes.
4/4/2022	12:05:58 PM	Start degas stage 3 of 4: ramp to 250 °C at 10 °C/min/min and hold for 820 minutes.
4/5/2022	2:05:58 AM	Start degas stage 4 of 4: ramp to 25 °C at 10 °C/min/min and hold for 60 minutes.
4/5/2022	4:32:58 AM	Start degas cooldown.
4/5/2022	9:51:00 AM	Started analysis of file 1.SMP on port 1.
4/5/2022	9:51:00 AM	System volume: 36.2726 cm³
4/5/2022	9:53:21 AM	Port 1 1000 mmHg transducer scale changed from 518,4809 to 518,4631 mmHg (fraction of nominal: 1.01).
4/5/2022	10:42:56 AM	Sample port 1 leak rate measured (interval: 50 s, rate: -0,000700 mmHg/min).
4/5/2022	10:50:07 AM	Ambient free-space measurement on sample port 1 complete (elapsed: 3545 s, qty in free-space: 16,3455 cm³, P1: 798,1717 mmHg, P2: 406,8109 mmHg, Tman: 45,0 °C, Tport: 45,0 °C).
4/5/2022	11:03:33 AM	Analysis free-space measurement on sample port 1 complete (elapsed: 4350 s, qty in free-space: 57,7940 cm³, P3: 170,7155 mmHg, Tport: 45,0 °C).
4/5/2022	11:43:44 AM	Psat port is charged with N2 at 748,1649 mmHg
4/5/2022	11:57:42 AM	Port 1 vacuum level is 1,79e-05 mmHg
4/5/2022	11:57:47 AM	Data collection started on sample port 1 (gas: N2).
4/5/2022	5:26:03 PM	Analysis termination started.
4/5/2022	5:37:32 PM	Finished a sample analysis for C:\data\Fride M\1.SMP on port 1.

Sample: prøve3
Operator:
Submitter:
File: C:\data\Fride M\3.SMP

Started:	4/5/2022 9:51:00 AM	Analysis adsorptive:	N2
Completed:	4/5/2022 5:37:32 PM	Analysis bath temp.:	-195,902 °C
Report time:	4/5/2022 5:57:07 PM	Thermal correction:	Yes
Sample mass:	1,4208 g	Ambient free space:	16,1254 cm³ Measured
Analysis free space:	56,9626 cm³	Equilibration interval:	10 s
Low pressure dose:	None	Sample density:	1,000 g/cm³
Automatic degas:	Yes		

Comments: prøve3.

Sample prep: Stage	Temperature (°C)	Ramp Rate (°C/min)	Time (min)
1	30	10	10
2	90	10	60
3	250	10	820
4	25	10	60

Summary Report

Surface Area

Single point surface area at p/p° = 0,298683301: 11,3854 m²/g

BET Surface Area: 11,7457 m²/g

Pore Volume

Single point desorption total pore volume of pores less than 1 934,646 Å diameter at p/p° = 0,990000000: 0,065867 cm³/g

Pore Size

Adsorption average pore diameter (4V/A by BET): 221,121 Å

Desorption average pore diameter (4V/A by BET): 224,308 Å

Sample: prøve3
Operator:
Submitter:
File: C:\data\Fride M\3.SMP

Started: 4/5/2022 9:51:00 AM
Completed: 4/5/2022 5:37:32 PM
Report time: 4/5/2022 5:57:07 PM
Sample mass: 1,4208 g
Analysis free space: 56,9626 cm³
Low pressure dose: None
Automatic degas: Yes

Analysis adsorptive: N2
Analysis bath temp.: -195,902 °C
Thermal correction: Yes
Ambient free space: 16,1254 cm³ Measured
Equilibration interval: 10 s
Sample density: 1,000 g/cm³

Comments: prøve3.

Sample prep: Stage	Temperature (°C)	Ramp Rate (°C/min)	Time (min)
1	30	10	10
2	90	10	60
3	250	10	820
4	25	10	60

Isotherm Tabular Report

Relative Pressure (p/p°)	Absolute Pressure (mmHg)	Quantity Adsorbed (cm³/g STP)	Elapsed Time (h:min)	Saturation Pressure (mmHg)
			01:52	748.194153
0.009557558	7.179074	1.7710	02:32	751.140991
0.035804618	26.880369	2.2290	02:39	750.751465
0.067379052	50.588093	2.5147	02:48	750.798523
0.079379101	59.587513	2.6013	02:52	750.670044
0.099651175	74.824554	2.7328	02:58	750.864746
0.119548002	89.783432	2.8505	03:02	751.024109
0.139541981	104.822311	2.9603	03:06	751.188354
0.159419835	119.764618	3.0645	03:09	751.252930
0.179389048	134.775909	3.1658	03:12	751.305115
0.200342330	150.526276	3.2684	03:15	751.345337
0.247283771	185.723846	3.4903	03:18	751.055542
0.298683301	224.374527	3.7298	03:21	751.212158
0.349212100	262.344269	3.9676	03:24	751.246216
0.399192710	299.914185	4.2062	03:27	751.301758
0.448903125	337.193237	4.4513	03:30	751.149231
0.499165473	374.879059	4.7145	03:33	751.011597
0.548571327	412.028931	4.9946	03:36	751.094543
0.598332248	449.271667	5.3063	03:38	750.873230
0.719029317	540.194824	6.3294	03:42	751.283447
0.823206841	618.204773	8.4268	03:49	750.971375
0.876723744	658.699341	12.4904	03:57	751.319153
0.903168579	678.234070	17.1898	04:08	750.949585
0.921335329	691.996948	21.9471	04:20	751.080444
0.938361940	704.476257	26.4883	04:31	750.751099
0.954888102	716.963196	30.7597	04:42	750.834778
0.972402298	729.835999	35.3894	04:57	750.549438
0.977306776	733.654724	37.2715	05:05	750.690308
0.993537808	745.440369	43.1940	05:22	750.288879
0.978048617	733.771423	40.1863	05:31	750.240234
0.949481085	712.454468	34.9214	05:46	750.361938
0.930735573	698.366394	31.8333	05:55	750.338135
0.902344647	677.068115	27.1869	06:09	750.343140
0.880367993	660.349609	22.5597	06:22	750.083618
0.852266080	639.097656	16.1646	06:38	749.880432
0.828928843	621.430054	12.8147	06:48	749.678406
0.806100176	604.109253	10.7927	06:56	749.422058
0.723612475	542.261780	7.4298	07:03	749.381470

Sample: prøve3
Operator:
Submitter:
File: C:\data\Fride M\3.SMP

Started: 4/5/2022 9:51:00 AM
Completed: 4/5/2022 5:37:32 PM
Report time: 4/5/2022 5:57:07 PM
Sample mass: 1,4208 g
Analysis free space: 56,9626 cm³
Low pressure dose: None
Automatic degas: Yes

Analysis adsorptive: N2
Analysis bath temp.: -195,902 °C
Thermal correction: Yes
Ambient free space: 16,1254 cm³ Measured
Equilibration interval: 10 s
Sample density: 1,000 g/cm³

Comments: prøve3.

Sample prep: Stage	Temperature (°C)	Ramp Rate (°C/min)	Time (min)
1	30	10	10
2	90	10	60
3	250	10	820
4	25	10	60

Isotherm Tabular Report

Relative Pressure (p/p°)	Absolute Pressure (mmHg)	Quantity Adsorbed (cm³/g STP)	Elapsed Time (h:min)	Saturation Pressure (mmHg)
0.300599847	225.294998	3.8368	07:25	749.484741
0.250358076	187.553406	3.5986	07:27	749.140625
0.200270589	150.008698	3.3592	07:31	749.030090
0.143419323	107.543098	3.0730	07:35	749.850830

Sample: prøve3
Operator:
Submitter:
File: C:\data\Fride M\3.SMP

Started:	4/5/2022 9:51:00 AM	Analysis adsorptive:	N2
Completed:	4/5/2022 5:37:32 PM	Analysis bath temp.:	-195,902 °C
Report time:	4/5/2022 5:57:07 PM	Thermal correction:	Yes
Sample mass:	1,4208 g	Ambient free space:	16,1254 cm³ Measured
Analysis free space:	56,9626 cm³	Equilibration interval:	10 s
Low pressure dose:	None	Sample density:	1,000 g/cm³
Automatic degas:	Yes		

Comments: prøve3.

Sample prep: Stage	Temperature (°C)	Ramp Rate (°C/min)	Time (min)
1	30	10	10
2	90	10	60
3	250	10	820
4	25	10	60

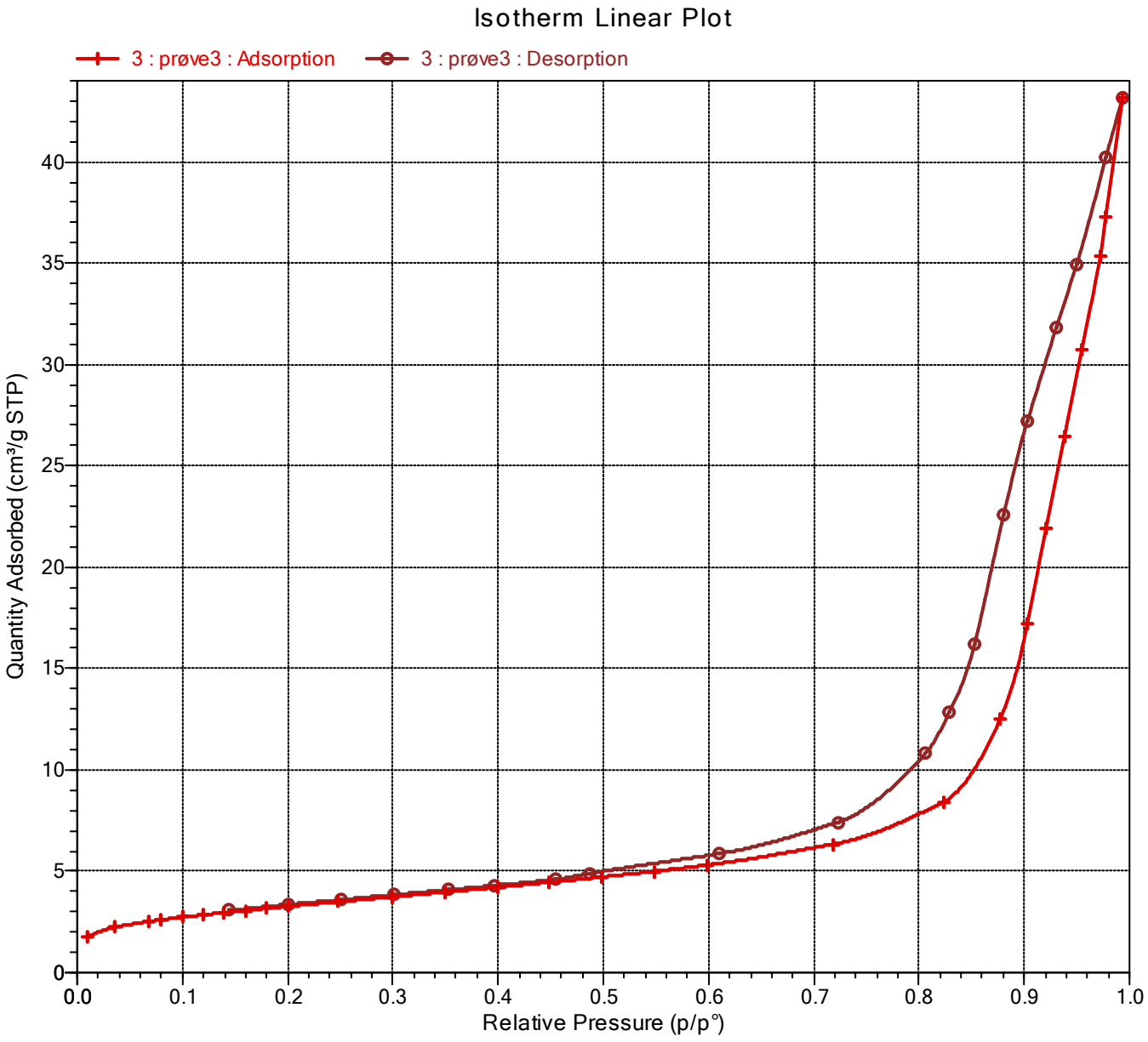

Sample: prøve3
Operator:
Submitter:
File: C:\data\Fride M\3.SMP

Started: 4/5/2022 9:51:00 AM
Completed: 4/5/2022 5:37:32 PM
Report time: 4/5/2022 5:57:07 PM
Sample mass: 1,4208 g
Analysis free space: 56,9626 cm³
Low pressure dose: None
Automatic degas: Yes

Analysis adsorptive: N2
Analysis bath temp.: -195,902 °C
Thermal correction: Yes
Ambient free space: 16,1254 cm³ Measured
Equilibration interval: 10 s
Sample density: 1,000 g/cm³

Comments: prøve3.

Sample prep: Stage	Temperature (°C)	Ramp Rate (°C/min)	Time (min)
1	30	10	10
2	90	10	60
3	250	10	820
4	25	10	60

BET Report

BET surface area: 11,7457 ± 0,0683 m²/g
Slope: 0,366848 ± 0,002122 g/cm³ STP
Y-intercept: 0,003718 ± 0,000369 g/cm³ STP
C: 99,671852
Qm: 2,6986 cm³/g STP
Correlation coefficient: 0,9998661
Molecular cross-sectional area: 0,1620 nm²

Relative Pressure (p/p°)	Quantity Adsorbed (cm³/g STP)	1/[Q(p°/p - 1)]
0.067379052	2.5147	0.028730
0.079379101	2.6013	0.033146
0.099651175	2.7328	0.040500
0.119548002	2.8505	0.047634
0.139541981	2.9603	0.054782
0.159419835	3.0645	0.061888
0.179389048	3.1658	0.069053
0.200342330	3.2684	0.076653
0.247283771	3.4903	0.094123
0.298683301	3.7298	0.114185

Sample: prøve3
Operator:
Submitter:
File: C:\data\Fride M\3.SMP

Started:	4/5/2022 9:51:00 AM	Analysis adsorptive:	N2
Completed:	4/5/2022 5:37:32 PM	Analysis bath temp.:	-195,902 °C
Report time:	4/5/2022 5:57:07 PM	Thermal correction:	Yes
Sample mass:	1,4208 g	Ambient free space:	16,1254 cm³ Measured
Analysis free space:	56,9626 cm³	Equilibration interval:	10 s
Low pressure dose:	None	Sample density:	1,000 g/cm³
Automatic degas:	Yes		

Comments: prøve3.

Sample prep: Stage	Temperature (°C)	Ramp Rate (°C/min)	Time (min)
1	30	10	10
2	90	10	60
3	250	10	820
4	25	10	60

BET Surface Area Plot

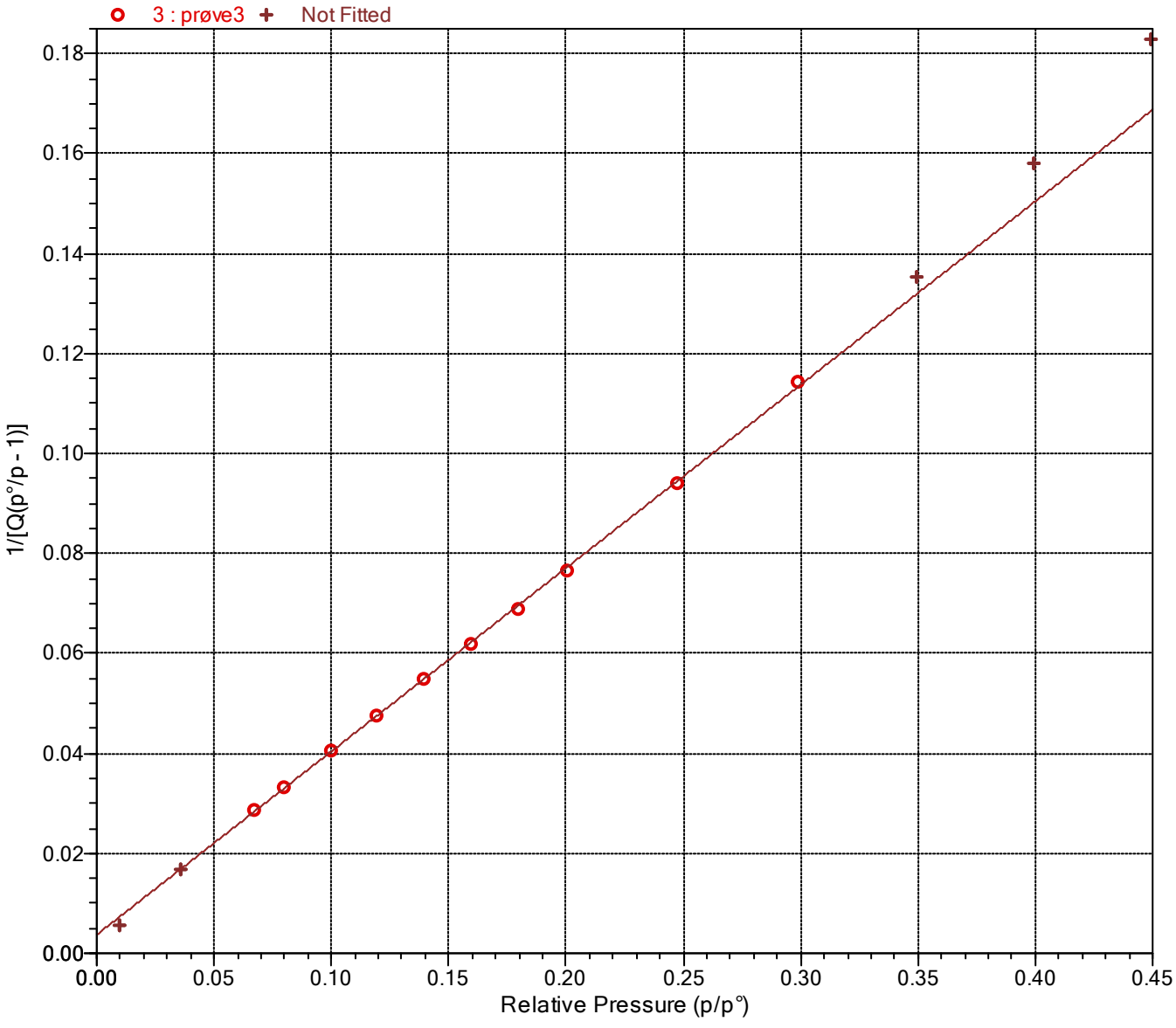

Sample: prøve3
Operator:
Submitter:
File: C:\data\Fride M\3.SMP

Started:	4/5/2022 9:51:00 AM	Analysis adsorptive:	N2
Completed:	4/5/2022 5:37:32 PM	Analysis bath temp.:	-195,902 °C
Report time:	4/5/2022 5:57:07 PM	Thermal correction:	Yes
Sample mass:	1,4208 g	Ambient free space:	16,1254 cm³ Measured
Analysis free space:	56,9626 cm³	Equilibration interval:	10 s
Low pressure dose:	None	Sample density:	1,000 g/cm³
Automatic degas:	Yes		

Comments: prøve3.

Sample prep: Stage	Temperature (°C)	Ramp Rate (°C/min)	Time (min)
1	30	10	10
2	90	10	60
3	250	10	820
4	25	10	60

BET Isotherm Plot

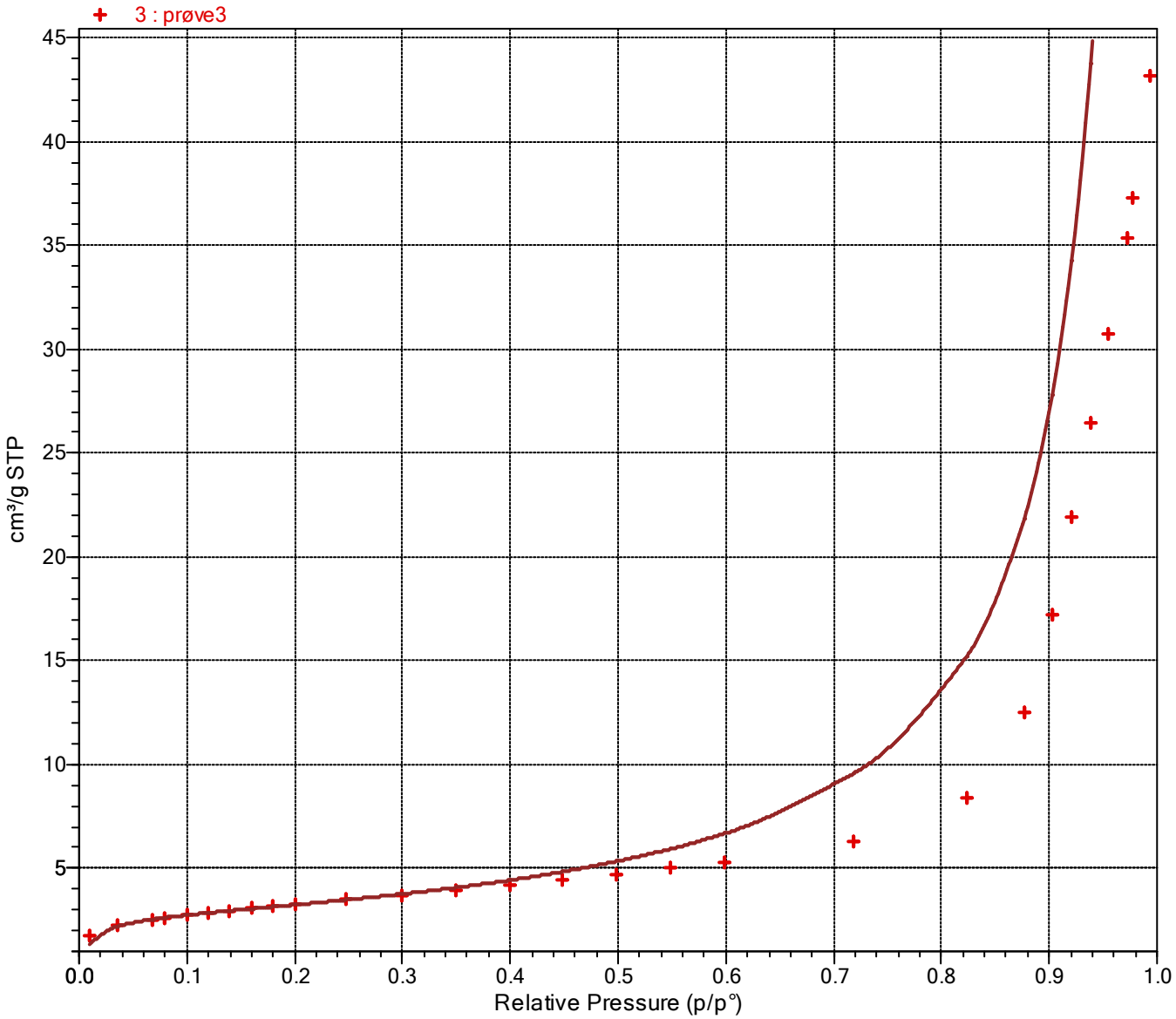

Sample: prøve3
Operator:
Submitter:
File: C:\data\Fride M\3.SMP

Started:	4/5/2022 9:51:00 AM	Analysis adsorptive:	N2
Completed:	4/5/2022 5:37:32 PM	Analysis bath temp.:	-195,902 °C
Report time:	4/5/2022 5:57:07 PM	Thermal correction:	Yes
Sample mass:	1,4208 g	Ambient free space:	16,1254 cm³ Measured
Analysis free space:	56,9626 cm³	Equilibration interval:	10 s
Low pressure dose:	None	Sample density:	1,000 g/cm³
Automatic degas:	Yes		

Comments: prøve3.

Sample prep: Stage	Temperature (°C)	Ramp Rate (°C/min)	Time (min)
1	30	10	10
2	90	10	60
3	250	10	820
4	25	10	60

t-Plot Report

Micropore volume:	-0,000129 cm³/g
Micropore area:	*
External surface area:	11,8761 m²/g
Slope:	0,766423 ± 0,005092 cm³/g·Å STP
Y-intercept:	-0,083269 ± 0,020676 cm³/g STP
Correlation coefficient:	0,999868
Surface area correction factor:	1,000
Density conversion factor:	0,0015495
Total surface area (BET):	11,7457 m²/g
Thickness range:	3,5000 to 5,0000 Å
Thickness equation:	Harkins and Jura

Thickness Curve

$$t = [\ 13.99 / (\ 0.034 - \log(p/p^\circ)\ )\ ]^{\wedge}\ 0.5$$

t-Plot Report - Data

Relative Pressure (p/p°)	Statistical Thickness (Å)	Quantity Adsorbed (cm³/g STP)	Fitted
0.067379052	3.4067	2.5147	
0.079379101	3.5119	2.6013	*
0.099651175	3.6756	2.7328	*
0.119548002	3.8245	2.8505	*
0.139541981	3.9663	2.9603	*
0.159419835	4.1019	3.0645	*
0.179389048	4.2345	3.1658	*
0.200342330	4.3711	3.2684	*
0.247283771	4.6725	3.4903	*
0.298683301	5.0036	3.7298	
0.349212100	5.3384	3.9676	
0.399192710	5.6853	4.2062	
0.448903125	6.0529	4.4513	
0.499165473	6.4550	4.7145	
0.548571327	6.8892	4.9946	
0.598332248	7.3772	5.3063	

* The micropore area is not reported because either the micropore volume is negative or the calculated external surface area is larger than the total surface area.

Sample: prøve3
Operator:
Submitter:
File: C:\data\Fride M\3.SMP

Started:	4/5/2022 9:51:00 AM	Analysis adsorptive:	N2
Completed:	4/5/2022 5:37:32 PM	Analysis bath temp.:	-195,902 °C
Report time:	4/5/2022 5:57:07 PM	Thermal correction:	Yes
Sample mass:	1,4208 g	Ambient free space:	16,1254 cm³ Measured
Analysis free space:	56,9626 cm³	Equilibration interval:	10 s
Low pressure dose:	None	Sample density:	1,000 g/cm³
Automatic degas:	Yes		

Comments: prøve3.

Sample prep: Stage	Temperature (°C)	Ramp Rate (°C/min)	Time (min)
1	30	10	10
2	90	10	60
3	250	10	820
4	25	10	60

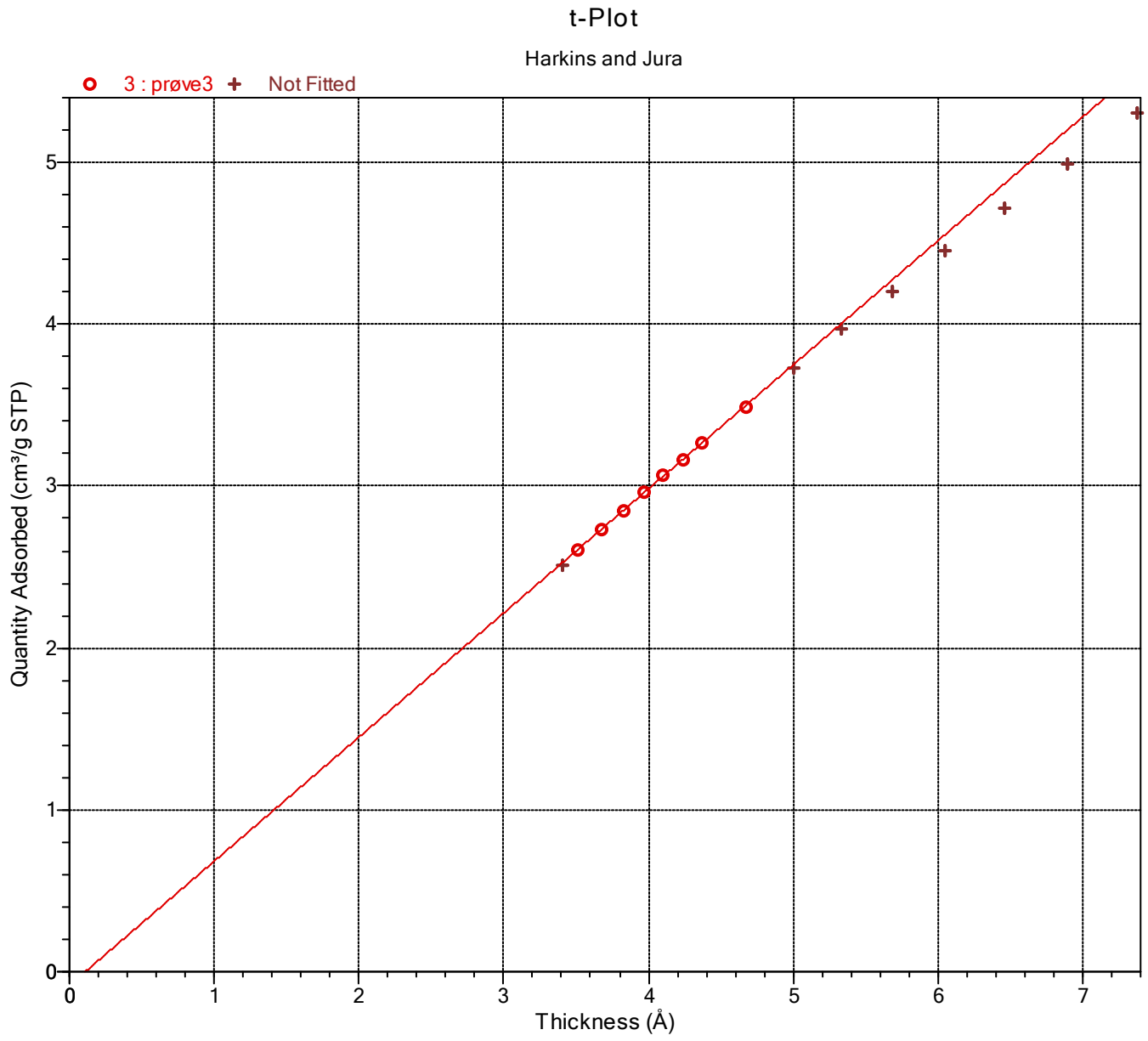

Sample: prøve3
Operator:
Submitter:
File: C:\data\Fride M\3.SMP

Started: 4/5/2022 9:51:00 AM
Completed: 4/5/2022 5:37:32 PM
Report time: 4/5/2022 5:57:07 PM
Sample mass: 1,4208 g
Analysis free space: 56,9626 cm³
Low pressure dose: None
Automatic degas: Yes

Analysis adsorptive: N2
Analysis bath temp.: -195,902 °C
Thermal correction: Yes
Ambient free space: 16,1254 cm³ Measured
Equilibration interval: 10 s
Sample density: 1,000 g/cm³

Comments: prøve3.

Sample prep: Stage	Temperature (°C)	Ramp Rate (°C/min)	Time (min)
1	30	10	10
2	90	10	60
3	250	10	820
4	25	10	60

BJH Adsorption Pore Distribution Report

Faas Correction
Harkins and Jura
$t = [13.99 / (0.034 - \log(p/p°))]^{0.5}$

Diameter range: 17,000 to 3 000,000 Å
Adsorbate property factor: 9,53000 Å
Density conversion factor: 0,0015495
Fraction of pores open at both ends: 0,00

Pore Diameter Range (Å)	Average Diameter (Å)	Incremental Pore Volume (cm³/g)	Cumulative Pore Volume (cm³/g)	Incremental Pore Area (m²/g)	Cumulative Pore Area (m²/g)
2977.8 - 864.9	1021.4	0.009832	0.009832	0.385	0.385
864.9 - 714.8	775.2	0.003171	0.013003	0.164	0.549
714.8 - 444.0	517.0	0.008043	0.021046	0.622	1.171
444.0 - 328.7	368.6	0.007666	0.028712	0.832	2.003
328.7 - 259.9	285.9	0.008396	0.037108	1.175	3.178
259.9 - 212.8	231.4	0.009025	0.046133	1.560	4.738
212.8 - 168.6	185.2	0.009012	0.055145	1.946	6.684
168.6 - 118.6	134.4	0.007490	0.062635	2.228	8.913
118.6 - 74.5	86.1	0.002524	0.065159	1.173	10.086
74.5 - 50.8	57.8	0.000331	0.065491	0.229	10.315
50.8 - 44.5	47.2	0.000034	0.065524	0.029	10.343
44.5 - 39.3	41.5	0.000033	0.065558	0.032	10.375
39.3 - 34.8	36.8	0.000038	0.065596	0.042	10.417
34.8 - 31.1	32.7	0.000045	0.065641	0.056	10.473
31.1 - 27.7	29.2	0.000063	0.065704	0.087	10.559
27.7 - 24.7	26.0	0.000083	0.065787	0.127	10.687
24.7 - 21.9	23.1	0.000091	0.065879	0.158	10.844
21.9 - 19.5	20.6	0.000091	0.065970	0.177	11.022
19.5 - 18.5	19.0	0.000047	0.066017	0.100	11.122
18.5 - 17.5	18.0	0.000051	0.066068	0.113	11.234
17.5 - 16.5	17.0	0.000052	0.066120	0.122	11.356

Sample: prøve3
Operator:
Submitter:
File: C:\data\Fride M\3.SMP

Started: 4/5/2022 9:51:00 AM
Completed: 4/5/2022 5:37:32 PM
Report time: 4/5/2022 5:57:07 PM
Sample mass: 1,4208 g
Analysis free space: 56,9626 cm³
Low pressure dose: None
Automatic degas: Yes

Analysis adsorptive: N2
Analysis bath temp.: -195,902 °C
Thermal correction: Yes
Ambient free space: 16,1254 cm³ Measured
Equilibration interval: 10 s
Sample density: 1,000 g/cm³

Comments: prøve3.

Sample prep: Stage	Temperature (°C)	Ramp Rate (°C/min)	Time (min)
1	30	10	10
2	90	10	60
3	250	10	820
4	25	10	60

BJH Desorption Pore Distribution Report

Faas Correction
Harkins and Jura
t = [13.99 / (0.034 - log(p/p°))] ^ 0.5

Diameter range: 17,000 to 3 000,000 Å
Adsorbate property factor: 9,53000 Å
Density conversion factor: 0,0015495
Fraction of pores open at both ends: 0,00

Pore Diameter Range (Å)	Average Diameter (Å)	Incremental Pore Volume (cm³/g)	Cumulative Pore Volume (cm³/g)	Incremental Pore Area (m²/g)	Cumulative Pore Area (m²/g)
2976.6 - 892.2	1056.5	0.004971	0.004971	0.188	0.188
892.2 - 396.8	474.0	0.009218	0.014189	0.778	0.966
396.8 - 292.5	328.4	0.005563	0.019752	0.678	1.644
292.5 - 209.9	237.1	0.008693	0.028445	1.467	3.110
209.9 - 172.3	187.2	0.008982	0.037428	1.920	5.030
172.3 - 140.2	152.7	0.012769	0.050197	3.344	8.374
140.2 - 121.3	129.3	0.006574	0.056771	2.034	10.408
121.3 - 107.1	113.2	0.003776	0.060547	1.334	11.742
107.1 - 74.5	84.6	0.005429	0.065976	2.566	14.308
74.5 - 51.3	58.4	0.000901	0.066877	0.618	14.925
51.3 - 34.1	35.4	0.000202	0.067079	0.228	15.153

Sample: prøve3
Operator:
Submitter:
File: C:\data\Fride M\3.SMP

Started:	4/5/2022 9:51:00 AM	Analysis adsorptive:	N2
Completed:	4/5/2022 5:37:32 PM	Analysis bath temp.:	-195,902 °C
Report time:	4/5/2022 5:57:07 PM	Thermal correction:	Yes
Sample mass:	1,4208 g	Ambient free space:	16,1254 cm³ Measured
Analysis free space:	56,9626 cm³	Equilibration interval:	10 s
Low pressure dose:	None	Sample density:	1,000 g/cm³
Automatic degas:	Yes		

Comments: prøve3.

Sample prep: Stage	Temperature (°C)	Ramp Rate (°C/min)	Time (min)
1	30	10	10
2	90	10	60
3	250	10	820
4	25	10	60

Sample Log

Date	Time	Log Message
4/4/2022	10:35:58 AM	Start degas stage 1 of 4: ramp to 30 °C at 10 °C/min/min and hold for 10 minutes.
4/4/2022	10:53:58 AM	Start degas stage 2 of 4: ramp to 90 °C at 10 °C/min/min and hold for 60 minutes.
4/4/2022	12:04:58 PM	Start degas stage 3 of 4: ramp to 250 °C at 10 °C/min/min and hold for 820 minutes.
4/5/2022	2:03:58 AM	Start degas stage 4 of 4: ramp to 25 °C at 10 °C/min/min and hold for 60 minutes.
4/5/2022	4:35:58 AM	Start degas cooldown.
4/5/2022	9:51:01 AM	Started analysis of file 3.SMP on port 3.
4/5/2022	9:51:01 AM	System volume: 36.2726 cm³
4/5/2022	9:53:21 AM	Port 3 1000 mmHg transducer scale changed from 517,7170 to 517,6793 mmHg (fraction of nominal: 1.01).
4/5/2022	10:42:56 AM	Sample port 3 leak rate measured (interval: 50 s, rate: 0,000963 mmHg/min).
4/5/2022	10:52:27 AM	Ambient free-space measurement on sample port 3 complete (elapsed: 3684 s, qty in free-space: 16,1254 cm³, P1: 801,7168 mmHg, P2: 410,9649 mmHg, Tman: 45,0 °C, Tport: 45,0 °C).
4/5/2022	11:03:33 AM	Analysis free-space measurement on sample port 3 complete (elapsed: 4350 s, qty in free-space: 56,9626 cm³, P3: 172,7313 mmHg, Tport: 45,0 °C).
4/5/2022	11:43:44 AM	Psat port is charged with N2 at 748,1649 mmHg
4/5/2022	11:57:42 AM	Port 3 vacuum level is 1,79e-05 mmHg
4/5/2022	11:57:47 AM	Data collection started on sample port 3 (gas: N2).
4/5/2022	5:26:04 PM	Analysis termination started.
4/5/2022	5:37:32 PM	Finished a sample analysis for C:\data\Fride M\3.SMP on port 3.

Sample: prøve8
Operator:
Submitter:
File: C:\data\Fride M\8.SMP

Started:	4/22/2022 11:41:17 AM	Analysis adsorptive:	N2
Completed:	4/22/2022 7:19:10 PM	Analysis bath temp.:	-195,582 °C
Report time:	4/23/2022 10:43:41 AM	Thermal correction:	Yes
Sample mass:	1,3256 g	Ambient free space:	16,0910 cm³ Measured
Analysis free space:	56,8169 cm³	Equilibration interval:	10 s
Low pressure dose:	None	Sample density:	1,000 g/cm³
Automatic degas:	Yes		

Comments: prøve8 fra takvent

Sample prep: Stage	Temperature (°C)	Ramp Rate (°C/min)	Time (min)
1	30	10	10
2	90	10	60
3	250	10	820
4	25	10	60

Summary Report

Surface Area

Single point surface area at p/p° = 0,299018432: 5,7847 m²/g

BET Surface Area: 6,0138 m²/g

Pore Volume

Single point desorption total pore volume of pores less than 1 929,645 Å diameter at p/p° = 0,989973725: 0,028585 cm³/g

Pore Size

Adsorption average pore diameter (4V/A by BET): 190,128 Å

Desorption average pore diameter (4V/A by BET): 190,128 Å

Sample: prøve8
Operator:
Submitter:
File: C:\data\Fride M\8.SMP

Started: 4/22/2022 11:41:17 AM
Completed: 4/22/2022 7:19:10 PM
Report time: 4/23/2022 10:43:41 AM
Sample mass: 1,3256 g
Analysis free space: 56,8169 cm³
Low pressure dose: None
Automatic degas: Yes

Analysis adsorptive: N2
Analysis bath temp.: -195,582 °C
Thermal correction: Yes
Ambient free space: 16,0910 cm³ Measured
Equilibration interval: 10 s
Sample density: 1,000 g/cm³

Comments: prøve8 fra takvent

Sample prep: Stage	Temperature (°C)	Ramp Rate (°C/min)	Time (min)
1	30	10	10
2	90	10	60
3	250	10	820
4	25	10	60

Isotherm Tabular Report

Relative Pressure (p/p°)	Absolute Pressure (mmHg)	Quantity Adsorbed (cm³/g STP)	Elapsed Time (h:min)	Saturation Pressure (mmHg)
			01:52	778.452454
0.009664524	7.548883	0.8124	02:18	781.092102
0.036585837	28.575155	1.0743	02:34	781.044189
0.058332170	45.554573	1.1930	02:41	780.951111
0.079062772	61.728626	1.2809	02:44	780.754639
0.099636045	77.828461	1.3550	02:47	781.127563
0.119530055	93.373299	1.4206	02:51	781.170044
0.139529888	108.968269	1.4815	02:54	780.967224
0.159593099	124.627823	1.5381	02:56	780.909851
0.179470057	140.164154	1.5938	03:00	780.989075
0.199470287	155.774643	1.6458	03:02	780.941589
0.248206849	193.828476	1.7690	03:05	780.915100
0.299018432	233.494431	1.8960	03:08	780.869690
0.349729221	273.051239	2.0236	03:11	780.750427
0.399397028	311.910187	2.1541	03:14	780.952698
0.449043001	350.647797	2.2918	03:17	780.877991
0.499067110	389.717010	2.4419	03:19	780.890991
0.548828906	428.635040	2.6062	03:22	780.999390
0.598693158	467.595398	2.7967	03:25	781.026794
0.713080072	556.859131	3.3925	03:29	780.920898
0.820180077	640.454163	4.4434	03:33	780.870178
0.900304853	703.035828	6.3458	03:39	780.886414
0.942071832	735.451111	9.1952	03:47	780.674133
0.980736464	765.587402	16.1942	04:00	780.625000
0.989973725	773.167969	18.4139	04:03	780.998474
0.979113999	764.578552	17.1884	04:08	780.888184
0.949617450	741.222961	12.3427	04:23	780.549011
0.918234614	716.808777	9.7229	04:31	780.637939
0.899950058	702.581848	8.7203	04:38	780.689819
0.884213122	686.611511	7.7305	04:43	776.522644
0.875620790	679.969299	7.3860	04:47	776.556824
0.849934427	660.151550	6.5595	04:52	776.708801
0.826164415	641.452881	5.9773	04:56	776.422791
0.801572621	622.434937	5.4922	05:00	776.517212
0.698684267	542.447693	4.0925	05:04	776.384583
0.586470464	455.292084	3.2396	05:08	776.325684
0.551912247	428.476318	3.0535	05:11	776.348633
0.501985487	389.726715	2.7922	05:16	776.370483

Sample: prøve8
Operator:
Submitter:
File: C:\data\Fride M\8.SMP

Started:	4/22/2022 11:41:17 AM	Analysis adsorptive:	N2
Completed:	4/22/2022 7:19:10 PM	Analysis bath temp.:	-195,582 °C
Report time:	4/23/2022 10:43:41 AM	Thermal correction:	Yes
Sample mass:	1,3256 g	Ambient free space:	16,0910 cm³ Measured
Analysis free space:	56,8169 cm³	Equilibration interval:	10 s
Low pressure dose:	None	Sample density:	1,000 g/cm³
Automatic degas:	Yes		

Comments: prøve8 fra takvent

Sample prep: Stage	Temperature (°C)	Ramp Rate (°C/min)	Time (min)
1	30	10	10
2	90	10	60
3	250	10	820
4	25	10	60

Isotherm Tabular Report

Relative Pressure (p/p°)	Absolute Pressure (mmHg)	Quantity Adsorbed (cm³/g STP)	Elapsed Time (h:min)	Saturation Pressure (mmHg)
0.200235352	155.436798	1.6910	05:37	776.270508
0.141556099	109.870705	1.5300	05:39	776.163696

Sample: prøve8
Operator:
Submitter:
File: C:\data\Fride M\8.SMP

Started: 4/22/2022 11:41:17 AM
Completed: 4/22/2022 7:19:10 PM
Report time: 4/23/2022 10:43:41 AM
Sample mass: 1,3256 g
Analysis free space: 56,8169 cm³
Low pressure dose: None
Automatic degas: Yes

Analysis adsorptive: N2
Analysis bath temp.: -195,582 °C
Thermal correction: Yes
Ambient free space: 16,0910 cm³ Measured
Equilibration interval: 10 s
Sample density: 1,000 g/cm³

Comments: prøve8 fra takvent

Sample prep: Stage	Temperature (°C)	Ramp Rate (°C/min)	Time (min)
1	30	10	10
2	90	10	60
3	250	10	820
4	25	10	60

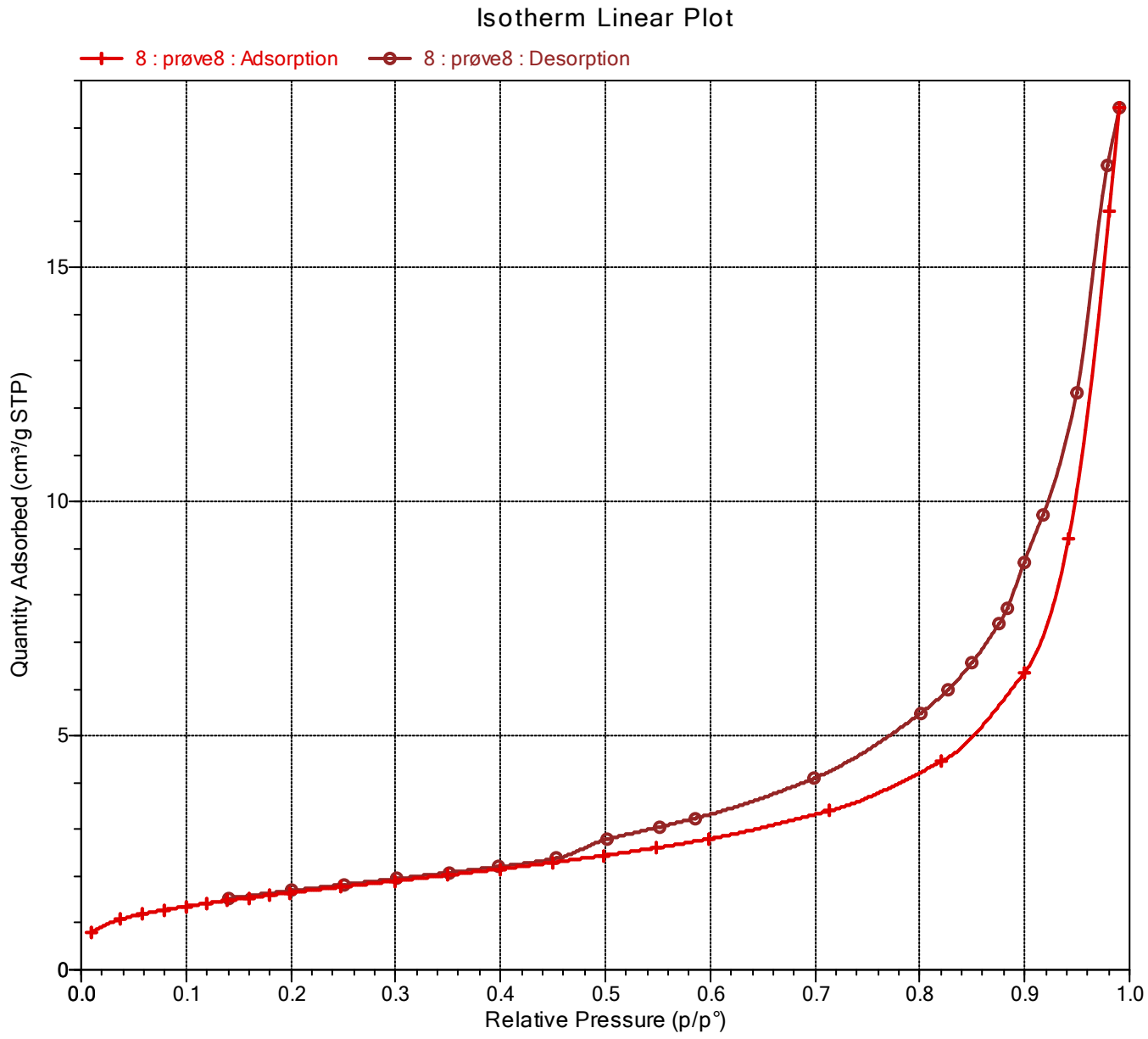

Sample: prøve8
Operator:
Submitter:
File: C:\data\Fride M\8.SMP

Started: 4/22/2022 11:41:17 AM
Completed: 4/22/2022 7:19:10 PM
Report time: 4/23/2022 10:43:41 AM
Sample mass: 1,3256 g
Analysis free space: 56,8169 cm³
Low pressure dose: None
Automatic degas: Yes

Analysis adsorptive: N2
Analysis bath temp.: -195,582 °C
Thermal correction: Yes
Ambient free space: 16,0910 cm³ Measured
Equilibration interval: 10 s
Sample density: 1,000 g/cm³

Comments: prøve8 fra takvent

Sample prep: Stage	Temperature (°C)	Ramp Rate (°C/min)	Time (min)
1	30	10	10
2	90	10	60
3	250	10	820
4	25	10	60

BET Report

BET surface area: 6,0138 ± 0,0306 m²/g
Slope: 0,713731 ± 0,003624 g/cm³ STP
Y-intercept: 0,010035 ± 0,000630 g/cm³ STP
C: 72,126979
Qm: 1,3817 cm³/g STP
Correlation coefficient: 0,9998969
Molecular cross-sectional area: 0,1620 nm²

Relative Pressure (p/p°)	Quantity Adsorbed (cm³/g STP)	1/[Q(p°/p - 1)]
0.058332170	1.1930	0.051925
0.079062772	1.2809	0.067021
0.099636045	1.3550	0.081669
0.119530055	1.4206	0.095566
0.139529888	1.4815	0.109457
0.159593099	1.5381	0.123463
0.179470057	1.5938	0.137233
0.199470287	1.6458	0.151400
0.248206849	1.7690	0.186637
0.299018432	1.8960	0.224989

Sample: prøve8
Operator:
Submitter:
File: C:\data\Fride M\8.SMP

Started:	4/22/2022 11:41:17 AM	Analysis adsorptive:	N2
Completed:	4/22/2022 7:19:10 PM	Analysis bath temp.:	-195,582 °C
Report time:	4/23/2022 10:43:41 AM	Thermal correction:	Yes
Sample mass:	1,3256 g	Ambient free space:	16,0910 cm³ Measured
Analysis free space:	56,8169 cm³	Equilibration interval:	10 s
Low pressure dose:	None	Sample density:	1,000 g/cm³
Automatic degas:	Yes		

Comments: prøve8 fra takvent

Sample prep: Stage	Temperature (°C)	Ramp Rate (°C/min)	Time (min)
1	30	10	10
2	90	10	60
3	250	10	820
4	25	10	60

BET Surface Area Plot

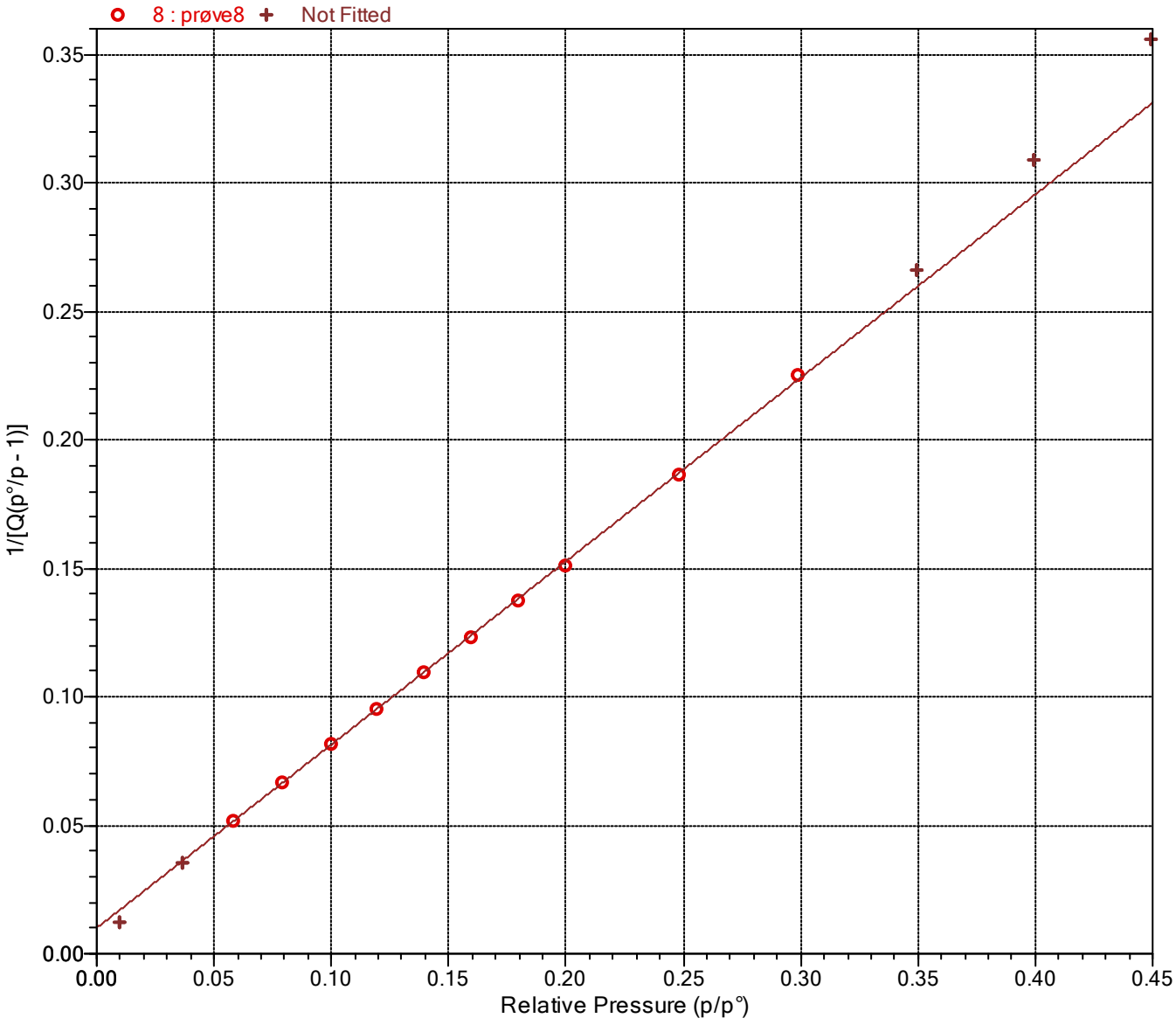

Sample: prøve8
Operator:
Submitter:
File: C:\data\Fride M\8.SMP

Started:	4/22/2022 11:41:17 AM	Analysis adsorptive:	N2
Completed:	4/22/2022 7:19:10 PM	Analysis bath temp.:	-195,582 °C
Report time:	4/23/2022 10:43:41 AM	Thermal correction:	Yes
Sample mass:	1,3256 g	Ambient free space:	16,0910 cm³ Measured
Analysis free space:	56,8169 cm³	Equilibration interval:	10 s
Low pressure dose:	None	Sample density:	1,000 g/cm³
Automatic degas:	Yes		

Comments: prøve8 fra takvent

Sample prep: Stage	Temperature (°C)	Ramp Rate (°C/min)	Time (min)
1	30	10	10
2	90	10	60
3	250	10	820
4	25	10	60

BET Isotherm Plot

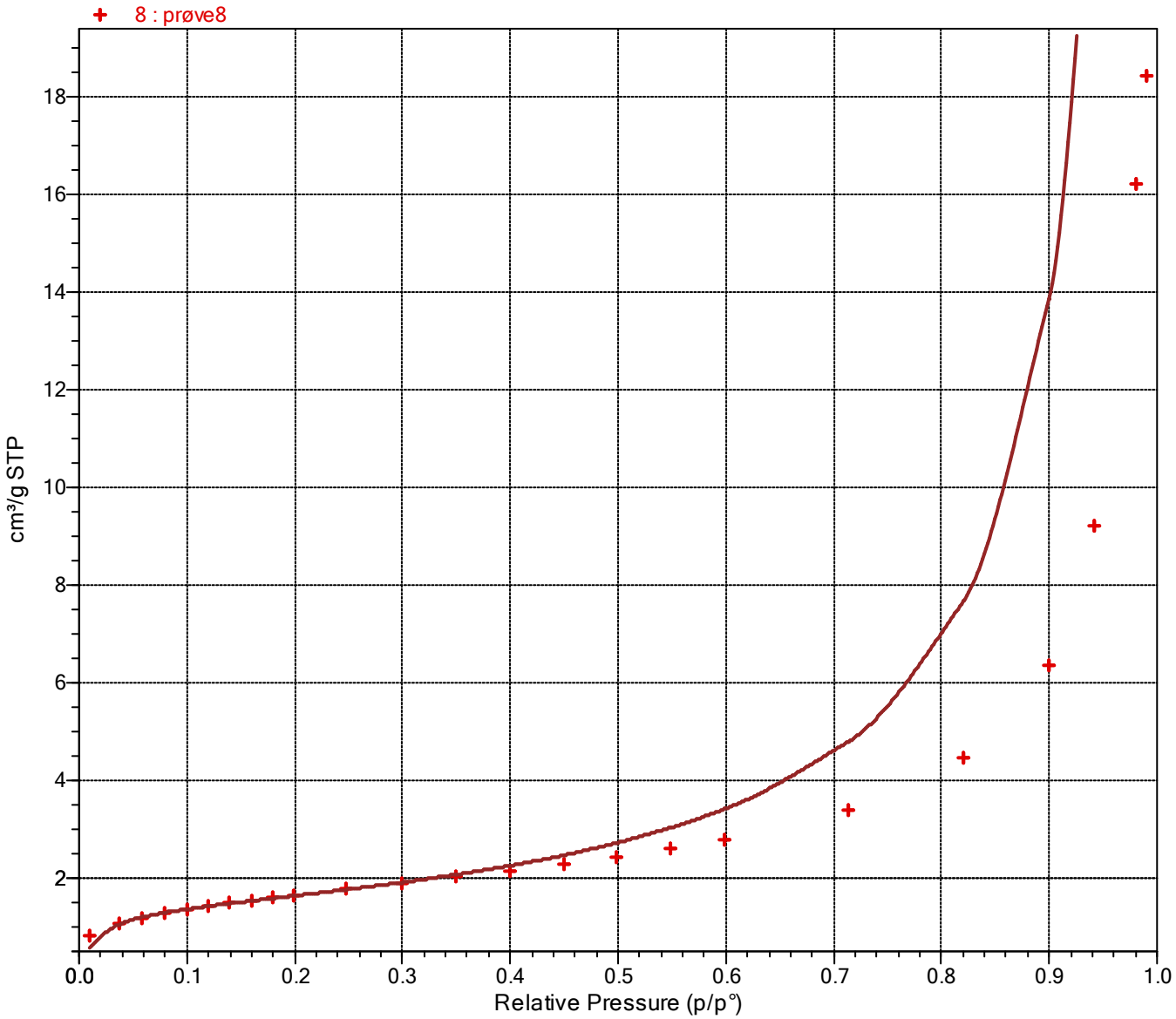

Sample: prøve8
Operator:
Submitter:
File: C:\data\Fride M\8.SMP

Started: 4/22/2022 11:41:17 AM
Completed: 4/22/2022 7:19:10 PM
Report time: 4/23/2022 10:43:41 AM
Sample mass: 1,3256 g
Analysis free space: 56,8169 cm³
Low pressure dose: None
Automatic degas: Yes

Analysis adsorptive: N2
Analysis bath temp.: -195,582 °C
Thermal correction: Yes
Ambient free space: 16,0910 cm³ Measured
Equilibration interval: 10 s
Sample density: 1,000 g/cm³

Comments: prøve8 fra takvent

Sample prep: Stage	Temperature (°C)	Ramp Rate (°C/min)	Time (min)
1	30	10	10
2	90	10	60
3	250	10	820
4	25	10	60

t-Plot Report

Micropore volume: -0,000279 cm³/g
Micropore area: *
External surface area: 6,4883 m²/g
Slope: 0,417966 ± 0,004425 cm³/g·Å STP
Y-intercept: -0,179955 ± 0,017966 cm³/g STP
Correlation coefficient: 0,999664
Surface area correction factor: 1,000
Density conversion factor: 0,0015523
Total surface area (BET): 6,0138 m²/g
Thickness range: 3,5000 to 5,0000 Å
Thickness equation: Harkins and Jura

Thickness Curve

$$t = [\ 13.99 / (\ 0.034 - \log(p/p^\circ)\ )\ ]^{\wedge} 0.5$$

t-Plot Report - Data

Relative Pressure (p/p°)	Statistical Thickness (Å)	Quantity Adsorbed (cm³/g STP)	Fitted
0.058332170	3.3215	1.1930	
0.079062772	3.5093	1.2809	*
0.099636045	3.6755	1.3550	*
0.119530055	3.8244	1.4206	*
0.139529888	3.9662	1.4815	*
0.159593099	4.1031	1.5381	*
0.179470057	4.2351	1.5938	*
0.199470287	4.3654	1.6458	*
0.248206849	4.6784	1.7690	*
0.299018432	5.0058	1.8960	
0.349729221	5.3419	2.0236	
0.399397028	5.6868	2.1541	
0.449043001	6.0540	2.2918	
0.499067110	6.4542	2.4419	
0.548828906	6.8916	2.6062	
0.598693158	7.3810	2.7967	

* The micropore area is not reported because either the micropore volume is negative or the calculated external surface area is larger than the total surface area.

Sample: prøve8
Operator:
Submitter:
File: C:\data\Fride M\8.SMP

Started:	4/22/2022 11:41:17 AM	Analysis adsorptive:	N2
Completed:	4/22/2022 7:19:10 PM	Analysis bath temp.:	-195,582 °C
Report time:	4/23/2022 10:43:41 AM	Thermal correction:	Yes
Sample mass:	1,3256 g	Ambient free space:	16,0910 cm³ Measured
Analysis free space:	56,8169 cm³	Equilibration interval:	10 s
Low pressure dose:	None	Sample density:	1,000 g/cm³
Automatic degas:	Yes		

Comments: prøve8 fra takvent

Sample prep: Stage	Temperature (°C)	Ramp Rate (°C/min)	Time (min)
1	30	10	10
2	90	10	60
3	250	10	820
4	25	10	60

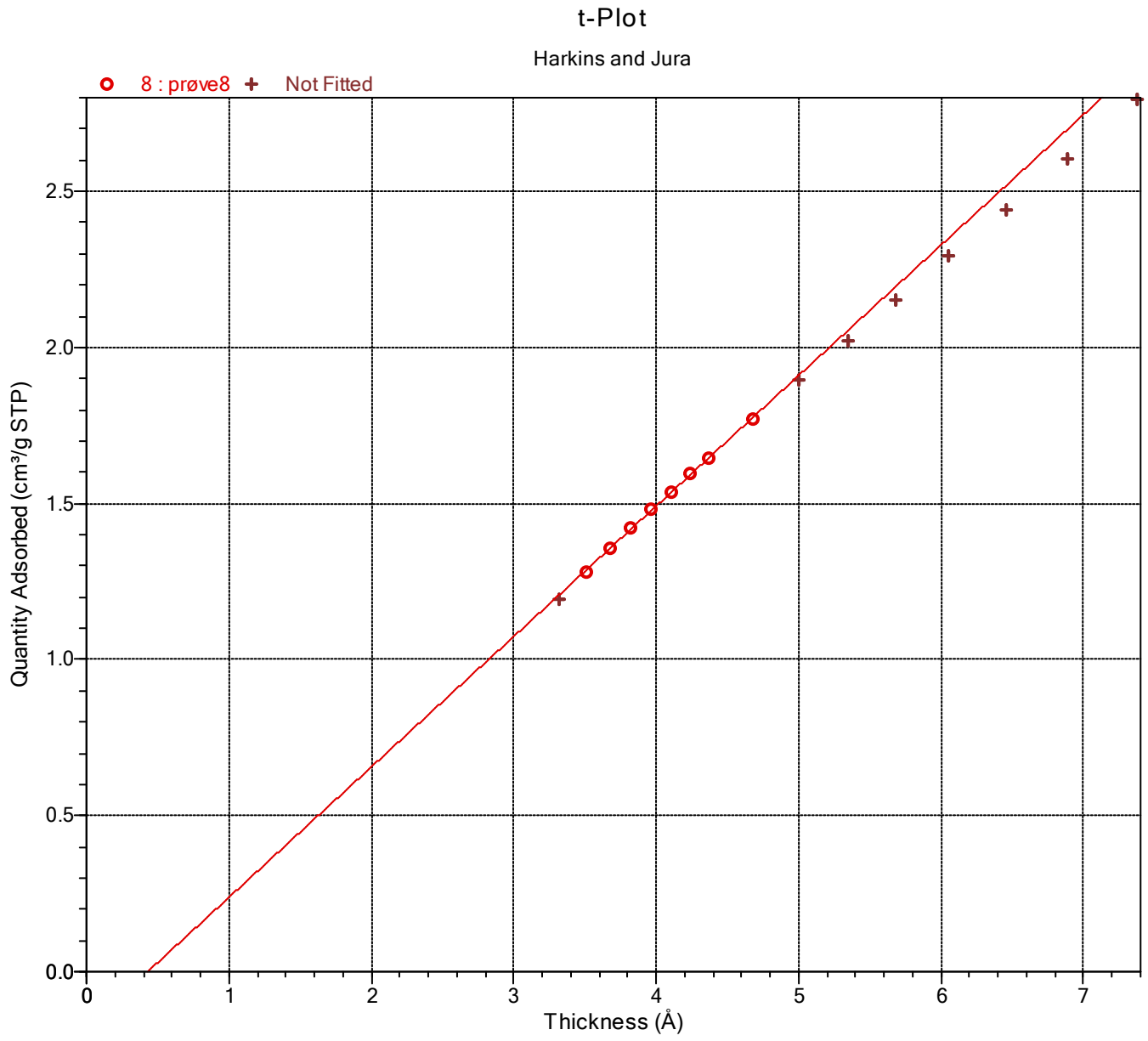

Sample: prøve8
Operator:
Submitter:
File: C:\data\Fride M\8.SMP

Started: 4/22/2022 11:41:17 AM
Completed: 4/22/2022 7:19:10 PM
Report time: 4/23/2022 10:43:41 AM
Sample mass: 1,3256 g
Analysis free space: 56,8169 cm³
Low pressure dose: None
Automatic degas: Yes

Analysis adsorptive: N2
Analysis bath temp.: -195,582 °C
Thermal correction: Yes
Ambient free space: 16,0910 cm³ Measured
Equilibration interval: 10 s
Sample density: 1,000 g/cm³

Comments: prøve8 fra takvent

Sample prep: Stage	Temperature (°C)	Ramp Rate (°C/min)	Time (min)
1	30	10	10
2	90	10	60
3	250	10	820
4	25	10	60

BJH Adsorption Pore Distribution Report

Faas Correction
Harkins and Jura
$t = [13.99 / (0.034 - \log(p/p^\circ))]^{0.5}$

Diameter range: 17,000 to 3 000,000 Å
Adsorbate property factor: 9,53000 Å
Density conversion factor: 0,0015523
Fraction of pores open at both ends: 0,00

Pore Diameter Range (Å)	Average Diameter (Å)	Incremental Pore Volume (cm³/g)	Cumulative Pore Volume (cm³/g)	Incremental Pore Area (m²/g)	Cumulative Pore Area (m²/g)
1927.9 - 1014.4	1207.9	0.003652	0.003652	0.121	0.121
1014.4 - 348.2	412.8	0.012516	0.016168	1.213	1.334
348.2 - 206.2	241.2	0.005178	0.021346	0.859	2.193
206.2 - 116.0	136.1	0.003356	0.024702	0.987	3.179
116.0 - 72.2	83.6	0.001591	0.026292	0.761	3.941
72.2 - 50.1	56.9	0.000696	0.026988	0.489	4.430
50.1 - 43.8	46.5	0.000179	0.027167	0.154	4.583
43.8 - 38.6	40.8	0.000137	0.027304	0.134	4.718
38.6 - 34.1	36.1	0.000119	0.027423	0.132	4.850
34.1 - 30.4	32.0	0.000104	0.027527	0.130	4.980
30.4 - 27.1	28.5	0.000096	0.027623	0.135	5.115
27.1 - 24.0	25.3	0.000090	0.027713	0.142	5.257
24.0 - 21.3	22.5	0.000090	0.027803	0.161	5.418
21.3 - 18.8	19.9	0.000086	0.027889	0.172	5.590
18.8 - 17.8	18.3	0.000036	0.027925	0.078	5.668
17.8 - 16.8	17.3	0.000046	0.027971	0.108	5.775

Sample: prøve8
Operator:
Submitter:
File: C:\data\Fride M\8.SMP

Started: 4/22/2022 11:41:17 AM
Completed: 4/22/2022 7:19:10 PM
Report time: 4/23/2022 10:43:41 AM
Sample mass: 1,3256 g
Analysis free space: 56,8169 cm³
Low pressure dose: None
Automatic degas: Yes

Analysis adsorptive: N2
Analysis bath temp.: -195,582 °C
Thermal correction: Yes
Ambient free space: 16,0910 cm³ Measured
Equilibration interval: 10 s
Sample density: 1,000 g/cm³

Comments: prøve8 fra takvent

Sample prep: Stage	Temperature (°C)	Ramp Rate (°C/min)	Time (min)
1	30	10	10
2	90	10	60
3	250	10	820
4	25	10	60

BJH Desorption Pore Distribution Report

Faas Correction
Harkins and Jura
$t = [13.99 / (0.034 - \log(p/p^\circ))]^{0.5}$

Diameter range: 17,000 to 3 000,000 Å
Adsorbate property factor: 9,53000 Å
Density conversion factor: 0,0015523
Fraction of pores open at both ends: 0,00

Pore Diameter Range (Å)	Average Diameter (Å)	Incremental Pore Volume (cm³/g)	Cumulative Pore Volume (cm³/g)	Incremental Pore Area (m²/g)	Cumulative Pore Area (m²/g)
1928.9 - 938.2	1122.4	0.002028	0.002028	0.072	0.072
938.2 - 399.4	476.9	0.008575	0.010602	0.719	0.792
399.4 - 250.7	290.9	0.004797	0.015399	0.660	1.451
250.7 - 206.5	224.0	0.001850	0.017248	0.330	1.781
206.5 - 179.4	190.9	0.001894	0.019142	0.397	2.178
179.4 - 167.4	173.0	0.000640	0.019782	0.148	2.326
167.4 - 139.6	150.7	0.001536	0.021319	0.408	2.734
139.6 - 120.9	128.8	0.001069	0.022388	0.332	3.066
120.9 - 106.1	112.5	0.000879	0.023267	0.313	3.379
106.1 - 69.5	79.8	0.002570	0.025837	1.289	4.667
69.5 - 49.4	55.8	0.001350	0.027187	0.968	5.635
49.4 - 45.1	47.0	0.000234	0.027421	0.199	5.835
45.1 - 39.8	42.1	0.000352	0.027773	0.335	6.169
39.8 - 35.4	37.3	0.000893	0.028666	0.957	7.126
35.4 - 31.3	33.0	0.000041	0.028708	0.050	7.177

Sample: prøve8
Operator:
Submitter:
File: C:\data\Fride M\8.SMP

Started: 4/22/2022 11:41:17 AM
Completed: 4/22/2022 7:19:10 PM
Report time: 4/23/2022 10:43:41 AM
Sample mass: 1,3256 g
Analysis free space: 56,8169 cm³
Low pressure dose: None
Automatic degas: Yes

Analysis adsorptive: N2
Analysis bath temp.: -195,582 °C
Thermal correction: Yes
Ambient free space: 16,0910 cm³ Measured
Equilibration interval: 10 s
Sample density: 1,000 g/cm³

Comments: prøve8 fra takvent

Sample prep: Stage	Temperature (°C)	Ramp Rate (°C/min)	Time (min)
1	30	10	10
2	90	10	60
3	250	10	820
4	25	10	60

Sample Log

Date	Time	Log Message
4/21/2022	12:54:43 PM	Start degas stage 1 of 4: ramp to 30 °C at 10 °C/min/min and hold for 10 minutes.
4/21/2022	1:13:43 PM	Start degas stage 2 of 4: ramp to 90 °C at 10 °C/min/min and hold for 60 minutes.
4/21/2022	2:24:43 PM	Start degas stage 3 of 4: ramp to 250 °C at 10 °C/min/min and hold for 820 minutes.
4/22/2022	4:23:43 AM	Start degas stage 4 of 4: ramp to 25 °C at 10 °C/min/min and hold for 60 minutes.
4/22/2022	6:53:43 AM	Start degas cooldown.
4/22/2022	11:41:17 AM	Started analysis of file 8.SMP on port 1.
4/22/2022	11:41:17 AM	System volume: 36.2726 cm³
4/22/2022	11:42:45 AM	Port 1 1000 mmHg transducer scale changed from 518,5526 to 518,5535 mmHg (fraction of nominal: 1.01).
4/22/2022	12:32:14 PM	Sample port 1 leak rate measured (interval: 50 s, rate: 0,001054 mmHg/min).
4/22/2022	12:39:24 PM	Ambient free-space measurement on sample port 1 complete (elapsed: 3485 s, qty in free-space: 16,0910 cm³, P1: 798,2021 mmHg, P2: 408,5869 mmHg, Tman: 45,0 °C, Tport: 45,0 °C).
4/22/2022	12:51:40 PM	Analysis free-space measurement on sample port 1 complete (elapsed: 4222 s, qty in free-space: 56,8169 cm³, P3: 172,3641 mmHg, Tport: 45,0 °C).
4/22/2022	1:33:59 PM	Psat port is charged with N2 at 778,3698 mmHg
4/22/2022	1:47:55 PM	Port 1 vacuum level is 1,18e-05 mmHg
4/22/2022	1:48:00 PM	Data collection started on sample port 1 (gas: N2).
4/22/2022	7:07:25 PM	Analysis termination started.
4/22/2022	7:19:10 PM	Finished a sample analysis for C:\data\Fride M\8.SMP on port 1.

micromeritics®

Micromeritics Instrument Corporation

Sample: prøve11
Operator:
Submitter:
File: C:\data\Fride M\11.SMP

Started:	4/22/2022 11:41:17 AM	Analysis adsorptive:	N2
Completed:	4/22/2022 7:19:10 PM	Analysis bath temp.:	-195,591 °C
Report time:	4/23/2022 10:44:09 AM	Thermal correction:	Yes
Sample mass:	1,4597 g	Ambient free space:	16,0736 cm³ Measured
Analysis free space:	55,6293 cm³	Equilibration interval:	10 s
Low pressure dose:	None	Sample density:	1,000 g/cm³
Automatic degas:	Yes		

Comments: prøve 11 fra gulv vifterom

Sample prep: Stage	Temperature (°C)	Ramp Rate (°C/min)	Time (min)
1	30	10	10
2	90	10	60
3	250	10	820
4	25	10	60

Summary Report

Surface Area

Single point surface area at p/p° = 0,299476124: 12,0381 m²/g

BET Surface Area: 12,3691 m²/g

Pore Volume

Single point desorption total pore volume of pores less than 1 837,906 Å diameter at p/p° = 0,989465986: 0,063133 cm³/g

Pore Size

Adsorption average pore diameter (4V/A by BET): 204,166 Å

Desorption average pore diameter (4V/A by BET): 204,166 Å

Sample: prøve11
Operator:
Submitter:
File: C:\data\Fride M\11.SMP

Started: 4/22/2022 11:41:17 AM
Completed: 4/22/2022 7:19:10 PM
Report time: 4/23/2022 10:44:09 AM
Sample mass: 1,4597 g
Analysis free space: 55,6293 cm³
Low pressure dose: None
Automatic degas: Yes

Analysis adsorptive: N2
Analysis bath temp.: -195,591 °C
Thermal correction: Yes
Ambient free space: 16,0736 cm³ Measured
Equilibration interval: 10 s
Sample density: 1,000 g/cm³

Comments: prøve 11 fra gulv vifterom

Sample prep: Stage	Temperature (°C)	Ramp Rate (°C/min)	Time (min)
1	30	10	10
2	90	10	60
3	250	10	820
4	25	10	60

Isotherm Tabular Report

Relative Pressure (p/p°)	Absolute Pressure (mmHg)	Quantity Adsorbed (cm³/g STP)	Elapsed Time (h:min)	Saturation Pressure (mmHg)
			01:52	778.452454
0.009589691	7.490704	1.9243	02:31	781.120483
0.036091413	28.184547	2.4177	02:39	780.921143
0.057356995	44.797325	2.6191	02:42	781.026367
0.078538646	61.329742	2.7784	02:46	780.886169
0.099674030	77.865372	2.9158	02:49	781.200195
0.119674652	93.465706	3.0349	02:52	780.998352
0.139599879	109.029610	3.1464	02:56	781.015076
0.159619703	124.669174	3.2533	02:59	781.038757
0.180062504	140.608704	3.3588	03:01	780.888306
0.199540518	155.800430	3.4572	03:04	780.795959
0.248120123	193.749817	3.6962	03:07	780.871033
0.299476124	233.846527	3.9481	03:10	780.851990
0.349805368	273.154694	4.1967	03:13	780.876221
0.399131749	311.661530	4.4454	03:16	780.848755
0.449019047	350.694153	4.7075	03:19	781.022888
0.499038942	389.761841	4.9840	03:22	781.024902
0.548913419	428.684998	5.2813	03:25	780.970154
0.599062876	467.799988	5.6126	03:28	780.886292
0.706440885	551.713257	6.5484	03:32	780.975830
0.802994921	626.973328	8.2092	03:37	780.793640
0.860997247	672.221130	11.2424	03:46	780.747131
0.891112662	695.772217	15.0742	03:56	780.790405
0.910260510	710.645447	19.0759	04:07	780.705566
0.935446010	730.375793	26.5403	04:21	780.778137
0.960575951	749.708130	33.4478	04:37	780.477722
0.975733150	757.889587	36.1629	04:47	776.738586
0.989465986	768.208069	40.6716	05:03	776.386536
0.978047068	759.355469	39.4656	05:10	776.399719
0.955716475	741.999512	35.9331	05:22	776.380371
0.921664760	715.356201	30.6761	05:38	776.156616
0.905059346	702.476196	27.7283	05:48	776.165894
0.879003129	682.054871	22.0695	06:04	775.941345
0.848195541	657.911072	15.6387	06:23	775.659668
0.825399550	640.116394	12.6426	06:34	775.523071
0.805820793	624.821167	10.9983	06:42	775.384766
0.730319585	566.143127	7.8416	06:50	775.199158
0.629883631	488.290527	6.3078	06:54	775.207520

Sample: prøve11
Operator:
Submitter:
File: C:\data\Fride M\11.SMP

Started: 4/22/2022 11:41:17 AM
Completed: 4/22/2022 7:19:10 PM
Report time: 4/23/2022 10:44:09 AM
Sample mass: 1,4597 g
Analysis free space: 55,6293 cm³
Low pressure dose: None
Automatic degas: Yes

Analysis adsorptive: N2
Analysis bath temp.: -195,591 °C
Thermal correction: Yes
Ambient free space: 16,0736 cm³ Measured
Equilibration interval: 10 s
Sample density: 1,000 g/cm³

Comments: prøve 11 fra gulv vifterom

Sample prep: Stage	Temperature (°C)	Ramp Rate (°C/min)	Time (min)
1	30	10	10
2	90	10	60
3	250	10	820
4	25	10	60

Isotherm Tabular Report

Relative Pressure (p/p°)	Absolute Pressure (mmHg)	Quantity Adsorbed (cm³/g STP)	Elapsed Time (h:min)	Saturation Pressure (mmHg)
0.300251749	232.814407	4.0205	07:14	775.397339
0.250394340	194.107147	3.7758	07:17	775.205811
0.200282262	155.261856	3.5277	07:21	775.215210
0.140378077	108.798485	3.2175	07:26	775.039001

Sample: prøve11
Operator:
Submitter:
File: C:\data\Fride M\11.SMP

Started:	4/22/2022 11:41:17 AM	Analysis adsorptive:	N2
Completed:	4/22/2022 7:19:10 PM	Analysis bath temp.:	-195,591 °C
Report time:	4/23/2022 10:44:09 AM	Thermal correction:	Yes
Sample mass:	1,4597 g	Ambient free space:	16,0736 cm³ Measured
Analysis free space:	55,6293 cm³	Equilibration interval:	10 s
Low pressure dose:	None	Sample density:	1,000 g/cm³
Automatic degas:	Yes		

Comments: prøve 11 fra gulv vifterom

Sample prep: Stage	Temperature (°C)	Ramp Rate (°C/min)	Time (min)
1	30	10	10
2	90	10	60
3	250	10	820
4	25	10	60

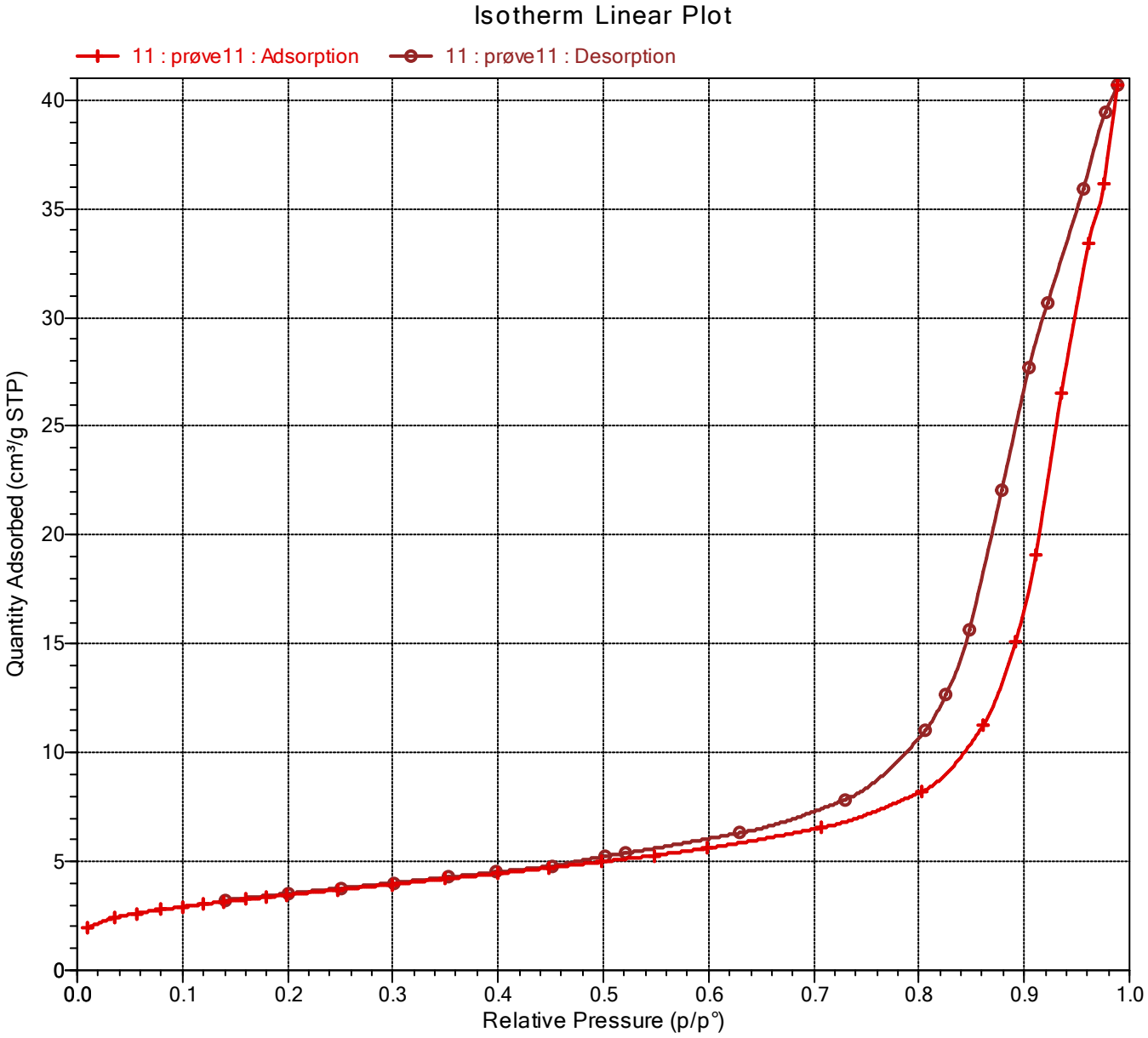

Sample: prøve11
Operator:
Submitter:
File: C:\data\Fride M\11.SMP

Started: 4/22/2022 11:41:17 AM
Completed: 4/22/2022 7:19:10 PM
Report time: 4/23/2022 10:44:09 AM
Sample mass: 1,4597 g
Analysis free space: 55,6293 cm³
Low pressure dose: None
Automatic degas: Yes

Analysis adsorptive: N2
Analysis bath temp.: -195,591 °C
Thermal correction: Yes
Ambient free space: 16,0736 cm³ Measured
Equilibration interval: 10 s
Sample density: 1,000 g/cm³

Comments: prøve 11 fra gulv vifterom

Sample prep: Stage	Temperature (°C)	Ramp Rate (°C/min)	Time (min)
1	30	10	10
2	90	10	60
3	250	10	820
4	25	10	60

BET Report

BET surface area: 12,3691 ± 0,0665 m²/g
Slope: 0,348911 ± 0,001865 g/cm³ STP
Y-intercept: 0,002981 ± 0,000324 g/cm³ STP
C: 118,045189
Qm: 2,8418 cm³/g STP
Correlation coefficient: 0,9998858
Molecular cross-sectional area: 0,1620 nm²

Relative Pressure (p/p°)	Quantity Adsorbed (cm³/g STP)	1/[Q(p°/p - 1)]
0.057356995	2.6191	0.023232
0.078538646	2.7784	0.030676
0.099674030	2.9158	0.037969
0.119674652	3.0349	0.044794
0.139599879	3.1464	0.051567
0.159619703	3.2533	0.058383
0.180062504	3.3588	0.065382
0.199540518	3.4572	0.072105
0.248120123	3.6962	0.089281
0.299476124	3.9481	0.108281

Sample: prøve11
Operator:
Submitter:
File: C:\data\Fride M\11.SMP

Started:	4/22/2022 11:41:17 AM	Analysis adsorptive:	N2
Completed:	4/22/2022 7:19:10 PM	Analysis bath temp.:	-195,591 °C
Report time:	4/23/2022 10:44:09 AM	Thermal correction:	Yes
Sample mass:	1,4597 g	Ambient free space:	16,0736 cm³ Measured
Analysis free space:	55,6293 cm³	Equilibration interval:	10 s
Low pressure dose:	None	Sample density:	1,000 g/cm³
Automatic degas:	Yes		

Comments: prøve 11 fra gulv vifterom

Sample prep: Stage	Temperature (°C)	Ramp Rate (°C/min)	Time (min)
1	30	10	10
2	90	10	60
3	250	10	820
4	25	10	60

BET Surface Area Plot

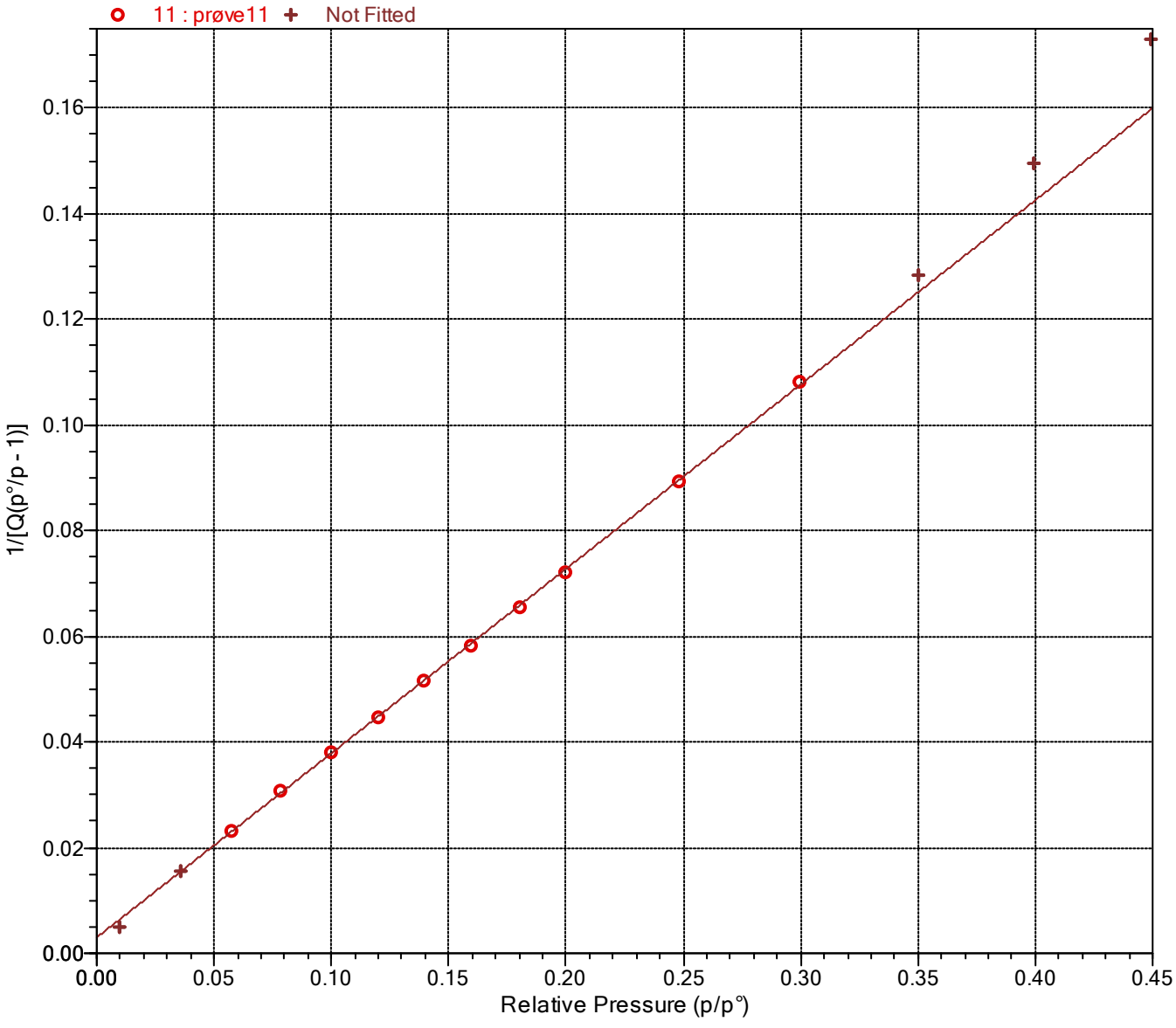

Sample: prøve11
Operator:
Submitter:
File: C:\data\Fride M\11.SMP

Started:	4/22/2022 11:41:17 AM	Analysis adsorptive:	N2
Completed:	4/22/2022 7:19:10 PM	Analysis bath temp.:	-195,591 °C
Report time:	4/23/2022 10:44:09 AM	Thermal correction:	Yes
Sample mass:	1,4597 g	Ambient free space:	16,0736 cm³ Measured
Analysis free space:	55,6293 cm³	Equilibration interval:	10 s
Low pressure dose:	None	Sample density:	1,000 g/cm³
Automatic degas:	Yes		

Comments: prøve 11 fra gulv vifterom

Sample prep: Stage	Temperature (°C)	Ramp Rate (°C/min)	Time (min)
1	30	10	10
2	90	10	60
3	250	10	820
4	25	10	60

BET Isotherm Plot

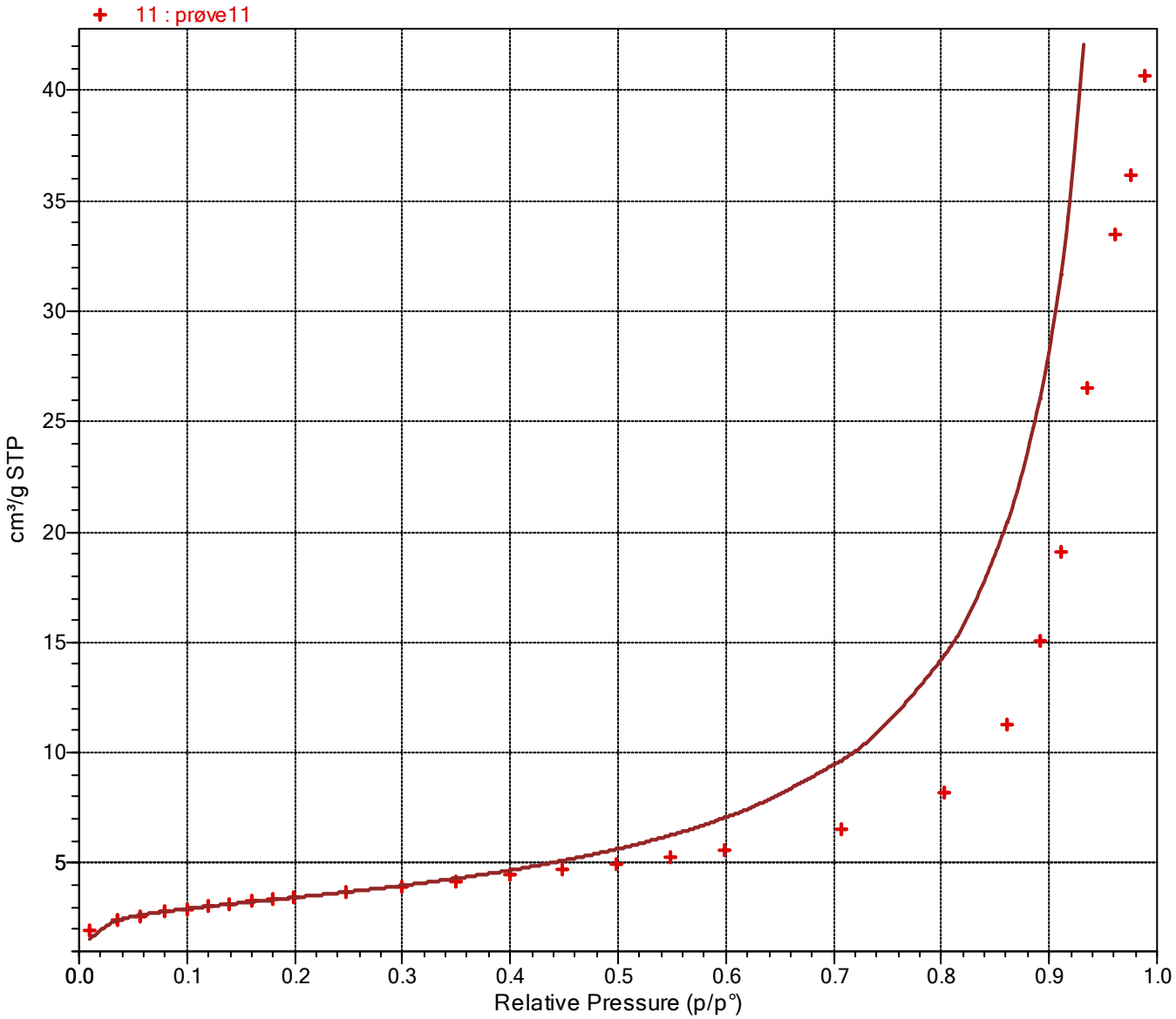

Sample: prøve11
Operator:
Submitter:
File: C:\data\Fride M\11.SMP

Started:	4/22/2022 11:41:17 AM	Analysis adsorptive:	N2
Completed:	4/22/2022 7:19:10 PM	Analysis bath temp.:	-195,591 °C
Report time:	4/23/2022 10:44:09 AM	Thermal correction:	Yes
Sample mass:	1,4597 g	Ambient free space:	16,0736 cm³ Measured
Analysis free space:	55,6293 cm³	Equilibration interval:	10 s
Low pressure dose:	None	Sample density:	1,000 g/cm³
Automatic degas:	Yes		

Comments: prøve 11 fra gulv vifterom

Sample prep: Stage	Temperature (°C)	Ramp Rate (°C/min)	Time (min)
1	30	10	10
2	90	10	60
3	250	10	820
4	25	10	60

t-Plot Report

Micropore volume:	0,000062 cm³/g
Micropore area:	0,2225 m²/g
External surface area:	12,1466 m²/g
Slope:	0,782501 ± 0,002939 cm³/g·Å STP
Y-intercept:	0,040042 ± 0,011933 cm³/g STP
Correlation coefficient:	0,999958
Surface area correction factor:	1,000
Density conversion factor:	0,0015523
Total surface area (BET):	12,3691 m²/g
Thickness range:	3,5000 to 5,0000 Å
Thickness equation:	Harkins and Jura

Thickness Curve

$$t = [\ 13.99 / (\ 0.034 - \log(p/p^\circ)\ )\ ]^{\wedge} 0.5$$

t-Plot Report - Data

Relative Pressure (p/p°)	Statistical Thickness (Å)	Quantity Adsorbed (cm³/g STP)	Fitted
0.057356995	3.3119	2.6191	
0.078538646	3.5048	2.7784	*
0.099674030	3.6758	2.9158	*
0.119674652	3.8254	3.0349	*
0.139599879	3.9667	3.1464	*
0.159619703	4.1033	3.2533	*
0.180062504	4.2389	3.3588	*
0.199540518	4.3659	3.4572	*
0.248120123	4.6778	3.6962	*
0.299476124	5.0088	3.9481	
0.349805368	5.3424	4.1967	
0.399131749	5.6849	4.4454	
0.449019047	6.0538	4.7075	
0.499038942	6.4540	4.9840	
0.548913419	6.8924	5.2813	
0.599062876	7.3849	5.6126	

Sample: prøve11
Operator:
Submitter:
File: C:\data\Fride M\11.SMP

Started:	4/22/2022 11:41:17 AM	Analysis adsorptive:	N2
Completed:	4/22/2022 7:19:10 PM	Analysis bath temp.:	-195,591 °C
Report time:	4/23/2022 10:44:09 AM	Thermal correction:	Yes
Sample mass:	1,4597 g	Ambient free space:	16,0736 cm³ Measured
Analysis free space:	55,6293 cm³	Equilibration interval:	10 s
Low pressure dose:	None	Sample density:	1,000 g/cm³
Automatic degas:	Yes		

Comments: prøve 11 fra gulv vifterom

Sample prep: Stage	Temperature (°C)	Ramp Rate (°C/min)	Time (min)
1	30	10	10
2	90	10	60
3	250	10	820
4	25	10	60

t-Plot

Harkins and Jura

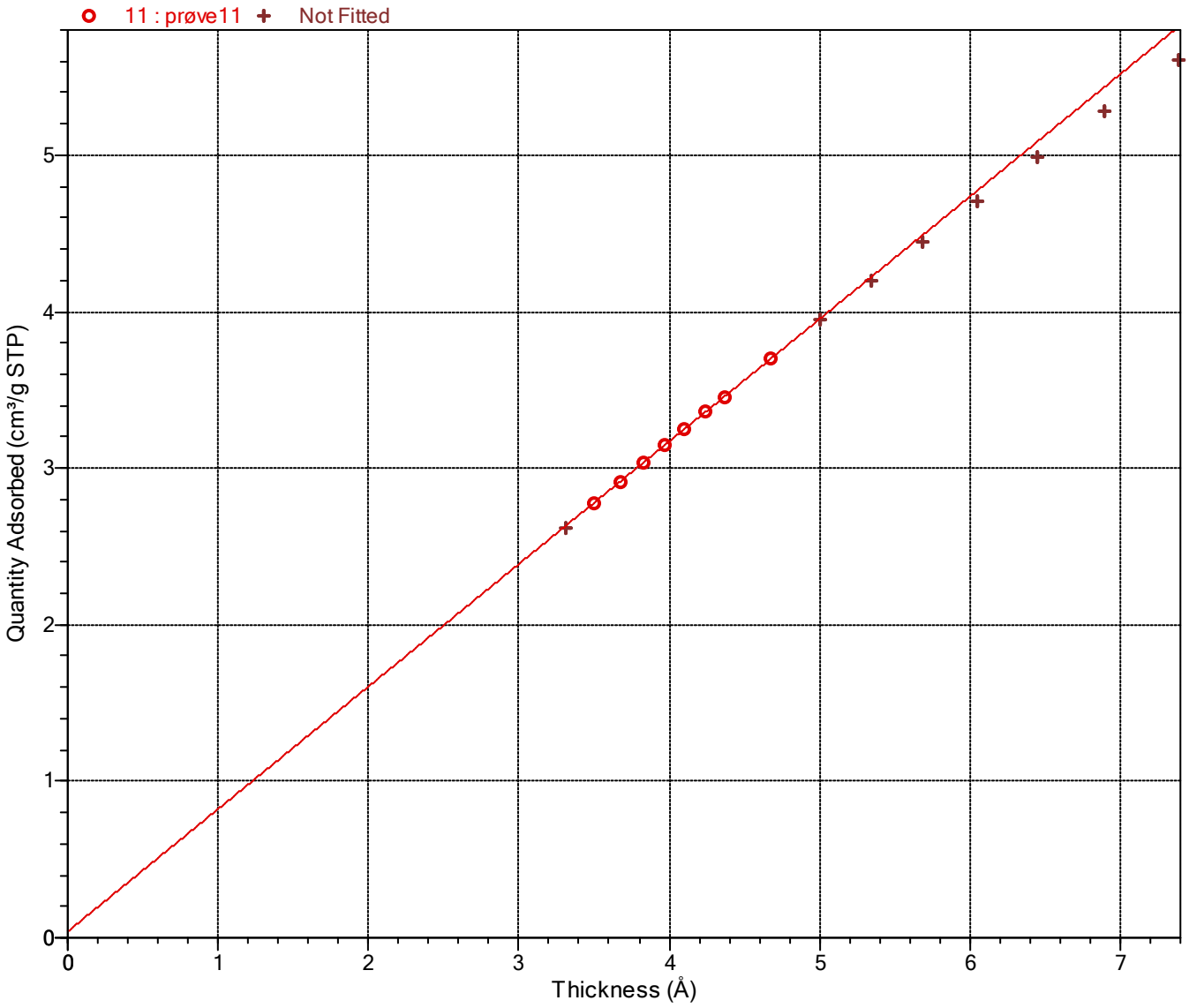

Sample: prøve11
Operator:
Submitter:
File: C:\data\Fride M\11.SMP

Started: 4/22/2022 11:41:17 AM
Completed: 4/22/2022 7:19:10 PM
Report time: 4/23/2022 10:44:09 AM
Sample mass: 1,4597 g
Analysis free space: 55,6293 cm³
Low pressure dose: None
Automatic degas: Yes

Analysis adsorptive: N2
Analysis bath temp.: -195,591 °C
Thermal correction: Yes
Ambient free space: 16,0736 cm³ Measured
Equilibration interval: 10 s
Sample density: 1,000 g/cm³

Comments: prøve 11 fra gulv vifterom

Sample prep: Stage	Temperature (°C)	Ramp Rate (°C/min)	Time (min)
1	30	10	10
2	90	10	60
3	250	10	820
4	25	10	60

BJH Adsorption Pore Distribution Report

Faas Correction
Harkins and Jura
$t = [13.99 / (0.034 - \log(p/p°))]^{0.5}$

Diameter range: 17,000 to 3 000,000 Å
Adsorbate property factor: 9,53000 Å
Density conversion factor: 0,0015523
Fraction of pores open at both ends: 0,00

Pore Diameter Range (Å)	Average Diameter (Å)	Incremental Pore Volume (cm³/g)	Cumulative Pore Volume (cm³/g)	Incremental Pore Area (m²/g)	Cumulative Pore Area (m²/g)
1837.0 - 810.4	971.6	0.007524	0.007524	0.310	0.310
810.4 - 506.0	588.9	0.004674	0.012198	0.317	0.627
506.0 - 314.6	365.8	0.012531	0.024729	1.370	1.998
314.6 - 229.2	257.9	0.014103	0.038832	2.187	4.185
229.2 - 190.3	205.9	0.007656	0.046488	1.488	5.673
190.3 - 150.3	165.2	0.007308	0.053797	1.769	7.442
150.3 - 106.8	120.7	0.005310	0.059107	1.760	9.202
106.8 - 71.4	81.6	0.001810	0.060917	0.887	10.089
71.4 - 51.1	57.6	0.000418	0.061336	0.291	10.380
51.1 - 44.7	47.4	0.000082	0.061418	0.070	10.449
44.7 - 39.5	41.7	0.000075	0.061493	0.072	10.521
39.5 - 35.0	36.9	0.000079	0.061572	0.086	10.606
35.0 - 31.2	32.9	0.000091	0.061663	0.111	10.718
31.2 - 28.0	29.4	0.000098	0.061761	0.133	10.851
28.0 - 25.0	26.3	0.000112	0.061874	0.171	11.022
25.0 - 22.2	23.4	0.000123	0.061997	0.211	11.233
22.2 - 19.7	20.7	0.000113	0.062110	0.217	11.450
19.7 - 18.7	19.2	0.000048	0.062157	0.100	11.550
18.7 - 17.7	18.2	0.000050	0.062208	0.110	11.660
17.7 - 16.7	17.2	0.000051	0.062258	0.118	11.778

Sample: prøve11
Operator:
Submitter:
File: C:\data\Fride M\11.SMP

Started: 4/22/2022 11:41:17 AM
Completed: 4/22/2022 7:19:10 PM
Report time: 4/23/2022 10:44:09 AM
Sample mass: 1,4597 g
Analysis free space: 55,6293 cm³
Low pressure dose: None
Automatic degas: Yes

Analysis adsorptive: N2
Analysis bath temp.: -195,591 °C
Thermal correction: Yes
Ambient free space: 16,0736 cm³ Measured
Equilibration interval: 10 s
Sample density: 1,000 g/cm³

Comments: prøve 11 fra gulv vifterom

Sample prep: Stage	Temperature (°C)	Ramp Rate (°C/min)	Time (min)
1	30	10	10
2	90	10	60
3	250	10	820
4	25	10	60

BJH Desorption Pore Distribution Report

Faas Correction
Harkins and Jura
t = [13.99 / (0.034 - log(p/p°))] ^ 0.5

Diameter range: 17,000 to 3 000,000 Å
Adsorbate property factor: 9,53000 Å
Density conversion factor: 0,0015523
Fraction of pores open at both ends: 0,00

Pore Diameter Range (Å)	Average Diameter (Å)	Incremental Pore Volume (cm³/g)	Cumulative Pore Volume (cm³/g)	Incremental Pore Area (m²/g)	Cumulative Pore Area (m²/g)
1836.3 - 892.9	1068.1	0.001998	0.001998	0.075	0.075
892.9 - 451.5	537.3	0.006154	0.008152	0.458	0.533
451.5 - 260.5	305.8	0.009685	0.017836	1.267	1.800
260.5 - 216.4	234.1	0.005596	0.023433	0.956	2.756
216.4 - 171.1	188.1	0.011124	0.034557	2.365	5.121
171.1 - 137.2	150.2	0.012984	0.047541	3.459	8.580
137.2 - 119.6	127.1	0.005936	0.053477	1.868	10.448
119.6 - 107.6	112.9	0.003102	0.056579	1.099	11.547
107.6 - 77.2	87.0	0.005259	0.061837	2.417	13.964
77.2 - 55.1	62.2	0.001173	0.063010	0.755	14.719
55.1 - 39.0	39.9	0.000003	0.063013	0.003	14.722
39.0 - 34.5	36.4	0.000285	0.063298	0.313	15.034

Sample: prøve11
Operator:
Submitter:
File: C:\data\Fride M\11.SMP

Started:	4/22/2022 11:41:17 AM	Analysis adsorptive:	N2
Completed:	4/22/2022 7:19:10 PM	Analysis bath temp.:	-195,591 °C
Report time:	4/23/2022 10:44:09 AM	Thermal correction:	Yes
Sample mass:	1,4597 g	Ambient free space:	16,0736 cm³ Measured
Analysis free space:	55,6293 cm³	Equilibration interval:	10 s
Low pressure dose:	None	Sample density:	1,000 g/cm³
Automatic degas:	Yes		

Comments: prøve 11 fra gulv vifterom

Sample prep: Stage	Temperature (°C)	Ramp Rate (°C/min)	Time (min)
1	30	10	10
2	90	10	60
3	250	10	820
4	25	10	60

Sample Log

Date	Time	Log Message
4/21/2022	12:56:22 PM	Start degas stage 1 of 4: ramp to 30 °C at 10 °C/min/min and hold for 10 minutes.
4/21/2022	1:10:22 PM	Start degas stage 2 of 4: ramp to 90 °C at 10 °C/min/min and hold for 60 minutes.
4/21/2022	2:21:22 PM	Start degas stage 3 of 4: ramp to 250 °C at 10 °C/min/min and hold for 820 minutes.
4/22/2022	4:20:22 AM	Start degas stage 4 of 4: ramp to 25 °C at 10 °C/min/min and hold for 60 minutes.
4/22/2022	7:10:22 AM	Start degas cooldown.
4/22/2022	11:41:17 AM	Started analysis of file 11.SMP on port 2.
4/22/2022	11:41:17 AM	System volume: 36.2726 cm³
4/22/2022	11:42:45 AM	Port 2 1000 mmHg transducer scale changed from 517,6125 to 517,6033 mmHg (fraction of nominal: 1.01).
4/22/2022	12:32:19 PM	Sample port 2 leak rate measured (interval: 50 s, rate: 0,000151 mmHg/min).
4/22/2022	12:40:34 PM	Ambient free-space measurement on sample port 2 complete (elapsed: 3555 s, qty in free-space: 16,0736 cm³, P1: 802,8527 mmHg, P2: 332,0007 mmHg, Tman: 45,0 °C, Tport: 45,0 °C).
4/22/2022	12:51:40 PM	Analysis free-space measurement on sample port 2 complete (elapsed: 4222 s, qty in free-space: 55,6293 cm³, P3: 175,2588 mmHg, Tport: 45,0 °C).
4/22/2022	1:33:59 PM	Psat port is charged with N2 at 778,3698 mmHg
4/22/2022	1:47:55 PM	Port 2 vacuum level is 1,18e-05 mmHg
4/22/2022	1:48:00 PM	Data collection started on sample port 2 (gas: N2).
4/22/2022	7:07:25 PM	Analysis termination started.
4/22/2022	7:19:10 PM	Finished a sample analysis for C:\data\Fride M\11.SMP on port 2.

B SEM

B.1 Chemical Composition analyses

Mapping sample 1 -Airborne Høyanger

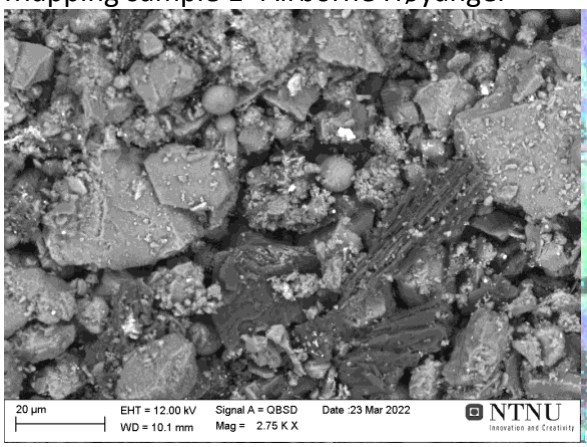

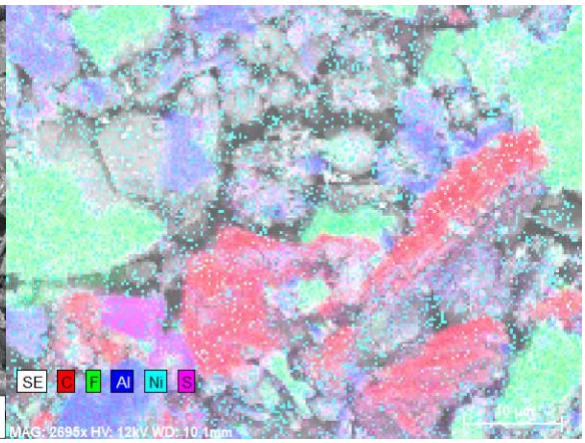

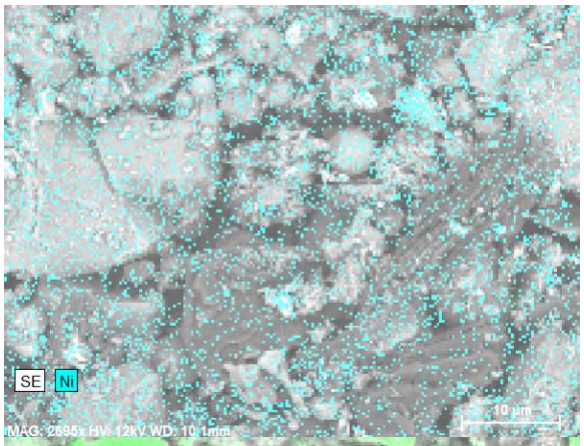

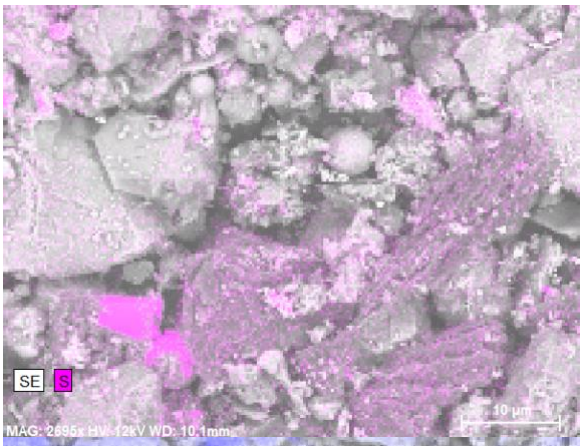

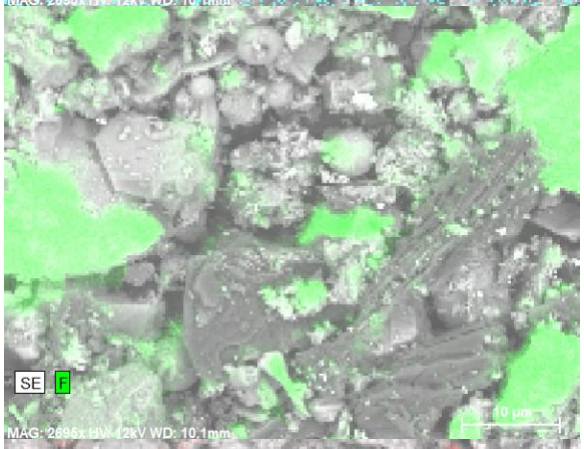

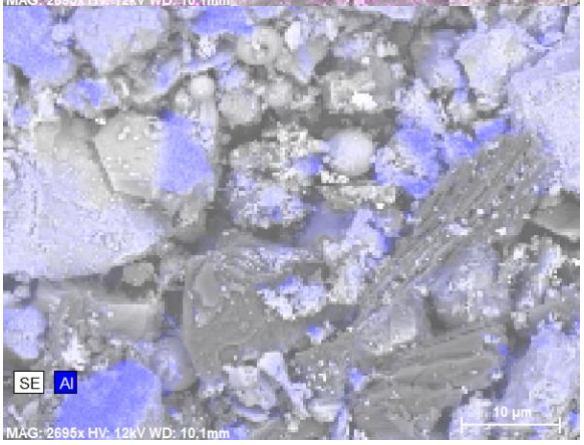

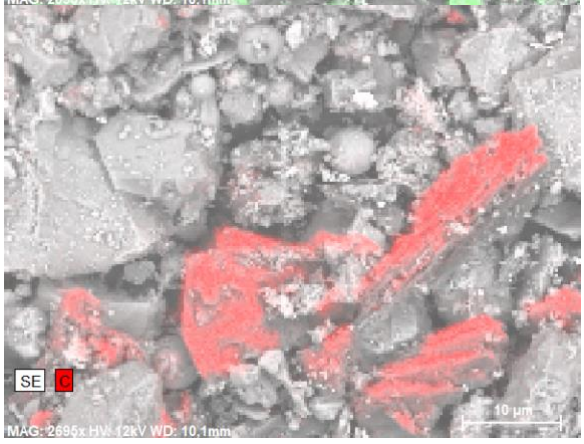

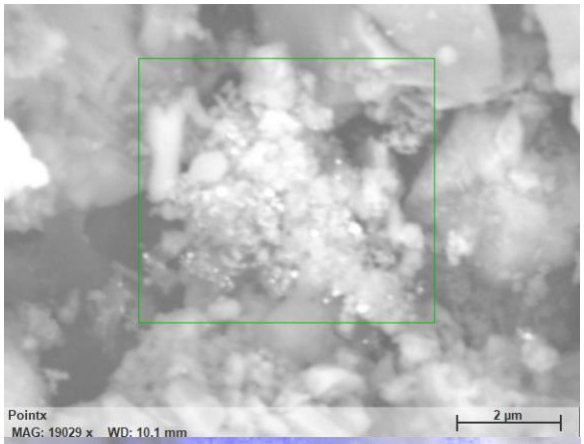
Pointx
MAG: 19029 x WD: 10,1 mm
2 µm

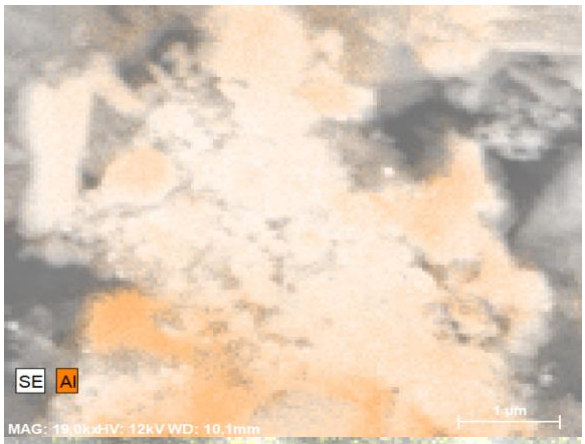
SE Al
MAG: 19,0kx HV: 12kV WD: 10,1mm
1 µm

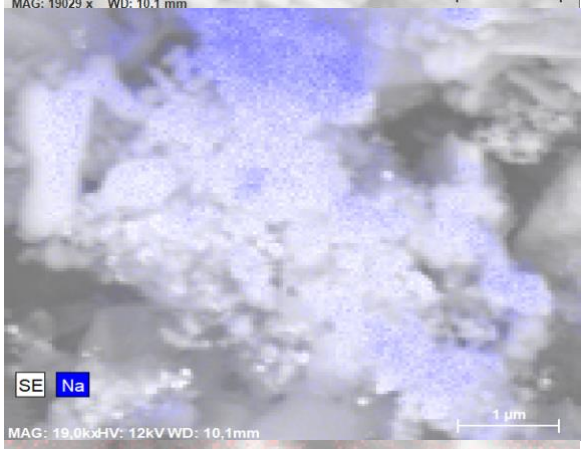
SE Na
MAG: 19,0kx HV: 12kV WD: 10,1mm
1 µm

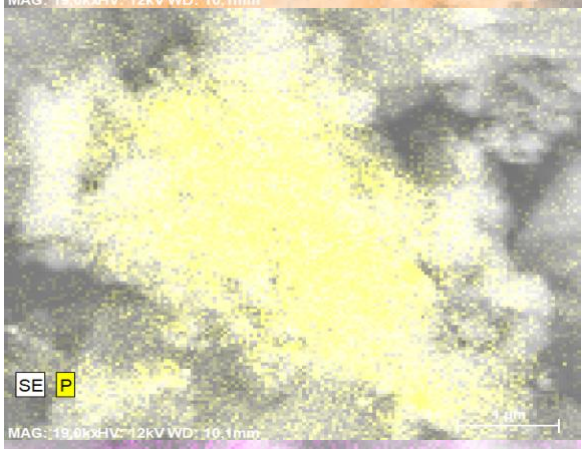
SE P
MAG: 19,0kx HV: 12kV WD: 10,1mm
1 µm

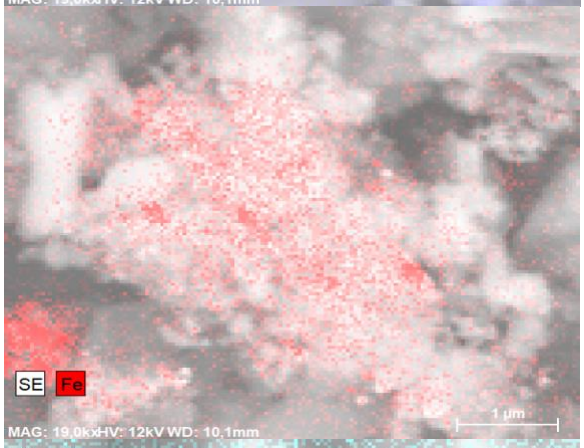
SE Fe
MAG: 19,0kx HV: 12kV WD: 10,1mm
1 µm

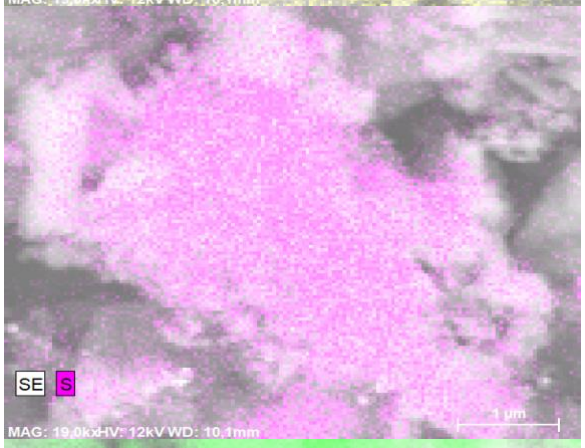
SE S
MAG: 19,0kx HV: 12kV WD: 10,1mm
1 µm

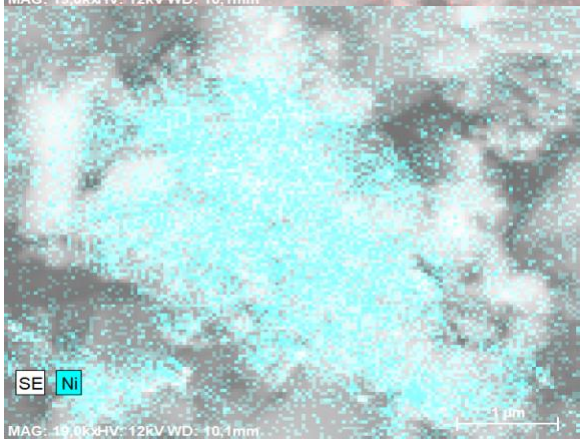
SE Ni
MAG: 19,0kx HV: 12kV WD: 10,1mm
1 µm

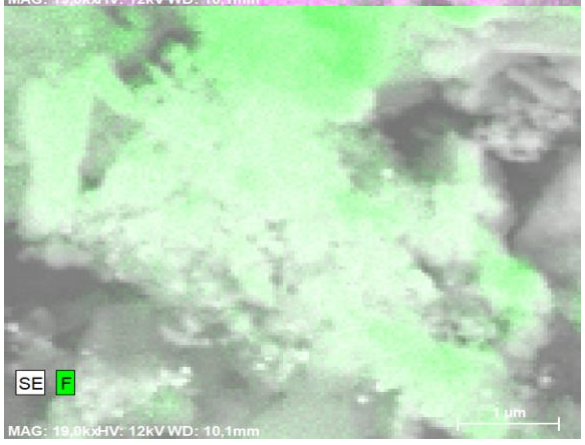
SE F
MAG: 19,0kx HV: 12kV WD: 10,1mm
1 µm

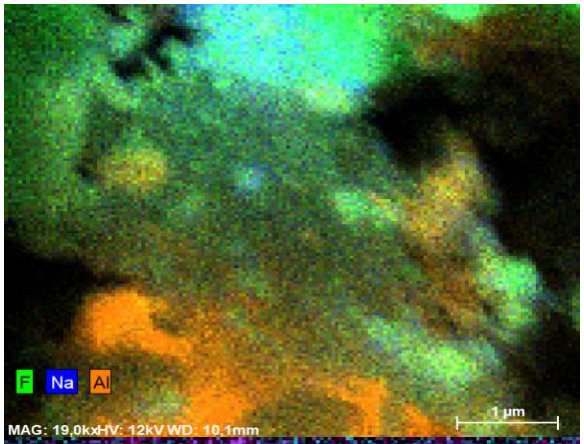

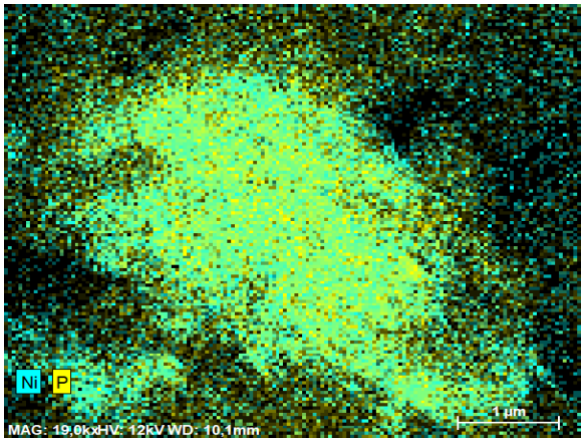

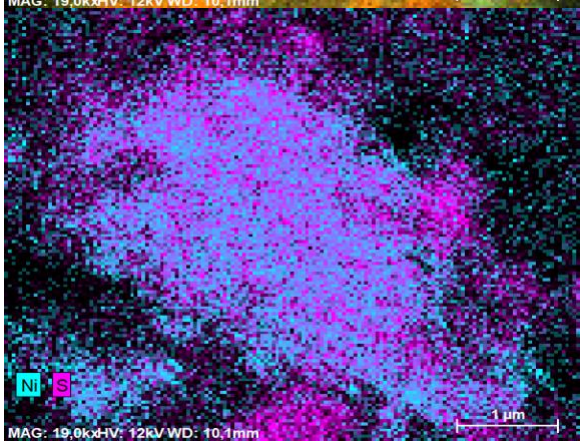

Point analysis sample 1

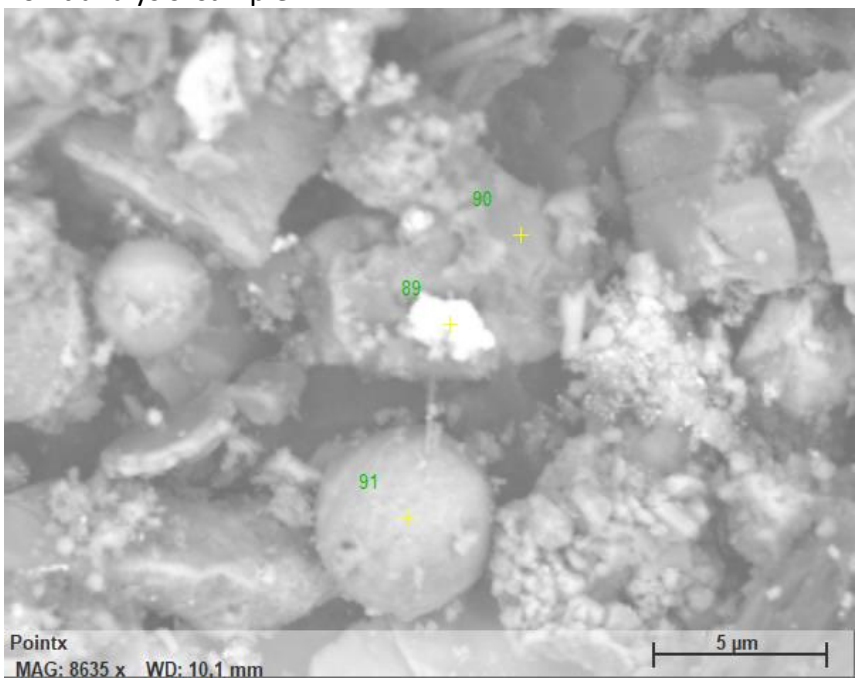

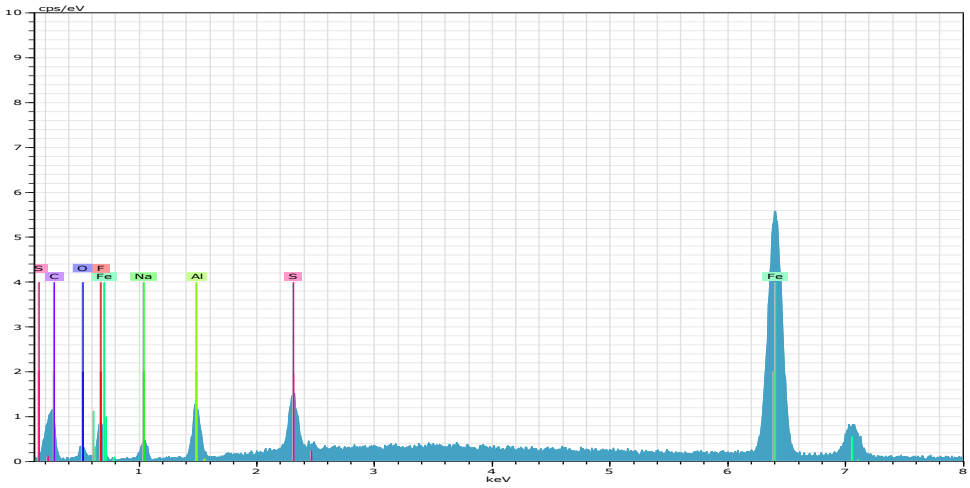
cps/eV
S
C
O
F
Fe
Na
Al
S
Fe
keV

89

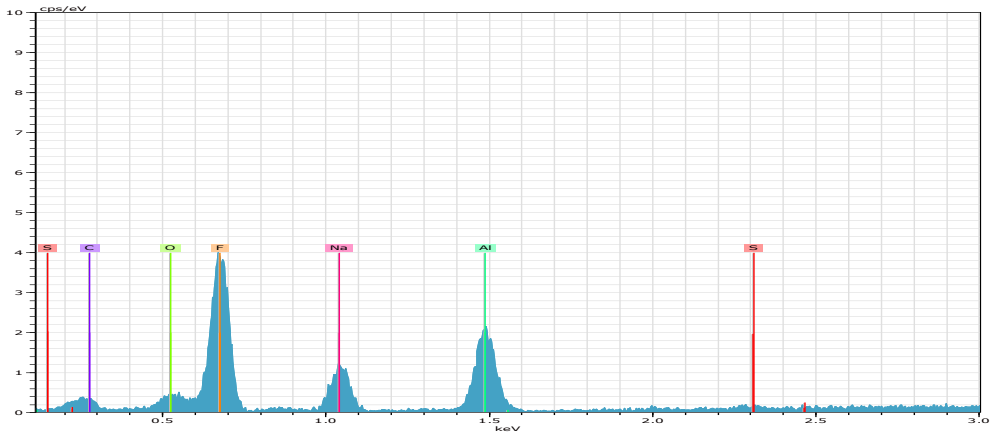
cps/eV
S
C
O
F
Na
Al
S
keV

90

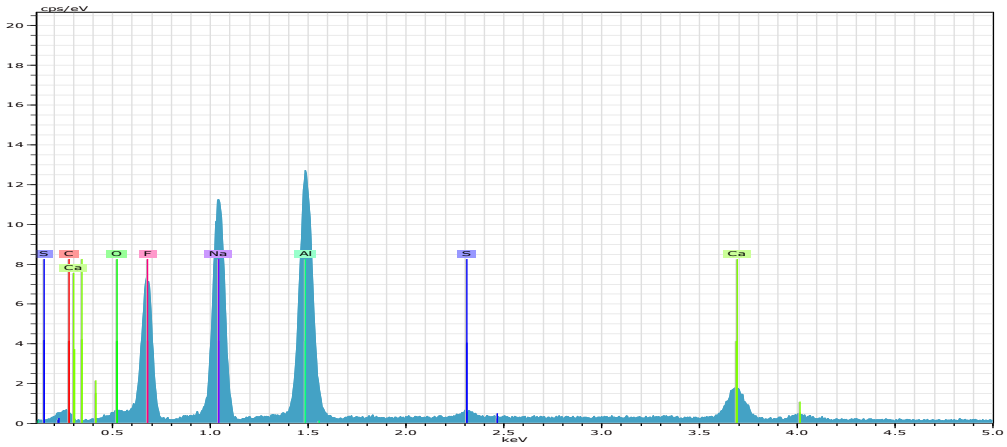
cps/eV
S
C
Ca
O
F
Na
Al
S
Ca
keV

91

89 Date:08.10.2018 14:30:29 HV:12,0kV Puls th.:3,51kcps

El	AN	Series	unn. C [wt.%]	norm. C [wt.%]	Atom. C [at.%]	Error (1 Sigma) [wt.%]
Fe	26	K-series	118,23	93,71	80,68	4,16
C	6	K-series	4,71	3,73	14,93	0,99
S	16	K-series	1,75	1,39	2,08	0,10
Al	13	K-series	1,05	0,83	1,48	0,09
F	9	K-series	0,32	0,26	0,65	0,13
Na	11	K-series	0,11	0,09	0,18	0,04
O	8	K-series	0,00	0,00	0,00	0,00
		Total:	126,16	100,00	100,00	

90 Date:08.10.2018 14:30:59 HV:12,0kV Puls th.:2,07kcps

El	AN	Series	unn. C [wt.%]	norm. C [wt.%]	Atom. C [at.%]	Error (1 Sigma) [wt.%]
F	9	K-series	4,20	54,59	55,26	0,65
Al	13	K-series	1,57	20,39	14,53	0,11
C	6	K-series	0,91	11,78	18,85	0,31
Na	11	K-series	0,82	10,67	8,93	0,09
O	8	K-series	0,11	1,47	1,76	0,08
S	16	K-series	0,09	1,11	0,67	0,03
		Total:	7,70	100,00	100,00	

91 Date:08.10.2018 14:31:30 HV:12,0kV Puls th.:4,74kcps

El	AN	Series	unn. C [wt.%]	norm. C [wt.%]	Atom. C [at.%]	Error (1 Sigma) [wt.%]
Al	13	K-series	9,95	28,64	24,10	0,48
Na	11	K-series	8,82	25,38	25,06	0,56
F	9	K-series	8,51	24,48	29,25	1,18
Ca	20	K-series	4,57	13,15	7,45	0,18
C	6	K-series	2,01	5,78	10,92	0,51
O	8	K-series	0,68	1,96	2,78	0,20
S	16	K-series	0,22	0,62	0,44	0,04
		Total:	34,76	100,00	100,00	

Mapping sample 2- Airborne Høyanger

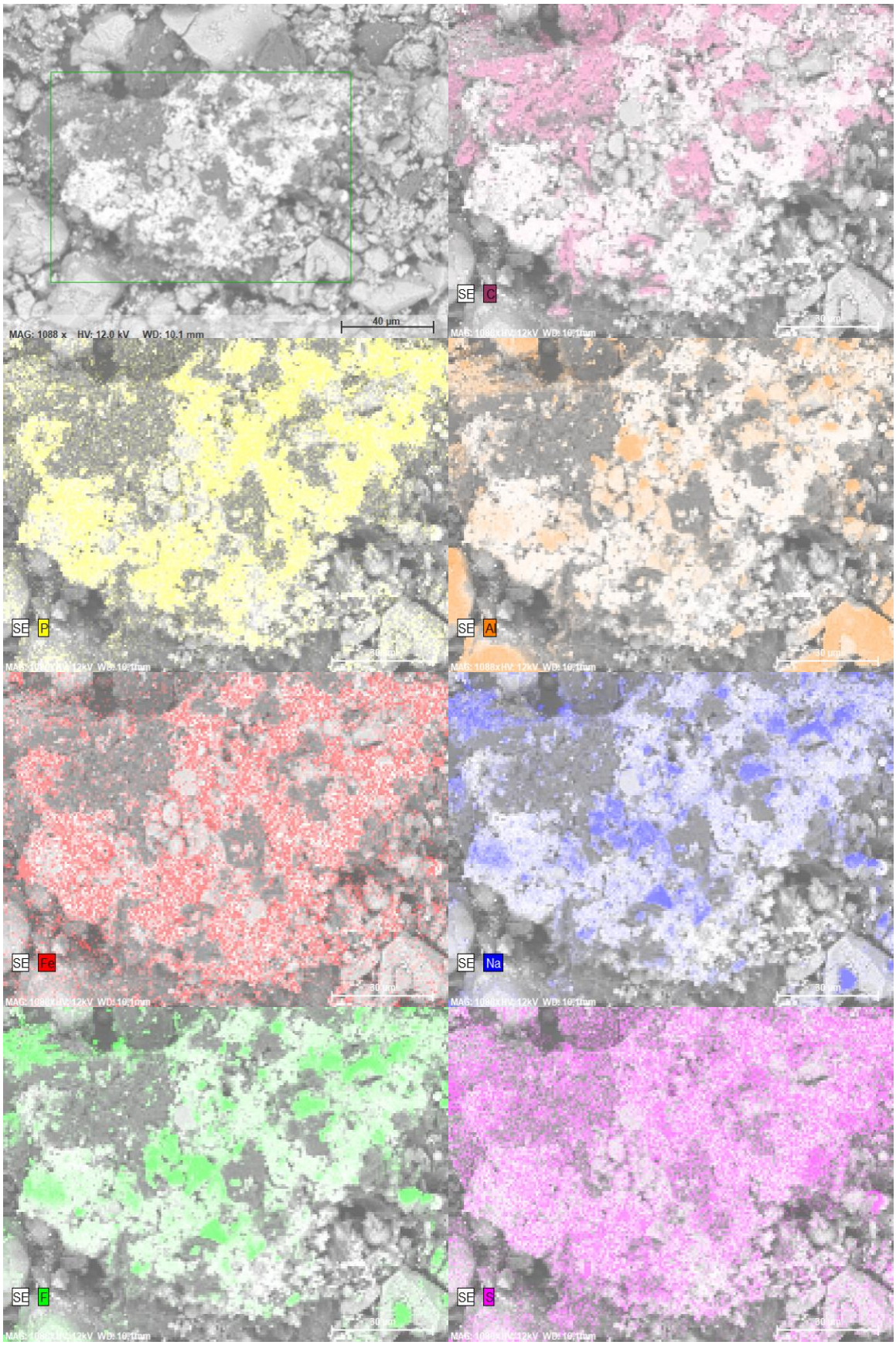

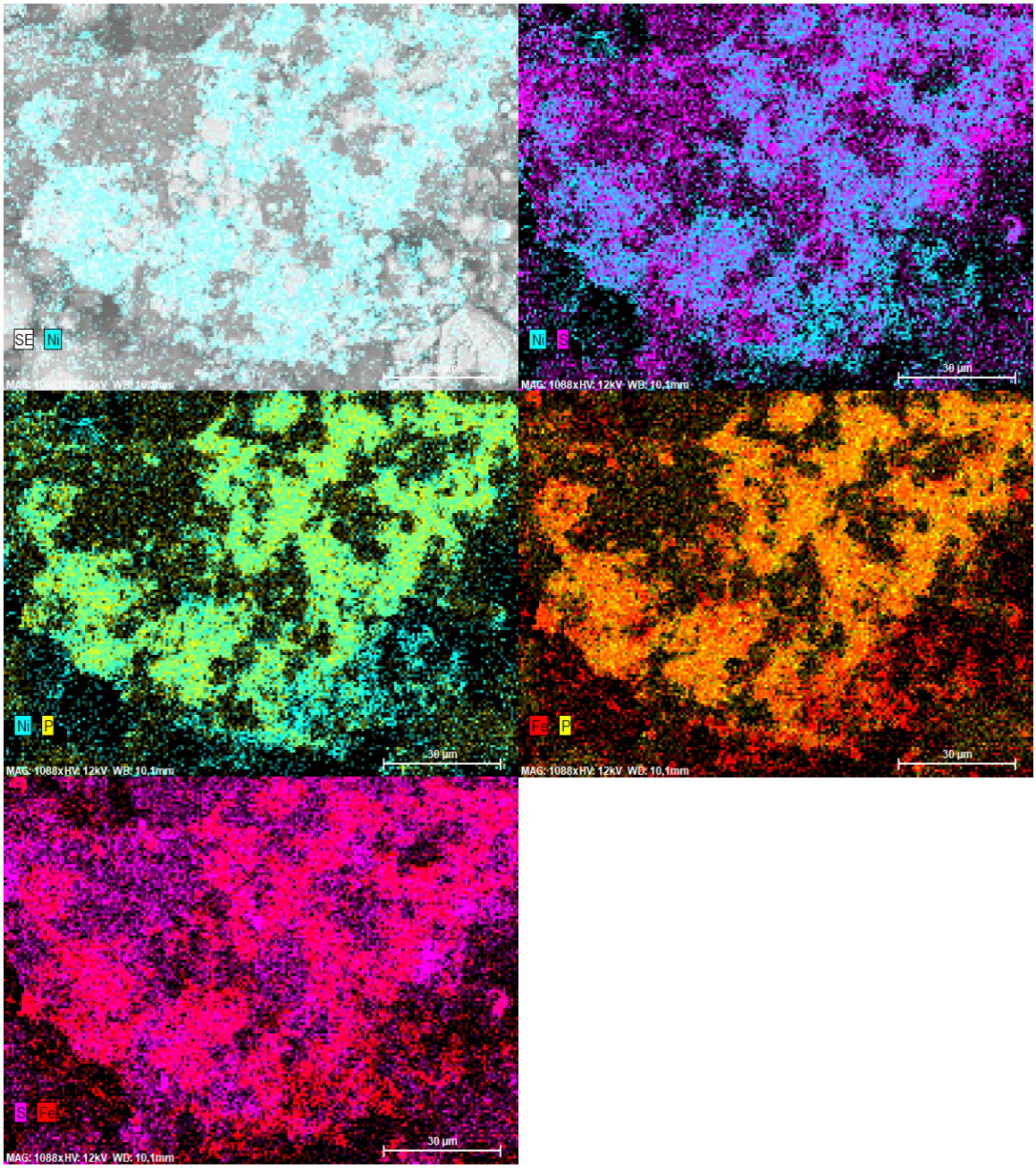
SE Ni
Ni S
30 µm
MAG: 1088x HV: 12kV WD: 10.1mm
Ni P
Fe P
S Fe

Point analysis sample 2

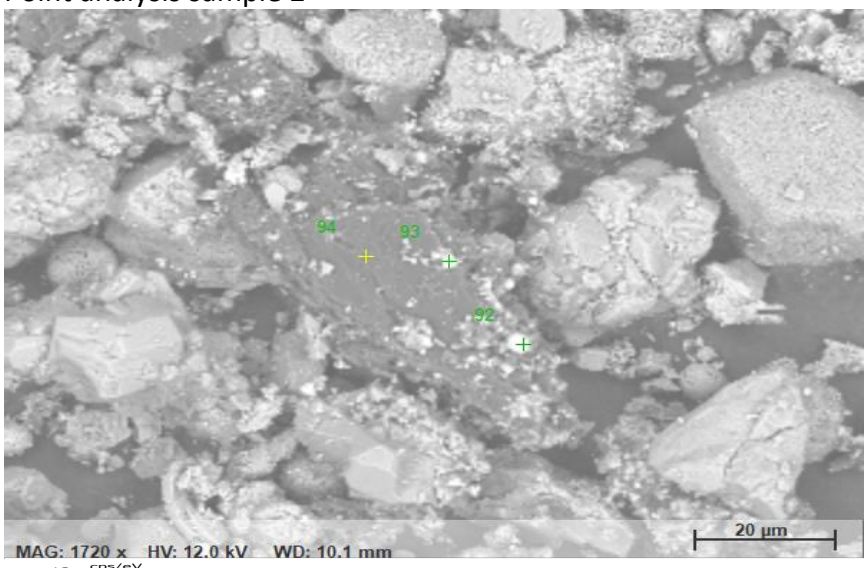

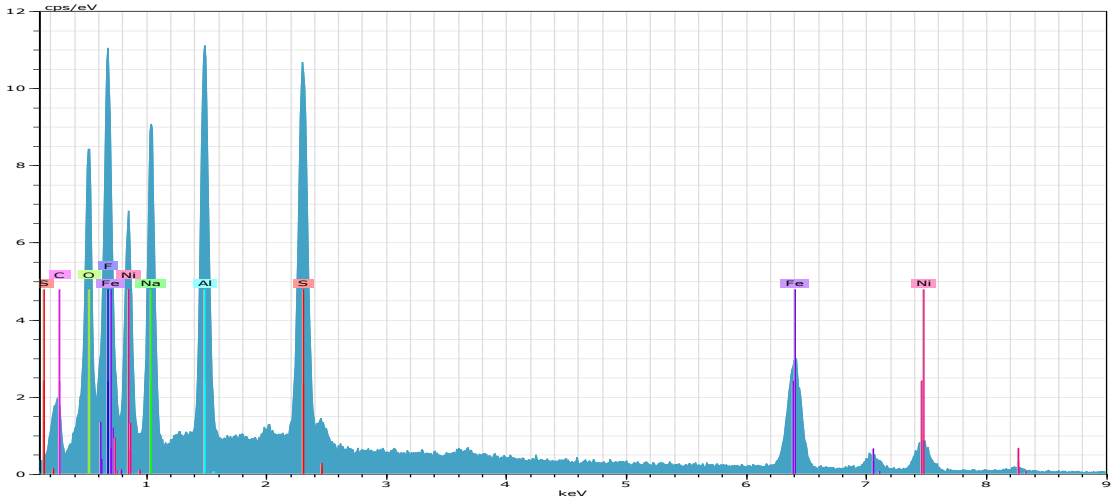

92

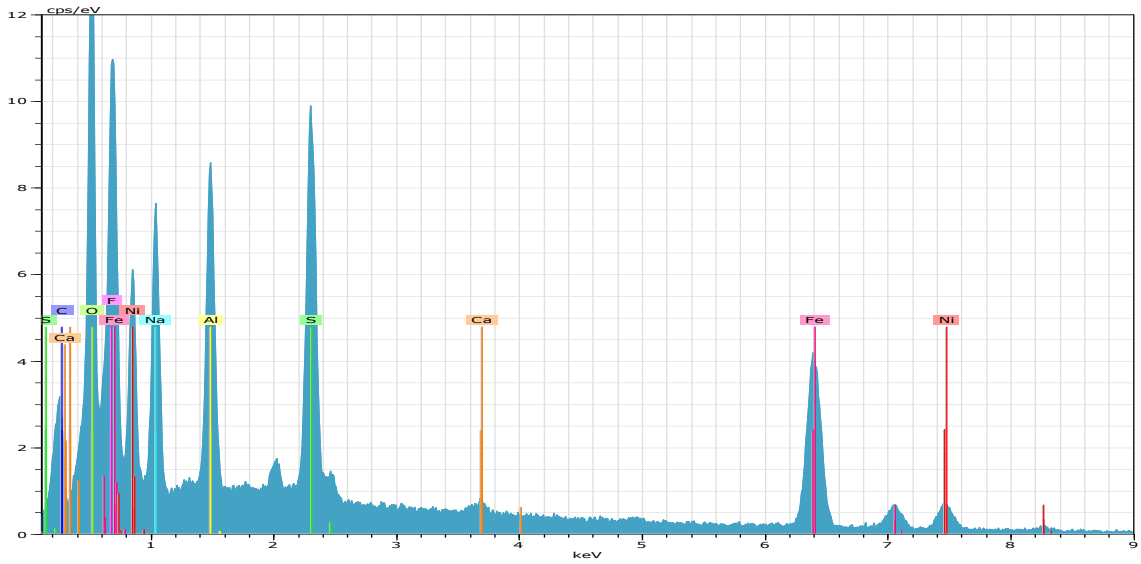

93

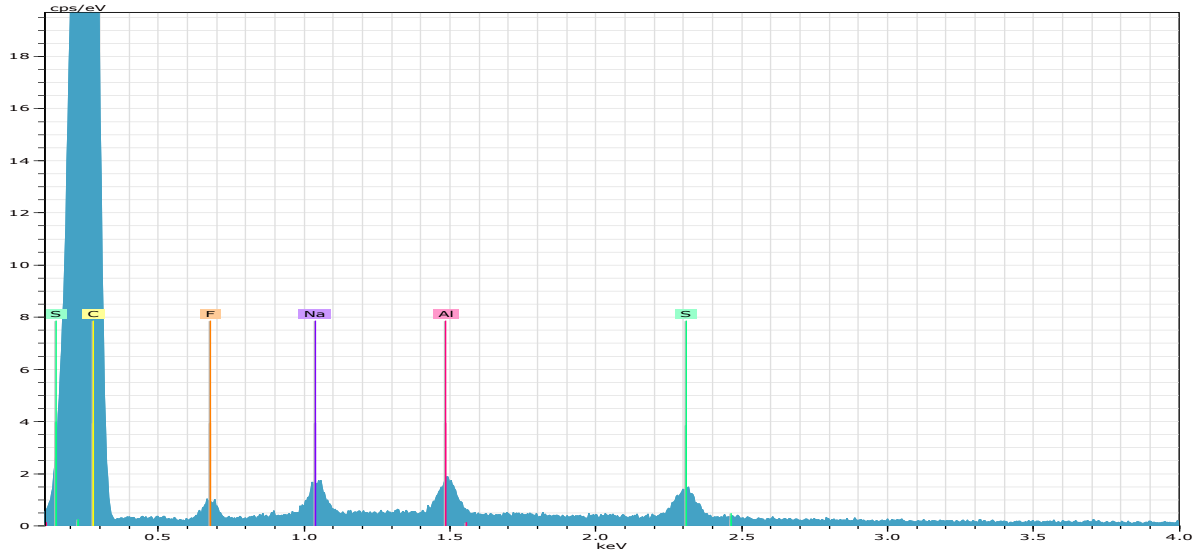

- 92 Date:08.10.2018 14:56:13 HV:12,0kV Puls th.:9,55kcps

El	AN	Series	unn. C [wt.%]	norm. C [wt.%]	Atom. C [at.%]	Error (1 Sigma) [wt.%]
Fe	26	K-series	27,01	32,31	17,21	0,99
Ni	28	K-series	15,60	18,67	9,46	0,72
O	8	K-series	8,17	9,78	18,17	1,12
S	16	K-series	7,51	8,99	8,34	0,30
Na	11	K-series	7,13	8,53	11,04	0,46
F	9	K-series	6,82	8,16	12,78	0,94
Al	13	K-series	6,43	7,70	8,49	0,32
C	6	K-series	4,90	5,86	14,52	0,89
		Total:	83,58	100,00	100,00	

- 93 Date:08.10.2018 14:56:44 HV:12,0kV Puls th.:10,22kcps

El	AN	Series	unn. C [wt.%]	norm. C [wt.%]	Atom. C [at.%]	Error (1 Sigma) [wt.%]
Fe	26	K-series	37,52	41,22	21,82	1,35
O	8	K-series	12,89	14,16	26,16	1,66
Ni	28	K-series	12,71	13,97	7,03	0,60
S	16	K-series	6,37	7,00	6,45	0,26
C	6	K-series	6,08	6,68	16,45	1,03
Na	11	K-series	5,64	6,19	7,96	0,37
F	9	K-series	4,88	5,37	8,35	0,71
Al	13	K-series	4,53	4,97	5,45	0,24
Ca	20	K-series	0,39	0,43	0,32	0,04
		Total:	91,02	100,00	100,00	

- 94 Date:08.10.2018 14:57:14 HV:12,0kV Puls th.:6,71kcps

El	AN	Series	unn. C [wt.%]	norm. C [wt.%]	Atom. C [at.%]	Error (1 Sigma) [wt.%]
C	6	K-series	92,72	92,72	96,23	10,69
F	9	K-series	2,15	2,15	1,41	0,48
S	16	K-series	1,97	1,97	0,77	0,11
Na	11	K-series	1,60	1,60	0,87	0,13
Al	13	K-series	1,57	1,57	0,73	0,11
		Total:	100,00	100,00	100,00	

Mapping sample 13 - from filter Høyanger

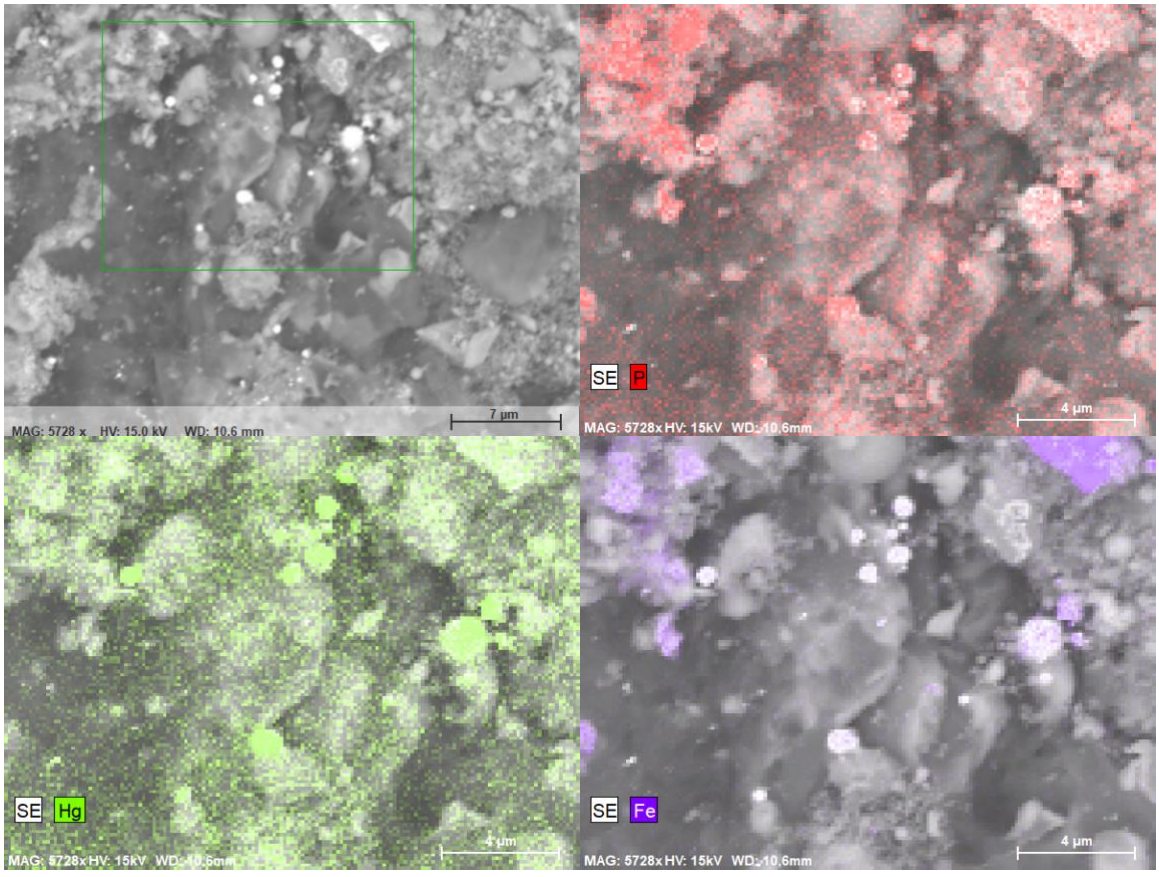

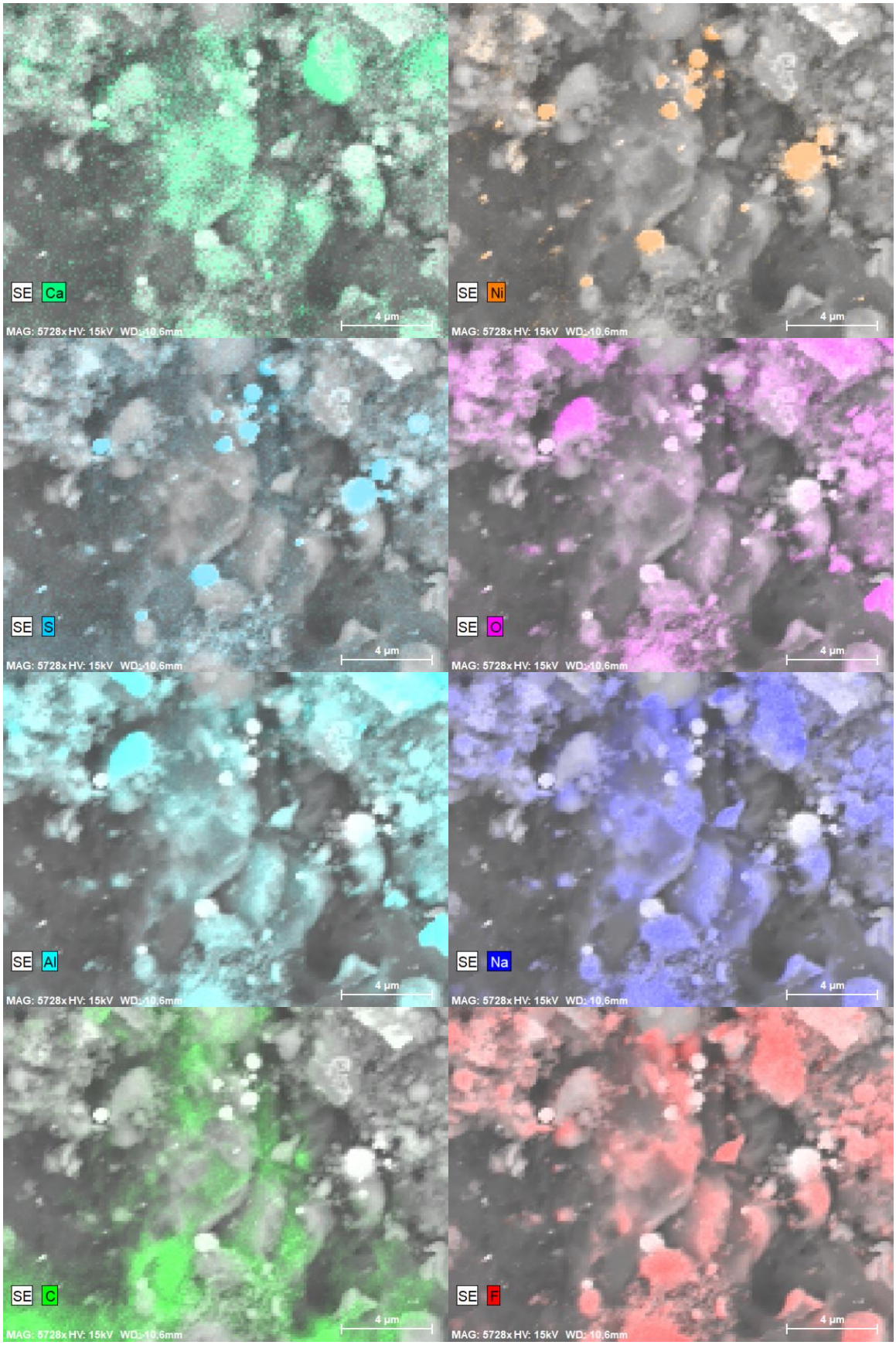
SE Ca
4 µm
MAG: 5728x HV: 15kV WD: 10.6mm
SE Ni
4 µm
MAG: 5728x HV: 15kV WD: 10.6mm
SE S
4 µm
MAG: 5728x HV: 15kV WD: 10.6mm
SE O
4 µm
MAG: 5728x HV: 15kV WD: 10.6mm
SE Al
4 µm
MAG: 5728x HV: 15kV WD: 10.6mm
SE Na
4 µm
MAG: 5728x HV: 15kV WD: 10.6mm
SE C
4 µm
MAG: 5728x HV: 15kV WD: 10.6mm
SE F
4 µm
MAG: 5728x HV: 15kV WD: 10.6mm

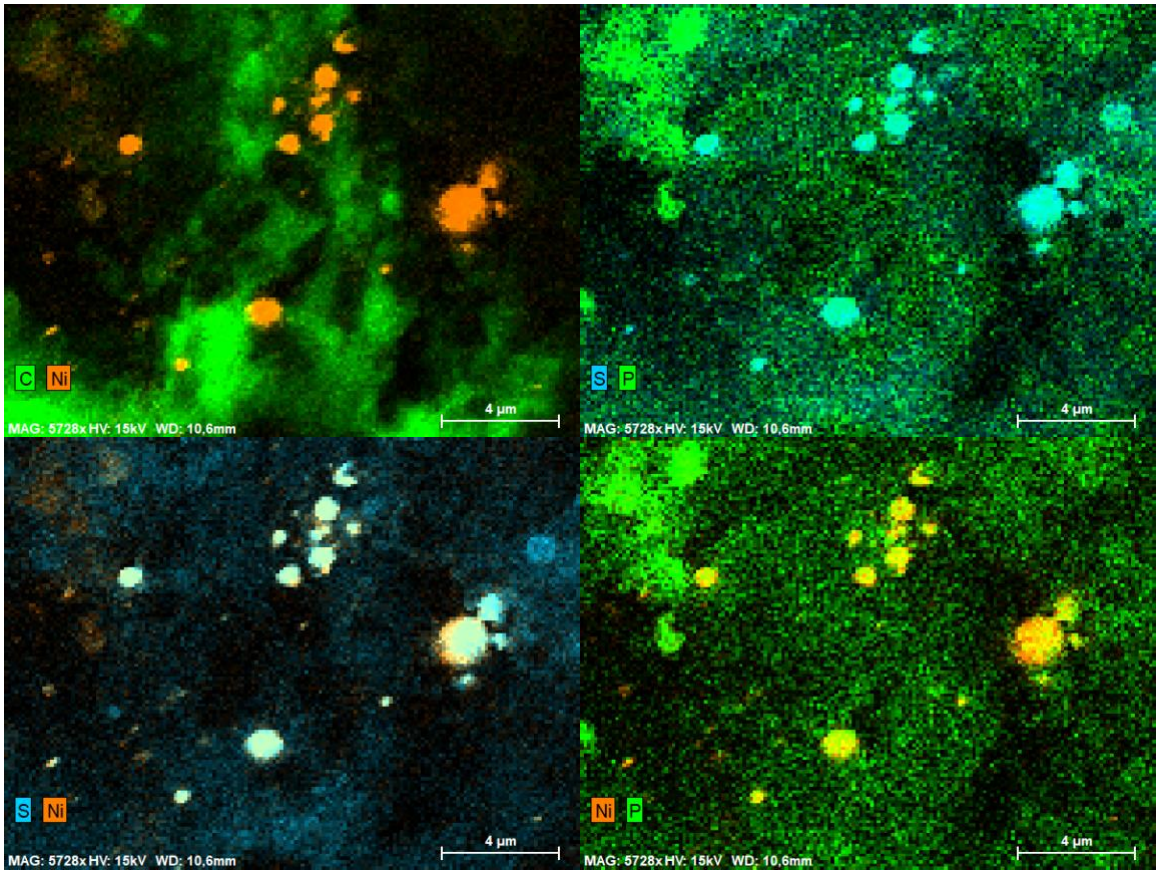

Mapping sample 13

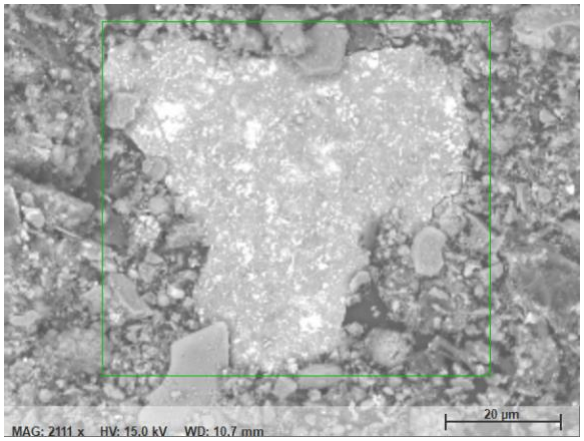

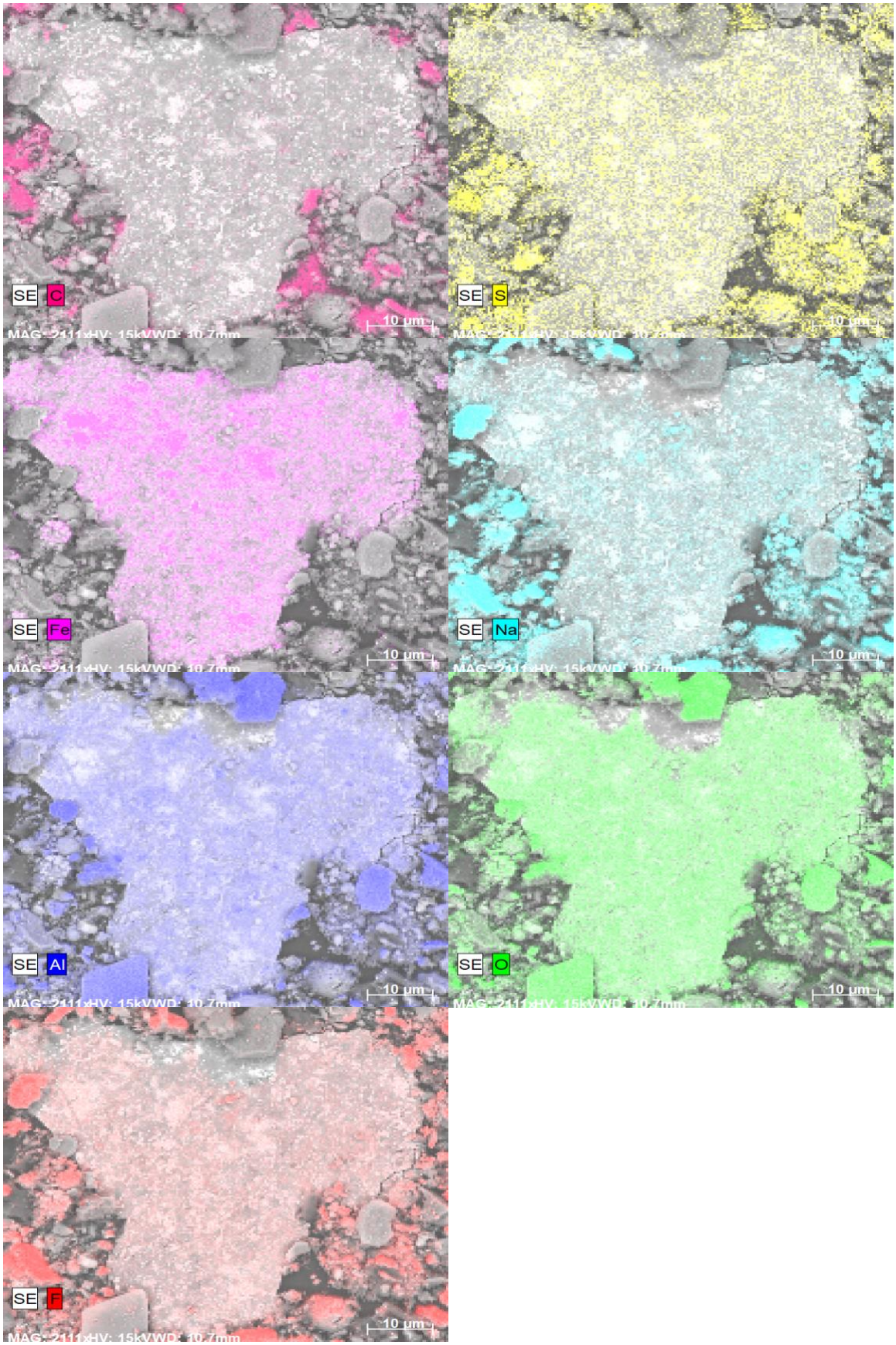
SE C
10 µm
SE S
10 µm
SE Fe
10 µm
SE Na
10 µm
SE Al
10 µm
SE O
10 µm
SE F
10 µm

Point analysis sample 13

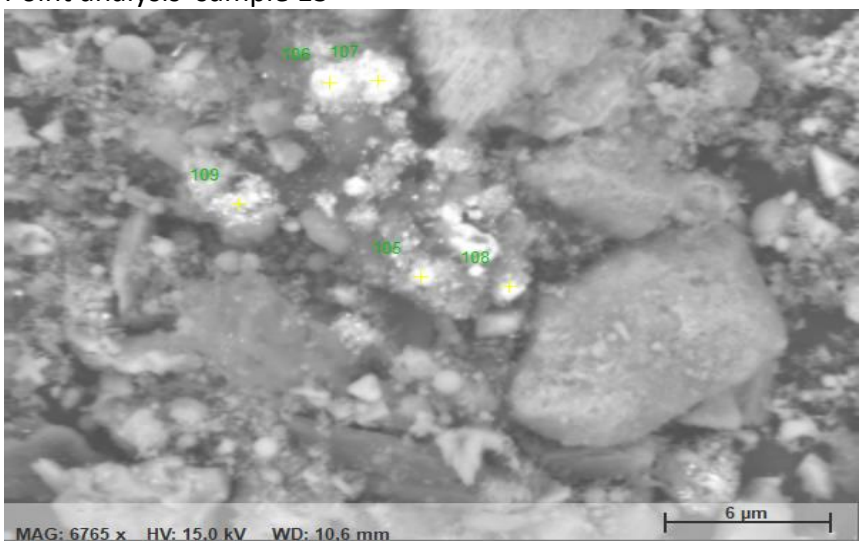

105

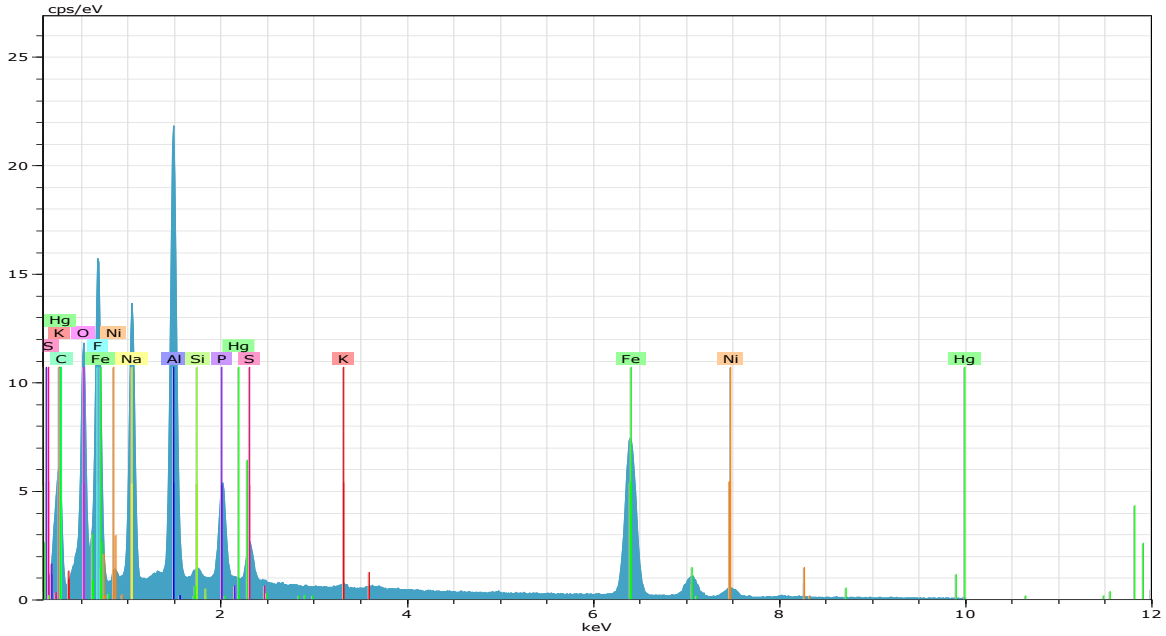

106

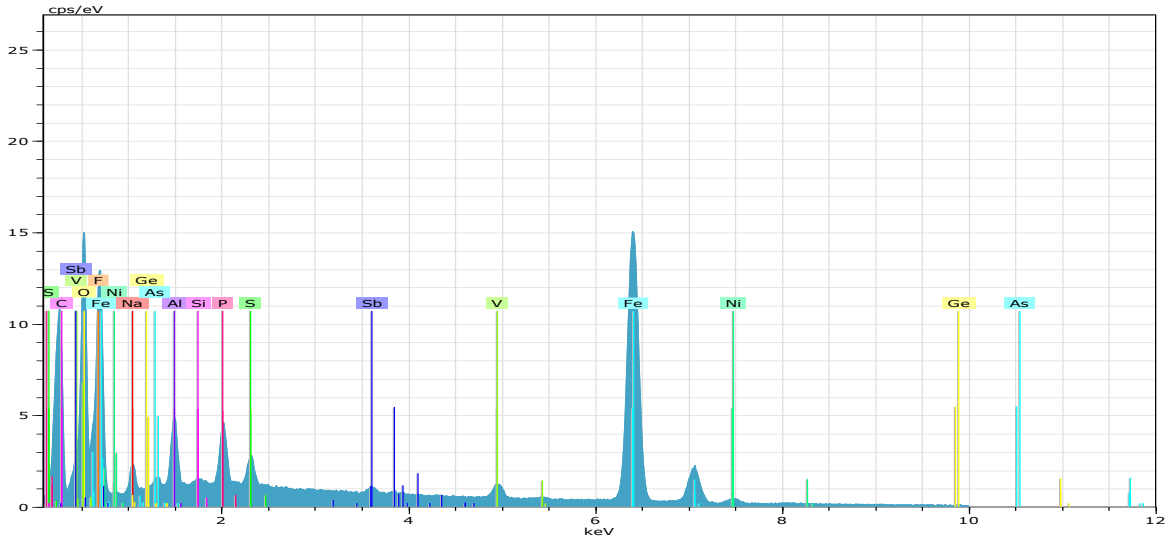
cps/eV
keV
Sb
V
F
Ge
S
O
Ni
As
C
Fe
Na
Al
Si
P
S
Sb
V
Fe
Ni
Ge
As

107

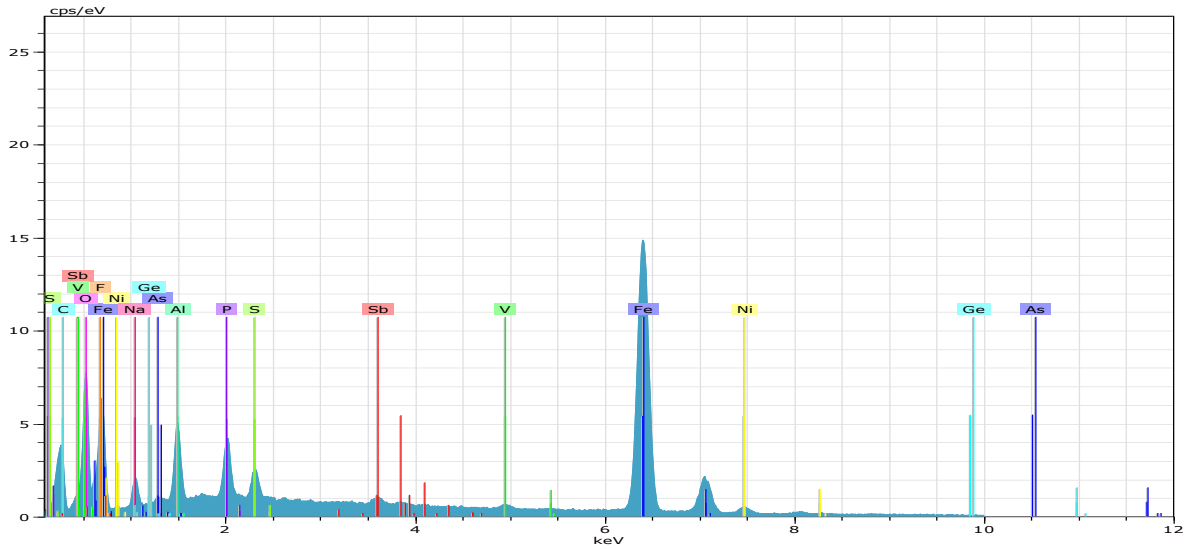
cps/eV
keV
Sb
V
F
Ge
S
O
Ni
As
C
Fe
Na
Al
P
S
Sb
V
Fe
Ni
Ge
As

108

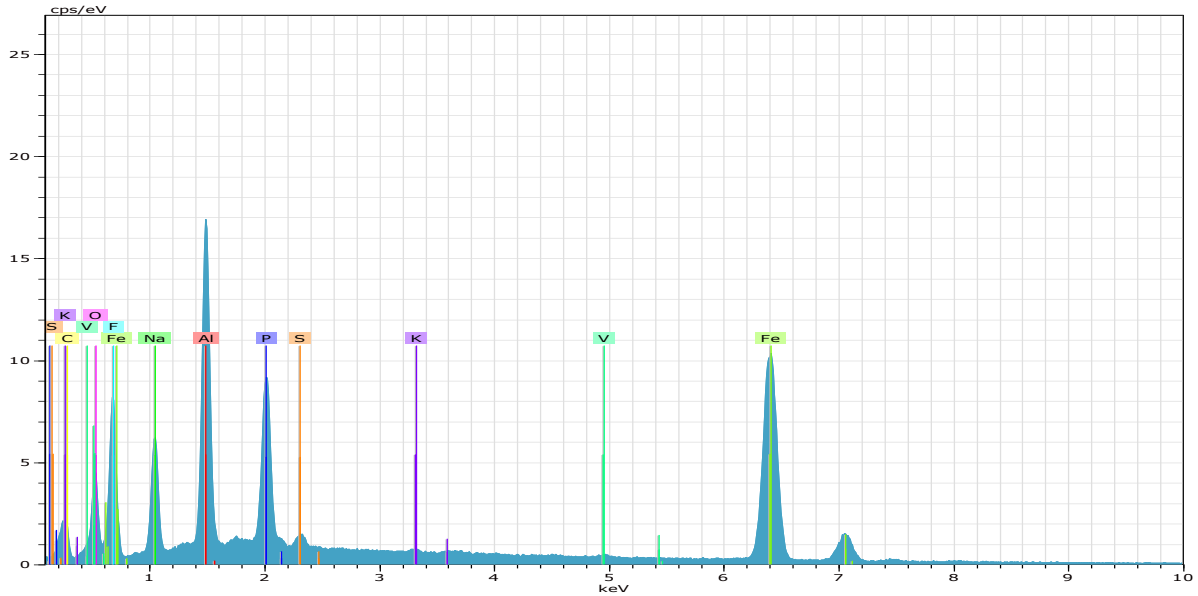
cps/eV
keV
K
O
S
V
F
C
Fe
Na
Al
P
S
K
V
Fe

109

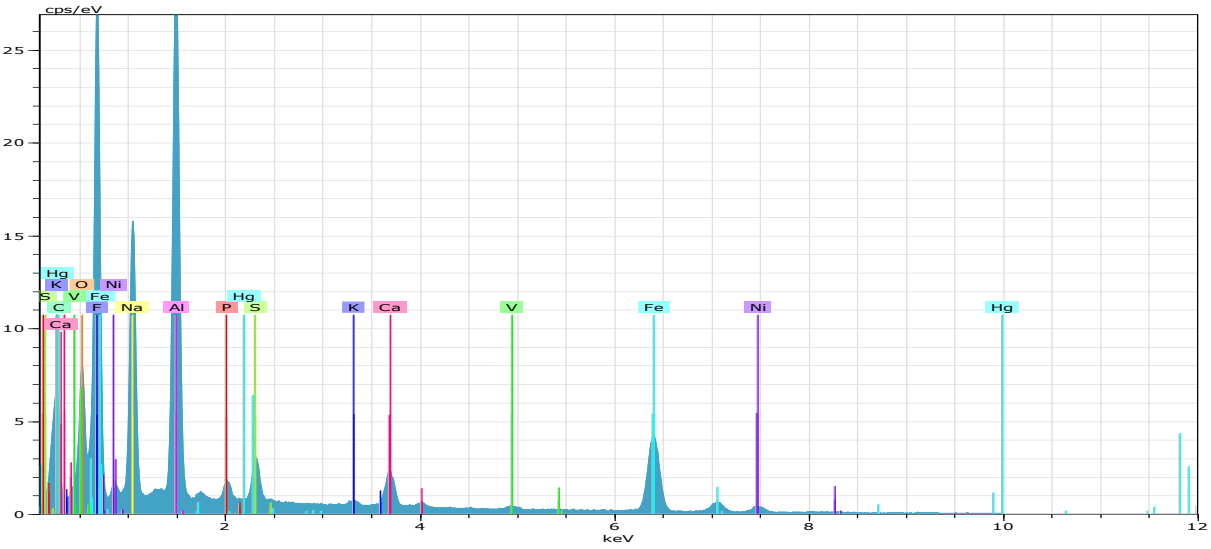

105 Date:09.10.2018 10:43:22 HV:15,0kV Puls th.:13,24kcps

El	AN	Series	unn. C [wt.%]	norm. C [wt.%]	Atom. C [at.%]	Error (1 Sigma) [wt.%]
Fe	26	K-series	34,26	37,97	18,79	1,04
Al	13	K-series	11,84	13,13	13,44	0,58
F	9	K-series	11,30	12,52	18,20	1,36
O	8	K-series	11,10	12,30	21,24	1,36
Na	11	K-series	10,83	12,00	14,43	0,70
Ni	28	K-series	3,52	3,90	1,83	0,15
C	6	K-series	3,07	3,40	7,82	0,56
P	15	K-series	2,76	3,06	2,73	0,13
S	16	K-series	1,13	1,25	1,08	0,07
Si	14	K-series	0,36	0,40	0,39	0,04
K	19	K-series	0,07	0,08	0,05	0,03
Hg	80	M-series	0,00	0,00	0,00	0,00
		Total:	90,23	100,00	100,00	

106 Date:09.10.2018 10:44:23 HV:15,0kV Puls th.:14,44kcps

El	AN	Series	unn. C [wt.%]	norm. C [wt.%]	Atom. C [at.%]	Error (1 Sigma) [wt.%]
Fe	26	K-series	52,69	55,03	25,59	1,57
C	6	K-series	18,78	19,62	42,43	2,32
O	8	K-series	10,69	11,17	18,13	1,31
F	9	K-series	5,44	5,68	7,76	0,71
Ni	28	K-series	1,72	1,80	0,80	0,09
Al	13	K-series	1,52	1,58	1,53	0,10
P	15	K-series	1,34	1,40	1,17	0,08
V	23	K-series	1,15	1,20	0,61	0,06
Na	11	K-series	1,03	1,07	1,21	0,09
S	16	K-series	0,64	0,66	0,54	0,05
Sb	51	L-series	0,44	0,46	0,10	0,04
As	33	L-series	0,28	0,29	0,10	0,04
Si	14	K-series	0,03	0,03	0,03	0,03
Ge	32	L-series	0,00	0,00	0,00	0,00

107 Date:09.10.2018 10:45:23 HV:15,0kV Puls th.:11,65kcps

El	AN	Series	unn. C [wt.%]	norm. C [wt.%]	Atom. C [at.%]	Error (1 Sigma) [wt.%]
Fe	26	K-series	64,02	69,99	42,75	1,90
C	6	K-series	9,02	9,86	28,00	1,27
O	8	K-series	5,92	6,47	13,79	0,79
Ni	28	K-series	2,61	2,85	1,66	0,12
F	9	K-series	2,43	2,66	4,77	0,36
Al	13	K-series	2,30	2,51	3,17	0,13
P	15	K-series	1,73	1,89	2,09	0,09
Na	11	K-series	1,39	1,52	2,26	0,12
S	16	K-series	0,83	0,91	0,97	0,06
Sb	51	L-series	0,80	0,87	0,24	0,05
V	23	K-series	0,39	0,43	0,29	0,04
As	33	L-series	0,04	0,04	0,02	0,03
Ge	32	L-series	0,00	0,00	0,00	0,00

108 Date:09.10.2018 10:46:24 HV:15,0kV Puls th.:11,50kcps

El	AN	Series	unn. C [wt.%]	norm. C [wt.%]	Atom. C [at.%]	Error (1 Sigma) [wt.%]
Fe	26	K-series	49,78	60,91	38,58	1,49
Al	13	K-series	10,09	12,34	16,18	0,49
Na	11	K-series	5,64	6,91	10,63	0,38
P	15	K-series	5,55	6,79	7,75	0,24
F	9	K-series	5,19	6,36	11,83	0,68
O	8	K-series	3,60	4,40	9,73	0,52
C	6	K-series	1,27	1,55	4,56	0,31
S	16	K-series	0,41	0,50	0,56	0,04
V	23	K-series	0,15	0,18	0,13	0,03
K	19	K-series	0,04	0,05	0,05	0,03
		Total:	81,72	100,00	100,00	

109 Date:09.10.2018 10:47:24 HV:15,0kV Puls th.:13,71kcps

El	AN	Series	unn. C [wt.%]	norm. C [wt.%]	Atom. C [at.%]	Error (1 Sigma) [wt.%]
F	9	K-series	21,79	24,24	31,86	2,49
Fe	26	K-series	20,84	23,19	10,37	0,65
Al	13	K-series	16,29	18,12	16,77	0,78
Na	11	K-series	12,12	13,48	14,64	0,78
O	8	K-series	6,79	7,55	11,78	0,89
C	6	K-series	4,01	4,46	9,27	0,69
Ni	28	K-series	2,81	3,12	1,33	0,13
Ca	20	K-series	2,46	2,74	1,71	0,10
S	16	K-series	1,51	1,68	1,31	0,08
P	15	K-series	0,67	0,74	0,60	0,05
V	23	K-series	0,38	0,43	0,21	0,04
K	19	K-series	0,23	0,25	0,16	0,03
Hg	80	M-series	0,00	0,00	0,00	0,00
		Total:	89,90	100,00	100,00	

Mapping sample 3 - Settled Høyanger

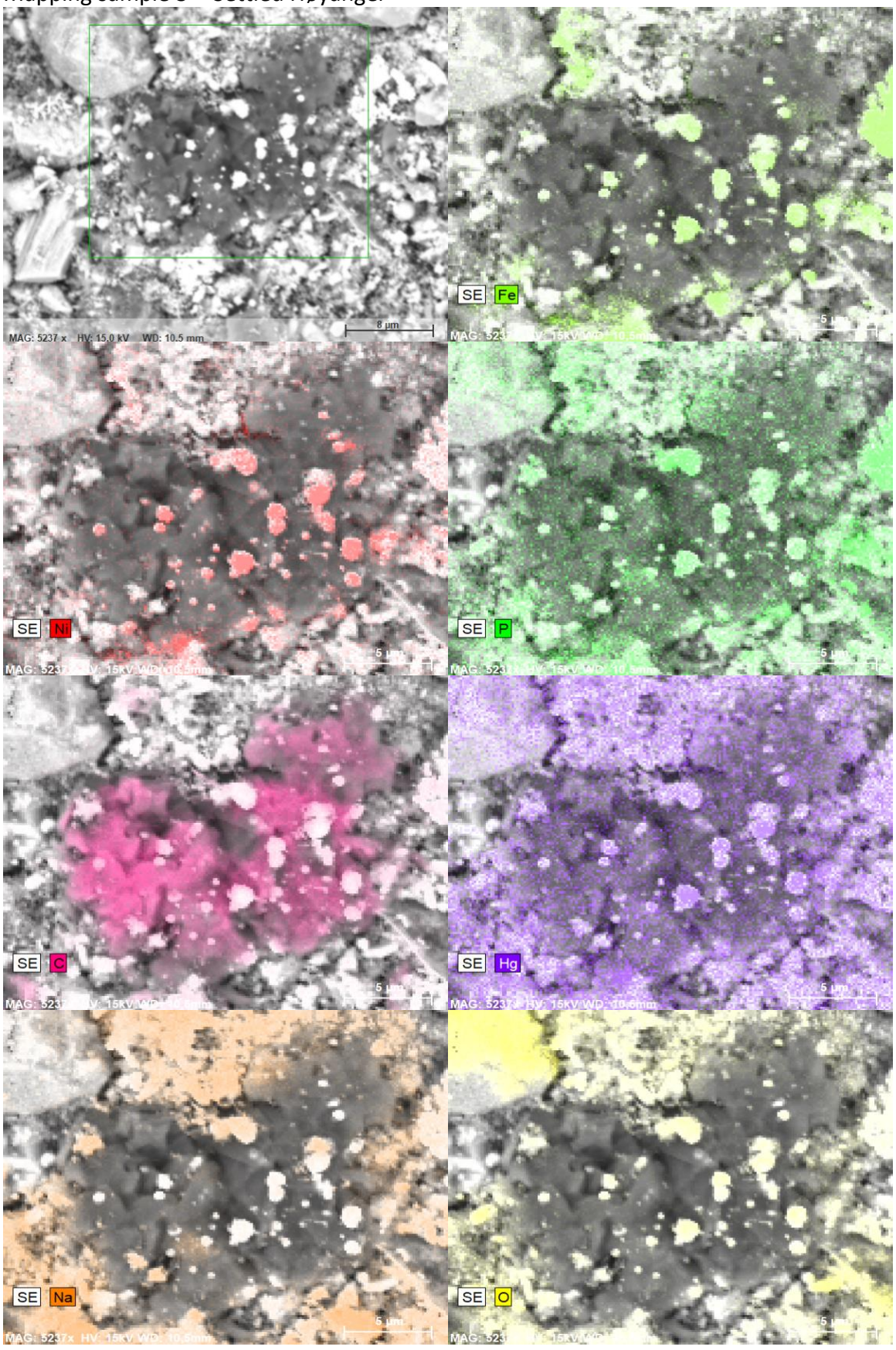

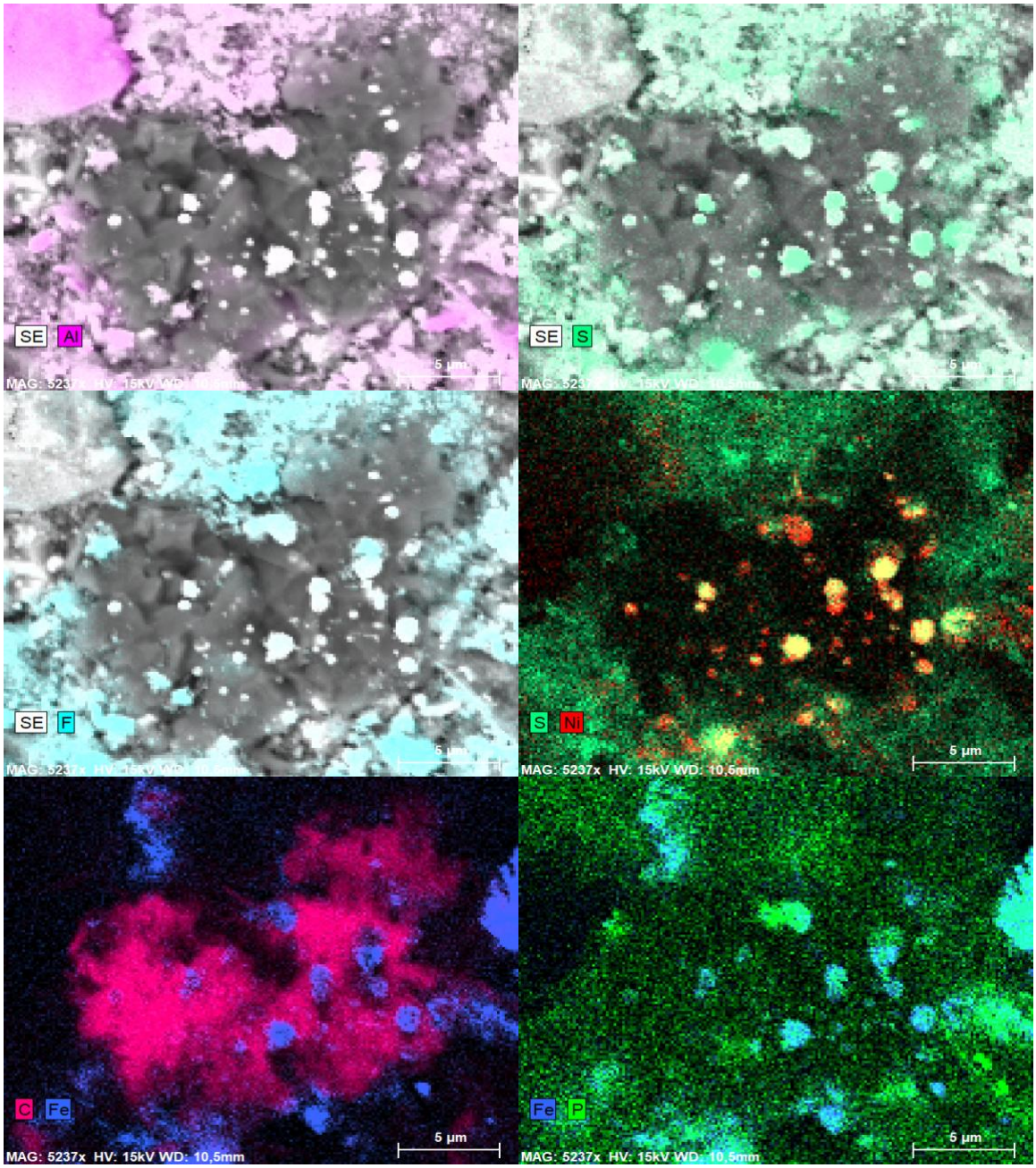

Sample 3

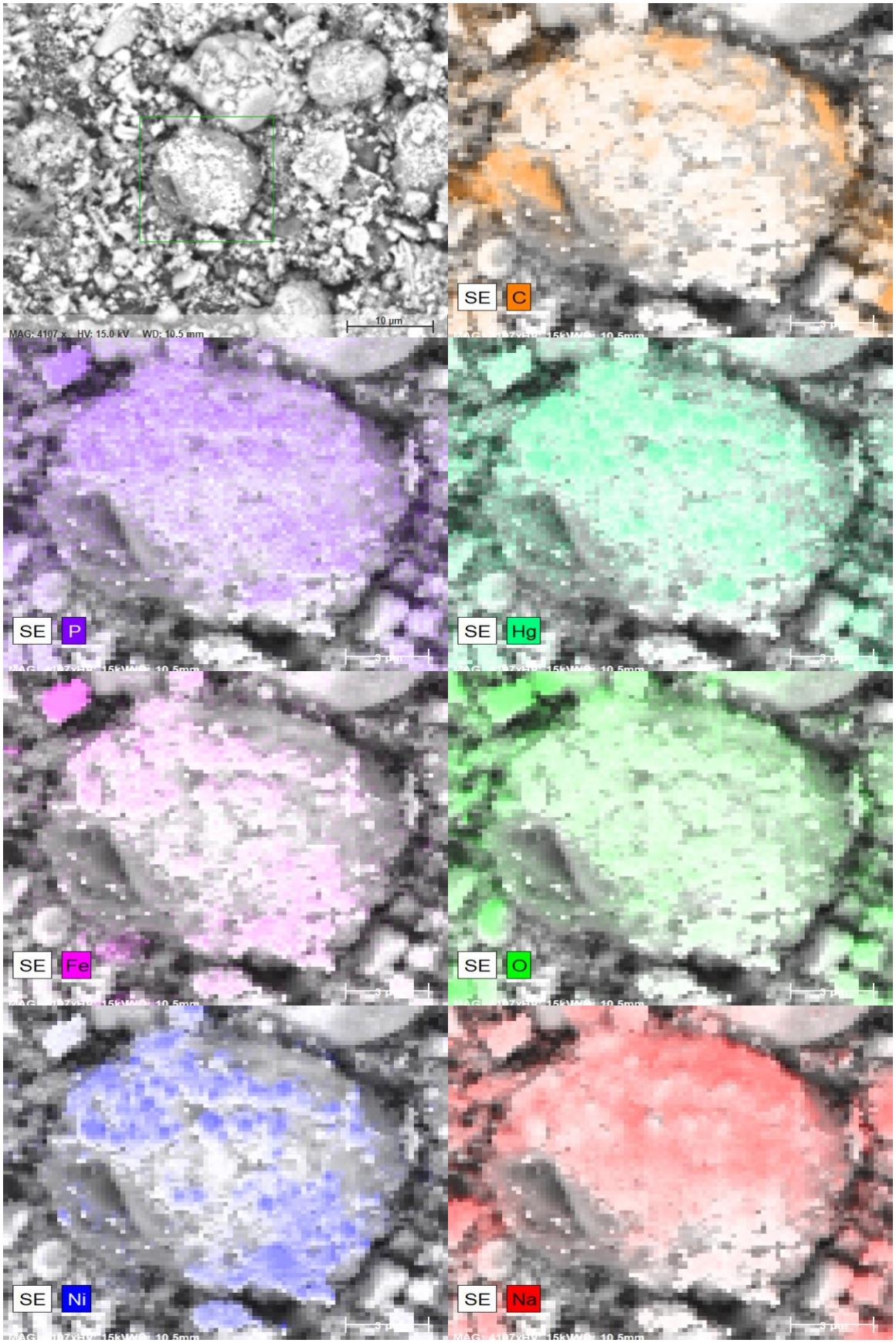
10 µm
MAG: 4107 x HV: 15.0 kV WD: 10.5 mm
SE C
SE P
SE Hg
SE Fe
SE O
SE Ni
SE Na

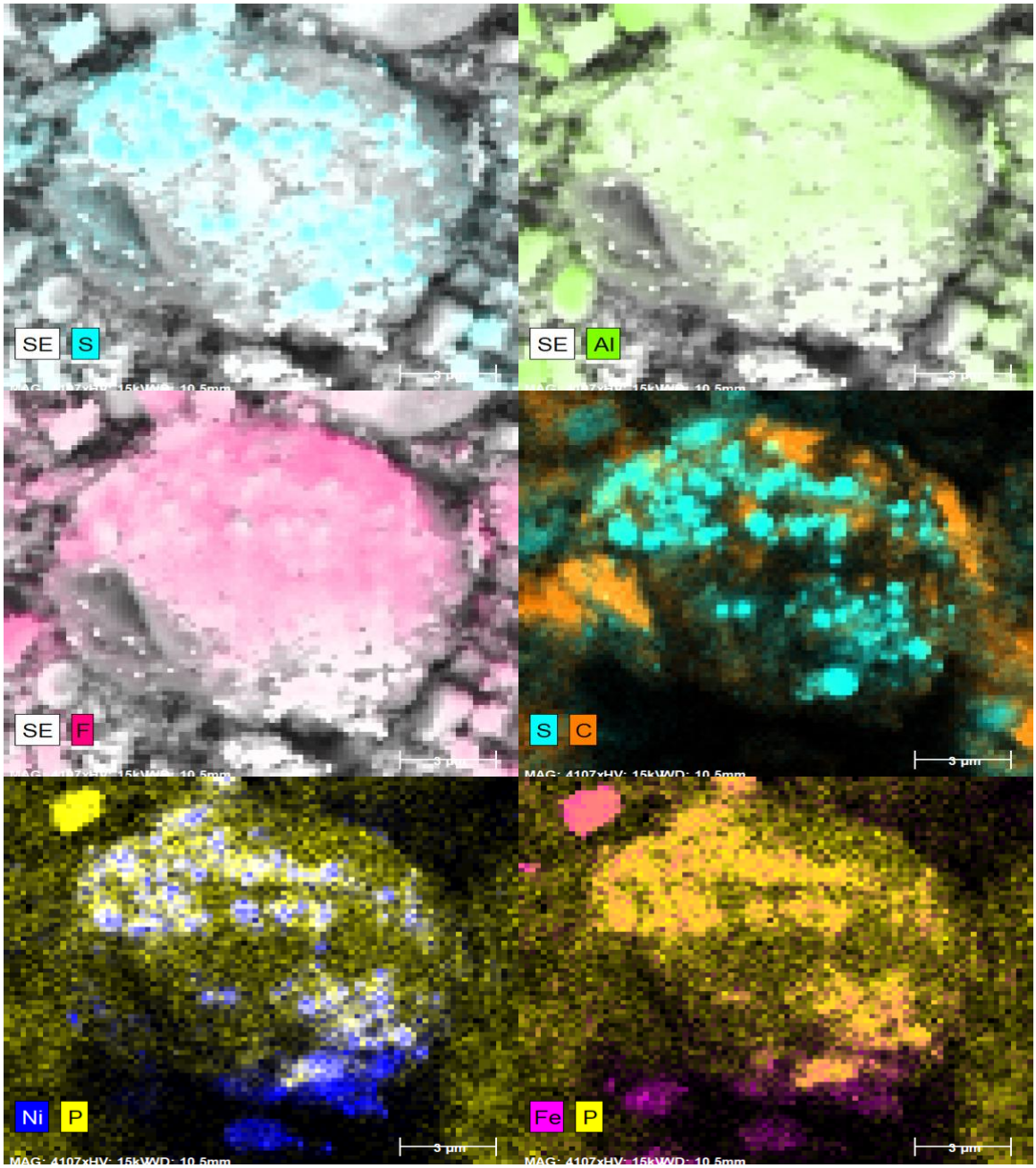
SE S
SE Al
SE F
S C
3 μm
Ni P
Fe P
MAG: 4107x HV: 15kV WD: 10.5mm

B.2 Morphology

Sample 13 Høyanger - filter

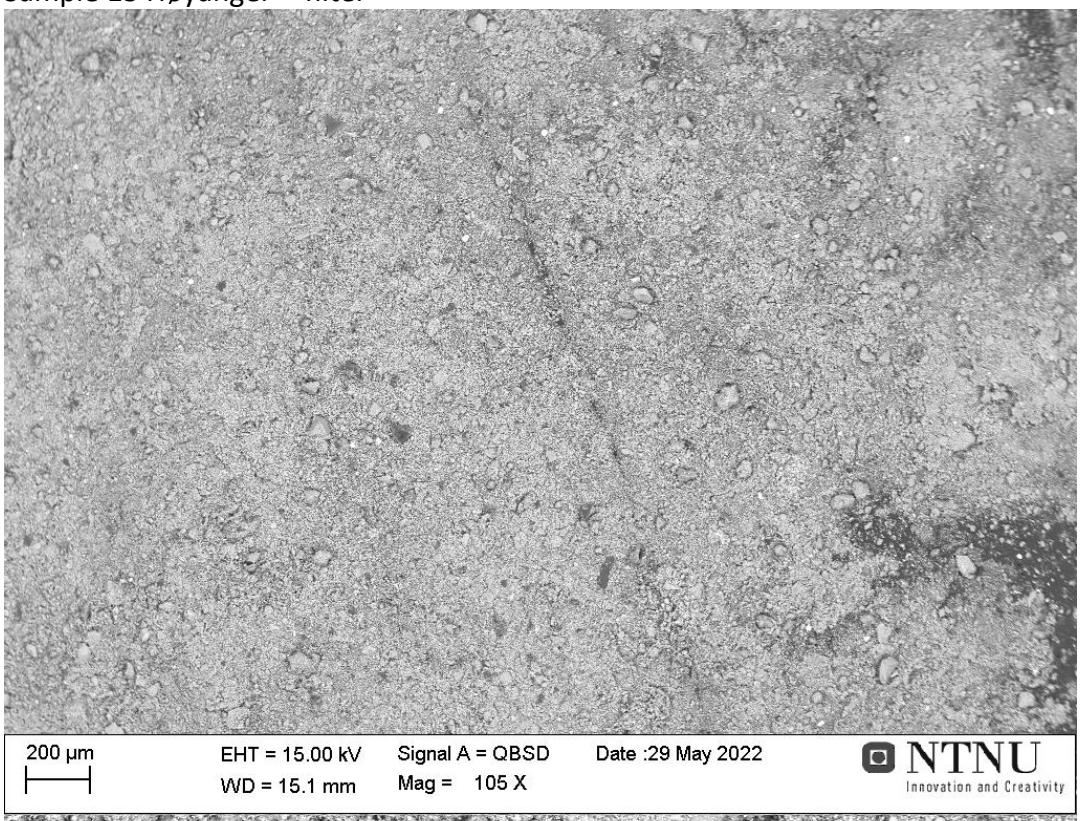

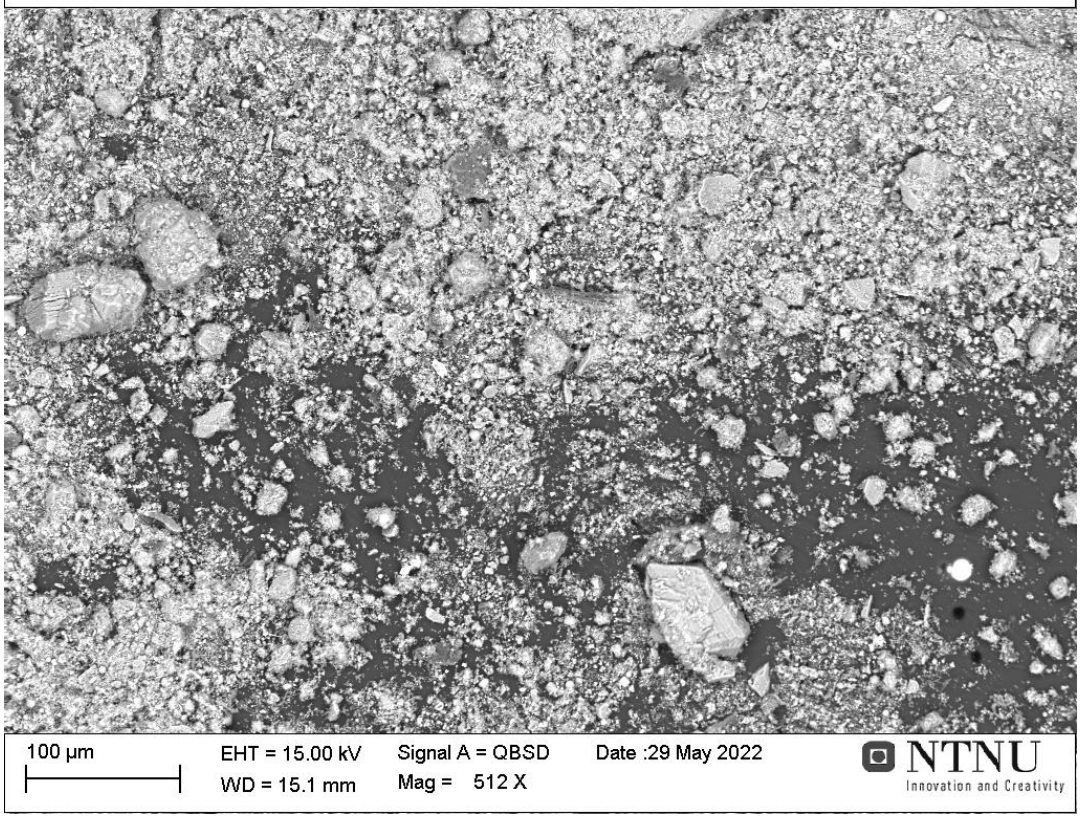

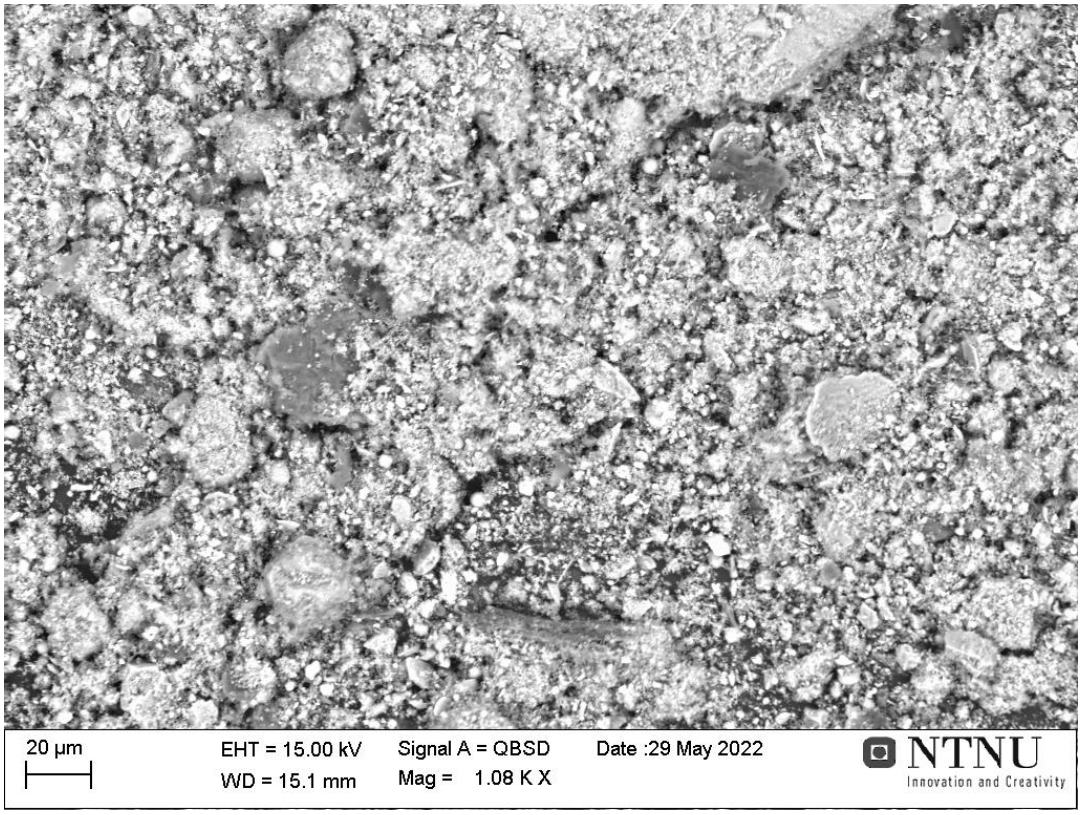

Sample 9 Høyanger-Airborne

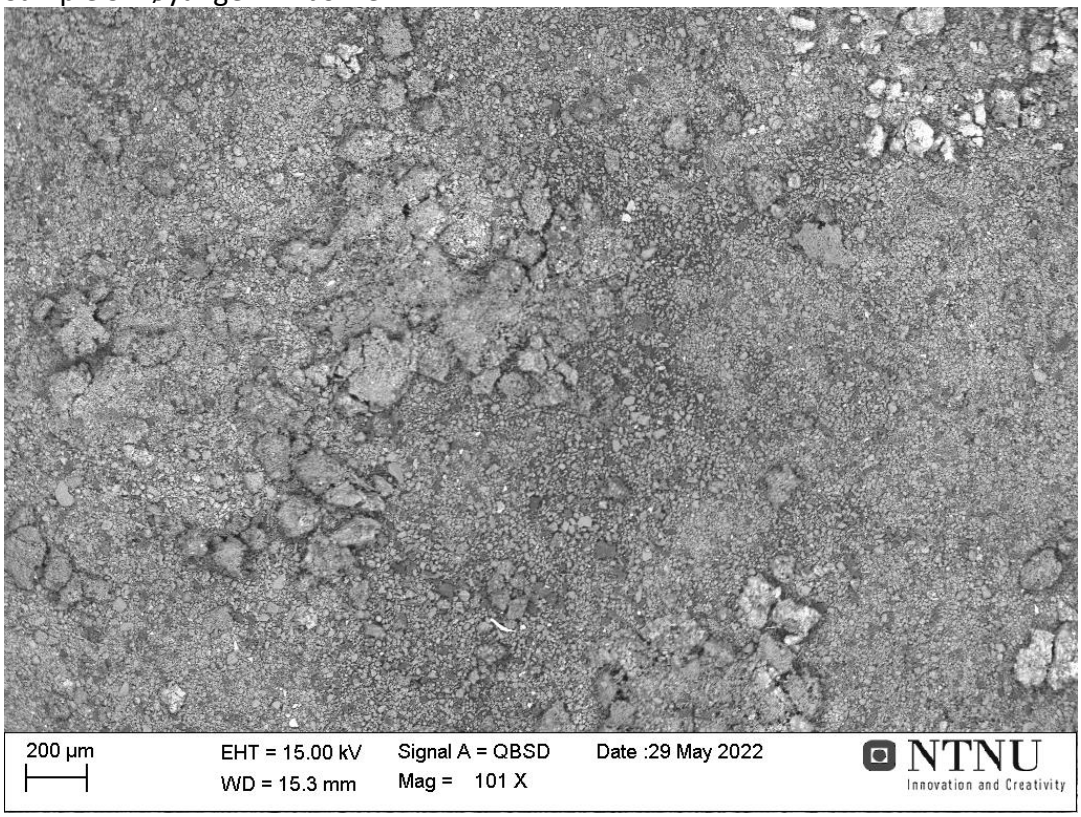

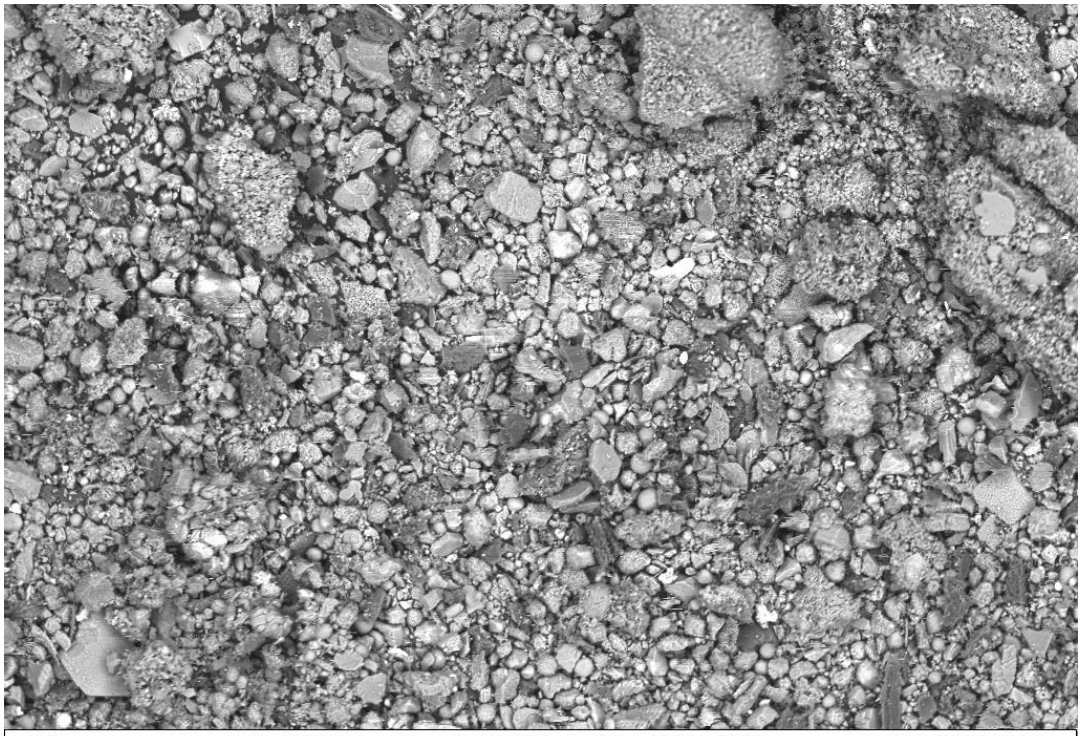
100 µm
EHT = 15.00 kV
WD = 15.1 mm
Signal A = QBSD
Mag = 512 X
Date :29 May 2022
NTNU
Innovation and Creativity

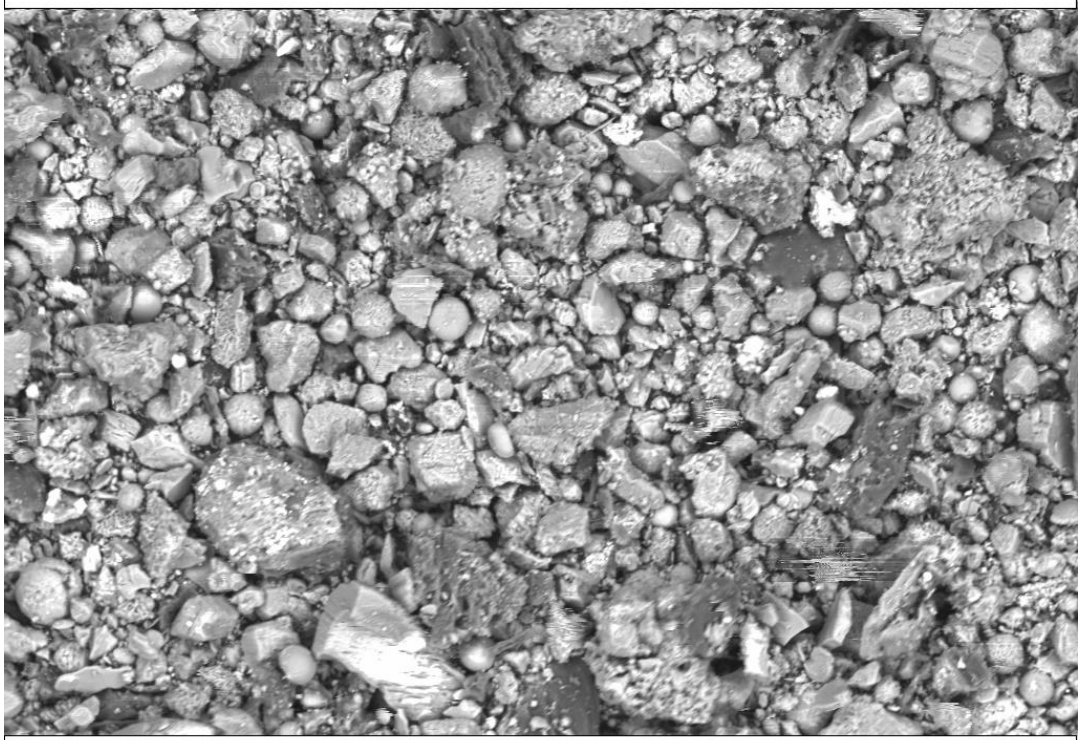
20 µm
EHT = 15.00 kV
WD = 15.1 mm
Signal A = QBSD
Mag = 1.04 K X
Date :29 May 2022
NTNU
Innovation and Creativity

Sample 3 Høyanger- Settled

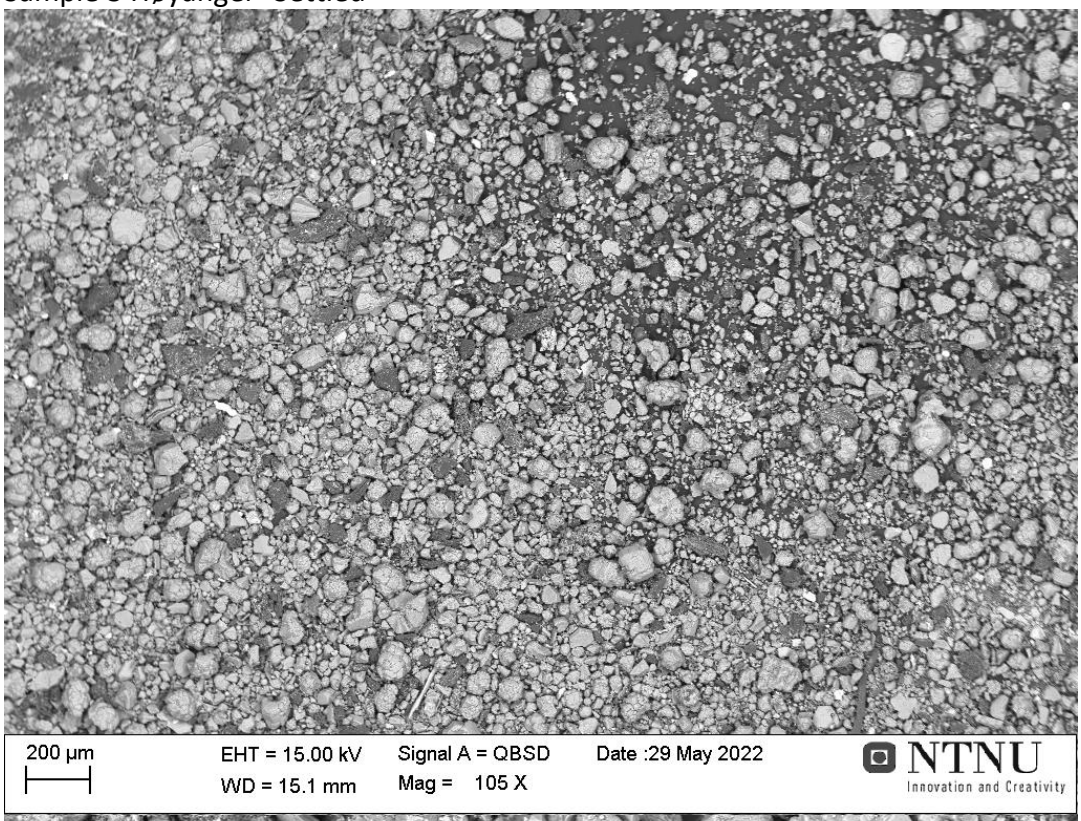

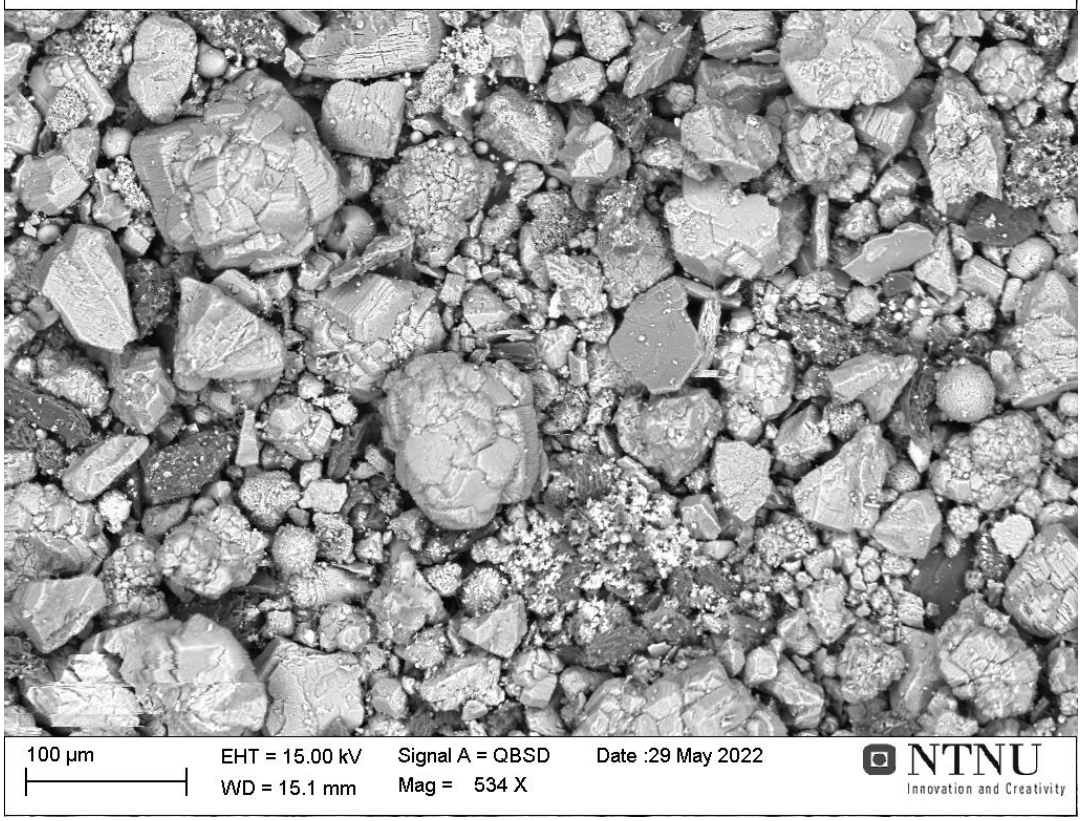

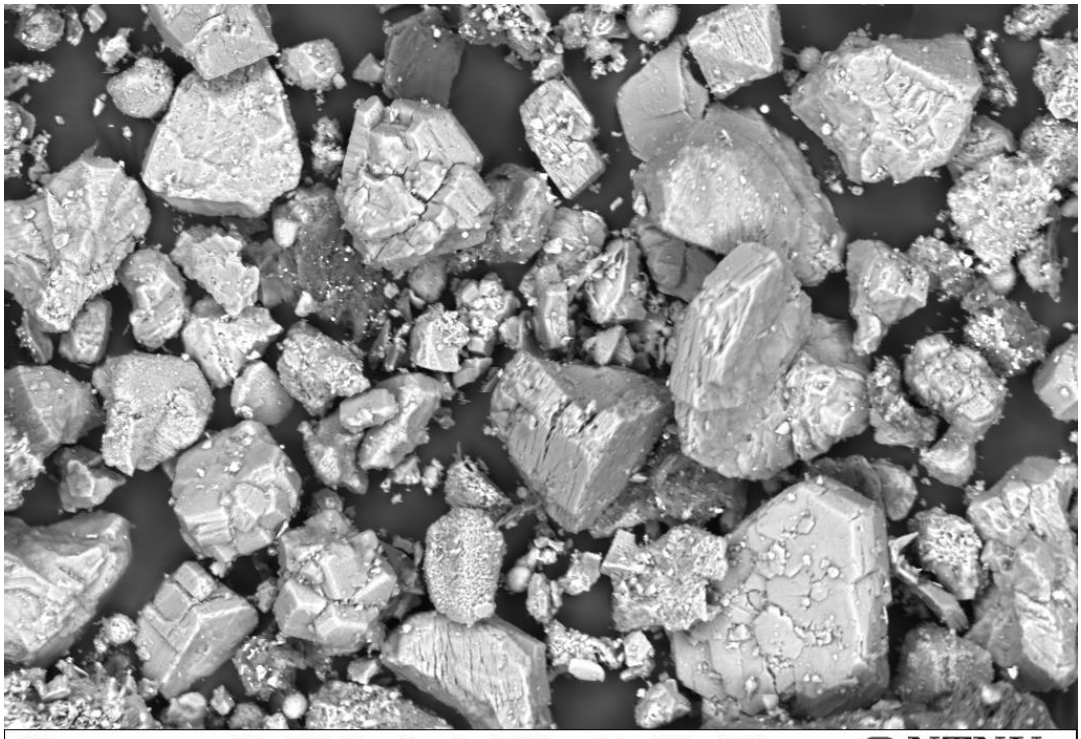
20 µm
EHT = 15.00 kV
WD = 15.1 mm
Signal A = QBSD
Mag = 1.04 K X
Date :29 May 2022
NTNU
Innovation and Creativity

C XRD

SH3 (Coupled TwoTheta/Theta)

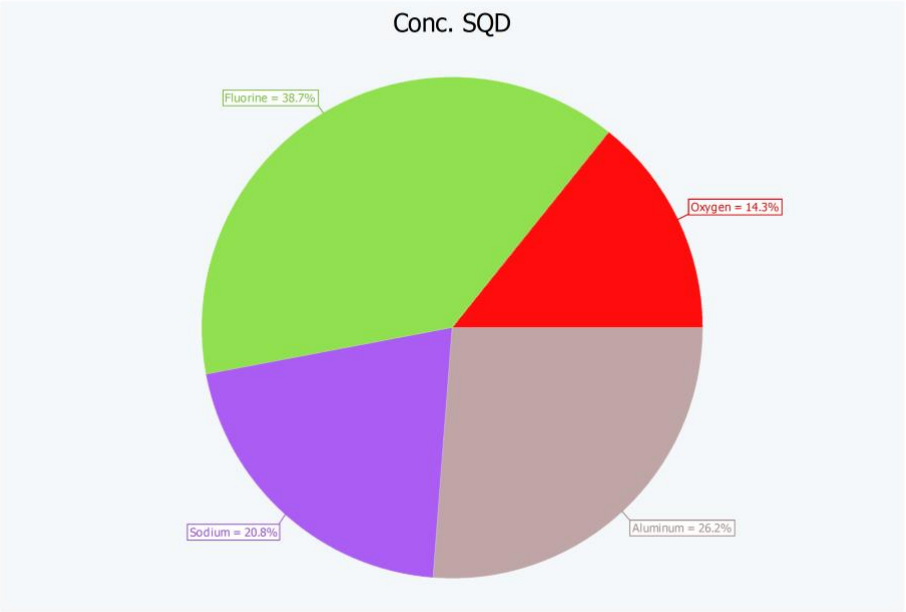

SH3 (Coupled TwoTheta/Theta)

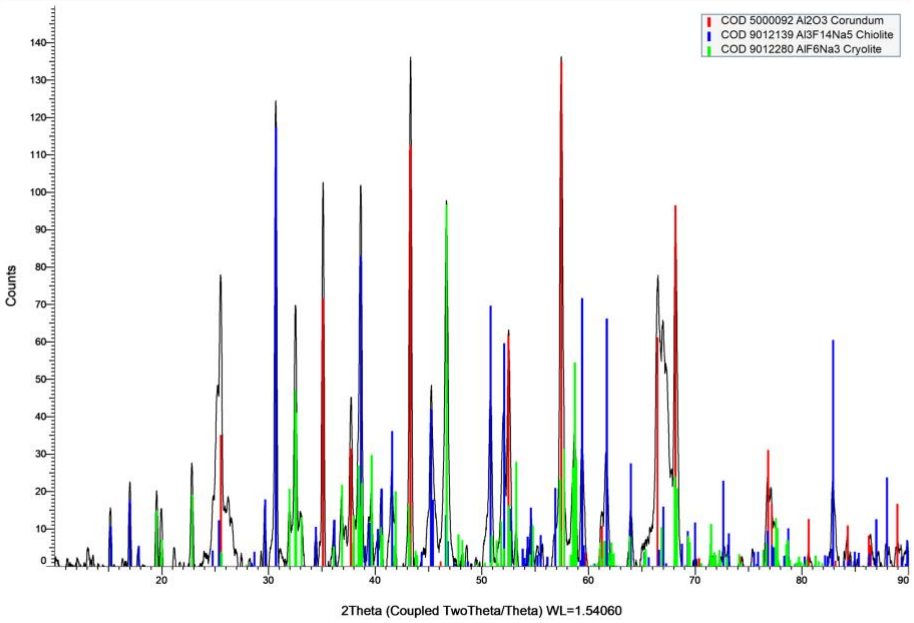

AH8 (Coupled TwoTheta/Theta)

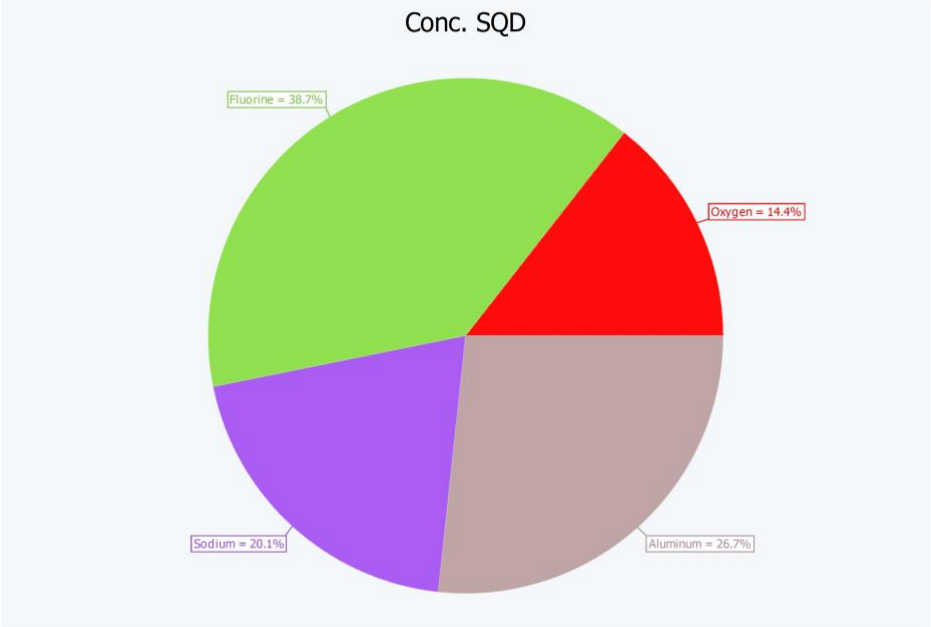

AH8 (Coupled TwoTheta/Theta)

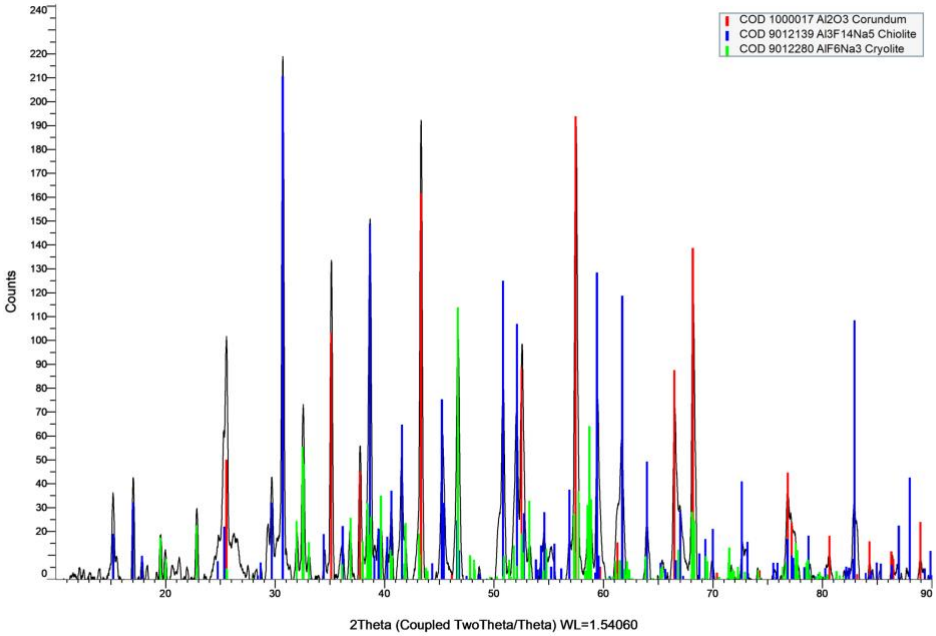

AH9 (Coupled TwoTheta/Theta)

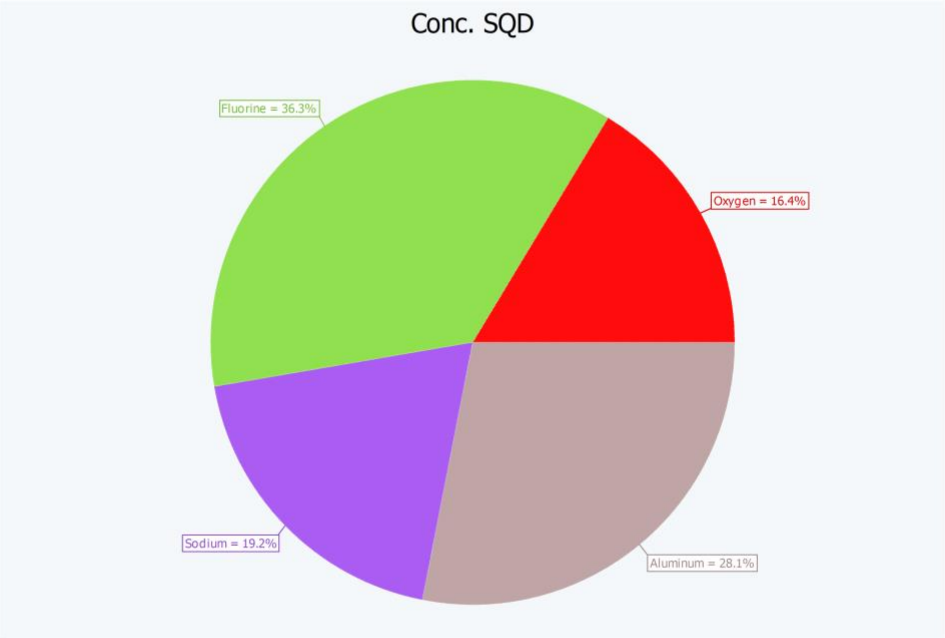

AH9 (Coupled TwoTheta/Theta)

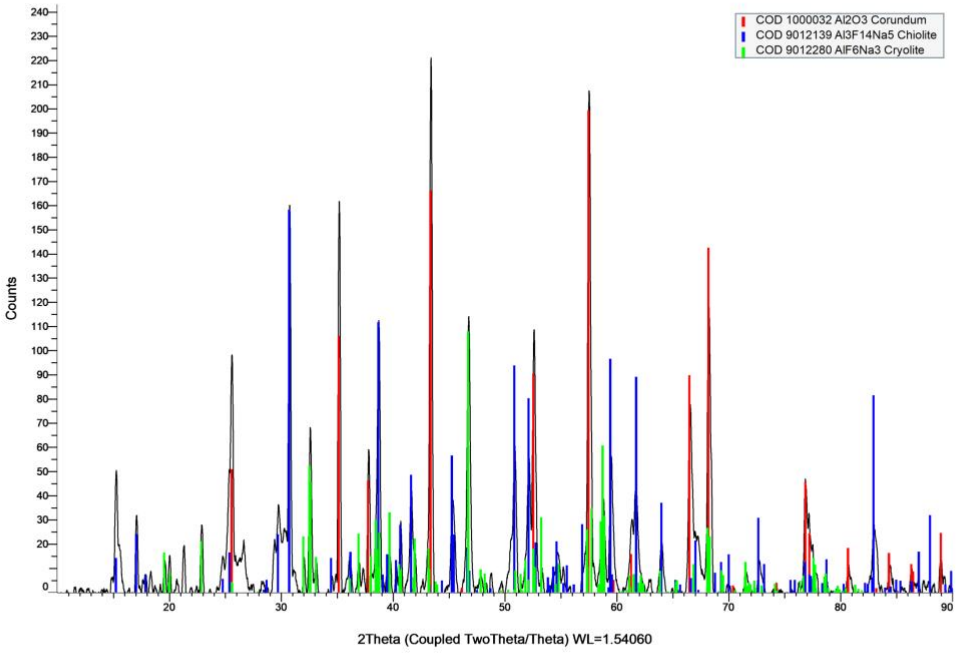

SH11 (Coupled TwoTheta/Theta)

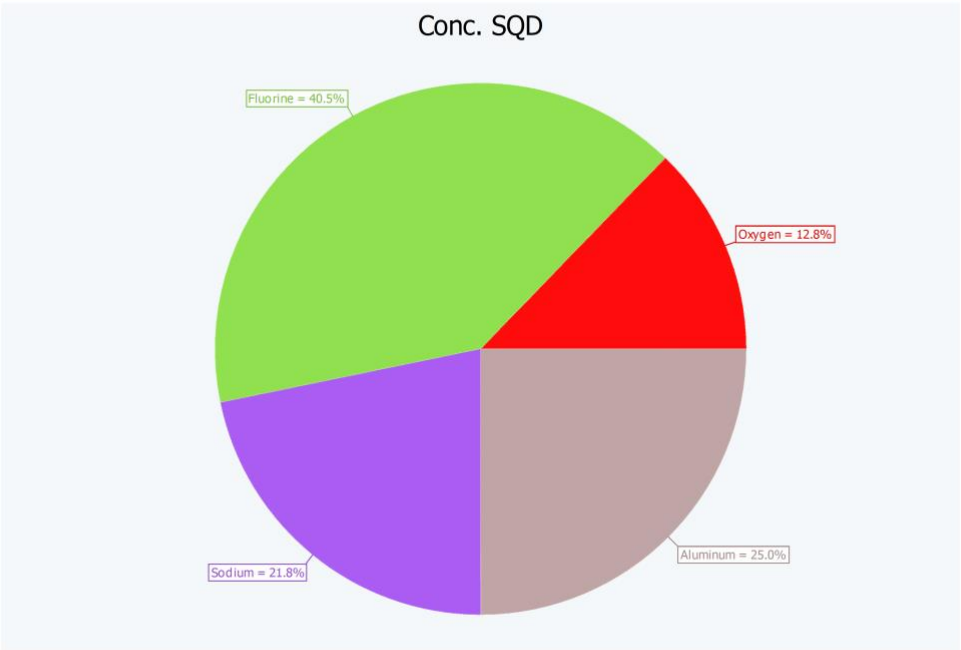

SH11 (Coupled TwoTheta/Theta)

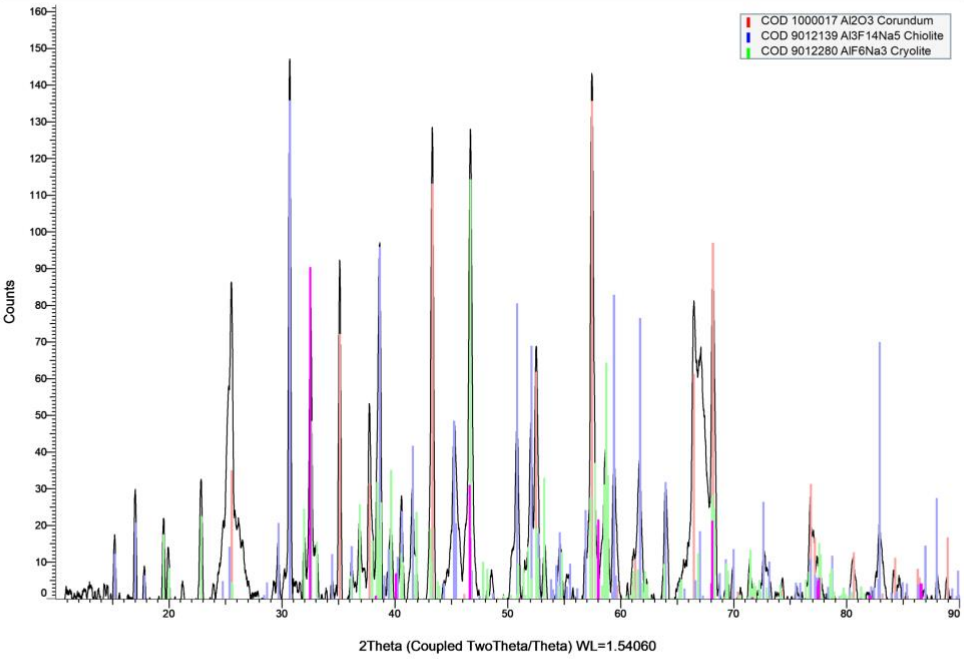

D ICP-MS

ANALYSIS REPORT

Semi-quantitative screening analysis by ICP

Issued by:	ALS Scandinavia Luleå, Aurorum 10, SE-977 75 LULEÅ, Sweden
Client:	NTNU Institutt for Materialteknolog
Date of receipt:	2022-04-08
Date of analysis:	2022-04-22
Order number(our):	LE2204221
Your reference:	Fride Müller
Our reference:	Steffen Eisele
Sample name:	1
Sample description:	
Lab number(our)	LE2204221-001

Aluminum, Al	190000 mg/kg	Nickel, Ni	720 mg/kg
Antimony, Sb	62 mg/kg	Niobium, Nb	0.63 mg/kg
Arsenic, As	200 mg/kg	Osmium, Os	< 0.02 mg/kg
Barium, Ba	140 mg/kg	Palladium, Pd	< 0.05 mg/kg
Beryllium, Be	10 mg/kg	Phosphorus, P	1200 mg/kg
Bismuth, Bi	37 mg/kg	Platinum, Pt	< 0.02 mg/kg
Boron, B	< 5 mg/kg	Potassium, K	3800 mg/kg
Bromine, Br	39 mg/kg	Praseodymium, Pr	0.19 mg/kg
Cadmium, Cd	3.2 mg/kg	Rhenium, Re	0.047 mg/kg
Calcium, Ca	7900 mg/kg	Rhodium, Rh	< 0.03 mg/kg
Cerium, Ce	1.8 mg/kg	Rubidium, Rb	20 mg/kg
Cesium, Cs	2.3 mg/kg	Ruthenium, Ru	< 0.03 mg/kg
Chromium, Cr	25 mg/kg	Samarium, Sm	0.14 mg/kg
Cobalt, Co	9.4 mg/kg	Scandium, Sc	0.37 mg/kg
Copper, Cu	21 mg/kg	Selenium, Se	8.2 mg/kg
Dysprosium, Dy	0.098 mg/kg	Silicon, Si	4600 mg/kg
Erbium, Er	0.067 mg/kg	Silver, Ag	0.052 mg/kg
Europium, Eu	0.070 mg/kg	Sodium, Na	110000 mg/kg
Gadolinium, Gd	0.12 mg/kg	Strontium, Sr	45 mg/kg
Gallium, Ga	280 mg/kg	Sulfur, S	2400 mg/kg
Germanium, Ge	2.5 mg/kg	Tantalum, Ta	< 0.05 mg/kg
Gold, Au	< 0.05 mg/kg	Tellurium, Te	10 mg/kg
Hafnium, Hf	0.85 mg/kg	Terbium, Tb	0.19 mg/kg
Holmium, Ho	< 0.05 mg/kg	Thallium, Tl	0.22 mg/kg
Iodine, I	1.9 mg/kg	Thorium, Th	0.24 mg/kg
Iridium, Ir	< 0.005 mg/kg	Thulium, Tm	0.011 mg/kg
Iron, Fe	8400 mg/kg	Tin, Sn	3.3 mg/kg
Lanthanum, La	2.3 mg/kg	Titanium, Ti	260 mg/kg
Lead, Pb	61 mg/kg	Tungsten, W	5.8 mg/kg
Lithium, Li	3.4 mg/kg	Uranium, U	0.15 mg/kg
Lutetium, Lu	0.0077 mg/kg	Vanadium, V	450 mg/kg
Magnesium, Mg	770 mg/kg	Ytterbium, Yb	0.093 mg/kg
Manganese, Mn	72 mg/kg	Yttrium, Y	2.1 mg/kg
Mercury, Hg	0.024 mg/kg	Zinc, Zn	1200 mg/kg
Molybdenum, Mo	4.4 mg/kg	Zirconium, Zr	130 mg/kg
Neodymium, Nd	0.59 mg/kg		

Comments

The analysis is carried out by ICP-SMS (HR-ICP-MS).
The trace elements are determined using 18 scans over the mass range, resulting in a total measurement time of 300 s.
All concentrations are within ± 50% of the reported value.This may not apply to Br, Cl and I.
Elements marked with '<' are below the detection limit.
Elements marked with*** were not detectable.
Elements marked with ----- are not measured.

Signature

ANALYSIS REPORT

Semi-quantitative screening analysis by ICP

Issued by:	ALS Scandinavia Luleå, Aurorum 10, SE-977 75 LULEÅ, Sweden
Client:	NTNU Institutt for Materialteknolog
Date of receipt:	2022-04-08
Date of analysis:	2022-04-22
Order number(our):	LE2204221
Your reference:	Fride Müller
Our reference:	Steffen Eisele
Sample name:	2
Sample description:	
Lab number(our)	LE2204221-002

Aluminum, Al	200000 mg/kg	Nickel, Ni	1000 mg/kg
Antimony, Sb	33 mg/kg	Niobium, Nb	0.49 mg/kg
Arsenic, As	120 mg/kg	Osmium, Os	< 0.02 mg/kg
Barium, Ba	130 mg/kg	Palladium, Pd	< 0.05 mg/kg
Beryllium, Be	9.6 mg/kg	Phosphorus, P	810 mg/kg
Bismuth, Bi	15 mg/kg	Platinum, Pt	< 0.02 mg/kg
Boron, B	< 5 mg/kg	Potassium, K	1800 mg/kg
Bromine, Br	< 50 mg/kg	Praseodymium, Pr	0.15 mg/kg
Cadmium, Cd	1.7 mg/kg	Rhenium, Re	0.048 mg/kg
Calcium, Ca	9000 mg/kg	Rhodium, Rh	< 0.03 mg/kg
Cerium, Ce	1.1 mg/kg	Rubidium, Rb	8.7 mg/kg
Cesium, Cs	1.0 mg/kg	Ruthenium, Ru	< 0.03 mg/kg
Chromium, Cr	24 mg/kg	Samarium, Sm	0.088 mg/kg
Cobalt, Co	13 mg/kg	Scandium, Sc	0.18 mg/kg
Copper, Cu	26 mg/kg	Selenium, Se	3.5 mg/kg
Dysprosium, Dy	0.072 mg/kg	Silicon, Si	3100 mg/kg
Erbium, Er	0.064 mg/kg	Silver, Ag	0.12 mg/kg
Europium, Eu	0.071 mg/kg	Sodium, Na	96000 mg/kg
Gadolinium, Gd	< 0.05 mg/kg	Strontium, Sr	47 mg/kg
Gallium, Ga	160 mg/kg	Sulfur, S	1900 mg/kg
Germanium, Ge	1.0 mg/kg	Tantalum, Ta	< 0.05 mg/kg
Gold, Au	< 0.05 mg/kg	Tellurium, Te	6.7 mg/kg
Hafnium, Hf	0.59 mg/kg	Terbium, Tb	0.18 mg/kg
Holmium, Ho	< 0.05 mg/kg	Thallium, Tl	0.078 mg/kg
Iodine, I	1.2 mg/kg	Thorium, Th	0.12 mg/kg
Iridium, Ir	< 0.005 mg/kg	Thulium, Tm	0.013 mg/kg
Iron, Fe	7400 mg/kg	Tin, Sn	2 mg/kg
Lanthanum, La	2.0 mg/kg	Titanium, Ti	250 mg/kg
Lead, Pb	32 mg/kg	Tungsten, W	4.9 mg/kg
Lithium, Li	5.7 mg/kg	Uranium, U	0.16 mg/kg
Lutetium, Lu	0.016 mg/kg	Vanadium, V	320 mg/kg
Magnesium, Mg	650 mg/kg	Ytterbium, Yb	0.079 mg/kg
Manganese, Mn	86 mg/kg	Yttrium, Y	2.9 mg/kg
Mercury, Hg	< 0.02 mg/kg	Zinc, Zn	1700 mg/kg
Molybdenum, Mo	5.9 mg/kg	Zirconium, Zr	25 mg/kg
Neodymium, Nd	0.44 mg/kg		

Comments

The analysis is carried out by ICP-SMS (HR-ICP-MS).
The trace elements are determined using 18 scans over the mass range, resulting in a total measurement time of 300 s.
All concentrations are within ± 50% of the reported value.This may not apply to Br, Cl and I.
Elements marked with '<' are below the detection limit.
Elements marked with*** were not detectable.
Elements marked with ----- are not measured.

Signature 

ANALYSIS REPORT

Semi-quantitative screening analysis by ICP

Issued by:	ALS Scandinavia Luleå, Aurorum 10, SE-977 75 LULEÅ, Sweden
Client:	NTNU Institutt for Materialteknolog
Date of receipt:	2022-04-08
Date of analysis:	2022-04-22
Order number(our):	LE2204221
Your reference:	Fride Müller
Our reference:	Steffen Eisele
Sample name:	3
Sample description:	
Lab number(our)	LE2204221-003

Aluminum, Al	260000 mg/kg	Nickel, Ni	850 mg/kg
Antimony, Sb	36 mg/kg	Niobium, Nb	0.29 mg/kg
Arsenic, As	43 mg/kg	Osmium, Os	< 0.02 mg/kg
Barium, Ba	110 mg/kg	Palladium, Pd	< 0.05 mg/kg
Beryllium, Be	8.8 mg/kg	Phosphorus, P	640 mg/kg
Bismuth, Bi	5.3 mg/kg	Platinum, Pt	< 0.02 mg/kg
Boron, B	< 5 mg/kg	Potassium, K	1100 mg/kg
Bromine, Br	< 50 mg/kg	Praseodymium, Pr	0.071 mg/kg
Cadmium, Cd	0.50 mg/kg	Rhenium, Re	0.071 mg/kg
Calcium, Ca	8500 mg/kg	Rhodium, Rh	< 0.03 mg/kg
Cerium, Ce	0.63 mg/kg	Rubidium, Rb	4.8 mg/kg
Cesium, Cs	0.71 mg/kg	Ruthenium, Ru	< 0.03 mg/kg
Chromium, Cr	22 mg/kg	Samarium, Sm	0.0.65 mg/kg
Cobalt, Co	9.2 mg/kg	Scandium, Sc	0.084 mg/kg
Copper, Cu	25 mg/kg	Selenium, Se	1.2 mg/kg
Dysprosium, Dy	0.072 mg/kg	Silicon, Si	2900 mg/kg
Erbium, Er	0.062 mg/kg	Silver, Ag	0.067 mg/kg
Europium, Eu	0.069 mg/kg	Sodium, Na	75000 mg/kg
Gadolinium, Gd	< 0.05 mg/kg	Strontium, Sr	38 mg/kg
Gallium, Ga	110 mg/kg	Sulfur, S	900 mg/kg
Germanium, Ge	0.36 mg/kg	Tantalum, Ta	< 0.05 mg/kg
Gold, Au	< 0.05 mg/kg	Tellurium, Te	2.6 mg/kg
Hafnium, Hf	0.40 mg/kg	Terbium, Tb	< 0.01 mg/kg
Holmium, Ho	< 0.05 mg/kg	Thallium, Tl	0.035 mg/kg
Iodine, I	1.1 mg/kg	Thorium, Th	0.057 mg/kg
Iridium, Ir	< 0.005 mg/kg	Thulium, Tm	< 0.005 mg/kg
Iron, Fe	5100 mg/kg	Tin, Sn	1 mg/kg
Lanthanum, La	1.6 mg/kg	Titanium, Ti	85 mg/kg
Lead, Pb	15 mg/kg	Tungsten, W	4.1 mg/kg
Lithium, Li	6.1 mg/kg	Uranium, U	0.19 mg/kg
Lutetium, Lu	0.011 mg/kg	Vanadium, V	210 mg/kg
Magnesium, Mg	540 mg/kg	Ytterbium, Yb	0.065 mg/kg
Manganese, Mn	39 mg/kg	Yttrium, Y	2.6 mg/kg
Mercury, Hg	< 0.02 mg/kg	Zinc, Zn	25 mg/kg
Molybdenum, Mo	7.6 mg/kg	Zirconium, Zr	13 mg/kg
Neodymium, Nd	0.19 mg/kg		

Comments

The analysis is carried out by ICP-SMS (HR-ICP-MS).
The trace elements are determined using 18 scans over the mass range, resulting in a total measurement time of 300 s.
All concentrations are within ± 50% of the reported value.This may not apply to Br, Cl and I.
Elements marked with '<' are below the detection limit.
Elements marked with*** were not detectable.
Elements marked with ----- are not measured.

Signature

ANALYSIS REPORT

Semi-quantitative screening analysis by ICP

Issued by:	ALS Scandinavia Luleå, Aurorum 10, SE-977 75 LULEÅ, Sweden
Client:	NTNU Institutt for Materialteknolog
Date of receipt:	2022-04-08
Date of analysis:	2022-04-22
Order number(our):	LE2204221
Your reference:	Fride Müller
Our reference:	Steffen Eisele
Sample name:	4
Sample description:	
Lab number(our)	LE2204221-004

Aluminum, Al	200000 mg/kg	Nickel, Ni	4100 mg/kg
Antimony, Sb	470 mg/kg	Niobium, Nb	0.71 mg/kg
Arsenic, As	420 mg/kg	Osmium, Os	< 0.02 mg/kg
Barium, Ba	95 mg/kg	Palladium, Pd	< 0.05 mg/kg
Beryllium, Be	8.8 mg/kg	Phosphorus, P	980 mg/kg
Bismuth, Bi	100 mg/kg	Platinum, Pt	< 0.03 mg/kg
Boron, B	100 mg/kg	Potassium, K	4100 mg/kg
Bromine, Br	< 300 mg/kg	Praseodymium, Pr	0.23 mg/kg
Cadmium, Cd	2.9 mg/kg	Rhenium, Re	0.48 mg/kg
Calcium, Ca	8800 mg/kg	Rhodium, Rh	0.028 mg/kg
Cerium, Ce	1.9 mg/kg	Rubidium, Rb	18 mg/kg
Cesium, Cs	2.4 mg/kg	Ruthenium, Ru	< 0.03 mg/kg
Chromium, Cr	110 mg/kg	Samarium, Sm	0.080 mg/kg
Cobalt, Co	110 mg/kg	Scandium, Sc	0.48 mg/kg
Copper, Cu	1600 mg/kg	Selenium, Se	9.5 mg/kg
Dysprosium, Dy	0.14 mg/kg	Silicon, Si	4200 mg/kg
Erbium, Er	0.073 mg/kg	Silver, Ag	0.79 mg/kg
Europium, Eu	0.088 mg/kg	Sodium, Na	100000 mg/kg
Gadolinium, Gd	0.079 mg/kg	Strontium, Sr	31 mg/kg
Gallium, Ga	210 mg/kg	Sulfur, S	8900 mg/kg
Germanium, Ge	3.1 mg/kg	Tantalum, Ta	0.050 mg/kg
Gold, Au	< 0.05 mg/kg	Tellurium, Te	150 mg/kg
Hafnium, Hf	0.44 mg/kg	Terbium, Tb	0.023 mg/kg
Holmium, Ho	< 0.05 mg/kg	Thallium, Tl	0.78 mg/kg
Iodine, I	< 2 mg/kg	Thorium, Th	0.28 mg/kg
Iridium, Ir	< 0.005 mg/kg	Thulium, Tm	0.020 mg/kg
Iron, Fe	10000 mg/kg	Tin, Sn	55 mg/kg
Lanthanum, La	2.8 mg/kg	Titanium, Ti	390 mg/kg
Lead, Pb	270 mg/kg	Tungsten, W	7.2 mg/kg
Lithium, Li	5.3 mg/kg	Uranium, U	0.30 mg/kg
Lutetium, Lu	0.029 mg/kg	Vanadium, V	230 mg/kg
Magnesium, Mg	910 mg/kg	Ytterbium, Yb	0.10 mg/kg
Manganese, Mn	190 mg/kg	Yttrium, Y	2.1 mg/kg
Mercury, Hg	0.13 mg/kg	Zinc, Zn	1600 mg/kg
Molybdenum, Mo	51 mg/kg	Zirconium, Zr	17 mg/kg
Neodymium, Nd	0.76 mg/kg		

Comments

The analysis is carried out by ICP-SMS (HR-ICP-MS).
The trace elements are determined using 18 scans over the mass range, resulting in a total measurement time of 300 s.
All concentrations are within ± 50% of the reported value.This may not apply to Br, Cl and I.
Elements marked with '<' are below the detection limit.
Elements marked with*** were not detectable.
Elements marked with ----- are not measured.

Signature 

ANALYSIS REPORT

Semi-quantitative screening analysis by ICP

Issued by:	ALS Scandinavia Luleå, Aurorum 10, SE-977 75 LULEÅ, Sweden
Client:	NTNU Institutt for Materialteknolog
Date of receipt:	2022-04-08
Date of analysis:	2022-04-22
Order number(our):	LE2204221
Your reference:	Fride Müller
Our reference:	Steffen Eisele
Sample name:	5
Sample description:	
Lab number(our)	LE2204221-005

Aluminum, Al	230000 mg/kg	Nickel, Ni	770 mg/kg
Antimony, Sb	85 mg/kg	Niobium, Nb	0.48 mg/kg
Arsenic, As	85 mg/kg	Osmium, Os	< 0.02 mg/kg
Barium, Ba	76 mg/kg	Palladium, Pd	< 0.05 mg/kg
Beryllium, Be	9.5 mg/kg	Phosphorus, P	1000 mg/kg
Bismuth, Bi	26 mg/kg	Platinum, Pt	< 0.02 mg/kg
Boron, B	< 5 mg/kg	Potassium, K	3300 mg/kg
Bromine, Br	< 50 mg/kg	Praseodymium, Pr	0.10 mg/kg
Cadmium, Cd	0.42 mg/kg	Rhenium, Re	0.098 mg/kg
Calcium, Ca	8300 mg/kg	Rhodium, Rh	< 0.03 mg/kg
Cerium, Ce	1.3 mg/kg	Rubidium, Rb	18 mg/kg
Cesium, Cs	2.3 mg/kg	Ruthenium, Ru	< 0.03 mg/kg
Chromium, Cr	44 mg/kg	Samarium, Sm	0.087 mg/kg
Cobalt, Co	20 mg/kg	Scandium, Sc	0.085 mg/kg
Copper, Cu	140 mg/kg	Selenium, Se	1.8 mg/kg
Dysprosium, Dy	0.098 mg/kg	Silicon, Si	2400 mg/kg
Erbium, Er	0.076 mg/kg	Silver, Ag	0.067 mg/kg
Europium, Eu	< 0.05 mg/kg	Sodium, Na	96000 mg/kg
Gadolinium, Gd	0.11 mg/kg	Strontium, Sr	26 mg/kg
Gallium, Ga	200 mg/kg	Sulfur, S	2000 mg/kg
Germanium, Ge	2.5 mg/kg	Tantalum, Ta	< 0.05 mg/kg
Gold, Au	< 0.05 mg/kg	Tellurium, Te	26 mg/kg
Hafnium, Hf	0.27 mg/kg	Terbium, Tb	0.021 mg/kg
Holmium, Ho	< 0.05 mg/kg	Thallium, Tl	0.14 mg/kg
Iodine, I	1.2 mg/kg	Thorium, Th	0.14 mg/kg
Iridium, Ir	< 0.005 mg/kg	Thulium, Tm	0.016 mg/kg
Iron, Fe	9000 mg/kg	Tin, Sn	4.2 mg/kg
Lanthanum, La	2.2 mg/kg	Titanium, Ti	240 mg/kg
Lead, Pb	47 mg/kg	Tungsten, W	8.2 mg/kg
Lithium, Li	0.83 mg/kg	Uranium, U	0.22 mg/kg
Lutetium, Lu	0.012 mg/kg	Vanadium, V	260 mg/kg
Magnesium, Mg	630 mg/kg	Ytterbium, Yb	0.073 mg/kg
Manganese, Mn	120 mg/kg	Yttrium, Y	1.9 mg/kg
Mercury, Hg	< 0.02 mg/kg	Zinc, Zn	66 mg/kg
Molybdenum, Mo	8.3 mg/kg	Zirconium, Zr	11 mg/kg
Neodymium, Nd	0.56 mg/kg		

Comments

The analysis is carried out by ICP-SMS (HR-ICP-MS).
The trace elements are determined using 18 scans over the mass range, resulting in a total measurement time of 300 s.
All concentrations are within ± 50% of the reported value.This may not apply to Br, Cl and I.
Elements marked with '<' are below the detection limit.
Elements marked with*** were not detectable.
Elements marked with ----- are not measured.

Signature S. Eisele

ANALYSIS REPORT

Semi-quantitative screening analysis by ICP

Issued by:	ALS Scandinavia Luleå, Aurorum 10, SE-977 75 LULEÅ, Sweden
Client:	NTNU Institutt for Materialteknolog
Date of receipt:	2022-04-08
Date of analysis:	2022-04-22
Order number(our):	LE2204221
Your reference:	Fride Müller
Our reference:	Steffen Eisele
Sample name:	6
Sample description:	
Lab number(our)	LE2204221-006

Aluminum, Al	230000 mg/kg	Nickel, Ni	940 mg/kg
Antimony, Sb	91 mg/kg	Niobium, Nb	0.72 mg/kg
Arsenic, As	80 mg/kg	Osmium, Os	< 0.02 mg/kg
Barium, Ba	71 mg/kg	Palladium, Pd	< 0.05 mg/kg
Beryllium, Be	7.6 mg/kg	Phosphorus, P	860 mg/kg
Bismuth, Bi	25 mg/kg	Platinum, Pt	< 0.02 mg/kg
Boron, B	6.0 mg/kg	Potassium, K	3600 mg/kg
Bromine, Br	< 50 mg/kg	Praseodymium, Pr	0.096 mg/kg
Cadmium, Cd	0.31 mg/kg	Rhenium, Re	0.098 mg/kg
Calcium, Ca	8200 mg/kg	Rhodium, Rh	< 0.03 mg/kg
Cerium, Ce	0.73 mg/kg	Rubidium, Rb	17 mg/kg
Cesium, Cs	2.0 mg/kg	Ruthenium, Ru	< 0.03 mg/kg
Chromium, Cr	62 mg/kg	Samarium, Sm	0.051 mg/kg
Cobalt, Co	21 mg/kg	Scandium, Sc	0.18 mg/kg
Copper, Cu	220 mg/kg	Selenium, Se	2.6 mg/kg
Dysprosium, Dy	< 0.05 mg/kg	Silicon, Si	2700 mg/kg
Erbium, Er	0.062 mg/kg	Silver, Ag	0.075 mg/kg
Europium, Eu	< 0.05 mg/kg	Sodium, Na	100000 mg/kg
Gadolinium, Gd	< 0.05 mg/kg	Strontium, Sr	24 mg/kg
Gallium, Ga	180 mg/kg	Sulfur, S	1900 mg/kg
Germanium, Ge	1.2 mg/kg	Tantalum, Ta	< 0.05 mg/kg
Gold, Au	< 0.05 mg/kg	Tellurium, Te	27 mg/kg
Hafnium, Hf	0.30 mg/kg	Terbium, Tb	< 0.01 mg/kg
Holmium, Ho	< 0.05 mg/kg	Thallium, Tl	0.12 mg/kg
Iodine, I	1.4 mg/kg	Thorium, Th	0.10 mg/kg
Iridium, Ir	< 0.005 mg/kg	Thulium, Tm	< 0.005 mg/kg
Iron, Fe	9200 mg/kg	Tin, Sn	6.4 mg/kg
Lanthanum, La	1.7 mg/kg	Titanium, Ti	150 mg/kg
Lead, Pb	60 mg/kg	Tungsten, W	7.5 mg/kg
Lithium, Li	0.71 mg/kg	Uranium, U	0.14 mg/kg
Lutetium, Lu	0.0064 mg/kg	Vanadium, V	270 mg/kg
Magnesium, Mg	600 mg/kg	Ytterbium, Yb	< 0.05 mg/kg
Manganese, Mn	92 mg/kg	Yttrium, Y	1.4 mg/kg
Mercury, Hg	< 0.02 mg/kg	Zinc, Zn	240 mg/kg
Molybdenum, Mo	9.3 mg/kg	Zirconium, Zr	8.8 mg/kg
Neodymium, Nd	0.30 mg/kg		

Comments

The analysis is carried out by ICP-SMS (HR-ICP-MS).
The trace elements are determined using 18 scans over the mass range, resulting in a total measurement time of 300 s.
All concentrations are within ± 50% of the reported value.This may not apply to Br, Cl and I.
Elements marked with '<' are below the detection limit.
Elements marked with*** were not detectable.
Elements marked with ----- are not measured.

Signature

ANALYSIS REPORT

Semi-quantitative screening analysis by ICP

Issued by:	ALS Scandinavia Luleå, Aurorum 10, SE-977 75 LULEÅ, Sweden
Client:	NTNU Institutt for Materialteknolog
Date of receipt:	2022-04-08
Date of analysis:	2022-04-22
Order number(our):	LE2204221
Your reference:	Fride Müller
Our reference:	Steffen Eisele
Sample name:	7
Sample description:	
Lab number(our)	LE2204221-007

Aluminum, Al	220000 mg/kg	Nickel, Ni	5100 mg/kg
Antimony, Sb	360 mg/kg	Niobium, Nb	0.65 mg/kg
Arsenic, As	320 mg/kg	Osmium, Os	< 0.02 mg/kg
Barium, Ba	78 mg/kg	Palladium, Pd	< 0.05 mg/kg
Beryllium, Be	7.3 mg/kg	Phosphorus, P	1000 mg/kg
Bismuth, Bi	70 mg/kg	Platinum, Pt	< 0.03 mg/kg
Boron, B	18 mg/kg	Potassium, K	2700 mg/kg
Bromine, Br	< 300 mg/kg	Praseodymium, Pr	0.087 mg/kg
Cadmium, Cd	2.6 mg/kg	Rhenium, Re	0.41 mg/kg
Calcium, Ca	10000 mg/kg	Rhodium, Rh	0.031 mg/kg
Cerium, Ce	0.92 mg/kg	Rubidium, Rb	13 mg/kg
Cesium, Cs	1.4 mg/kg	Ruthenium, Ru	< 0.03 mg/kg
Chromium, Cr	77 mg/kg	Samarium, Sm	0.069 mg/kg
Cobalt, Co	110 mg/kg	Scandium, Sc	0.12 mg/kg
Copper, Cu	2000 mg/kg	Selenium, Se	7.1 mg/kg
Dysprosium, Dy	0.062 mg/kg	Silicon, Si	2800 mg/kg
Erbium, Er	0.052 mg/kg	Silver, Ag	0.61 mg/kg
Europium, Eu	0.051 mg/kg	Sodium, Na	87000 mg/kg
Gadolinium, Gd	0.069 mg/kg	Strontium, Sr	31 mg/kg
Gallium, Ga	180 mg/kg	Sulfur, S	6900 mg/kg
Germanium, Ge	2.1 mg/kg	Tantalum, Ta	0.058 mg/kg
Gold, Au	< 0.05 mg/kg	Tellurium, Te	71 mg/kg
Hafnium, Hf	0.35 mg/kg	Terbium, Tb	< 0.01 mg/kg
Holmium, Ho	< 0.05 mg/kg	Thallium, Tl	0.32 mg/kg
Iodine, I	6.1 mg/kg	Thorium, Th	0.12 mg/kg
Iridium, Ir	< 0.005 mg/kg	Thulium, Tm	< 0.005 mg/kg
Iron, Fe	8400 mg/kg	Tin, Sn	110 mg/kg
Lanthanum, La	2.4 mg/kg	Titanium, Ti	180 mg/kg
Lead, Pb	230 mg/kg	Tungsten, W	8.5 mg/kg
Lithium, Li	4 mg/kg	Uranium, U	0.16 mg/kg
Lutetium, Lu	0.012 mg/kg	Vanadium, V	220 mg/kg
Magnesium, Mg	810 mg/kg	Ytterbium, Yb	0.076 mg/kg
Manganese, Mn	93 mg/kg	Yttrium, Y	1.7 mg/kg
Mercury, Hg	0.061 mg/kg	Zinc, Zn	1300 mg/kg
Molybdenum, Mo	39 mg/kg	Zirconium, Zr	9.2 mg/kg
Neodymium, Nd	0.39 mg/kg		

Comments

The analysis is carried out by ICP-SMS (HR-ICP-MS).
The trace elements are determined using 18 scans over the mass range, resulting in a total measurement time of 300 s.
All concentrations are within ± 50% of the reported value.This may not apply to Br, Cl and I.
Elements marked with '<' are below the detection limit.
Elements marked with*** were not detectable.
Elements marked with ----- are not measured.

Signature S. Eisele

ANALYSIS REPORT

Semi-quantitative screening analysis by ICP

Issued by:	ALS Scandinavia Luleå, Aurorum 10, SE-977 75 LULEÅ, Sweden
Client:	NTNU Institutt for Materialteknolog
Date of receipt:	2022-04-08
Date of analysis:	2022-04-22
Order number(our):	LE2204221
Your reference:	Fride Müller
Our reference:	Steffen Eisele
Sample name:	8
Sample description:	
Lab number(our)	LE2204221-008

Aluminum, Al	180000 mg/kg	Nickel, Ni	920 mg/kg
Antimony, Sb	31 mg/kg	Niobium, Nb	0.60 mg/kg
Arsenic, As	110 mg/kg	Osmium, Os	< 0.02 mg/kg
Barium, Ba	130 mg/kg	Palladium, Pd	< 0.05 mg/kg
Beryllium, Be	8.2 mg/kg	Phosphorus, P	1100 mg/kg
Bismuth, Bi	18 mg/kg	Platinum, Pt	< 0.02 mg/kg
Boron, B	< 5 mg/kg	Potassium, K	3100 mg/kg
Bromine, Br	< 50 mg/kg	Praseodymium, Pr	0.13 mg/kg
Cadmium, Cd	1.1 mg/kg	Rhenium, Re	0.034 mg/kg
Calcium, Ca	12000 mg/kg	Rhodium, Rh	< 0.03 mg/kg
Cerium, Ce	1.5 mg/kg	Rubidium, Rb	13 mg/kg
Cesium, Cs	1.6 mg/kg	Ruthenium, Ru	< 0.03 mg/kg
Chromium, Cr	23 mg/kg	Samarium, Sm	0.13 mg/kg
Cobalt, Co	14 mg/kg	Scandium, Sc	0.22 mg/kg
Copper, Cu	21 mg/kg	Selenium, Se	4.1 mg/kg
Dysprosium, Dy	0.071 mg/kg	Silicon, Si	3000 mg/kg
Erbium, Er	0.066 mg/kg	Silver, Ag	0.13 mg/kg
Europium, Eu	0.094 mg/kg	Sodium, Na	110000 mg/kg
Gadolinium, Gd	0.076 mg/kg	Strontium, Sr	53 mg/kg
Gallium, Ga	160 mg/kg	Sulfur, S	1200 mg/kg
Germanium, Ge	2.0 mg/kg	Tantalum, Ta	0.063 mg/kg
Gold, Au	< 0.05 mg/kg	Tellurium, Te	7.3 mg/kg
Hafnium, Hf	0.44 mg/kg	Terbium, Tb	0.019 mg/kg
Holmium, Ho	< 0.05 mg/kg	Thallium, Tl	0.069 mg/kg
Iodine, I	1.2 mg/kg	Thorium, Th	0.14 mg/kg
Iridium, Ir	< 0.005 mg/kg	Thulium, Tm	0.011 mg/kg
Iron, Fe	8600 mg/kg	Tin, Sn	2 mg/kg
Lanthanum, La	2.1 mg/kg	Titanium, Ti	450 mg/kg
Lead, Pb	36 mg/kg	Tungsten, W	6.1 mg/kg
Lithium, Li	3.2 mg/kg	Uranium, U	0.12 mg/kg
Lutetium, Lu	0.023 mg/kg	Vanadium, V	280 mg/kg
Magnesium, Mg	1500 mg/kg	Ytterbium, Yb	0.083 mg/kg
Manganese, Mn	70 mg/kg	Yttrium, Y	2.9 mg/kg
Mercury, Hg	< 0.02 mg/kg	Zinc, Zn	670 mg/kg
Molybdenum, Mo	5.2 mg/kg	Zirconium, Zr	17 mg/kg
Neodymium, Nd	0.62 mg/kg		

Comments

The analysis is carried out by ICP-SMS (HR-ICP-MS).
The trace elements are determined using 18 scans over the mass range, resulting in a total measurement time of 300 s.
All concentrations are within ± 50% of the reported value.This may not apply to Br, Cl and I.
Elements marked with '<' are below the detection limit.
Elements marked with*** were not detectable.
Elements marked with ----- are not measured.

Signature

ANALYSIS REPORT

Semi-quantitative screening analysis by ICP

Issued by:	ALS Scandinavia Luleå, Aurorum 10, SE-977 75 LULEÅ, Sweden
Client:	NTNU Institutt for Materialteknolog
Date of receipt:	2022-04-08
Date of analysis:	2022-04-22
Order number(our):	LE2204221
Your reference:	Fride Müller
Our reference:	Steffen Eisele
Sample name:	9
Sample description:	
Lab number(our)	LE2204221-009

Aluminum, Al	210000 mg/kg	Nickel, Ni	780 mg/kg
Antimony, Sb	23 mg/kg	Niobium, Nb	0.80 mg/kg
Arsenic, As	170 mg/kg	Osmium, Os	< 0.02 mg/kg
Barium, Ba	140 mg/kg	Palladium, Pd	< 0.05 mg/kg
Beryllium, Be	8.7 mg/kg	Phosphorus, P	1000 mg/kg
Bismuth, Bi	15 mg/kg	Platinum, Pt	< 0.02 mg/kg
Boron, B	< 5 mg/kg	Potassium, K	3100 mg/kg
Bromine, Br	< 50 mg/kg	Praseodymium, Pr	0.20 mg/kg
Cadmium, Cd	1.2 mg/kg	Rhenium, Re	0.035 mg/kg
Calcium, Ca	9800 mg/kg	Rhodium, Rh	< 0.03 mg/kg
Cerium, Ce	1.7 mg/kg	Rubidium, Rb	11 mg/kg
Cesium, Cs	1.1 mg/kg	Ruthenium, Ru	< 0.03 mg/kg
Chromium, Cr	26 mg/kg	Samarium, Sm	0.13 mg/kg
Cobalt, Co	8.5 mg/kg	Scandium, Sc	0.22 mg/kg
Copper, Cu	18 mg/kg	Selenium, Se	6.2 mg/kg
Dysprosium, Dy	0.12 mg/kg	Silicon, Si	3500 mg/kg
Erbium, Er	0.062 mg/kg	Silver, Ag	0.067 mg/kg
Europium, Eu	0.074 mg/kg	Sodium, Na	93000 mg/kg
Gadolinium, Gd	0.079 mg/kg	Strontium, Sr	50 mg/kg
Gallium, Ga	270 mg/kg	Sulfur, S	1600 mg/kg
Germanium, Ge	1.5 mg/kg	Tantalum, Ta	0.064 mg/kg
Gold, Au	< 0.05 mg/kg	Tellurium, Te	5.9 mg/kg
Hafnium, Hf	0.28 mg/kg	Terbium, Tb	0.023 mg/kg
Holmium, Ho	< 0.05 mg/kg	Thallium, Tl	0.10 mg/kg
Iodine, I	1.8 mg/kg	Thorium, Th	0.19 mg/kg
Iridium, Ir	< 0.005 mg/kg	Thulium, Tm	0.013 mg/kg
Iron, Fe	9300 mg/kg	Tin, Sn	2.3 mg/kg
Lanthanum, La	1.6 mg/kg	Titanium, Ti	600 mg/kg
Lead, Pb	44 mg/kg	Tungsten, W	5.3 mg/kg
Lithium, Li	5.1 mg/kg	Uranium, U	0.17 mg/kg
Lutetium, Lu	0.016 mg/kg	Vanadium, V	510 mg/kg
Magnesium, Mg	870 mg/kg	Ytterbium, Yb	0.085 mg/kg
Manganese, Mn	74 mg/kg	Yttrium, Y	1.8 mg/kg
Mercury, Hg	< 0.02 mg/kg	Zinc, Zn	2200 mg/kg
Molybdenum, Mo	4.5 mg/kg	Zirconium, Zr	11 mg/kg
Neodymium, Nd	0.66 mg/kg		

Comments

The analysis is carried out by ICP-SMS (HR-ICP-MS).
The trace elements are determined using 18 scans over the mass range, resulting in a total measurement time of 300 s.
All concentrations are within ± 50% of the reported value.This may not apply to Br, Cl and I.
Elements marked with '<' are below the detection limit.
Elements marked with*** were not detectable.
Elements marked with ----- are not measured.

Signature

ANALYSIS REPORT

Semi-quantitative screening analysis by ICP

Issued by:	ALS Scandinavia Luleå, Aurorum 10, SE-977 75 LULEÅ, Sweden
Client:	NTNU Institutt for Materialteknolog
Date of receipt:	2022-04-08
Date of analysis:	2022-04-22
Order number(our):	LE2204221
Your reference:	Fride Müller
Our reference:	Steffen Eisele
Sample name:	10
Sample description:	
Lab number(our)	LE2204221-010

Aluminum, Al	200000 mg/kg	Nickel, Ni	810 mg/kg
Antimony, Sb	30 mg/kg	Niobium, Nb	0.82 mg/kg
Arsenic, As	120 mg/kg	Osmium, Os	< 0.02 mg/kg
Barium, Ba	110 mg/kg	Palladium, Pd	< 0.05 mg/kg
Beryllium, Be	9.0 mg/kg	Phosphorus, P	1000 mg/kg
Bismuth, Bi	13 mg/kg	Platinum, Pt	< 0.02 mg/kg
Boron, B	< 5 mg/kg	Potassium, K	1700 mg/kg
Bromine, Br	< 50 mg/kg	Praseodymium, Pr	0.20 mg/kg
Cadmium, Cd	2.4 mg/kg	Rhenium, Re	0.046 mg/kg
Calcium, Ca	9000 mg/kg	Rhodium, Rh	< 0.03 mg/kg
Cerium, Ce	1.4 mg/kg	Rubidium, Rb	8.8 mg/kg
Cesium, Cs	0.94 mg/kg	Ruthenium, Ru	< 0.03 mg/kg
Chromium, Cr	30 mg/kg	Samarium, Sm	0.076 mg/kg
Cobalt, Co	9.8 mg/kg	Scandium, Sc	0.031 mg/kg
Copper, Cu	23 mg/kg	Selenium, Se	6.4 mg/kg
Dysprosium, Dy	0.091 mg/kg	Silicon, Si	3200 mg/kg
Erbium, Er	0.075 mg/kg	Silver, Ag	0.081 mg/kg
Europium, Eu	0.070 mg/kg	Sodium, Na	96000 mg/kg
Gadolinium, Gd	< 0.05 mg/kg	Strontium, Sr	46 mg/kg
Gallium, Ga	270 mg/kg	Sulfur, S	2000 mg/kg
Germanium, Ge	2.1 mg/kg	Tantalum, Ta	< 0.05 mg/kg
Gold, Au	< 0.05 mg/kg	Tellurium, Te	6.1 mg/kg
Hafnium, Hf	0.25 mg/kg	Terbium, Tb	0.013 mg/kg
Holmium, Ho	< 0.05 mg/kg	Thallium, Tl	0.13 mg/kg
Iodine, I	1.5 mg/kg	Thorium, Th	0.15 mg/kg
Iridium, Ir	< 0.005 mg/kg	Thulium, Tm	0.24 mg/kg
Iron, Fe	20000 mg/kg	Tin, Sn	3 mg/kg
Lanthanum, La	1.9 mg/kg	Titanium, Ti	440 mg/kg
Lead, Pb	47 mg/kg	Tungsten, W	5.7 mg/kg
Lithium, Li	3.6 mg/kg	Uranium, U	0.16 mg/kg
Lutetium, Lu	0.016 mg/kg	Vanadium, V	630 mg/kg
Magnesium, Mg	720 mg/kg	Ytterbium, Yb	0.061 mg/kg
Manganese, Mn	76 mg/kg	Yttrium, Y	2.5 mg/kg
Mercury, Hg	< 0.02 mg/kg	Zinc, Zn	1800 mg/kg
Molybdenum, Mo	6.4 mg/kg	Zirconium, Zr	9.9 mg/kg
Neodymium, Nd	0.71 mg/kg		

Comments

The analysis is carried out by ICP-SMS (HR-ICP-MS).
The trace elements are determined using 18 scans over the mass range, resulting in a total measurement time of 300 s.
All concentrations are within ± 50% of the reported value.This may not apply to Br, Cl and I.
Elements marked with '<' are below the detection limit.
Elements marked with*** were not detectable.
Elements marked with ----- are not measured.

Signature

ANALYSIS REPORT

Semi-quantitative screening analysis by ICP

Issued by:	ALS Scandinavia Luleå, Aurorum 10, SE-977 75 LULEÅ, Sweden
Client:	NTNU Institutt for Materialteknolog
Date of receipt:	2022-04-08
Date of analysis:	2022-04-22
Order number(our):	LE2204221
Your reference:	Fride Müller
Our reference:	Steffen Eisele
Sample name:	11
Sample description:	
Lab number(our)	LE2204221-011

Aluminum, Al	250000 mg/kg	Nickel, Ni	970 mg/kg
Antimony, Sb	44 mg/kg	Niobium, Nb	0.34 mg/kg
Arsenic, As	38 mg/kg	Osmium, Os	< 0.02 mg/kg
Barium, Ba	110 mg/kg	Palladium, Pd	< 0.05 mg/kg
Beryllium, Be	9.0 mg/kg	Phosphorus, P	740 mg/kg
Bismuth, Bi	3.7 mg/kg	Platinum, Pt	< 0.02 mg/kg
Boron, B	< 5 mg/kg	Potassium, K	1000 mg/kg
Bromine, Br	< 50 mg/kg	Praseodymium, Pr	0.060 mg/kg
Cadmium, Cd	0.35 mg/kg	Rhenium, Re	0.088 mg/kg
Calcium, Ca	8900 mg/kg	Rhodium, Rh	< 0.03 mg/kg
Cerium, Ce	0.71 mg/kg	Rubidium, Rb	3.4 mg/kg
Cesium, Cs	0.36 mg/kg	Ruthenium, Ru	< 0.03 mg/kg
Chromium, Cr	23 mg/kg	Samarium, Sm	0.088 mg/kg
Cobalt, Co	9.5 mg/kg	Scandium, Sc	0.27 mg/kg
Copper, Cu	28 mg/kg	Selenium, Se	1.5 mg/kg
Dysprosium, Dy	0.084 mg/kg	Silicon, Si	1900 mg/kg
Erbium, Er	0.074 mg/kg	Silver, Ag	0.13 mg/kg
Europium, Eu	0.080 mg/kg	Sodium, Na	79000 mg/kg
Gadolinium, Gd	< 0.05 mg/kg	Strontium, Sr	42 mg/kg
Gallium, Ga	110 mg/kg	Sulfur, S	950 mg/kg
Germanium, Ge	0.19 mg/kg	Tantalum, Ta	< 0.05 mg/kg
Gold, Au	< 0.05 mg/kg	Tellurium, Te	1.9 mg/kg
Hafnium, Hf	0.31 mg/kg	Terbium, Tb	< 0.01 mg/kg
Holmium, Ho	< 0.05 mg/kg	Thallium, Tl	0.036 mg/kg
Iodine, I	1.1 mg/kg	Thorium, Th	0.84 mg/kg
Iridium, Ir	< 0.005 mg/kg	Thulium, Tm	< 0.005 mg/kg
Iron, Fe	5100 mg/kg	Tin, Sn	0.92 mg/kg
Lanthanum, La	1.8 mg/kg	Titanium, Ti	64 mg/kg
Lead, Pb	16 mg/kg	Tungsten, W	4.6 mg/kg
Lithium, Li	9.7 mg/kg	Uranium, U	0.19 mg/kg
Lutetium, Lu	0.015 mg/kg	Vanadium, V	230 mg/kg
Magnesium, Mg	314 mg/kg	Ytterbium, Yb	0.080 mg/kg
Manganese, Mn	36 mg/kg	Yttrium, Y	2.8 mg/kg
Mercury, Hg	< 0.02 mg/kg	Zinc, Zn	14 mg/kg
Molybdenum, Mo	9.8 mg/kg	Zirconium, Zr	7.6 mg/kg
Neodymium, Nd	0.25 mg/kg		

Comments

The analysis is carried out by ICP-SMS (HR-ICP-MS).
The trace elements are determined using 18 scans over the mass range, resulting in a total measurement time of 300 s.
All concentrations are within ± 50% of the reported value.This may not apply to Br, Cl and I.
Elements marked with '<' are below the detection limit.
Elements marked with*** were not detectable.
Elements marked with ----- are not measured.

Signature

ANALYSIS REPORT

Semi-quantitative screening analysis by ICP

Issued by:	ALS Scandinavia Luleå, Aurorum 10, SE-977 75 LULEÅ, Sweden
Client:	NTNU Institutt for Materialteknolog
Date of receipt:	2022-04-08
Date of analysis:	2022-04-22
Order number(our):	LE2204221
Your reference:	Fride Müller
Our reference:	Steffen Eisele
Sample name:	12
Sample description:	
Lab number(our)	LE2204221-012

Aluminum, Al	71000 mg/kg	Nickel, Ni	97 mg/kg
Antimony, Sb	2.5 mg/kg	Niobium, Nb	0.18 mg/kg
Arsenic, As	7.3 mg/kg	Osmium, Os	< 0.02 mg/kg
Barium, Ba	32 mg/kg	Palladium, Pd	< 0.05 mg/kg
Beryllium, Be	2.5 mg/kg	Phosphorus, P	120 mg/kg
Bismuth, Bi	0.24 mg/kg	Platinum, Pt	< 0.02 mg/kg
Boron, B	< 5 mg/kg	Potassium, K	2100 mg/kg
Bromine, Br	< 50 mg/kg	Praseodymium, Pr	0.070 mg/kg
Cadmium, Cd	< 0.01 mg/kg	Rhenium, Re	0.0052 mg/kg
Calcium, Ca	37000 mg/kg	Rhodium, Rh	< 0.03 mg/kg
Cerium, Ce	0.55 mg/kg	Rubidium, Rb	1.6 mg/kg
Cesium, Cs	0.087 mg/kg	Ruthenium, Ru	< 0.03 mg/kg
Chromium, Cr	5.6 mg/kg	Samarium, Sm	< 0.05 mg/kg
Cobalt, Co	1.5 mg/kg	Scandium, Sc	0.18 mg/kg
Copper, Cu	1.4 mg/kg	Selenium, Se	1.3 mg/kg
Dysprosium, Dy	< 0.05 mg/kg	Silicon, Si	7200 mg/kg
Erbium, Er	< 0.05 mg/kg	Silver, Ag	< 0.02 mg/kg
Europium, Eu	0.065 mg/kg	Sodium, Na	120000 mg/kg
Gadolinium, Gd	< 0.05 mg/kg	Strontium, Sr	410 mg/kg
Gallium, Ga	31 mg/kg	Sulfur, S	16000 mg/kg
Germanium, Ge	< 0.05 mg/kg	Tantalum, Ta	< 0.05 mg/kg
Gold, Au	< 0.1 mg/kg	Tellurium, Te	0.39 mg/kg
Hafnium, Hf	0.20 mg/kg	Terbium, Tb	< 0.01 mg/kg
Holmium, Ho	< 0.05 mg/kg	Thallium, Tl	< 0.005 mg/kg
Iodine, I	0.72 mg/kg	Thorium, Th	< 0.05 mg/kg
Iridium, Ir	< 0.005 mg/kg	Thulium, Tm	< 0.005 mg/kg
Iron, Fe	3000 mg/kg	Tin, Sn	0.18 mg/kg
Lanthanum, La	1.5 mg/kg	Titanium, Ti	28 mg/kg
Lead, Pb	1.3 mg/kg	Tungsten, W	1.4 mg/kg
Lithium, Li	0.99 mg/kg	Uranium, U	0.11 mg/kg
Lutetium, Lu	0.0056 mg/kg	Vanadium, V	73 mg/kg
Magnesium, Mg	50000 mg/kg	Ytterbium, Yb	0.087 mg/kg
Manganese, Mn	6.6 mg/kg	Yttrium, Y	1.5 mg/kg
Mercury, Hg	< 0.02 mg/kg	Zinc, Zn	0.74 mg/kg
Molybdenum, Mo	1.7 mg/kg	Zirconium, Zr	6.3 mg/kg
Neodymium, Nd	0.25 mg/kg		

Comments

The analysis is carried out by ICP-SMS (HR-ICP-MS).
The trace elements are determined using 18 scans over the mass range, resulting in a total measurement time of 300 s.
All concentrations are within ± 50% of the reported value.This may not apply to Br, Cl and I.
Elements marked with '<' are below the detection limit.
Elements marked with*** were not detectable.
Elements marked with ----- are not measured.

Signature S. Eisele

Fride Müller

Heavy Metal Emissions from Primary Aluminium Production

NTNU
Norwegian University of
Science and Technology